University of Southampton

Faculty of Environmental and Life Sciences

School of Geography and Environmental Science

Examining Large-Scale Interactions between Hazards, Exposure, and Vulnerability in Coastal Built Environments

by

Sofía Nadime Aldabet Muñoz

ORCID ID 0000-0002-6822-8330

Thesis for the degree of Doctor of Philosophy (PhD)

July 2024

University of Southampton

Abstract

Faculty of Environmental and Life Sciences

School of Geography and Environmental Science

Doctor of Philosophy

Examining Large-Scale Interactions between Hazards, Exposure, and Vulnerability in Coastal Built Environments

by

Sofía Nadime Aldabet Muñoz

Coastal areas stand out as the most densely populated and economically active regions on the planet, with growth rates surpassing those of inland areas. Yet, the conversion of natural coastlines into human-modified built environments carries significant implications. Coastal landscapes are inherently dynamic, continuously changing their shape and location, especially in response to rising sea levels. This ongoing transformation exposes coastal communities and their built environments to various natural hazards, which are often exacerbated by anthropogenic activities. Human-made structures and modifications to natural land formations, particularly those intended to protect these areas, have a profound impact on the morphology of the coast and its natural processes. These changes, in turn, give rise to dynamics that fundamentally differ from those observed in natural settings. In most developed coasts, human alterations are so extensive that coastlines no longer adhere to natural behaviors. Instead, they have evolved into complex human-landscape systems, where human actions and landscape changes are intricately intertwined. This interdependence between the human and natural components of the system leads to unexpected dynamics that unfold over extended periods, often resulting in self-reinforcing feedbacks that amplify coastal risk and its associated costs. The present thesis explores empirical signatures of the interplay between natural hazards and the physical and socio-economic characteristics of coastal built environment at large spatial scales, using only publicly available data. Its main objective is to bridge theory with data to deepen our understanding of the complex dynamics shaping coastal risk and offer insights into the implications and consequences of these interconnected factors for coastal communities. By enhancing our comprehension of the multifaceted nature of coastal risk, this work underscores the critical need for thoughtful and informed decision-making in the formulation of strategies for effective coastal risk reduction.

Table of Contents

Table of Contents **3**
Table of Tables **8**
Table of Figures **9**
Research Thesis: Declaration of Authorship **15**
Acknowledgements **16**
Chapter 1 Introduction **18**
1.1 Preamble **18**
1.2 Background **20**
1.2.1 Coupled human-landscape systems 20
1.2.1.1 Sculptors of the Earth's surface 20
1.2.1.2 Interconnectedness of human actions and landscape changes 21
1.2.1.3 Developed coasts as dynamic coupled human-landscape systems 22
1.2.2 The components of coastal risk 24
1.2.2.1 Hazard 25
1.2.2.2 Exposure 26
1.2.2.3 Vulnerability 26
1.2.3 Systemic feedbacks exacerbating coastal risk 28
1.2.3.1 Unintended consequences of hazard protection: the levee effect and the safe development paradox 29
1.2.3.2 Self-reinforcing dynamics in coupled human-coastal systems .. 31
1.2.3.3 The disaster trap 33
1.2.4 The recipe for disaster 34
1.2.4.1 The expanding bull's-eye effect 34
1.2.4.2 Escalating exposure in hazard-prone zones 35
1.2.4.3 Building back bigger in hazard-prone zones 38
1.3 Contributions to the literature **39**
1.3.1 Research gap and thesis objectives 39
1.3.2 Data and methods 41

1.3.3 Research papers 42

1.3.3.1 Chapter 2: Exploring spatial relationships between coastal hazards, population exposure, and social vulnerability in England [Unpublished manuscript] 42

1.3.3.2 Chapter 3: The revalorizing effect of beach nourishment [Unpublished manuscript] 43

1.3.3.3 Chapter 4: Thresholds in Road Network Functioning on US Atlantic and Gulf Barrier Islands (Aldabet et al., 2021) 44

Chapter 2 Paper 1: Exploring spatial relationships between coastal hazards, population exposure, and social vulnerability in England 47

2.1 Abstract 47

2.2 Introduction 47

2.3 Background 49

2.4 Data and Methods 52

2.4.1 Definition of the coastal zone 52

2.4.2 The components of risk 53

2.4.2.1 Hazards 54

2.4.2.2 Exposure 55

2.4.2.3 Vulnerability 56

2.4.3 Exploring relationships between the components of risk 58

2.5 Results 58

2.5.1 Compound hazard, defenses, and policies 58

2.5.2 Patterns of social disadvantage 64

2.6 Implications 70

2.6.1 Comparative patterns 70

2.6.2 Spatial relationships alongshore 71

2.6.3 Data gaps and opportunities for insight 72

2.7 Conclusions 73

2.8 Acknowledgments 73

Chapter 3 Paper 2: The revalorizing effect of beach nourishment..... 74

3.1 Abstract 74

3.2 Introduction 74

3.3 Data and methods 79

3.3.1 Study area 79

3.3.2 Tax records 79

3.3.3 Beach nourishment 80

3.3.4 Historical Settlement Data Compilation for the United States (HISDAC-US) 80

3.3.5 Building footprints 81

3.3.6 Florida 82

3.3.7 United States 83

3.4 Results 83

3.4.1 Increased property price 83

3.4.2 Increased property size 85

3.4.3 Increased built-up intensity 87

3.4.4 Scaling relationships 89

3.4.4.1 Sale price versus property size 89

3.4.4.2 Total living area versus plan-view area 89

3.4.5 Florida 90

3.5 Implications 95

3.5.1 The revalorizing effect of beach nourishment 95

3.5.2 Increased exposure in high-risk coastal development in nourishing areas 96

3.5.3 Growth patterns in vulnerable zones 97

3.5.4 Building footprints as a proxy for total living area 98

3.6 Conclusions 99

3.7 Acknowledgments 100

Chapter 4 Paper 3: Thresholds in road network functioning on US Atlantic and Gulf barrier islands 101

4.1 Abstract 101

4.2 Introduction 102

4.3 Methods 105

4.3.1 Road networks and topography 106

4.3.2 Network response to node removal 107

4.3.3 Extreme water levels 108

4.3.4 Network robustness 110

4.4 Results 111

4.4.1 Barrier island road networks 111

4.4.2 Elevation-based node removal 112

4.4.3 Extreme water levels 114

4.4.4 Road network robustness 114

4.5 Implications 116

4.5.1 No single metric can be used to rank barrier susceptibility to disruption 116

4.5.2 Caveats: non-stationarity and interdependencies in hazard forcing 117

4.5.3 Identifying hotspots of concern 118

4.6 Acknowledgments 120

Chapter 5 Synthesis and conclusions 121

5.1 Key insights 121

5.1.1 Built environments as human-landscape systems 121

5.1.2 Advantages and drawbacks of large-scale analysis 123

5.1.3 Comparative patterns in coastal risk 125

5.1.4 Unintended consequences of hazard protection 127

5.1.5 Networks of critical infrastructure in evolving human-landscape systems 130

5.1.6 Impact of coastal engineering on the risk triangle 133

5.2 Future work 135

5.3 Reflections 137

List of References 139

Table of Contents

Table of Tables

Table 2.1 Exposure to natural hazards in England. 61

Table 2.2 Defenses on the coastal floodplain. 62

Table 2.3 Shoreline Management Plans strategies in the Short-Term (2005-2025) and Long-Term (2056–2105).....63

Table 2.4 Summary statistics for high and low disadvantage areas. 67

Table of Figures

Figure 1.1 The Risk Triangle (Crichton, 1999) 25

Figure 1.2 Hypothetical urbanization patterns without (a) and with (b) levees. Image retrieved from Di Baldassarre et al. (2018). 30

Figure 1.3 Beach nourishment as a driver of self-reinforcing dynamics in tourist-dependent coastal areas: (1) natural movement of sand creates areas of erosion and accretion; (2) wide beaches attract coastal development; (3) high-value built environment at risk of damage from natural hazards requires (4) investment in hazard protection which, in turn, justifies further development. Image retrieved from Lazarus et al. (2016). 33

Figure 1.4 Illustration of the expanding bull's eye effect. Image retrieved from Strader and Ashley (2015). 35

Figure 2.1 Definition of the coastal zone based on coastal floodplains: (a) vectors delineating Shoreline Management Plan Policy Units that intersect (b) the coastal floodplain are given a spatial dimension determined by (c) Euclidean allocation to the nearest coastal-floodplain polygon. This method captures over 3,000 km (~56%) of the total coastline of England. 53

Figure 2.2 Variables used to represent the components of coastal risk: (a) likelihood of flooding and (b) shoreline change represent natural hazards; (c) population and (d) buildings define exposure; (e) coastal defenses and (f) social disadvantage describe vulnerability. 54

Figure 2.3 Coastal-floodplain Policy Units exposed to (a) high likelihood of coastal flooding, (b) long-term shoreline erosion, and (c) both a high likelihood of coastal flooding and long-term shoreline erosion. 59

Figure 2.4 Population on the English coastal floodplain exposed to natural hazards: (a) number of Policy Units and (b) total area exposed to coastal flooding; (c) number of policy units and (d) total alongshore length exposed to shoreline change. 60

Figure 2.5 Proportion of developed area exposed to (a) coastal flooding and (b) modes of shoreline change. 61

Figure 2.6 Plots of (a) population and (b) buildings protected by coastal defenses. *Natural* refers to Policy Units that rely on natural structures for their protection against floods or coastal erosion; *engineered* comprises areas exclusively

protected with hard defenses; and *combined* includes both natural and engineered defenses. 62

Figure 2.7 Strategic policies defined in the Shoreline Management Plans for the Short-Term horizon (2005–2025). 63

Figure 2.8 Differences in affected coastal-floodplain population under shifts in long-term (2056–2105) Shoreline Management Policies: (a) Hold-the-Line, (b) Managed Realignment and (c) No Active Intervention. 64

Figure 2.9 Social disadvantage reported in the national River and Coastal Flood Disadvantage Index, mapped to coastal floodplain extents. (a) Policy Units with low and high disadvantage scores; (b) Policy Units with high and low disadvantage scores and exposed to both a high likelihood of flooding and long-term shoreline erosion. Summary statistics are provided in Table 4. 65

Figure 2.10 Social disparities in exposure to natural hazards: flood likelihood in areas of (a) low and (b) high disadvantage, and distribution of shoreline change in areas of (c) low and (d) high disadvantage. 66

Figure 2.11 Distribution of coastal defenses in areas of (a) low and (b) high disadvantage. 68

Figure 2.12 Relationships between the components of coastal risk in high and low disadvantage areas. (a) Relationship between rates of shoreline change (hazard) and coastal-floodplain development intensity (exposure). (b) Percentage of engineered defenses (vulnerability) relative to building density and (c) population density (exposure); symbols in (b) and (c) are scaled by total length, and medians (dark circles) are superimposed atop the full range of distributions (light circles). (d) Distribution of total shoreline length (exposure) in relation to the percentage of engineered defenses in high and low disadvantage areas (vulnerability). 69

Figure 2.13 Distribution of strategic policies according to Shoreline Management Plans: (a) low and (b) high disadvantage areas for the Short-Term horizon (2005–2025) and (c) low and (d) high disadvantage areas for the Long-Term horizon (2056–2105). 70

Figure 3.1 Beach nourishment in the barrier islands of New Jersey. (a) Barrier island outlines divided into nourishing (light blue) and non-nourishing (dark blue) municipalities. (b) Map of recorded beach nourishment projects carried out in the barrier islands of New Jersey between 1995 and 2016. (c) Cumulative

number of beach nourishment locations between 1940 and 2020 on the barrier islands of New Jersey and number of nourishment events per year. The gray square highlights our period of study (1995-2016). (d) Number of nourishing and non-nourishing municipalities that have jurisdiction in the barrier islands of New Jersey and, most specifically, in the first block of properties from the Atlantic shoreline. (e) Total area (in km2) of the nourishing and non-nourishing barrier and first block municipal sections. (f) Total length (in km) of the Atlantic shoreline in nourishing and non-nourishing areas of the New Jersey barrier islands.....78

Figure 3.2 The revalorizing effect of beach nourishment. Evolution of mean house price (in $/m^2$) for residential properties sold in the barrier islands of New Jersey (a) and the first block of properties from the Atlantic shoreline (b) between 1995 and 2016, compared to the national average. Relationship between sale prices (in $) and distance to the shoreline (in meters) for barrier islands (c) and first-block residential properties (d).....84

Figure 3.3 Changes in mean house size in the barrier islands of New Jersey (a) and the first block of properties from the Atlantic shoreline (b) between 1995 and 2016. 85

Figure 3.4 Changes in property size for houses sold more than once between 1995 and 2016 in the barrier islands of New Jersey and in the first block of properties. The scatterplots (a-d) compare the size of these properties the first and last time a sale was recorded in the tax database, both in nourishing (a-b) and non-nourishing municipalities (c-d). The histograms (e-h) represent the distributions of properties that increased their size over time according to their total living area the first time they were sold (in gray) and the last time their size was recorded in the database (in blue), both in nourishing (e-f) and non-nourishing areas (g-h). Insets in e-h show initial and final year distributions of all properties in a-d. 86

Figure 3.5 Changes in built-up intensity from 1995 to 2015 according to the HISDAC-US database. (a-b) Comparisons in built-up intensity for all raster cells located in nourishing areas of the barrier islands of New Jersey and the first block of properties. (c-d) Comparisons in built-up intensity for barrier and first-block cells located in non-nourishing municipalities. (e-f) Evolution of the mean built-up intensity during our period of study in nourishing and non-nourishing municipalities of the barrier islands and the first block of properties....88

Table of Figures

Figure 3.6 Scaling relationships between sale price and total living area (a-b) and total living area and building footprint (c-d) in the barrier islands of New Jersey and the first block of properties. 90

Figure 3.7 Changes in property price (a-c) and property size (d-f) of shorefront single-family houses in the Atlantic and Gulf Coasts of Florida. 91

Figure 3.8 Changes in property size for houses sold more than once between 2012 and 2017 in the Atlantic and Gulf Coasts of Florida. The scatterplots compare the size of these properties the first and last time a sale was recorded in the tax database in nourishing (a-c) and non-nourishing municipalities (g-i). The histograms represent the distributions of properties that increased their size over time according to their total living area the first time they were sold (in gray) and the last time their size was recorded in the database (in blue), both in nourishing (d-f) and non-nourishing areas (j-l). Insets in the histograms show initial and final year distributions of all properties in the database.92

Figure 3.9 Changes in property size for houses sold more than once between 2012 and 2017 in two storm-prone locations: Naples and Palm Beach. The scatterplots (a-b) compare the size of these properties the first and last time a sale was recorded in the tax database, and the histograms (c-d) represent the distributions of properties that increased their size over time, according to their total living area the first time they were sold (in gray) and the last time their size was recorded in the database (in blue). Insets in the histograms show initial and final year distributions of all properties in the database.94

Figure 4.1 US Atlantic and Gulf Coast barrier islands considered in this study, and their road networks. (a) Map of 184 barrier islands (Mulhern et al., 2017, 2021), of which 74 have road networks with >100 nodes (intersections). Of those, 72 (light blue) overlap with tiles currently available in the Continuously Updated Digital Elevation Model data from NOAA (Amante et al., 2021; CIRES, 2014). Box shows location of example barrier in panel below. (b) Example of drivable road network at Ocean Isle, North Carolina, USA, in which intersections are represented as nodes and roads as edges. Maps shown in Web Mercator projection (EPSG:3857). 105

Figure 4.2 Methodological workflow for assessing robustness to flood-induced failures in road networks on US Atlantic and Gulf barrier islands. Abbreviations are as follows: OSM is Open Street Map; OSMnx is an analytical toolbox (Boeing, 2017). CUDEM is the NOAA Continuously Updated Digital Elevation Model (Amante et al., 2021; CIRES, 2014). GCC is the giant connected component

of a network, or the large cluster of nodes connected in the original network. 106

Figure 4.3 Examples illustrating the methodology used to (a) explore the size decay of the first and second GCCs, (b) identify the critical node that leads to the fragmentation of the network, and (c) quantify overall network robustness to elevation-based node removal. Barrier example shown here is the drivable network at Ocean Isle, North Carolina, USA. In (a), the vertical axes show the first (left) and second (right) GCC size as a fraction of nodes in the original network, as a function of the fraction of nodes removed (q). Red dot in panels (a) and (b) marks the critical node in the GCC and in real physical space, respectively. In panel (c), robustness R is taken as the area (light green) under the decay curve for the first GCC (bold green). Dashed gray line shows the inverse 1:1 reference line, indicating the theoretical maximum for R = 0.5. Maps like the example shown in (b) for all 72 barrier road networks with >100 nodes can be found in the data repository.....108

Figure 4.4 Summary statistics for 72 US Atlantic and Gulf barrier-island road networks with >100 nodes. Panels show distributions of (a) total area, (b) total road length, and (c) the number of networked nodes for all 72 barriers. Panel (d) shows the distribution of elevation for all networked nodes in all 72 barriers.111

Figure 4.5 Network effects of node removal based on ranked list of elevation (from low to high). (a) Elevation of each networked node, sorted into a ranked list from lowest to highest, for 72 barriers with networks with >100 nodes. Network size is normalized to 1. (b) Size decay of each giant connected component under sequential node removal by elevation, from lowest to highest. Gray dashes are the inverse 1:1 reference line. (c) Elevation of the critical node (zc) for each of the 72 road networks with >100 nodes, ranked from lowest to highest. (d) Size decay of each giant connected component as a function of node elevation. 113

Figure 4.6 Relationships between road networks and extreme water levels. (a) Size decay of the giant connected component versus annual exceedance probability (AEP) of extreme high-water events, based on the elevation of each node removed. (b) Barrier islands ranked according to exceedance probability of the critical node (e_c). (c) Relationship between the exceedance probability of the critical node for each barrier (e_c) as a function of the critical-node elevation (z_c). 114

Figure 4.7 Road network robustness. (a) Normalized giant connected component size as a function of fraction of network nodes removed (as in Figure 4.5b), where

color represents values of robustness (purple ~ low; yellow ~ high). Dashed gray inverse 1:1 reference line denotes the curve for perfectly linear GCC decay with a theoretical maximum robustness of R = 0.5. (b) Rank-order plot of robustness values for the 72 barriers with >100 nodes. (c) Decay of giant component as a function of fraction of nodes removed for a network with high robustness to flooding disturbance (black line; R = 0.47; island FL28 in Mulhern et al. (2021)). Solid gray lines show comparatively distinct decay curves for the same network under random node removal. (d) Decay of giant component as a function of fraction of nodes removed for a network with low robustness to flooding disturbance (black line; R = 0.17; island SC1 in Mulhern et al. (2021)). Solid gray lines show similar decay curves for the same network under random node removal.....115

Figure 4.8 Parallel-coordinates plot of critical node elevation (z_c), exceedance probability (e_c), and robustness (*R*) for barriers with road networks of >100 nodes. In each column, respectively, barriers (labeled at far left) are ranked by z_c in ascending order, by e_c in descending order, and by *R* in ascending order. Each barrier is colored by z_c, and that color follows each barrier across the plot as its relative rank changes for e_c and *R*.....117

Figure 5.1 Interrelations between the components of risk explored in this thesis: hazard, exposure and vulnerability in Chapter 2, exposure and vulnerability in Chapter 3 and hazard and exposure in Chapter 4. 123

Research Thesis: Declaration of Authorship

Print name: Sofía Nadime Aldabet Muñoz

Title of thesis: Examining Large-Scale Interactions between Hazards, Exposure, and Vulnerability in Coastal Built Environments

I declare that this thesis and the work presented in it are my own and has been generated by me as the result of my own original research.

I confirm that:

1. This work was done wholly or mainly while in candidature for a research degree at this University;
2. Where any part of this thesis has previously been submitted for a degree or any other qualification at this University or any other institution, this has been clearly stated;
3. Where I have consulted the published work of others, this is always clearly attributed;
4. Where I have quoted from the work of others, the source is always given. With the exception of such quotations, this thesis is entirely my own work;
5. I have acknowledged all main sources of help;
6. Where the thesis is based on work done by myself jointly with others, I have made clear exactly what was done by others and what I have contributed myself;
7. Parts of this work have been published as:

Aldabet, S., Goldstein, E. B., and Lazarus, E. D. (2022) “Thresholds in road network functioning on US Atlantic and Gulf barrier islands”, *Earth’s Future*, 10(5), e2021EF002581. DOI: 10.1029/2021EF002581

Aldabet, S. contributed to the investigation, methodology, formal analysis, writing and data curation; Goldstein, E. B. contributed to the conceptualization, investigation, methodology, formal analysis, and writing; Lazarus, E. D. contributed to conceptualization, investigation, methodology, formal analysis, writing, supervision and funding acquisition.

Signature: ..... Date: 16/07/2024

Acknowledgements

After completing my degree in 2008, I knew I wanted to pursue a PhD. Not because I had ambitions of an academic career, but because I enjoy taking on personal challenges and have an insatiable thirst for knowledge. Almost by chance, a whole decade after I graduated, I stumbled upon a project that felt like the perfect fit. Now, as I reflect on five challenging years that included navigating a global pandemic and an illness, I want to express my most sincere gratitude to all those who stood by me throughout this journey and made it possible.

I want to begin by expressing my heartfelt thanks to my primary supervisor, Dr. Eli Lazarus. He believed in my potential, provided me with this opportunity, and expertly guided me through the entire process. I am also truly grateful for his encouragement, understanding and support, particularly during the challenging times of the pandemic and my illness, which resulted in a temporary halt in my research. I would also like to extend my gratitude to the other advisors that I have had during my PhD, Professor Emma Tompkins and Professor Robert Nicholls (now at the University of East Anglia), for their thoughtful insights. A special recognition also goes to Evan Goldstein, for being my (unofficial) technical mentor and patiently introducing me to tools that have become integral to my daily tasks. As a coauthor, I am also thankful for his valuable inputs and insights that greatly contributed to the completion and publication of Paper 3 (Chapter 4).

I would like to acknowledge the School of Geography and Environmental Science, as well as the Southampton Marine and Maritime Institute, for funding my doctoral studies and providing the essential support required for their completion. I am also grateful to the reviewers who have contributed to making the PhD progression meetings insightful and fruitful experiences: Professor Emma Tompkins (before becoming a supervisor), Dr. David Sear and Dr. Julian Leyland. Special thanks are also due to Chris Hill and Duncan Hornby from GeoData for their mentoring during the analysis in Chapter 2, as well as to Julie Drewitt, for her invaluable assistance over these five years.

I am profoundly grateful to my VIVA examiners, Dr. Irene Delgado Fernandez and Dr. Dianna Smith, for their invaluable insights and recommendations, and for making the nerve-wracking viva process an enjoyable experience.

My appreciation extends to Vizzuality for their support and understanding, which have allowed me to maintain a balance between my work and my personal project. I would also like to thank all my colleagues, with a special acknowledgement to the Science team, for their significant contributions to my learning and professional growth.

On a more personal note, I want to express my gratitude to my dearest friends: Alexia, my longstanding companion; Esther, my college partner-in-crime; and Nancy, forever bounded

by the twists of fate. Regardless of the physical distance or the extended periods between our get-togethers, I am sure that I can always rely on your support and affection. I also wish to extend my thanks to Giulia, my roommate during my time in Southampton, and to Sergio, with whom I shared many doubts and concerns throughout our PhD journeys. Additionally, my cousin Nour deserves my profound gratitude for her warm hospitality during numerous weekends and for introducing me to some of the most exceptional places in London.

Last but certainly not least, I would like to express my most profound appreciation to my loved ones for their unwavering love and support. A special recognition to my Galician family: my parents, Pili and Amadeo, who have consistently backed my decisions and dreams; my dear sister Cristina, the most precious gift from my parents; and my uncle Antonio and godmother Dolores, lifelong and beloved companions. I am also filled with gratitude for my Valencian family: Luis, my partner, for his unconditional love and acceptance, and Irene and Marta, for warmly welcoming me into their lives. This thesis is dedicated to each and every one of you.

Chapter 1 Introduction

1.1 Preamble

Coastal systems, profoundly shaped by human activities, constitute the most densely populated and economically valuable regions on the planet (McGranahan et al., 2007). Abundant in rich natural habitats, diverse recreational opportunities, and a wide range of economic activities including tourism, trade, and fishing, coasts have been sites of human settlements for tens of thousands, if not hundreds of thousands of years (Neumann et al., 2015; Nordstrom, 2005). Encompassing only 2% of the planet's landmass, low-lying coastal areas (below 10-meter elevation) currently house over 10% of the global population and 13% of the urban population, and continue to experience rapid growth rates that outpace national averages worldwide (McGranahan et al., 2007). This magnetism, however, comes at a steep price, generating a tremendous potential for catastrophe and escalating costs associated with coastal risk. Coastal regions, despite their significance and economic value, are paradoxically the most hazard-prone environments on Earth, especially to the physical impacts of powerful storms, which climate change and sea-level rise are compounding (Wong et al., 2014).

But coastal risk does not solely stem from the susceptibility of these regions to natural hazards. Instead, it is the convergence of natural hazards, the vulnerability of the exposed assets, and the values at stake that ultimately determines the level of risk (Crichton, 1999). Consequently, the rapid and uncontrolled urban development witnessed in coastal areas, particularly in recent decades, emerges as a primary and influential factor amplifying coastal risk. Human agency alters coastal morphology and natural dynamics, giving rise to novel processes that deviate significantly from those found in undisturbed environments (Lazarus, 2022a; Nordstrom, 1994). Anthropogenic activities also play a role in the deterioration of fragile ecosystems, which have dual significance as valuable resource providers and natural buffers against hazards (Mileti, 1999). For example, factors like population growth, infrastructure development, and the expansion of the tourism industry contribute to the degradation of beaches and dunes, affecting both their economic potential and their ability to offer natural protection (Lazarus, 2022b; Lazarus et al., 2016, 2011). Similarly, the conversion of natural landscapes into urban or suburban settings, accompanied by the expansion of impervious surfaces, disrupts hydrological systems, fragmenting drainage networks, and destroying natural defenses such as wetlands (Brody et al., 2008). Thus, the diminished capacity of natural ecosystems to retain water, coupled with increased runoff, leads to formerly secure areas unexpectedly succumbing to flood damage.

The persistent growth of human settlements also exposes an expanding population to increased risk from natural hazards (McGranahan et al., 2007). If current development trends persist and projected climate change impacts materialize, the combination of higher population density and expanded built-up areas along coastlines will inevitably amplify the potential for more frequent and severe disasters (McGranahan et al., 2007; Strader and Ashley, 2015). In efforts to reduce hazards along developed coastlines, various engineered measures like groins, seawalls, and beach nourishment have been widely used. Ironically, these protective interventions have been associated with increased risk during major hazardous events, as they can instill a false sense of safety among the protected population that might lead to further urbanization in hazard-prone areas (Burby, 2006; Di Baldasarre et al., 2015; Kates et al., 2006; Tobin, 1995; White, 1945). The devastating aftermath of Hurricane Katrina in New Orleans in 2005 might serve as a striking example of the detrimental impact of increased exposure resulting from the implementation of mitigation policies and hazard defenses (Burby, 2006).

While it is impossible to prevent large-scale natural events, acknowledging that major disasters are not mere strokes of bad luck, but rather the result of a complex interplay between political, financial, social, technical, and natural factors may significantly mitigate their impact (Lazarus et al., 2016; Werner and McNamara, 2007). This thesis delves into the domain of developed coastal areas, exploring them as dynamic, coupled human-landscape systems, where the built environment and physical and human-induced processes are intertwined. The intricate relationships between these elements often give rise to unforeseen dynamics that unfold over extended periods and large geographical scales, ultimately setting the stage for self-reinforcing feedbacks that magnify coastal risks and amplify their associated costs (Lazarus, 2022b).

Using publicly available geospatial data, this work examines indications of interactions and feedbacks among hazards, exposure, and vulnerability—the fundamental elements of risk—on developed coastlines, to identify significant large-scale patterns that may contribute to increased exposure and subsequently intensify the risk of disasters. The thesis comprises three manuscripts that I have led through intellectual contribution, analysis, and delivery, with one already published (Aldabet et al., 2022) and two currently in progress (undergoing review with the respective coauthors). The first paper, Chapter 2, examines potential indications of interdependence between the physical and social components of coastal risk at a national scale in England. For that, it assembles and analyzes a comprehensive portfolio of publicly available spatial datasets related to coastal hazards (flood likelihood and long-term erosion), population distribution, building infrastructure, social vulnerability, coastal defenses, and policy zones of shoreline-management plans. Chapter 3 investigates spatial development patterns in New Jersey and Florida, renowned hotspots of coastal risk. The analysis combines extensive housing data containing structural and economic information

with locations of historical beach nourishment projects. Chapter 4 (Aldabet et al., 2022) uses the quantitative tools of graph theory to identify potential thresholds in the functioning of road networks on developed barrier islands along the US Atlantic and Gulf coasts. Gaining insights into the functionality of critical infrastructure in built environments with high exposure to natural hazards is imperative for deepening our understanding and foresight regarding the future evolution of fragile coastal systems.

Together these papers provide complementary, data-driven perspectives on the challenges associated with mitigating damage risk posed by coastal hazards in developed coastal regions. This research illustrates the intricate interplay between physical processes and development patterns within hazard-prone coastal areas, thereby highlighting the unintended consequences of expanding the built environment and implementing human interventions, particularly those designed to safeguard infrastructure. By deepening our understanding of the multifaceted nature of coastal risk, this work underscores the critical need for thoughtful and informed decision-making in the formulation of strategies for effective coastal risk reduction.

1.2 Background

1.2.1 Coupled human-landscape systems

1.2.1.1 Sculptors of the Earth's surface

The significant role of human beings in shaping the Earth's ecosystems has led to the recognition of a new geological epoch, the so-called Anthropocene (Crutzen, 2002). While the precise onset of this era remains a subject of debate (Smith and Zeder, 2013), global-scale human influence on the environment has been acknowledged for centuries and even thousands of years. From the earliest days of human civilization, natural landscapes have been converted, shaped, or eliminated to suit human needs (Nordstrom, 1994). Particularly in the past century, population growth, built-up expansion, and technological advancements have contributed to the steady increase of anthropogenic land transformations, resulting in significant ecosystem alterations, biodiversity loss, and impacts on the climate (Hooke, 2000; Vitousek et al., 1997). This period marks a shift where the influence of nature on landscape dynamics is increasingly contested by what is known as the Anthropic Force, a term that captures the combined, direct and indirect effects of human activities (Haff, 2003).

With activities such as agriculture, mining, and infrastructure construction moving around 35 Gt of soil and rock annually, more than any other natural process of geomorphic transport (Hooke, 1994), we are, indeed, the most effective sculptors of the Earth's surface. The period from 1990 to 2015 alone witnessed a 30.3% increase in human-induced modifications that led to the destruction of approximately 3.3 M km^2 of natural land (Theobald et al., 2020;

2021). This is equivalent to an average 1.2% annual increase, with a daily loss of approximately 359 km^2 or nearly 25 hectares every minute. Consequently, recognizing human-induced geomorphic alterations as essential components of contemporary landscape dynamics has become imperative to fully understand modern and future landscape evolution (Church, 2010; Haff, 2003; Hooke, 1994; Lazarus, 2017, 2022a; Nordstrom, 1994, 2000, 2005).

1.2.1.2 Interconnectedness of human actions and landscape changes

Traditional research on Earth-surface processes has focused on undisturbed natural environments, where physical and biological processes shape the planet without human intervention (Murray et al., 2011). Yet, as human activities rapidly expand, the presence of pristine landscapes has significantly diminished, emphasizing the need to incorporate human agency as a fundamental component of landscape evolution rather than dismissing it as a mere “aberration” (Nordstrom, 1994). Effectively addressing this human component, however, requires acknowledging the interconnectedness of human actions and landscape changes, which exert mutual influence through—often unintended—feedback loops (Murray, 2011). Humans shape landscapes by moving sediments, enhancing erosion or accretion, altering ecosystems, or changing climate. Frequently, these actions respond to modifications in the landscape, or the processes that shape it, that were caused by previous human interventions (Werner and McNamara, 2007). Conversely, landscape processes impact human populations by determining the development and distribution of settlements, or by causing economic and personal harm to communities inhabiting areas prone to natural disasters. Given the complexity of these interconnections, human actions and landscape processes must be viewed not as separate entities but as parts of an interconnected, integrated system (Werner and McNamara, 2007).

The analysis of human and natural landscape changes as integrated, coupled systems might uncover and foresee emergent feedbacks and phenomena that less comprehensive perspectives may not reveal (Haff, 2003; Lazarus et al., 2016; Nordstrom, 1994; Werner and McNamara, 2007). Such human-landscape couplings are expected to be strongest on intermediate timescales (years to decades) where environmental forces can expose large areas of inhabited land to substantial transformations and risks, and where economic mechanisms attribute value to these lands, prompting initiatives to shield them from harm (Werner and McNamara, 2007). Developed coasts, where large-scale changes can occur at medium timescales, showcase some of the most exemplary cases of coupled human-environment systems in which anthropogenic interventions can, deliberately or unintentionally, lead to the development of novel landscape systems (Lazarus, 2017; Murray, 2011).

1.2.1.3 Developed coasts as dynamic coupled human-landscape systems

Coastlines, where the land meets the sea, are naturally sculpted by a complex interplay of geological, climatic, and oceanic forces, including sea level trends, and the actions of waves, currents, and tides (Walker et al., 2017; Wong et al., 2014). This continuous shaping underlines the diverse and evolving nature of coastal zones, which are home to a wide range of unique ecosystems, including mangroves and coral reefs. These areas are also fundamental to the livelihoods and economic stability of billions across the globe, providing indispensable services such as fishing, transportation and thriving tourism industries (McGranahan et al., 2007; Neumann et al., 2015). Furthermore, coastlines serve as protective barriers, shielding inland regions from the impacts of storm surges and sea-level rise (Wong et al., 2014).

Despite their significant role, the concept of “coastal zone” still lacks a universally accepted definition (Small and Nicholls, 2003; Wong et al., 2014). From a geomorphological perspective, a coastal zone may be defined as the narrow margin at the edge of a continent or island, shaped by the interplay between marine and terrestrial influences due to its proximity to the shoreline (Davidson-Arnott et al., 2019). Yet, the specific boundaries of the coastal zone, both inland and seaward, are intentionally kept vague. Inland, these boundaries can vary widely, from mere hundred meters from a cliff face to several kilometers inland in areas with extensive dune systems or tidal marshes. Seaward, the zone typically extends thousands of meters from the shoreline, though it can reach as far as the edge of the continental shelf or be determined by factors such as shipping routes, economic zones, or ecological criteria.

International bodies such as the IPCC emphasize the coast’s role as a nexus where terrestrial and marine environments intersect, but also struggle to demarcate its precise boundaries. While it is suggested that coastal waters might coincide with territorial seas, encompass the entire exclusive economic zone, or include shelf seas up to 200 meters deep, a definitive scientific or legal agreement on these boundaries remains elusive (IPCC, 2022). On the other hand, the review undertaken for the Millennium Ecosystem Assessment describes coastal ecosystems as areas extending up to 100 kilometers inland from the coastline or up to 50 meters above sea level—whichever is closer to the sea—with the seaward boundary set at the 50-meter depth contour where marine ecosystems begin (Millennium Ecosystem Assessment, 2005). This approach resonates with key studies defining “near-coastal zones” as regions within a 100-kilometer horizontal distance from the coastline and 100 meters vertically above sea level, a decision informed by the notable population density gradients found across these areas (Nicholls and Small; Small and Nicholls, 2003). Additionally, the concept of Low-Elevation Coastal Zone (LECZ), introduced by Mcgranahan et al. (2007), has gained widespread acceptance in the field (e.g., Nicholls

and Cazenave, 2013; Neumann et al., 2015; Wong et al., 2014). This term refers to land areas near the coast that are up to 10 meters above sea level. In some places, particularly near the mouths of significant rivers such as the Amazon and the Yenisey, the LECZ may extend over 100 kilometers inland. However, this expansive reach is more of an exception than the norm, with the zone generally being much narrower.

Amid different interpretations of coastal zones, there is a universal agreement that areas close to the shoreline contain significant and expanding concentrations of human populations, settlements, and socioeconomic activities. Notably, these regions encompass many of the world's most important urban centers and economic hubs (Small and Nicholls, 2003). Historically, coastal areas have been sites of incremental development, becoming the most densely populated and economically active regions on the planet, with growth rates surpassing those of inland areas—a trend expected to persist (McGranahan et al., 2007; Neumann et al., 2015; Nordstrom, 2004; Small and Nicholls, 2003; Wong et al., 2014). Currently, approximately 85% of the global coastlines have been significantly altered by human activities (Williams et al., 2022), transitioning from their original natural state to heavily human-influenced environments. This transformation has profound and far-reaching consequences.

Coastal landscapes are inherently dynamic, constantly shaped by variations in sea levels, oceanic forcing, and sediment exchanges between land and ocean (Davidson-Arnott et al., 2019). In settings with abundant sediment supply or falling sea levels, coastlines typically expand towards the sea, creating landforms such as deltas, barrier islands, and extensive sandy beaches. Conversely, areas with limited sediment supply or sea level rise are prone to erosion and shoreline retreat. These processes of accretion and erosion are fundamental to the resilience and evolution of coastal landforms and their supporting ecosystems. Key habitats such as mangroves, saltmarshes, and dunes, are also central to this resilience by stabilizing sediments and dissipating wave energy, thereby acting as frontline defenses against erosion and storm impacts (Salgado and Martinez, 2017). Natural interaction between physical processes and coastal ecosystems maintains a balanced sediment cycle that safeguards the intrinsic functions of coastlines, allowing them to adapt and recover from environmental changes and natural phenomena like storms and sea-level rise, which are essential aspects of coastal dynamics.

This delicate equilibrium, however, is compromised when the ever-changing forces of coastal environments collide with the static boundaries of human development. Anthropogenic structures and modifications to natural land formations, aimed at protecting human communities from coastal changes and accommodating increasing populations, profoundly affect coastal morphology and its inherent dynamics, leading to the emergence of novel processes that fundamentally differ from those observed in natural settings (Lazarus, 2022a;

Nordstrom, 1994). Recent research has identified a clear positive correlation between the degree of human development and changes in shoreline rates over long periods and across wide spatial scales (Armstrong and Lazarus, 2019a; Hapke et al., 2013). Even moderate levels of development have been linked to shifts in the expected rate of shoreline change, highlighting the significant and persistent impact of human actions, particularly those aimed at protecting infrastructure, on coastal dynamics. These findings suggest that natural shoreline patterns, as predicted by coastal geomorphology, are only observed in areas with sparse development (Hapke et al., 2013). In contrast, developed coastlines exemplify complex systems where human interventions and natural processes are inherently intertwined.

In coupled human-coastal systems, the human component is reflected through economic, political, and psychological mechanisms, while the landscape component is evident in physical processes such as sediment transport, wave climate, storm regime, and sea-level change. Alterations induced by human activities along the coastline have repercussions on the landscape, which in turn affects the environmental conditions to which the human component must adapt (McNamara and Lazarus, 2018). This interconnected relationship between human activities and physical processes at the coastline can give rise to unexpected and complex dynamics that manifest over years to decades (Werner and McNamara, 2007) and often result in self-reinforcing feedbacks that contribute to increased coastal risk and its associated costs (Lazarus, 2022b). Before delving into the dynamics behind these emergent patterns, the next section provides an overview of the key elements that define coastal risk.

1.2.2 The components of coastal risk

Because the definition of *risk* varies depending on the specific needs of the researcher or practitioner, as it is used across different disciplines, the term might lead to confusion when using technical language (Samuels and Gouldby, 2009). For the purpose of this thesis, risk, or most specifically coastal risk, is conceptualized according to the Hazard-Exposure-Vulnerability (HEV) model, also known as the *Crichton Risk Triangle* (Crichton, 1999, 2008). Extensively linked to natural hazards (Lavell et al., 2012), and regarded for its simplicity and comprehensiveness, this framework defines risk as:

> "...the probability of a loss, and this depends on three elements, hazard, vulnerability and exposure. If any of these three elements in risk increases or decreases, then risk increases or decreases respectively."
>
> **Samuels and Gouldby (2009) quoting Crichton (1999), p. 14**

By envisioning an acute-angled triangle with hazard, vulnerability, and exposure as its three sides (**Fig. 1.1**), the level of risk can be represented by the area of the triangle, following the expression:

$$Risk = Hazard \times Exposure \times Vulnerability$$

Therefore, any modifications made to these elements can either increase or decrease the associated risk and the complete absence of any element eliminates risk altogether (Crichton, 2008).

Figure 1.1 The Risk Triangle (Crichton, 1999)

1.2.2.1 Hazard

The Intergovernmental Panel on Climate Change (IPCC) defines *hazard* as:

> "The potential occurrence of a natural or human-induced physical event or trend that may cause loss of life, injury or other health impacts, as well as damage and loss to property, infrastructure, livelihoods, service provision, ecosystems and environmental resources"
>
> **IPCC (2022), p. 2911**

This definition is particularly useful for the research presented in this thesis as it encompasses a broad range of natural phenomena that may affect coastal communities and acknowledges the crucial role of human activity in exacerbating the impacts of natural hazards. Physical phenomena such as storms, sea-level rise, flooding, or shoreline change only become hazards where human beings, or the environmental resources that support them, are exposed to their potentially negative impacts and live under conditions that make them susceptible to harm (Lavell et al., 2012). Therefore, the term *hazard* in the context of this thesis specifically refers to the potential for adverse effects rather than the physical events themselves.

1.2.2.2 Exposure

Exposure plays a critical role in risk assessment as it determines the potential for loss and damage from hazards. The IPCC defines it as:

> "The presence of people; livelihoods; species or ecosystems; environmental functions, services, and resources; infrastructure; or economic, social, or cultural assets in places and settings that could be adversely affected."
>
> **IPCC (2022), p. 2908**

Within the context of this thesis, the exposure component is primarily represented by the built environment that is susceptible to experiencing the effects of coastal hazards, alongside the population residing within it. The built environment encompasses a range of physical infrastructure elements, including buildings, which are extensively analyzed in Chapter 2 and Chapter 3, and critical infrastructure such as road networks, thoroughly examined in Chapter 4.

1.2.2.3 Vulnerability

Vulnerability, the third component of risk, is a complex and controversial concept with multiple definitions (Samuels and Gouldby, 2009). The last Assessment Report (AR6) of the IPCC defines it as:

> "The propensity or predisposition to be adversely affected. Vulnerability encompasses a variety of concepts and elements, including sensitivity or susceptibility to harm and lack of capacity to cope and adapt"
>
> **IPCC (2022), p. 2927**

Nevertheless, even within the established framework of the Intergovernmental Panel on Climate Change there is an ongoing debate about the adequacy and accuracy of the current conceptualization of *vulnerability* for climate change assessments (Ishtiaque et al., 2022). For simplicity, in this thesis *vulnerability* is understood as the susceptibility of both the built environment and its inhabitants to suffer adverse effects from a change agent, which, in this case, refers to coastal hazards. This susceptibility is influenced by the characteristics of the hazard event itself, such as its nature and intensity, as well as the intrinsic attributes of the affected system, including its capacity to anticipate, cope with, resist, and recover from adverse events (Lavell et al., 2012; Nicholls et al., 2015; Wisner et al. 2004).

Vulnerability, and most specifically, social vulnerability, is a complex and multi-dimensional concept that cannot be fully encapsulated by a single metric (Cutter and Finch, 2008). Despite this complexity, quantitative tools like the Social Vulnerability Index (SoVI; Cutter et al., 2003), which is based on multiple socioeconomic and demographic factors, offer valuable

metrics for measuring vulnerability. These tools facilitate comparisons across geographic areas by mapping out a spectrum from higher to lower vulnerability levels within a specific study area. However, reducing the intricate nature of social vulnerability into a linear high-to-low scale can overlook the diversity of vulnerabilities present across different communities (Spielman et al., 2020).

Vulnerable populations are typically defined through a range of personal, social, and environmental factors that exhibit substantial variability among different communities and regions, illustrating that social vulnerability partially stems from social inequalities (Cutter et al., 2003; Cutter and Finch, 2008; England and Knox, 2014; Zsamboky et al., 2011). Among these elements, biophysical attributes such as age and health play a crucial role in determining an individual's susceptibility to the adverse effects of hazard-related events (England and Knox, 2014). The elderly, children, and those with chronic health conditions are especially at risk due to various reasons, including physical limitations that may affect their ability to evacuate or follow mandatory orders, heightened susceptibility to post-disaster psychological stress, and diminished ability to understand and act on hazard information (Cutter and Finch, 2008). Other important determinants including race/ethnicity, gender and socioeconomic considerations such as income, insurance coverage, social networks, and local knowledge, also influence the ability to anticipate, respond to, and recover from disasters (Cutter and Finch, 2008). Women, in particular, often encounter more obstacles during disaster recovery than men, due to their overrepresentation in sectors vulnerable to economic shocks, lower earnings, and caregiving responsibilities. Language and cultural barriers can also significantly restrict communities' access to essential aid and information following a disaster.

Additionally, living in areas prone to hazards or in economically disadvantaged conditions further amplifies vulnerability. The poorest individuals are often forced to settle in locations susceptible to floods or other natural threats, owing to the unaffordability of safer alternatives (McGranahan et al., 2007). Conversely, communities with higher socioeconomic status are better positioned to withstand and recover from disasters. This resilience is largely due to access to insurance, social safety nets, and entitlement programs, which collectively contribute to a more efficient recovery process (Cutter et al., 2003).

The characteristics of the built environment and the physical geography of a community also significantly impact its vulnerability to environmental hazards, either by intensifying or alleviating potential damage. For instance, residents living on the ground floor or in basements are particularly susceptible to severe flooding, while areas lacking efficient drainage systems or green/blue infrastructure to absorb water runoff face a greater risk of extensive flood damage (England and Knox, 2014). Moreover, the presence of hazard protection, whether in the form of hard structures (e.g., seawalls) or softer alternatives (e.g.,

beach nourishment), can influence the susceptibility of both the built environment and its inhabitants to damage or losses caused by natural events. Initially, such protection can reduce the likelihood of harm by creating a barrier between the hazard and the exposed population and assets. Yet, hazard defenses can also create a false sense of security among protected communities, leading to potential underestimation, minimization, or even denial of risk (De Marchi and Scolobig, 2012; Di Baldasarre et al., 2018). This misconception, in turn, can diminish risk awareness and preparedness, increasing their vulnerability in the event of disasters and perpetuating development in areas prone to disasters.

In this context, and given the escalating impacts of climate change and rising sea levels, which elevate the likelihood of coastal defense failures, along with the financial constraints on continuous government investments in such infrastructure (CCC, 2018), Chapter 2 of this thesis considers the presence of hard coastal structures as an indicator of heightened vulnerability. The protection of the population and assets behind these defenses relies on their proper operation and maintenance, but it remains uncertain whether this reliance can be sustained in the long term. In Chapter 3, a similar approach is applied to softer alternatives, specifically beach nourishment, based on the idea that any type of hazard protection can inadvertently encourage development in areas prone to disasters, triggering self-reinforcing feedbacks that may result in unforeseen increases in exposure and risk (Armstrong et al., 2016; Burby, 2006; Burton and Cutter, 2008; Di Baldasarre et al., 2018, 2013; Kates et al., 2006; Montz and Tobin, 2008; Tobin, 1995; White, 1945, 1994). These unintended consequences of hazard protection and their contribution to exacerbating coastal risk are examined in more detail in the subsequent section.

1.2.3 Systemic feedbacks exacerbating coastal risk

A growing body of research suggests that the components of risk do not necessarily function as independent variables, and instead may be interconnected in unintended ways (Armstrong et al., 2016; Armstrong and Lazarus, 2019a, 2019b; Brody et al., 2008, 2007; Burby, 2006; Di Baldassarre et al., 2018, 2013; Hutton et al., 2019; Kates et al., 2006; Lazarus et al., 2018; Mileti, 1999; Tobin, 1995; Wenger, 2015; White, 1945). For example, the installation of engineered defenses to mitigate natural hazards may unintentionally encourage development in disaster-prone areas (Burby, 2006; Burton and Cutter, 2008; Di Baldassarre et al., 2018, 2013; Kates et al., 2006; Montz and Tobin, 2008; Tobin, 1995; White, 1945). Paradoxically, increased exposure in high-risk zones has been identified as a significant contributor to the escalating losses caused by natural events (Ashley et al., 2014; Cutter and Emrich, 2005; Strader and Ashley, 2015). Furthermore, the modification of shorelines through engineering can disrupt natural processes and have long-term effects on coastal dynamics and ecosystems (Nordstrom, 1994, 2014), leading to new environmental conditions that, in turn, influence subsequent engineering decisions (Werner and McNamara,

2007). In human-coastal systems, such interconnected feedbacks can lead to the emergence of “undesirable and seemingly inescapable states”, where negative consequences tend to mutually reinforce and grow more severe over time (Lazarus, 2022b).

1.2.3.1 Unintended consequences of hazard protection: the levee effect and the safe development paradox

In his renowned thesis, “Human adjustment to floods” (1945), geographer Gilbert White wrote:

> “Floods are ‘acts of God’, but flood losses are largely acts of man.”
>
> **White (1945), p. 2**

This concise observation effectively conveys the notion that human actions play a significant role in the consequences of natural disasters. Even well-intentioned efforts to mitigate the risk of natural hazards can sometimes lead to unforeseen outcomes that exacerbate the perilous situation. Hard stabilization structures including groins or seawalls, or softer alternatives such as beach nourishment, are commonly used along developed coastlines to facilitate or protect existing development. But while these strategies might initially lower hazardous levels, particularly for frequent natural events (e.g. return periods of 100 years or less), they have also been paradoxically associated with increased risks when major hazard events occur (Burby et al., 2006; Di Baldasarre et al., 2018, 2013; Kates et al., 2006; Tobin, 1995). As far back as 1937, the literature acknowledged the unforeseen consequences of large-scale mitigation efforts, highlighting the concern that despite substantial investments in headwater reservoir systems—potentially costing hundreds of millions of dollars—greater occupancy and value in flood-prone areas could, over time, result in increased damages rather than diminished ones (Segoe, 1937).

Engineered hazard protection measures, such as levees, are effective in reducing the frequency of flooding and mitigating associated human and economic losses, but they can cause maximum loss when breached or overtopped (White, 1945). The presence of protective structures can create a false sense of security among the protected communities, leading to reduced awareness and preparedness for future hazards (Burby, 2006; Di Baldasarre et al., 2018, 2015; Tobin, 1995). Moreover, the complacency of the population can foster additional development in the protected areas, ultimately increasing exposure and, consequently, the associated risk. When a low-frequency, high-intensity event surpasses the design standards of the defenses, the resulting losses can be even more severe than they were before its construction, as more population and infrastructure are exposed to the hazard (Tobin, 1995). Thus, the installation of hazard protection typically results in a shift from frequent, yet minor, damage in rural or less densely populated areas to rare, but

potentially catastrophic, events in heavily urbanized and industrialized regions (Werner and McNamara, 2007).

The concerning relationship between increasing levels of hazard protection and unforeseen increases in exposure has been highlighted in the literature (Armstrong et al., 2016; Burby, 2006; Burton and Cutter, 2008; Di Baldasarre et al., 2018, 2013, 2015; Kates et al., 2006; Montz and Tobin, 2008; Tobin, 1995; White, 1945, 1994), and catastrophic losses such as those caused by Hurricane Katrina in New Orleans in 2005 have also been related to exacerbated urbanization fueled by the presence of hazard defenses (Burby, 2006). **Fig. 1.2**, extracted from Di Baldassarre et al. (2018), provides a visual representation of the *levee effect* (White, 1945; Tobin, 1995), showcasing the contrasting patterns of built environment expansion in a floodplain with and without hazard protection. The orange buildings in the figure represent the original built-up area. **Fig. 1.2a** illustrates development in an unprotected floodplain, based solely on socio-economic trends. Conversely, **Fig. 1.2b** depicts the impact of flood protection on the development of the area closer to the river, potentially resulting in increased flood exposure in the event of protection failure.

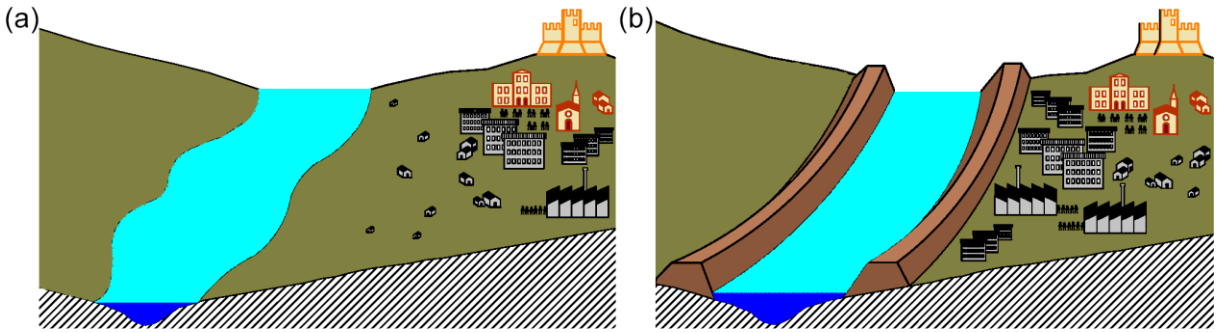

Figure 1.2 Hypothetical urbanization patterns without (a) and with (b) levees. Image retrieved from Di Baldassarre et al. (2018).

Continuous urban expansion in hazard-prone zones has also been favored by government policies that, in their attempt to accommodate population growth, have condoned their development provided that measures were taken to make them safe for human occupation. Burby (2006) used the aftermath of Hurricane Katrina in New Orleans as a prime example of the *safe development paradox*. He argued that, for years, the US government's policies encouraged the profitable use of hazardous land, which made the catastrophic damage caused by the storm entirely foreseeable. Among these policies were the installation of engineered structures to reduce the likelihood of occurrence and the impact of hazards, the adoption of new building designs and practices to enhance resilience, and the provision of disaster relief measures to help affected homeowners and businesses recover from their losses when other mechanisms failed. While these measures effectively facilitated development in hazardous areas, the resulting increased exposure ultimately contributed to the disaster. This reflects a paradox wherein attempts to make dangerous areas safe for

urban development inadvertently worsened the impact by allowing more construction in areas susceptible to natural hazards (Burby, 2006).

Regardless of the protection or insurance coverage provided to the residents, evidence shows that the intensification of land use in hazard-prone areas can eventually amplify pre-existing risks (Tobin, 1995). The effectiveness of hazard protection measures can be limited by inadequate design standards and potential flaws in construction, design, and maintenance, which can result in significant failures during severe events (Burby, 2006). However, communities often overlook these limitations when settling in hazard-prone areas. In Pre-Katrina New Orleans, for example, despite the unstable ground and the threat of dangerous flooding, the presence of improved hurricane protection and flood insurance led thousands of households to believe that the area was safe for occupation.

Consequently, the fundamental failure behind the *levee effect* or the *safe development paradox* stems from deficient land use planning and inadequate educational strategies that fail to warn residents about the risks associated with settling in such locations (Tobin, 1995). As observed by Gilbert White in 1975, hazard protection might prove ineffective if the benefits of reduced damage are outweighed by the heightened risk associated with new developments in flood-prone areas (White, 1975). Eventually, the ongoing construction or enhancement of hazard protection measures may not only be economically unsustainable but can also result in vicious lock-in cycles of ever-increasing expansion of exposed infrastructure and vulnerable and complacent populations, who remain unaware and unprepared for events that may exceed the design standards of the existing defense systems.

1.2.3.2 Self-reinforcing dynamics in coupled human-coastal systems

Developed coastlines with high market values and strong levels of protection exemplify tightly coupled human-landscape systems where human activities and natural processes interact in mutually responsive ways. This interconnectedness between the human and natural components of the system means that any changes in one part of the system can impact and influence the behavior of the other, creating self-reinforcing feedbacks that often lead the system towards an “undesired and seemingly inescapable state, with negative consequences that tend to amplify each other over time” (Lazarus, 2022b).

The model presented by McNamara and Werner (2008a, 2008b) provides an illustrative example of emergent phenomena resulting from self-reinforcing dynamics occurring in the interplay between barrier islands, resort development, and hazard structures. Initially, the presence of natural dunes in undeveloped areas of a barrier island may encourage the emergence of resort development. However, once this development is established, the need for artificial protection arises to safeguard the valuable built environment from natural hazard

impacts. Then, the presence of these newly built engineered defenses creates a false sense of security that legitimizes further development, which, in turn, will require further mitigation efforts. This relentless cycle ultimately leads to the formation of heavily protected barrier islands, where frequent but low-energy events are mitigated at the expense of amplifying the impact of infrequent but more catastrophic events.

In a similar vein, Lazarus et al. (2016) provide a conceptual framework, illustrated in **Fig. 1.3**, that offers valuable insights into how beach nourishment practices can trigger self-reinforcing dynamics in coastal areas that are highly dependent on tourism. Beaches can be regarded as a form of natural capital that yields economic benefits to tourism-related businesses, property owners facing coastal hazards, and coastal communities as a whole through factors such as real-estate values, hotel occupancy rates, and sale taxes (Lazarus et al., 2011). Various empirical studies have shown that wider beaches, frequently obtained via beach nourishment, can boost the value of oceanfront properties (Landry et al., 2003; Pompe and Rinehart, 1995; Qiu and Gopalakrishnan, 2018) and help property owners maintain home prices stable in areas that are prone to coastal hazards (Blackwell et al., 2011). Consequently, beach nourishment, a common “soft” engineering technique that involves importing sand to widen an eroding beach, has been the preferred form of protection in the US (NRC, 2014; Trembanis et al., 1999) and Europe (Hanson et al., 2002) since the 1960s. However, the effects of beach replenishment are temporary, as natural coastal processes rapidly redistribute the deposited sand offshore and alongshore. Population growth, built-up expansion, and the intensification of the tourism industry also contribute to the degradation of the coastal physical environment, including the erosion of beaches and dunes on which the demographic and economic development of the region depends for natural capital and natural hazard protection. As a result, tourism-dependent developed coasts that heavily rely on beach nourishment for hazard protection are typically locked in cycles of replenishment-development that may ultimately lead to *disaster traps* (Lazarus, 2022b; Lazarus et al., 2016, 2011).

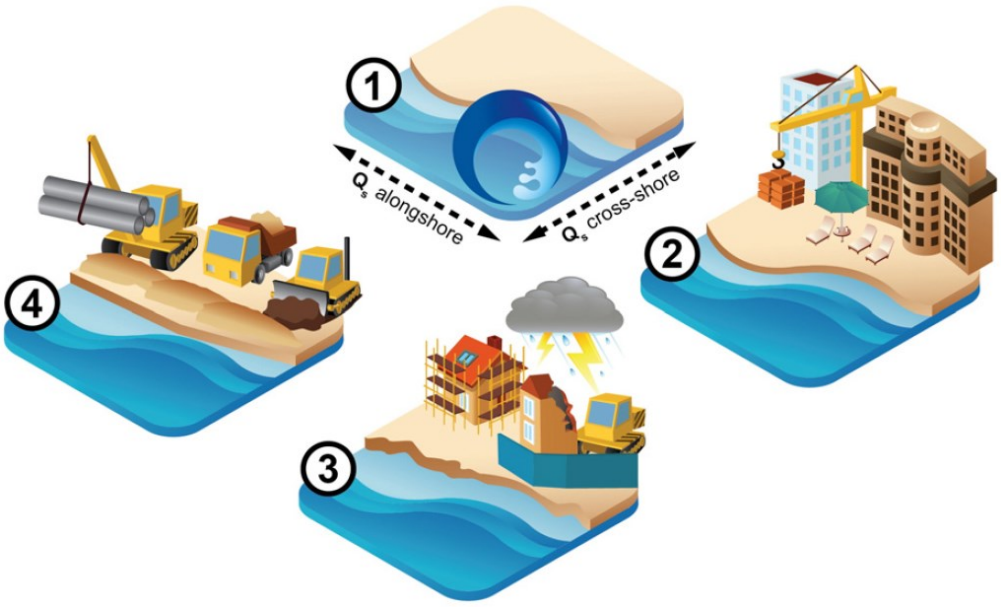

Figure 1.3 Beach nourishment as a driver of self-reinforcing dynamics in tourist-dependent coastal areas: (1) natural movement of sand creates areas of erosion and accretion; (2) wide beaches attract coastal development; (3) high-value built environment at risk of damage from natural hazards requires (4) investment in hazard protection which, in turn, justifies further development. Image retrieved from Lazarus et al. (2016).

1.2.3.3 The disaster trap

One of the most powerful and distinct dynamics that exemplifies these unintended interrelations between exposure, hazard protection, and heightened risk and could help explain the upward trend in economic costs associated with natural disasters is what Lazarus (2022b) termed *disaster trap*. Disaster traps arise from the coupling of two self-reinforcing dynamics: the *gilded trap*, which occurs when a local economy excessively relies on a highly profitable sector that is too lucrative to abandon; and the *safe-development trap*, where the implementation of hazard protection fosters the construction of high-value infrastructure in areas that are naturally prone to hazards. Disaster traps manifest when that high-value infrastructure, enabled and shielded by the safe-development trap, derives its economic value from the sector that drives the gilded trap.

Coastal areas prone to hazards and heavily reliant on tourism are highly susceptible to self-reinforcing dynamics that exacerbate coastal risks and increase their associated costs (Lazarus, 2022b). As the tourism industry becomes more crucial to the local economy, the strength of the gilded trap amplifies, leaving the entire coastal community at risk of economic shocks that could harm the sector. Simultaneously, the economic value of coastal resorts and other tourism infrastructure built to meet the sector's demands justifies artificial protection, driving the safe-development trap. The implementation of new protective

measures, in turn, promotes the expansion of the built environment, perpetuating a dangerous and seemingly inescapable cycle that can lead to disastrous consequences (Burby, 2006; Di Baldasarre et al., 2015; Lazarus, 2014; Lazarus et al., 2016; Mileti, 1999; Werner and McNamara, 2007).

The combination of the gilded trap and the safe-development trap is particularly concerning in coastal areas prone to hazards where climate-finance programs for climate-change adaptation continue to support hard infrastructure projects (Lazarus, 2022b). The expansion of the built environment behind coastal defenses can strengthen the trap and its negative consequences, making disaster-risk reduction increasingly difficult to achieve.

1.2.4 The recipe for disaster

Despite advancements in scientific knowledge, increased investment in hazard mitigation, and improved disaster response, the costs associated with natural disasters continue to rise (Mileti, 1999). Between 2000 and 2019, natural hazards affected over 4 billion people worldwide (many being impacted multiple times) and caused economic losses of approximately US$ 2.97 trillion (CRED and UNDRR, 2020). This is a substantial increase compared to the two decades prior (1980-1999), during which natural disasters impacted over 3 billion people and resulted in economic losses totaling about US$ 1.63 trillion.

Although these escalating costs have been partially attributed to climate change and the subsequent intensification, in frequency and magnitude, of extreme weather events (Batibeniz et al. 2020; Herring et al., 2020; Seneviratne et al., 2021; Van Aalst, 2006), mounting evidence suggests that increased exposure due to population growth and continued development in hazard-prone areas is largely contributing to these losses (Ashley and Strader, 2016; Ashley et al., 2014; Cutter and Emrich, 2005; Iglesias et al., 2021; Lazarus et al., 2018). Thus, to effectively assess the potential of future natural disasters and minimize their impact on society, it becomes essential to recognize the interaction between physical and social environments, as damages resulting from human-driven extremes may be outweighed by the damages caused by increased exposure in hazard-prone areas (Janković and Schultz, 2017).

1.2.4.1 The expanding bull’s-eye effect

The connection between the rising frequency and severity of disasters and the continuous expansion of the built environment over time can be easily understood through the lens of the *expanding bull’s-eye effect* (Ashley et al., 2014; Strader and Ashley, 2015). This framework uses the analogy of an archery target, in which the population and their assets represent the rings of the target and hazard events are depicted as arrows. As the rings of the target enlarge over time, the likelihood of arrows hitting an inner ring increases.

Accordingly, as populations and the built environment continue to expand, the probability of a hazard impacting developed land and causing a disaster that affects a larger number of people and assets also increases (Ashley and Stradler, 2016). The illustration provided by Strader and Ashley (2015) in **Fig. 1.4** showcases the occurrence of the expanding bull's-eye effect in a hypothetical location (A) and in Wichita, Kansas (B) from 1950 to 2100, using a tornado scenario as an example of natural hazard.

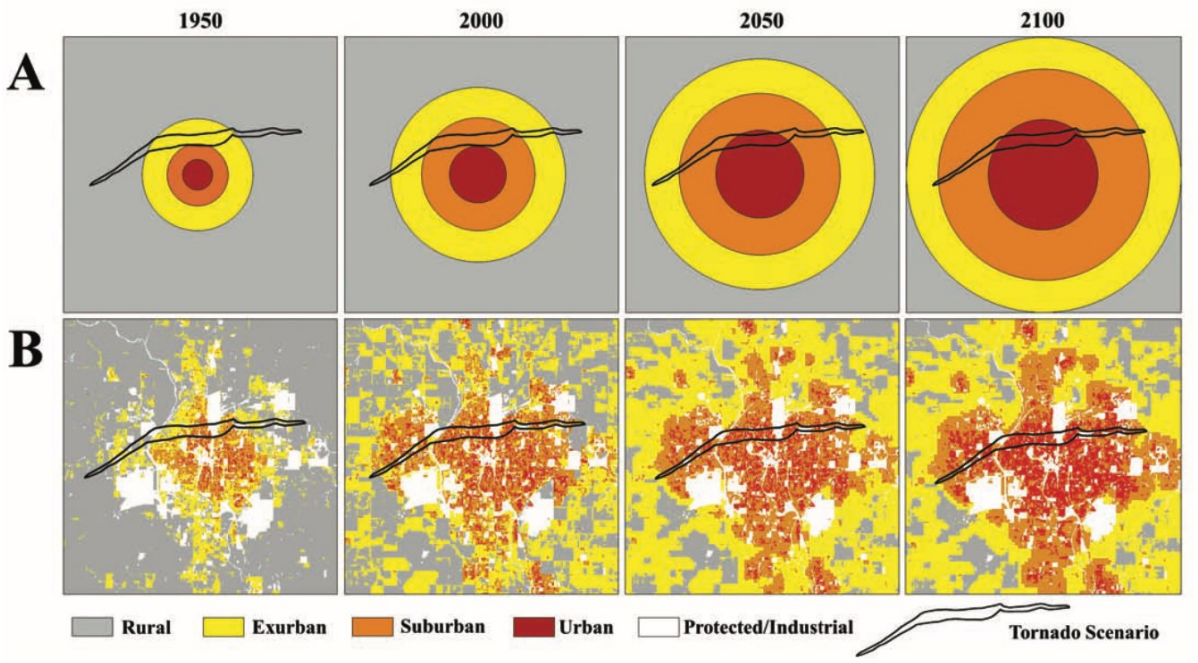

Figure 1.4 Illustration of the expanding bull's eye effect. Image retrieved from Strader and Ashley (2015).

If future development patterns remain similar to current trends, it becomes evident that the persistent growth of the population and assets could have significant implications for developed areas, resulting in increased susceptibility to disasters. When coupled with a hazardous landscape that is potentially being reshaped by climate change, the expanding bull's-eye effect suggests that there is a heightened risk of future disasters, which could be more frequent and severe than ever before (Strader and Ashley, 2015).

1.2.4.2 Escalating exposure in hazard-prone zones

While increasing exposure has been recognized as a major contributor to long-term growth in economic losses from natural disasters (Cutter and Emrich, 2005; Iglesias et al., 2021; Lazarus et al., 2018), empirical evidence consistently underscores an ongoing pattern of population expansion and urban development within physically vulnerable regions (Ashley and Strader, 2016; Braswell et al., 2022; Chen et al., 2019; Iglesias et al., 2021; McGranahan et al., 2007; Nicholls and Small 2002; Rentschler et al., 2023). Recent research demonstrates that human settlements have rapidly expanded in hazard-prone zones around the world over the last decades, consistently outpacing the growth in areas safe from natural

disasters (Braswell et al., 2022; Chen et al., 2019; Ehrlich et al., 2018; Iglesias et al., 2021; Lazarus et al., 2018; Rentschler et al., 2023). Global estimates for 2015 reveal that about 20% of all built-up areas on Earth are located in regions facing medium to high risk from flooding, and at least 11.3% are at high or very high risk of flood hazards (Rentschler et al., 2023). This exposes over one billion people and approximately 80,000 square kilometers of developed area to the risk of floods with a 100-year return period (Ehrlich et al., 2018). Similarly, almost one-third of the world's population and urbanized land are located in areas prone to potentially destructive earthquakes, one billion individuals live in regions at risk of Category 1 and 2 cyclone winds, and around 600 million are exposed to Category 3 storms or higher (Ehrlich et al., 2018). Sea-level surge, primarily impacting low-lying coastal areas prone to cyclones, also has the potential to affect approximately 160 million people and 25,000 square kilometers of developed land. Overall, these figures indicate a significant increase compared to previous decades, with both population and developed areas more than doubling over four decades (Ehrlich et al., 2018; Rentschler et al., 2023).

The global trend toward increased development in hazard-prone regions is especially evident in countries like China, where the urbanized area more than doubled between 1995 and 2015 (Chen et al., 2019). By the end of this period, approximately 80% of the population, 77% of developed land, and 68% of cropland are located in areas susceptible to at least one type of natural hazard, while around 4% of the population, 3% of built-up land, and 3% of cropland face exposure to more than three types of hazards. Likewise, in the United States, a nation that has also experienced sustained population growth and heightened urban development in recent decades, over 57% of the existing buildings is built in locations highly susceptible to hazards (Iglesias et al., 2021). Furthermore, the number of structures concentrated in regions prone to two or more categories of natural hazards substantially increased over the last seven decades, from about 173,000 buildings in 1945 to 1.5 million by 2015.

The generalized intensification of urban development and land utilization in hazard-prone zones has been particularly dramatic in coastal regions worldwide. Compared to inland regions, coastal areas tend to exhibit higher population densities and experience faster population growth and urbanization rates (McGranahan et al., 2007; Small and Nicholls, 2002). In Bangladesh and China, for instance, the population living in low-lying coastal areas expanded at twice the national growth rate between 1990 and 2000, with coastal China experiencing urban population growth rates three times higher than the national average (McGranahan et al., 2007). This surge in coastal population exposure in the most populous nation on Earth can be attributed to long-standing development strategies and trade-oriented economic policies that have actively promoted urbanization and migration toward coastal regions since the early 1980s, resulting in the creation of an urban landscape that consistently attracts people to the coast.

The economic boom driven by readily accessible credit during the late 20th and early 21st centuries also spurred significant growth within the construction sector at a global scale. Real estate played a crucial role during this period, resulting in remarkable spikes in property prices and a significant escalation in new property construction, particularly in coastal areas (Cooper and McKenna, 2009; Perez, 2010). Across Europe, extensive stretches of coastal land were transformed into complexes of apartments, condominiums, and houses, primarily intended for use as vacation homes. In many cases, pre-existing structures, hotels, shops, and residential and commercial buildings were demolished to make space for the construction of new and more valuable coastal housing, giving rise to subsequent environmental and socioeconomic implications (Cooper and McKenna, 2009).

The expansion of coastal built environments was particularly pronounced in popular sun-and-beach destinations across Southern Europe, including Spain, Italy, and Greece. Spain, in particular, emerged as the European Union nation with the highest number of residences per thousand inhabitants and the greatest quantity of second homes (Perez, 2010). Encouraged by the surge in residential and infrastructure development, Spain's construction sector consistently increased its GDP contribution during this timeframe, rising from 6.9% in 1995 to 10.8% in 2006. This growth, in turn, led to the expansion of artificial surfaces, particularly in tourism-oriented municipalities along the entire Mediterranean coast. Similarly, Eastern European countries, benefiting from improved mobility and increased political stability, also saw the expansion of the European second-home market along their coasts, notably along the Black Sea shorelines of Romania and Bulgaria, both northern and southern regions of Cyprus, and newly established Balkan nations (Cooper and McKenna, 2009). Even European coastal regions with typically below-average population and growth rates, and higher levels of deprivation, such as those in Great Britain (Office for National Statistics, 2020), experienced a significant surge in coastal property values over this period, with prices doubling in just a two-year span (Cooper and McKenna, 2009). One remarkable example can be found in Wales, where even modest beach huts without access to water and electricity, and unsuitable for accommodation, saw their prices rise from £20,000 (US$29,000) in 2002 to £28,000 (US$45,000) in 2003, ultimately peaking at £56,000 (US$100,000) in 2004.

This global construction surge, driven by the growing demand for coastal residential properties, left a profound imprint across the globe. In the Middle East, the significant surge in coastal development, primarily targeting foreign buyers, drove the construction of apartments and villas on existing arid land and prompted ambitious engineering projects to create new construction-ready spaces as available land became scarce (Cooper and McKenna, 2009). Similarly, Australia's Gold Coast witnessed extensive development of apartment blocks aimed at a global market on narrow sand barriers with limited space, resulting in a vertical expansion in real estate. In the United States, the significant expansion in developed coastal land and housing stock experienced in recent decades has also led to

coastal communities with denser and more intensively developed built environments compared to inland areas (Braswell et al., 2022). Together, these examples demonstrate that most coastal areas around the world have undergone significant changes and development over recent decades, despite the looming challenges derived from natural disasters. Even amid the compounded risks posed by climate change, this transformation is projected to persist in the future (Neumann et al., 2015).

1.2.4.3 Building back bigger in hazard-prone zones

Escalating exposure to natural hazards goes beyond population growth or the mere proliferation of structures. When communities rebuild after major disasters, they often undergo transformations rather than simply returning to their previous state. Unfortunately, these changes tend to undermine efforts to mitigate disaster risk, leaving both individuals and their built environments more susceptible to future hazardous events (Burby, 2006; Cutter and Emrich, 2005; Kates et al., 2006; Mileti, 1999). An illustrating example of this phenomenon is observed along the US Atlantic and Gulf coasts, where empirical evidence has shown that the size of buildings, as measured by their footprint, tends to increase during periods of calm between destructive hurricanes (Lazarus et al., 2018). This *building back bigger* pattern is not limited to renovated properties but also extends to new constructions, ultimately leading to heightened levels of development and, consequently, exposure to natural hazards. Recent research reinforces these observations, underscoring that US coastal regions affected by hurricanes have expanded their residential footprint over the last decades and now display more densely developed built environments compared to areas with lower risk (Braswell et al., 2022).

Thus, despite awareness of the risks associated with urban and population growth, as well as the implementation of policies designed to enhance resilience and reduce vulnerability in developed coastal regions, disasters along human-altered coastlines seem to paradoxically result in the expansion of urban areas. The surge in development, in turn, leads to the proliferation of larger residences, denser infrastructure, increased investments, and a higher population density exposed to potential damage from future storms. The phenomenon of urban expansion after catastrophic events, which may be related to the *safe development paradox* and the *levee effect* (McNamara et al., 2023), significantly contributes to the overall growth of built environments in hazard-prone regions, exacerbating the frequency and severity of subsequent disasters.

1.3 Contributions to the literature

1.3.1 Research gap and thesis objectives

The continuous escalation of disaster-related losses is significantly tied to increased exposure resulting from population growth and sustained development within areas vulnerable to hazards (Ashley and Strader, 2016; Ashley et al., 2014; Cutter and Emrich, 2005; Iglesias et al., 2021; Lazarus et al., 2018). This trend highlights the intricate nature of interactions within human-landscape systems, demonstrating that the natural and socioeconomic components of risk are not standalone elements but are deeply interconnected, often in complex and subtle ways. Empirical research exploring connections between risk components often relies on unique case studies, each characterized by specific conditions and dynamics (Di Baldasarre et al., 2018). While these studies may shed light on self-reinforcing feedbacks exacerbating coastal risks, such as the *levee effect* or the *safe development paradox*, their idiosyncrasies pose challenges when attempting to draw generalized conclusions. Consequently, there is a growing need for comparative analyses that seek common patterns across multiple case studies or large-scale analyses that reveal widespread relationships (Collenteur et al., 2015; Di Baldasarre et al., 2018; Schultz and Elliott, 2013).

Conducting research at large scales, however, poses considerable challenges. Data for such extensive studies are often fragmented, spread out across various organizations, restricted by ownership or confidentiality constraints, or in some cases, completely inexistent (Lazarus et al., 2021). For instance, prior investigations in England and Wales have conducted comprehensive assessments of exposure and vulnerability to coastal hazards like flooding and erosion at a large scale (Rözer and Surminski, 2020; Sayers et al., 2018). Yet, these studies relied on proprietary or inaccessible datasets, such as the “National Receptors Database”, developed by the Environment Agency but based on Ordnance Survey data (OS “AddressBase Premium” dataset), or the “AddressBase Premium” database, imposing limitations on replicability and further analyses. Similarly, while earlier studies have explored the connection between coastal development and hazard protection, particularly in the context of beach nourishment (McNamara and Werner, 2008a, 2008b; McNamara et al., 2015; Smith et al., 2009), only one empirical study directly compares development patterns in protected and non-protected areas at a large scale (Armstrong et al., 2016). Constrained by data limitations, however, this work could only provide a spatial snapshot of the spatial characteristics of the built environment at the time of the assessment and had to rely on indirect metrics to infer property wealth.

In a similar vein, previous research has delved into the intricacies of fragile coastal systems like barrier islands, which serve as prime examples of tightly coupled human-landscape

systems (Lazarus et al., 2016; Lazarus & Goldstein, 2019; McNamara et al., 2015; McNamara & Keeler, 2013; McNamara & Werner, 2008a, 2008b; Nordstrom, 1994, 2004). Still, they have not directly addressed critical infrastructure networks, such as roads and public utilities, despite their indispensable role within the built environment. Road networks, for example, connect physical spaces and support the well-being and quality of life of our societies (Jennelius and Mattson, 2012). Frequently, as seen on the barrier islands of the United States, roads are essential for the transport of people and goods, and play a vital role in evacuation processes, emergency responses, and recovery operations following disasters (Anarde et al., 2018; Darestani et al., 2021; Frazier et al., 2013; Godschalk et al., 1989; Velasquez-Montoya et al., 2021). Thus, considering that the future evolution of developed barrier islands is likely to be deeply affected by both their built environments and the implementation of measures to mitigate hazards, it is crucial to examine their infrastructure networks and identify critical points at which these networks may fail. Understanding potential large-scale disruptions that could compromise the functionality of the entire built environment can help refine management and planning approaches and provide valuable insights into the long-term viability of these vulnerable human-landscape systems.

To overcome these gaps in existing literature, the present thesis aims to bridge theory with data and deepen our understanding of the complex dynamics shaping coastal risk, offering insights into the implications and consequences of these interconnected factors for coastal communities. The primary goals of this study are outlined as follows:

- Examine coastal built environments as interconnected human-natural systems, identifying empirical relationships between their natural and socio-economic components.
- Perform the analysis across large spatial extents, moving beyond the scope of traditional, localized case studies.
- Rely exclusively on publicly available data.

To achieve these objectives, the thesis adopts a comprehensive approach. Chapter 2 conducts an in-depth examination of the complex interplay among the three different elements of coastal risk in England. Chapter 3 builds upon the research initiated by Armstrong et al. (2016) to enhance our comprehension of the dynamic relationship between coastal development patterns and the protective mechanisms offered by beach nourishment. This extended investigation introduces a temporal dimension, facilitating a thorough examination of these dynamics over time, and includes the assessment of actual property values. Chapter 4 recognizes the importance of critical infrastructure, particularly road networks, within the broader context of the built environment, and aims to explore thresholds at which these networks fail when confronted with potential coastal flooding scenarios. Collectively, this research makes a substantial contribution to a more holistic understanding

of the intricate interplay between infrastructure and coastal risk, as well as the potential repercussions for susceptible built environments.

1.3.2 Data and methods

This thesis conceives coastal built environments as complex systems in which human interventions and natural processes are deeply intertwined. Recognizing that this interaction can increase the risk and severity of disasters, a notion supported by prior research, risk components—hazard, exposure, and vulnerability—are considered as interdependent variables rather than isolated factors. Thus, through the collection and analysis of datasets representing these elements, this work seeks to identify interactions and feedback mechanisms that might amplify coastal risk.

The research deliberately extends its scope beyond the confines of traditional, narrowly focused case studies, towards broader spatial scale analyses. This approach stems from the recognition that while case studies yield detailed, context-specific insights, examining data across larger geographical extents is crucial for achieving the generality needed to formulate meaningful, overarching conclusions. Hence, the datasets selected for this thesis are primarily chosen—though not solely—for their extensive scale, leading to the dismissal of potentially suitable datasets that do not offer the required coverage. Integral to this thesis is also the commitment to rely exclusively on open-access data. This approach is driven not just by financial constraints but also by a firm belief in the benefits of open data for promoting accessibility and transparency, fostering collaborative research, and stimulating the development of innovative solutions for societal challenges.

However, sourcing open-access data for large-scale analysis may be significantly more challenging than for localized case studies. This difficulty became apparent early on, particularly during the analysis detailed in Chapter 2. Initially, this study aimed to investigate temporal trends of coastal development in the United Kingdom and compare these with historical coastal defense efforts, aiming to uncover signs of the safe development paradox at a national scale. Unfortunately, the original scope of this research was significantly limited by the absence of comprehensive historical data on coastal defenses and difficulties in accessing historical records of building developments on the required scale. Consequently, after the completion of this chapter, the focus of the research shifted towards the United States, where the data required for a thorough examination at large scales seemed more accessible. This strategic move, though originally unplanned, proved beneficial, facilitating a comparative analysis between the distinct yet similarly at-risk regions of England’s open coast and the Atlantic and Gulf Coasts of the US.

Considering the spatial dimension and significant volume of the datasets acquired, this dissertation extensively used Geographic Information Systems (GIS) tools to investigate

spatial relationships among the variables under study. In the initial phases, specifically for Chapters 2 and 3, the research predominantly relied on the ESRI platform, particularly ArcMap 10.7, due to its user-friendly interface and robust spatial analysis features. For statistical analysis and the creation of graphs, Matlab was the primary software, whereas R was used mainly for data cleaning tasks in Chapter 3. The rationale behind using these two programming languages was twofold: the requirements of these sections of the thesis did not necessitate specialized software, and there was a personal interest in evaluating the potential of both tools.

The particular needs of the analysis presented in Chapter 4, however, required a transition to Python. This phase of the study involved extracting road networks from OpenStreetMap, for which the Python library OSMnx (Boeing, 2017) was particularly well-suited. Consequently, the research methodology for this final part of the thesis was reoriented to fully leverage the Python ecosystem, taking advantage of its comprehensive range of libraries for analyzing network connectivity and processing geospatial data. The Python environment was not only intuitive and efficient for this specific study but also appears to be exceptionally well-suited for any research involving geospatial data. The use of Jupyter notebooks enhanced the clarity and organization of the analytical workflow beyond what is typically achievable with ArcGIS, while the ability to share methodologies via GitHub repositories greatly improved the reproducibility of the work and the dissemination of its findings.

Before examining the specific papers that constitute this thesis, the subsequent section provides an overview of the driving motivations for each piece of research included in this work.

1.3.3 Research papers

1.3.3.1 Chapter 2: Exploring spatial relationships between coastal hazards, population exposure, and social vulnerability in England [Unpublished manuscript]

Coastal regions in England hold significant historical and environmental value and serve as vital hubs for economic and social activities. However, these areas also face substantial physical hazards, with coastal flooding and shoreline erosion identified as the primary climate-related risks affecting communities, businesses, and infrastructure (CCC, 2016). Compounding these challenges, coastal communities in England and the broader UK tend to exhibit distinct characteristics, including aging populations, geographic and social isolation, poor-quality housing, higher unemployment levels, and lower salaries (Zsamboky et al., 2011). Such features make them more susceptible and less resilient to hazardous events, which climate change is expected to intensify in the coming decades (Ramsbottom et al., 2012). Moreover, given the considerable financial burden associated with coastal risk

mitigation (Environment Agency, 2018; Penning-Rowsell, 2015; Priestley and Allen, 2017), continued investment in existing coastal infrastructure along the English coastlines becomes increasingly impracticable (CCC, 2018). Consequently, to reduce the human and economic toll of future hazard events, it is vital to thoroughly evaluate the interconnections among the fundamental risk elements—hazards, exposure, and vulnerability (Crichton, 1999)—instead of treating them in isolation. As such, Chapter 2 aims to assess potential linkages between the physical and social facets of coastal risk along the exposed coastline of England.

To investigate relationships between the three components of risk, we gather and analyze a range of publicly accessible datasets on coastal hazards (flood probability and long-term shoreline change), exposure (population and building data), and vulnerability (social disadvantage and presence of engineered coastal defenses). By examining these variables and their interconnections, the primary goal is to identify national-scale spatial patterns that allow us to draw comparisons with similar large-scale studies on coastal risk (e.g., Armstrong and Lazarus, 2019a, 2019b) and derive broader conclusions that transcend the specific details typically associated with conventional case studies (Schultz and Elliott, 2013; Collenteur et al., 2015; Di Baldasarre et al., 2018). Nevertheless, due to certain data limitations (which are elaborated further in Lazarus et al., 2021 and summarized in Chapter 5 of this thesis), the analysis primarily focuses on the spatial dimension, offering a snapshot of the prevailing conditions during the study period, rather than capturing their temporal dynamics (Armstrong and Lazarus, 2019a).

1.3.3.2 Chapter 3: The revalorizing effect of beach nourishment [Unpublished manuscript]

Between 1960 and 2019, natural disasters in the United States resulted in more than 250,000 injuries (252,361) and almost 35,000 fatalities (34,933), leading to significant direct losses totaling $1,143.9 billion for both properties ($946.3 billion) and crops ($197.6 billion) (CEMHS, 2022). These rising costs from natural disasters have been largely attributed to continuous population growth and the expansion of the built environment in high-risk areas (Ashley et al., 2014; Cutter and Emrich, 2005; Lavell, 2012). Indeed, recent assessments indicate that the number of buildings exposed to natural hazards in the United States has consistently risen over the last decades, so that, in 2015, more than half of the existing structures were located in areas prone to floods, tornadoes, hurricanes, wildfires, or earthquakes; and approximately 1.5 million buildings lied in the intersection of two or more hazard hotspots (Iglesias et al., 2021).

Surprisingly, regions historically prone to catastrophic events have also witnessed substantial increases in urban development density, often surpassing average trends (Braswell et al., 2022; Iglesias et al., 2021; Lazarus et al., 2018). Coastal areas, for example, face chronic erosion, frequent storm impacts, and rising sea levels, all of which are anticipated to worsen

due to climate change (Nicholls and Cazenave, 2010; Hinkel et al., 2014; McNamara et al., 2015). Yet, despite extensive regulatory efforts to decrease their vulnerability, US hazard-prone coastlines continue to experience population growth and escalating building density, often surpassing trends observed inland (Braswell et al., 2022; Lazarus et al., 2018). Thus, although coastal counties represent just 17% of the total land area, they accommodate more than half of the country's population (Crossett et al., 2004, 2013) and a disproportionate number of high-value properties (Nordstrom, 2004).

This chapter aims to investigate underlying dynamics that may be contributing to the continued urban development experienced in hazard-prone coastal areas across the United States. Specifically, it examines potential relationships between beach nourishment, a popular form of hazard protection, and the escalating exposure of valuable infrastructure. To achieve this, we use extensive housing data encompassing both structural and economic information about residential properties, along with the locations of historical beach nourishment projects, to compare spatial development patterns in nourishing versus non-nourishing areas.

While previous research (Armstrong et al., 2016) has delved into these dynamics, Chapter 3 of this thesis builds upon and expands prior findings by addressing their limitations. Privacy and financial constraints make access to high-quality, comprehensive property-scale data challenging, if not unfeasible (Lu et al., 2013). As a result, prior research often depended on surrogates for estimating house size (Lazarus et al., 2018) or evaluating relative property wealth (Armstrong et al., 2016). Moreover, due to the absence of temporal data in many publicly available datasets, the study and depiction of the built environment typically remained static, reflecting conditions at the time of assessment (Armstrong et al., 2016). Conversely, the tax records used in this investigation contain a comprehensive set of attributes, encompassing details such as total living area, sale date, and sale price. These details enable an analysis that can account for both spatial and temporal variations in the size and value of coastal residential properties. Additionally, to increase the reliability of the results and circumvent the potential for drawing overly narrow conclusions based solely on a specific case study (Di Baldasarre et al., 2018), the analysis encompasses two well-recognized large-scale coastal risk hotspots in the United States: the barrier islands of New Jersey and the Atlantic and Gulf Coast of Florida.

1.3.3.3 Chapter 4: Thresholds in Road Network Functioning on US Atlantic and Gulf Barrier Islands (Aldabet et al., 2021)

There is an increasing recognition of the significant costs imposed on societies by natural disasters and climate change, not only in terms of infrastructure damage but also through the disruption of essential services provided by these systems (Hallegatte et al., 2019). In low-lying environments, coastal hazards pose a particular risk to critical infrastructure systems,

including road networks, which are highly sensitive to climate-related events that exceed their design standards (Markolf et al., 2019; Suarez et al., 2005).

Dynamic coastal features such as the barrier islands of the US are particularly exposed to storm-driven flooding and sea-level rise, which climate change will only exacerbate (Moser et al. 2012; Seneviratne et al., 2021; Williams, 2013; Wong et al., 2014; Zhang and Leatherman, 2011). Unforeseen road network disruptions—mechanisms that cause reductions in mobility or increases in the costs necessary to maintain the desired levels of mobility (Markolf et al., 2019)—are not uncommon during hurricanes, tropical storms, and nor'easters (Dolan and Lins, 2000; Nordstrom, 2004; Nordstrom and Jackson, 1995; Spanger-Siegfried et al., 2014; Velasquez-Montoya et al., 2021). But not only catastrophic—and relatively infrequent—events have the capacity to cause extensive structural failure in these areas. Frequent small-magnitude events such as those caused by high tides, often called nuisance flooding, can also compromise the functionality of the transportation network, rendering roads impassable or hazardous for hours (Jacobs et al., 2018; Moftakhari et al., 2015; Spanger-Siegfried et al., 2014; Suarez et al., 2005). On certain barrier islands, tidal flooding is a recurring event, particularly during spring high tides, and there has been a significant increase in the frequency, depth, and extent of nuisance flooding along the coastlines of the US over the past few decades (Crossett et al., 2013; Moftakhari et al., 2015; Spanger-Siegfried et al., 2014; Sweet and Park, 2014). In low-lying coastal areas, even minor increases in sea level have the potential to amplify flood heights linked to meteorological or tidal events (Buchanan et al., 2017), and induce coastal flooding in regions that were previously only affected by severe events like hurricanes or major storm surges (Sweet and Park, 2014). As sea levels continue to rise and storms become more frequent and severe, the likelihood of flood-related disruptions to road networks is expected to increase not only in regions traditionally impacted by these events but also in areas located further inland (Jacobs et al., 2018; Spanger-Siegfried et al., 2014).

In the US, road networks play a central role in facilitating transportation and mobility within developed barrier islands, serving as the primary means for people and goods to reach their destinations and enabling effective hazard evacuation, emergency response, and recovery operation during and after catastrophic events (Anarde et al., 2018; Darestani et al., 2021; Frazier et al., 2013; Godschalk et al., 1989; Velasquez-Montoya et al., 2021). Thus, road network disruptions can have significant socio-economic impacts on affected communities, isolating neighborhoods, hindering evacuation efforts, and impeding access to critical services (Balomenos et al., 2019; Dong et al., 2020; Jenelius and Mattson, 2012; Spanger-Siegfried et al., 2014; Suarez et al., 2005). They also incur significant opportunity costs, including lost time, discomfort, and foregone earnings (He et al., 2021).

To tackle these challenges and minimize or potentially eliminate such disruptions, network criticality analysis can help identify specific components of road infrastructure that require targeted maintenance or investment. This is particularly relevant in situations where resources for adaptation are limited, and targeted actions can have a significant impact on mitigating the effects of increasingly frequent disturbances. Thus, the main objective of this research is to investigate—using open-access data sets—the robustness of road networks in the US Atlantic and Gulf barrier islands to disturbance from extreme high-water events and identify critical physical locations that, if disrupted, could lead to the complete functional failure of the entire island road network. For that, we analyze the road infrastructure of 72 barrier islands, representing each network as a graph of nodes and edges. By systematically removing nodes, starting from the lowest elevation, we identify the critical node where network functionality is compromised. We then link the elevation of this critical node to the local annual exceedance probability curves to assess their likelihood of coastal flooding. Additionally, we assess the overall robustness of each barrier network to provide a comprehensive measure of network performance beyond the specific critical threshold. Examining thresholds in network functioning represents a fundamental step in enhancing our understanding and foresight regarding the future trajectory of these fragile, human-altered coastal environments.

Chapter 2 Paper 1: Exploring spatial relationships between coastal hazards, population exposure, and social vulnerability in England

This manuscript is currently in progress and undergoing review with the respective coauthors. We anticipate making minor to moderate adjustments and revisions before its publication.

Initial authors: Aldabet S., Lazarus E.D., Nicholls R.J.

Aldabet S. contributed to the investigation, methodology, formal analysis, writing, data curation; Lazarus E.D. contributed to the conceptualization, investigation, methodology, formal analysis, writing, supervision; Nicholls R. J. contributed to the conceptualization, methodology, project administration, funding acquisition.

2.1 Abstract

Coastal flooding and shoreline erosion have been identified as the highest priority climate-driven hazards to communities, businesses, and infrastructure in the UK. Risk can be defined as a function of hazard, exposure, and vulnerability. Each component may vary independently, or they may be linked – perhaps in unexpected ways. Understanding relationships between components of risk is necessary for reducing the human and economic costs of hazard events. Here, we use publicly available datasets and GIS techniques to investigate indications of relationships between coastal hazard, population exposure, and social vulnerability along the open coast of England. We identify a large-scale spatial pattern in the national risk profile indicative of a social disparity in exposure to coastal hazard, where zones of especially high coastal hazard tend to coincide with areas of high social vulnerability.

2.2 Introduction

Coastal floodplains (below 10 m elevation) support approximately 10% of the world's population and disproportionately more of the global GDP (McGranahan et al., 2007; Wong et al., 2014), along with the world's largest and fastest-growing cities (Aerts et al., 2014). In recent decades, low-lying coastal zones have experienced intense development and occupation—a trend that is expected to continue in the future (Neumann et al., 2015), even as sea-level rise and land-use pressures on coastal floodplains are making coastal hazards

more frequent, more severe, more economically costly, and more difficult for conventional hazard defenses to mitigate (Aerts et al., 2014; McGranahan et al., 2007; Vitousek et al., 2017; Vousdoukas et al., 2017; Wong et al., 2014).

In the United Kingdom, coastal areas embody legacies of historical and environmental heritage and host vital economic and social activities. Approximately 30 million Britons live in coastal cities, and 40% of the industry and 60% of the most fertile agricultural land are located in areas near the coast; port trade, fishing, and recreational tourism also contribute significantly to national, regional, and local economies (Zsamboky et al., 2011). But the UK coastal zone also entails significant physical hazards. Coastal flooding and shoreline erosion have been identified as the highest priority climate-driven risks to communities, businesses, and infrastructure in the country (CCC, 2016). Climate change is expected to exacerbate coastal flooding and shoreline erosion in the coming decades (Ramsbottom et al., 2012). Extreme sea levels resulting from a combination of sea-level rise, astronomical tides, and episodic water fluctuations (waves and storm surges), will likely increase by the end of the century (Vousdoukas et al., 2017).

Managing such coastal flood and erosion risk already carries a heavy financial burden: £250–320M annually (Penning-Rowsell, 2015; Priestley and Allen, 2017), or double that in a major storm season (Environment Agency, 2018). Recent reports to the UK Government on flood risk (Priestley and Allen, 2017) have highlighted the need for more maintenance spending on flood protection, efficiency savings to offset costs of new defenses, and “value for money” analysis of flood protection at local scales. In England alone, a national assessment by the UK Committee on Climate Change (CCC, 2018; Jacobs 2018) estimates that more than 500,000 properties (of which 370,000 are residential) are currently located in the 200-year floodplain, meaning that they are exposed to 0.5% or greater annual risk of coastal flooding. Modeling suggests that by the 2080s, this total could increase to 1.5 million properties (1.2 million residential) in the absence of defenses (CCC, 2018; Jacobs, 2018). Furthermore, coastal erosion might affect more than 100,000 properties by the 2080s if current coastal defenses failed or were abandoned. The assessment emphasizes that roads, railways, and other infrastructures might also be seriously threatened by coastal flooding and erosion, along with historic landfill sites and significant areas of designed land that host rich ecosystems and productive natural resources (CCC, 2018; Jacobs, 2018).

Reducing human and economic costs of future hazard events requires not only a clear accounting of the primary components of risk—hazard, exposure, and vulnerability (Crichton, 1999)—but also of how these primary components may be systematically related to each other. Having assembled a portfolio of publicly available datasets of coastal hazard, exposure, and social vulnerability in the UK, here we explore potential relationships between physical and social components of coastal risk along the open coastline of England. Our

analysis is spatial, not temporal, reflecting a snapshot of current circumstances but not their evolution (Armstrong and Lazarus, 2019b). Our findings bear on active UK national policy measures intended to improve coastal resilience under climate change.

2.3 Background

Initial coastal-protection works in the UK had military or industrial purposes, but population growth and increasing economic dependence on recreation and tourism encouraged the propagation of hazard defenses along much of the coastline. Seawalls and other hard structures were constructed intensively until the 1960s, when the study of coastal processes motivated alternative, “soft-engineering” strategies, such as beach nourishment, which involves importing sand to replenish an eroding beach (Fleming, 1992; Nicholls et al., 2013). Through the 1970s and 1980s, coastal hazard was regarded as a problem best managed at a local level. However, the resulting patchwork of interventions exacerbated down-drift erosion and contributed to beach lowering, driving an overall deterioration of coastal environments (Leafe et al., 1998). An integrated perspective of coastal dynamics showed the need for a more regional approach to managing coastal hazards (Nicholls et al., 2013). One of the first strategic assessments of sea defenses was the Anglian Sea Defence Management Study, which examined 300 km of open coast in the east of England (Leafe et al., 1998). An early application of Geographical Information System (GIS) techniques, the study provided a better understanding of the coastal behavior and initial recommendations for the management of the coast (Townend et al., 1990). The English and Welsh governments subsequently prepared national guidance to define management units along the coast considering natural processes, coastal defenses, current and future land uses, and planning and environmental concerns (Cooper et al., 2002). Based on broad patterns of sediment transport, the national coastline was divided into 11 cells and 46 sub-cells—boundaries that later informed the Shoreline Management Plans that exist today (Cooper et al., 2002; Leafe et al., 1998; Nicholls et al., 2013). Shoreline Management Plans are non-statutory, large-scale, and long-term strategic plans that aim at reducing the impacts of coastal flooding and erosion on population, infrastructures, and natural environments (Cooper et al., 2002). The second generation of Shoreline Management Plans, developed between 2006 and 2011, consider a 100-year management framework and three different timescales: short-term or Epoch 1 (2005–2025); medium-term or Epoch 2 (2026–2055); and long-term or Epoch 3 (2056–2105). The 22 Shoreline Management Plans that extend the length of the coastline of England and Wales are subdivided into nearly 2000 Policy Units, of which 1,523 are in England. Each Policy Unit is designated with one of four strategic coastal-defense options (Defra, 2006; Nicholls et al., 2013):

- *Advance-the-Line* (ATL): implementation of new defenses on the seaward side of the current defense line to reclaim land.

- *Hold-the-Line* (HTL): maintenance or upgrade of existing defenses in their current location.
- *Managed Realignment* (MR): natural realignment of the shoreline (backwards or forwards) with management to control or limit the movement. This could involve building new defenses on the landward side of the original ones.
- *No Active Intervention* (NAI) or “do nothing”: cease investment in the maintenance of coastal defenses, allowing the shoreline to evolve naturally.

Most of the Shoreline Management Plans suggest landward realignment or abandonment of hazard defenses along hundreds of kilometers of coastline within the next 50 years. Implementation is estimated to cost around £18–30 billion (CCC, 2018). However, the non-statutory nature of Shoreline Management Plans makes them subject to political decisions and funding allocation, and reaches of the coast designated as *Hold-the-Line* may not have the resources necessary to carry out the strategic recommendations. Therefore, abandonment of coastal defenses or failures in these systems is expected to occur over the next decades, increasing overall vulnerability to coastal flooding and erosion.

Furthermore, because personal, social, and environmental factors influence social vulnerability, not all communities share the same capacity to respond to environmental hazards (Zsamboky et al., 2011). A person’s biophysical characteristics, such as age or health, can affect an individual’s sensitivity to a negative hazard-related event. The elderly, children, people with chronic illness, and people who are homeless tend to be the most susceptible to hazard-related harm. Factors that relate to the built environment and physical geography in which people live may enhance their exposure to environmental hazards: for example, people living at ground level or in basements are more likely to experience the worst flooding effects. Also, neighborhoods with poorly maintained drainage systems or with no green or blue infrastructure, which helps mitigate water runoff, tend to face greater damage. Adaptive capacity – the ability to prepare, respond, and recover from disasters – is further influenced by factors such as income, insurance, social networks, and local knowledge (England and Knox, 2014; Lindley et al., 2011).

In the UK, coastal communities are characterized by aging populations (due to youth out-migration and immigration of older people and retirees), geographic and social isolation, poor-quality housing, higher unemployment levels, and lower salaries (Zsamboky et al., 2011). They are thus considered more susceptible and less resilient to hazardous events such as coastal flooding and erosion. Low-income residents are the most vulnerable, since circumstances tend to steer them into settings more prone to hazard impacts (McGranahan et al., 2007), and they are less likely to have insurance or resources to prepare for, or recover from, disaster events (England and Knox, 2014).

Risk may also concentrate in disaster-prone places for reasons other than high social vulnerability. Disaster-risk reduction and adaptation to climate-driven hazards are now a global priority (UNISDR, 2015; Vousdoukas et al., 2017; Wong et al., 2014), but for decades disaster science has been troubled by a paradoxical trend: despite more comprehensive understanding of disaster events, more investment in hazard mitigation, and improvements in disaster response, the economic costs of environmental disaster events continue to rise (Burby, 2006; Mileti, 1999; Tobin, 1995). If risk is, in general terms, a function of hazard, exposure, and vulnerability, then a change in any one of these variables has a direct effect on risk overall (Crichton, 1999). Natural environmental phenomena are considered hazards where human communities or environmental resources that people use are threatened by potential damage associated with these events, and hazard is represented in terms of the likelihood of occurrence (Lavell et al., 2012). Exposure may refer to people, infrastructure, and socioeconomic and environmental assets that are subject to potential damage or loss in the event of a hazard occurrence. Vulnerability describes the level of predisposition of exposed people and infrastructure potentially affected by the hazard, and the value of these (non-human) assets (Lavell et al., 2012; Leuttich et al., 2014). A growing body of research suggests that the components of risk do not necessarily function as independent variables, and instead may be linked in unintended ways (Armstrong and Lazarus, 2019a, 2019b; Armstrong et al., 2016; Brody et al., 2008, 2007; Burby, 2006; Di Baldassarre et al., 2018, 2013; Hutton et al., 2019; Kates et al., 2006; Lazarus et al., 2018; Mileti, 1999; Tobin, 1995; White, 1945). For example, the installation of engineered defenses against hazards can have the counterproductive, if unintentional, effect of encouraging development in hazard-prone areas by conveying a false sense of safety. This dynamic is known as the *levee effect* (Tobin, 1995; White, 1945) or the *safe-development paradox* (Burby, 2006). When a hazard event occurs that exceeds the defense design standards, or if the defenses go unmaintained, the resulting losses are even higher than they might have been otherwise, given the increased exposure of population and assets behind the defenses (Di Baldassarre et al., 2018; Tobin, 1995).

To investigate potential indications of interdependence between physical and social components of coastal risk at a national scale in England, we assembled and analyzed a portfolio of publicly available spatial datasets for coastal hazard (flood likelihood, long-term erosion), population, buildings, social vulnerability, coastal defenses, and policy zones of shoreline-management plans. While components of risk may vary considerably across local scales (i.e., individual communities and/or multi-km segments of coastline), we identify some collective patterns in spatial relationships among components of risk that do emerge at the national scale. The patterns that we find set up comparisons to similar analyses of coastal risk elsewhere, such as along the Atlantic Coast of the USA (Armstrong and Lazarus, 2019a, 2019b), and help frame new questions for the next generation of policy instruments for shoreline management in the UK.

2.4 Data and Methods

2.4.1 Definition of the coastal zone

While representing the coast as a one-dimensional line is cartographically convenient, it fails to capture the significant landward aspects of coastal processes and environments. The challenge in defining the coastal zone lies in its varying inland reach, which is not consistently delineated across studies (Thumerer et al., 2000), leading to a lack of a globally recognized definition (Small and Nicholls, 2003). Definitions of the coastal zone differ dramatically between countries—for example, Denmark includes regions up to 3 km inland within its coastal zone (Lavalle et al., 2011), while Spain limits it to areas within 500 m of the shoreline (Balaguer et al., 2008). Synthesis by the Intergovernmental Panel on Climate Change (Wong et al., 2014) has relied on the Low-Elevation Coastal Zone (McGranahan et al., 2007), which includes coastal terrain under 10 m in elevation, although this measurement is highly dependent on the digital terrain model used (Lichter et al., 2011). With such varying criteria including elevation (McGranahan et al., 2007; Thumerer et al., 2000), proximity (Lavalle et al., 2011), or a combination of both (Small and Nicholls, 2003), defining the coastal zone remains complex. In this study, we identify the coastal floodplains as a more accurate representation of coastal hazard zones than simply using a fixed inland distance from the shore.

We define the coastline using the “Shoreline Management Plan Mapping” dataset, available from the UK Environment Agency (Environment Agency, 2019e). This polyline layer demarcates the national land-ocean interface and identifies the strategic policies recommended for each stretch of the coast. The “Flood Map for Planning (Rivers and Sea)” datasets provided by the Environment Agency (Environment Agency, 2019a, 2019b) supply the polygons for England’s coastal floodplains. These layers show potential flooding extent, assuming that defenses are absent, and provide information on the flood type (coastal, fluvial, or tidal). Yet, it is important to note that they are primarily based on modeled data, making them indicative rather than precise for specific locations. Additionally, they exclude other sources of flooding not directly related to river or sea flooding, such as high groundwater, overland runoff, or infrastructure failures. Thus, while the datasets provide a general overview of flood risks to areas of land, they lack the granularity needed to properly assess individual property risks due to the absence of information on property flood levels and flood characteristics such as depth, speed, or flow volume. In this analysis in particular, we focus on areas identified within “Flood Zone 3” (indicating a 0.5% or higher chance of annual flooding from the sea) and “Flood Zone 2” (denoting areas with a 0.1% annual chance of flooding, situated between Zone 3 and lesser risk zones), and specifically select polygons that are either coastal or tidal and intersect with the “Shoreline Management Plan Mapping”

dataset. These selected areas are subsequently dissolved into a single feature representing the coastal floodplain using ArcMap 10.7.

Then, since Policy Units within the “Shoreline Management Plan Mapping” dataset are delineated as polylines and lack a spatial dimension specifying their landward extent, we use the “Euclidean Allocation” tool in ArcGIS 10.7 to parcel the coastal floodplain according to the nearest Policy Unit. This technique effectively assigns a spatial dimension to all Policy Units intersecting the coastal floodplain (1,364 out of 1,523 Policy Units in England), as determined by Euclidean allocation within this floodplain (**Fig. 2.1**). Policy Units themselves vary in alongshore length, from 0.02 to 90.7 km, and the inland extent of our defined coastal zone likewise varies alongshore.

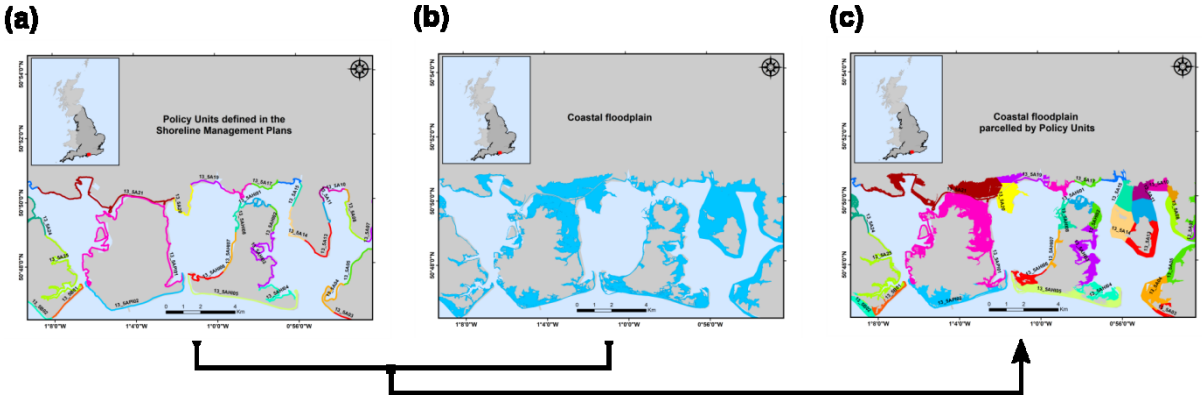

Figure 2.1 Definition of the coastal zone based on coastal floodplains: (a) vectors delineating Shoreline Management Plan Policy Units that intersect (b) the coastal floodplain are given a spatial dimension determined by (c) Euclidean allocation to the nearest coastal-floodplain polygon. This method captures over 3,000 km (~56%) of the total coastline of England.

2.4.2 The components of risk

Following the Risk Triangle model (Crichton, 1999), we represent coastal risk with the expression:

$$R = H \times E \times V$$

where R is coastal risk, H refers to natural hazards, E to exposure, and V to vulnerability. Here, we use erosion and the likelihood of coastal flooding to define the hazards component (H), population and buildings to represent exposure (E), and the type of coastal defenses and a social disadvantage index to describe vulnerability (V).

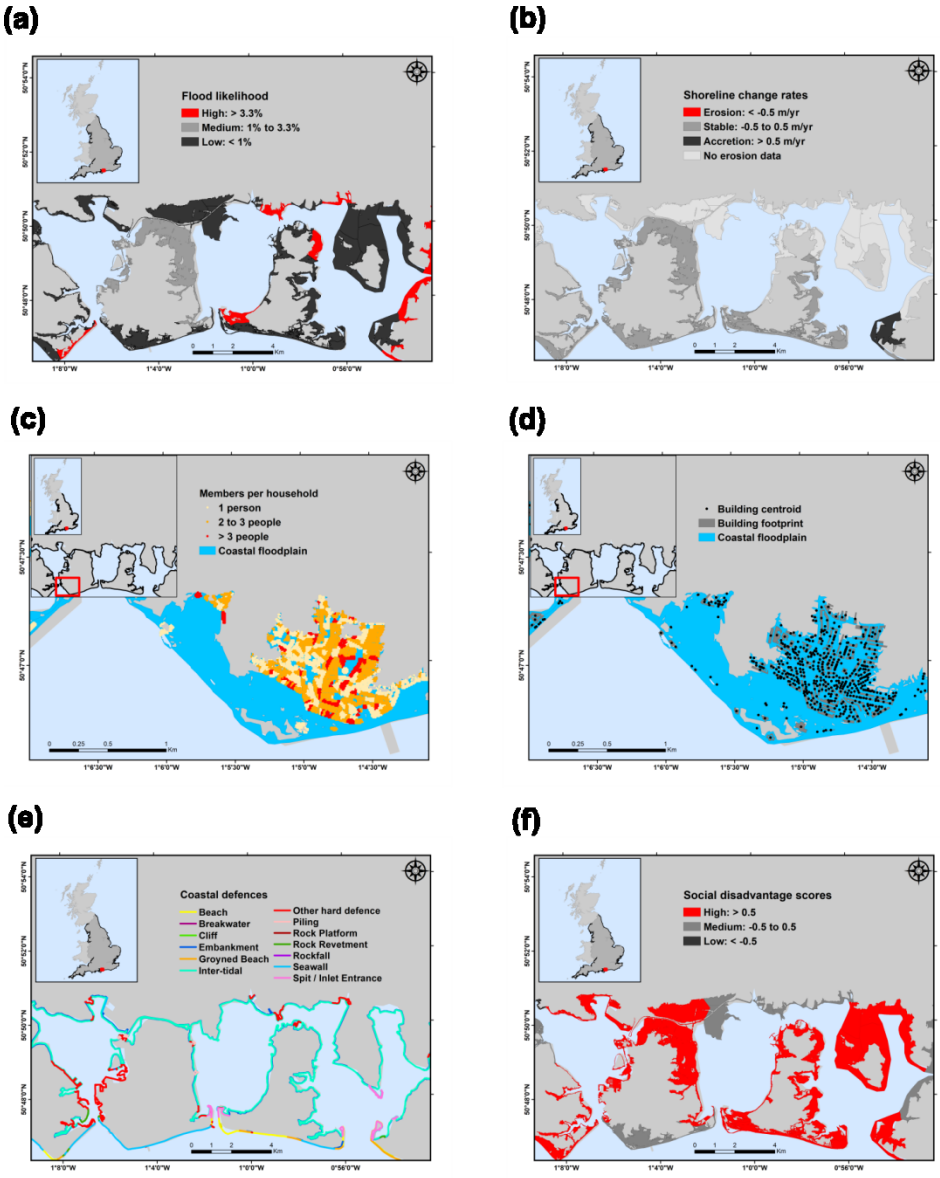

Figure 2.2 Variables used to represent the components of coastal risk: (a) likelihood of flooding and (b) shoreline change represent natural hazards; (c) population and (d) buildings define exposure; (e) coastal defenses and (f) social disadvantage describe vulnerability.

2.4.2.1 Hazards

The likelihood of coastal flooding in each Policy Unit is defined by the “Risk of Flooding by Rivers and Sea” dataset (Environment Agency, 2019d). This dataset evaluates the risk of flooding originating from rivers and/or the sea, taking into account the presence and condition of existing flood defenses, and classifies each 50m cell into one of four flood risk categories. A high-risk category is assigned for areas with a greater than 1 in 30 (3.3%) annual chance of flooding. Medium risk refers to areas with a flooding chance annually ranging from 1 in 30 (3.3%) to 1 in 100 (1%). The low-risk category is applied to regions with a flooding probability annually between 1 in 100 (1%) and 1 in 1000 (0.1%), and very low risk is used for areas with a less than 1 in 1000 (0.1%) chance of flooding each year. For our

analytical purposes, the original categories are reclassified into three classes using the 'Reclassify' tool in ArcMap 10.7:

- *High*: annual chance of flooding greater than 1 in 30 (3.3%)
- *Medium*: annual chance of flooding between 1 in 30 (3.3%) and 1 in 100 (1%)
- *Low*: annual chance of flooding less than 1 in 100 (1%)

Subsequently, the 'Zonal Statistics as Table' tool is employed to allocate to each Policy Unit the flood risk category that appears most frequently (*majority*) within its boundaries (**Fig. 2.2a**).

Erosion risk is estimated using long-term shoreline change rates (in units m/yr) calculated by Luijendijk et al. (2018) from Landsat satellite imagery over the period 1984–2016 (**Fig. 2.2b**). Given that no other national-scale dataset of shoreline change exists for the UK, the spatiotemporal resolution of this dataset is at present the most suitable option for assessing large-scale patterns of erosion and accretion for England. The shoreline-change data, provided at intervals of 500 meters along the coast, are integrated into the analysis by using the 'Zonal Statistics as Table' tool to attribute the median value of all shoreline-change data transects found within their boundaries to each Policy Unit. Then, we simplify the classification described in Luijendijk et al. (2018) into the following categories:

- *Erosion*: shoreline change less than -0.5 m/yr
- *Stable*: shoreline change between -0.5 and 0.5 m/yr
- *Accretion*: shoreline change greater than 0.5 m/yr

2.4.2.2 Exposure

We estimate the number of people exposed to coastal flooding using "OpenPopGrid", an open gridded population dataset that spatially redistributes 2011 UK census data over a grid based on Ordnance Survey residential building footprints (Murdock, 2015). This method improves the accuracy of population distribution by focusing on residential areas, providing a more precise alignment of population figures with actual residential locations. It is based on the latest Census available at the time of the assessment.

We calculate the number of buildings on the coastal floodplain from the "EDINA Digimap OS Open Map Local" data layer (Ordnance Survey Service, 2019), which provides an updated description of both residential and non-residential buildings. To avoid double-counting buildings with footprints that intersect more than one Policy Unit, we convert the population and building datasets from polygons to point layers using the 'Feature to Point' tool. This process represents each building by its centroid while preserving all the data attributes of the original feature. Subsequently, using a spatial join, we determine the count of people and buildings within each Policy Unit's boundaries (**Figs. 2.2c-d**).

2.4.2.3 Vulnerability

Because climate change and sea-level rise are expected to increase the likelihood of overtopping and failure in hard defenses (e.g., seawalls), and because continued government investment in existing hard coastal infrastructure around the UK is projected to become economically unviable (CCC, 2018), we treat the presence of engineered coastal defenses as an indicator of higher vulnerability. In the generic risk equation, the vulnerability term can function as a sort of buffer between hazard (which is an exogenous force on the risk system) and exposure. The vulnerability term can be imagined as inversely related to the age of the engineered protection: that is, vulnerability is arguably lowest when, for example, a seawall is new. But as the seawall ages, the more maintenance it sustains (and may require) and, if the safe-development paradox holds, the more time infrastructure has to accumulate behind it. Armstrong and Lazarus (2019b) explore a version of this assumption for beach nourishment.

Here, we use the "UK National Defences dataset" (CCO, 2014) to explore the distribution of natural and engineered coastal defenses for England (**Fig. 2.2e**). It is important to note that soft protection alternatives, such as beach nourishment, are not included in the analysis due to the absence of a compiled national dataset. The defenses dataset is a polyline layer, encompassing 32 categories that represent various combinations of 13 distinct protective measures. To systematically analyze the coastal defenses in place, we first establish separate columns for each of the 13 distinct defense measures identified in the dataset. Within these columns, for every segment of the dataset, we assign a 1 (indicating presence) or a 0 (indicating absence) to denote the existence of specific defenses. Subsequently, through a spatial join process, we map out which defense strategies are implemented within each Policy Unit. This allows us to categorize each Policy Unit based on the specific types of coastal defenses that have been deployed:

- *Natural*: only natural structures such as beaches, cliffs, intertidal, rock platforms, rockfall, and/or spit-inlet
- *Engineered*: only hard defenses such as breakwaters, embankments, groins, piling, rock revetment, seawalls, and/or other hard defenses
- *Combined*: any combination of natural and engineered defenses

Note that this dataset does not account for maintenance of defenses, and so includes structures both maintained and derelict. (A database of flood-defense infrastructure that does include maintenance activity is held by the UK Environment Agency, but its spatial coverage is not complete enough for this analysis.)

To account, at least in part, for social factors affecting vulnerability, we use the national "River and Coastal Flood Disadvantage Index", developed by Sarah Lindley and colleagues

in a 2011 study funded by the Joseph Rowntree Foundation (Lindley et al., 2011). This research, leveraging the IPCC framework, analyzed the interplay between social vulnerability and exposure to flooding in the UK, suggesting that flood disadvantage stems from this interaction, potentially intensifying negative outcomes for communities. Based on principles similar to the Index of Multiple Deprivation (Department for Levelling Up, Housing and Communities, 2019), the “River and Coastal Flood Disadvantage Index” derives from indicators that refer to the adaptive capacity, enhanced exposure, and personal sensitivity of the population at risk of flooding, lending it some reflection of the real implications of a flooding event in society (England and Knox, 2014). Adaptive capacity relates to the ability to prepare for, respond to, and recover from flooding, and it is influenced by various social factors including income, insurance, local knowledge, mobility, and social networks. Enhanced exposure covers environmental factors that could worsen flood effects, such as the absence of infrastructure to manage water run-off or homes with basements that are more likely to sustain damage. Personal sensitivity involves biophysical characteristics such as age and health that increase susceptibility to flood damage. By integrating these indicators and mapping areas of high vulnerability alongside flood exposure data, this index highlights locations at greatest risk of flood disadvantage, offering a better understanding of how floods impact society than the traditional measures of deprivation (England and Knox, 2014; Lindsey et al., 2011). Note, however, that this social vulnerability assessment does not directly account for the actual likelihood of flood events or the climatic factors influencing these probabilities. Consequently, the resulting maps highlight areas where community characteristics may amplify impacts but do not estimate the likelihood of such impacts occurring. The real significance of the social vulnerability maps emerges only if a community faces a genuine hazard, focusing solely on social and related factors (Lindsey et al., 2011). Detailed information on the indicators used for this index is outlined in Appendix I of Lindsey et al. (2011).

While this index’s outcomes were once accessible via the ‘Climate Just’ map tool (https://www.climatejust.org.uk/map), offering a lens on socio-spatial vulnerability and climate disadvantages in the UK, the current maps have been updated with newer flood data from a study conducted by Sayers and Partners LLP for the Joseph Rowntree Foundation (Sayers et al., 2017), which introduced the Neighbourhood Flood Vulnerability Index (NFVI) and Social Flood Risk Index (SFRI). Despite these updates, our study relies on the Lindsey et al. (2011) dataset, as it was the only publicly accessible resource available at the time of the assessment that specifically addressed flood vulnerability in our area of study. In England, the River and Coastal Flood Disadvantage Index is depicted through polygons that align with Middle Super Output Areas, with each area receiving a specific numerical score indicating its level of flood disadvantage. These scores are then divided into six distinct categories: acute, extremely high, relatively high, average, relatively low, and extremely low. Through a spatial join, we allocate to each Policy Unit the median of the flood disadvantage scores from all

intersecting polygons (**Fig. 2.2f**), subsequently categorizing the results into three levels of flood disadvantage:

- *Low disadvantage:* scores less than -0.5
- *Medium or average disadvantage:* scores between -0.5 and ≤ 0.5
- *High disadvantage:* scores greater than 0.5

2.4.3 Exploring relationships between the components of risk

To delve into the intricate aspects of coastal risk along the open coast of England, data layers capturing natural hazards, exposure, and vulnerability—once processed as outlined in the preceding sections—are merged through a series of spatial joins. This approach constructs an integrated matrix, associating each Shoreline Management Plan Policy Unit in England with comprehensive data on:

- Strategic policy in the short-term (2005–-2025)
- Strategic policy in the long-term (2056–2105)
- Probability of flooding
- Median shoreline change rate between 1984–2016
- Number of people on the coastal floodplain
- Number of buildings on the coastal floodplain
- Type of defenses used to protect the coast
- Median level of social disadvantage

By examining the interconnections between these various factors, we gain a deeper insight into the multifaceted nature of coastal risk.

2.5 Results

2.5.1 Compound hazard, defenses, and policies

Of the Shoreline Management Plan Policy Units in England that adjoin a coastal floodplain, approximately 76% are in places with a high likelihood of flooding (annual chance of flooding greater than 1 in 30) (**Fig. 2.3a**; **Fig. 2.4a**). Combined, these flood-prone areas account for 36% (1,541 km^2) of the coastal floodplain overall (**Fig. 2.4b**), and hold ~16% of the total coastal-floodplain population (113,880 people; **Table 2.1**). Coastal floodplains with a lower probability of flooding (annual chance of flooding less than 1 in 100) account for a slightly larger portion of the coastal floodplain overall (39%, 1,644 km^2) and more of the total population (462,844 people), and thus tend to be more densely populated (**Fig. 2.4a**). The most urbanized coastal-floodplain Policy Units—those in which buildings cover more than

20% of their total area—tend to be in places with a low probability of coastal flooding (**Fig. 2.5a**).

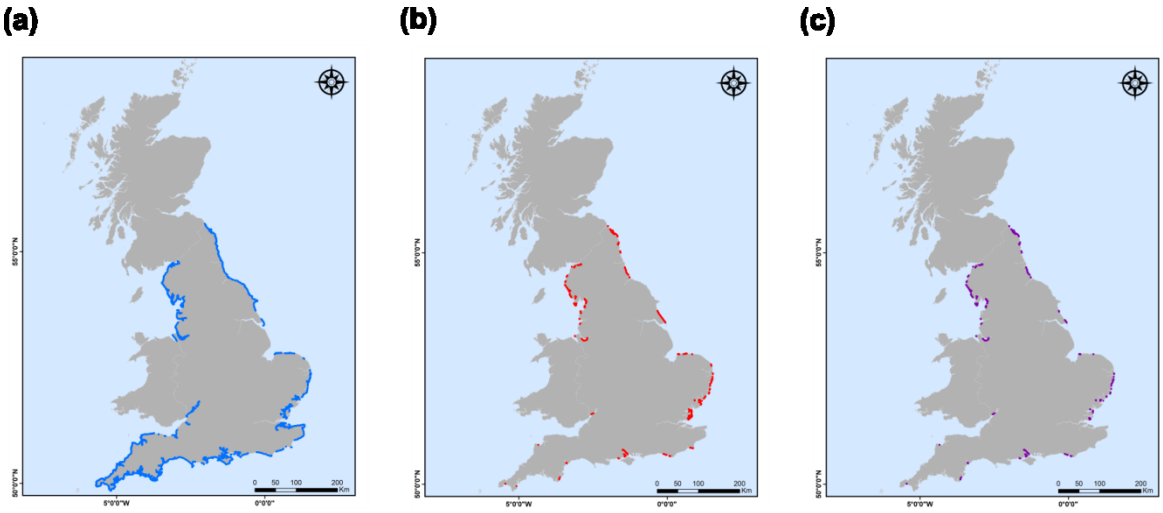

Figure 2.3 Coastal-floodplain Policy Units exposed to (a) high likelihood of coastal flooding, (b) long-term shoreline erosion, and (c) both a high likelihood of coastal flooding and long-term shoreline erosion.

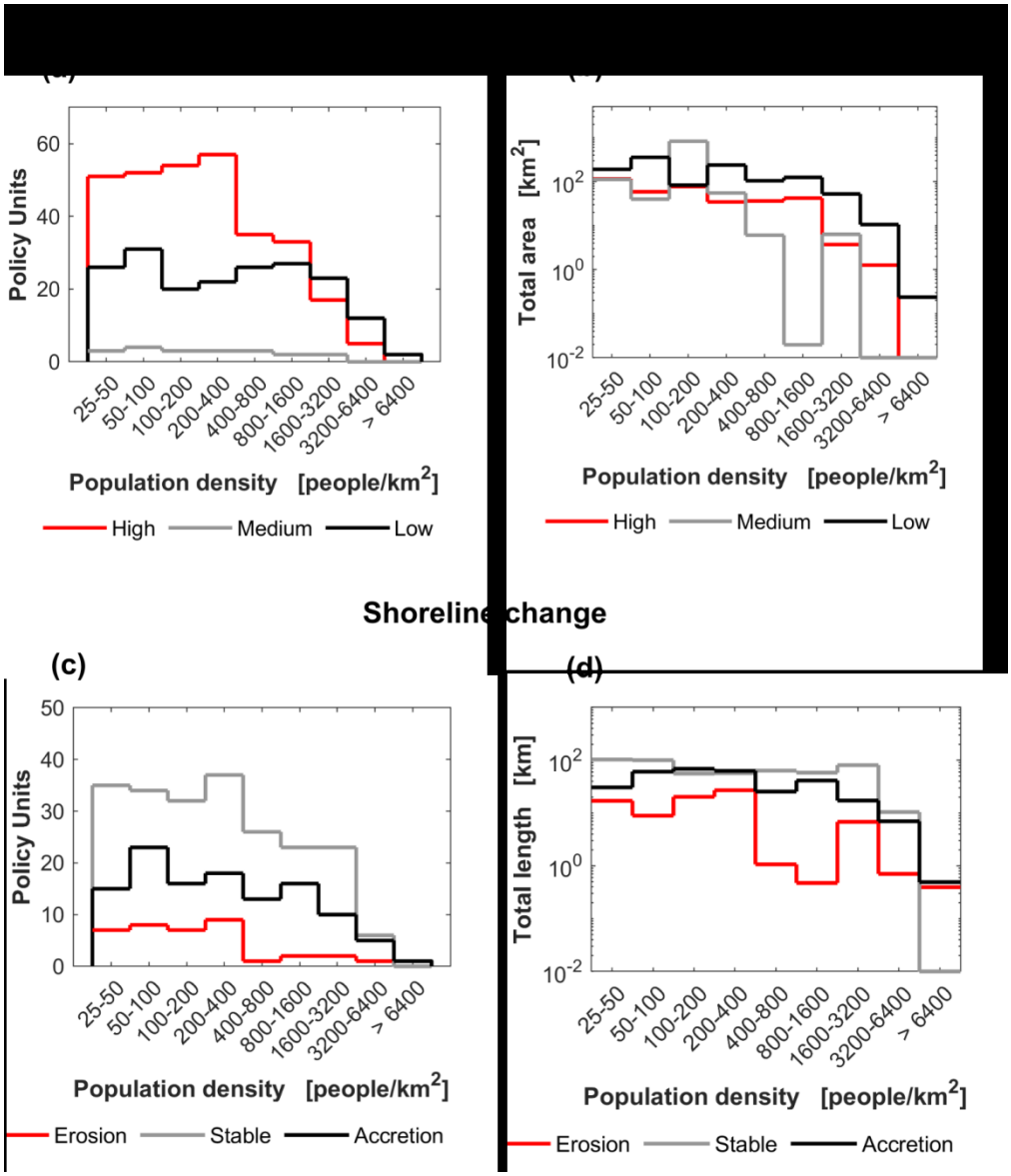

Figure 2.4 Population on the English coastal floodplain exposed to natural hazards: (a) number of Policy Units and (b) total area exposed to coastal flooding; (c) number of policy units and (d) total alongshore length exposed to shoreline change.

A comparatively smaller percentage of coastal-floodplain Policy Units (10%) and associated coastline (11% of the total coastline for all coastal floodplains, or 350 of 3,079 km) include zones of long-term erosion (**Fig. 2.3b**; **Figs. 2.4c-d**; **Table 2.1**). Policy Units affected by chronic coastal erosion are characterized by lower building densities (**Fig. 2.5b**). However, 80% of long-term erosion zones (approximately 9% of all coastal-floodplain Policy Units in England) are exposed to both chronic erosion and a high likelihood of flooding (**Fig. 2.3c**). The combination of these two hazards could potentially affect nearly 6,200 people and more than 2,200 buildings (**Table 2.1**).

Table 2.1 Exposure to natural hazards in England.

	Policy Units	%	Area [km2]	%	Length [km]	%	Population	%	Buildings	%
High flood likelihood	1,048	76.8	1,540.6	36.2	2004.7	65.1	113,880	15.5	30,284	14.6
Long-term coastal erosion	143	10.5	518.6	12.2	350.1	11.3	34,691	4.7	9,806	4.7
High flood likelihood & long-term erosion	115	8.4	303.6	7.1	261.4	8.5	6,179	0.8	2,263	1.1

From the Channel Coast Observatory dataset of national coastal defenses (CCO, 2014), we estimate that 42% of the English coastline (3,019 km) is currently fronted by one or more kinds of engineered protection (e.g., seawalls, rock revetments, and groins), maintained or derelict—the dataset does not include an assessment of condition. On coastal floodplains, specifically, engineering works are present along nearly 75% (2,295 km) of their shorelines (**Fig. 2.6**). The dataset indicates that hard structures tend to be co-located with natural features, such as beaches and marshes, which also contribute to reducing wave energy and flood damage and so are considered natural defenses. All but approximately 7% of the total population (**Fig. 2.6a**) and buildings (**Fig. 2.6b**) on the coastal floodplain are located behind such “combined” defenses, as we refer to them here (**Table 2.2**). Approximately 10% (281 km) of the coastal-floodplain coastline is fronted only by natural features. The exclusive presence of hard defenses is rare (3% of the coastal-floodplain coastline, or 83 km).

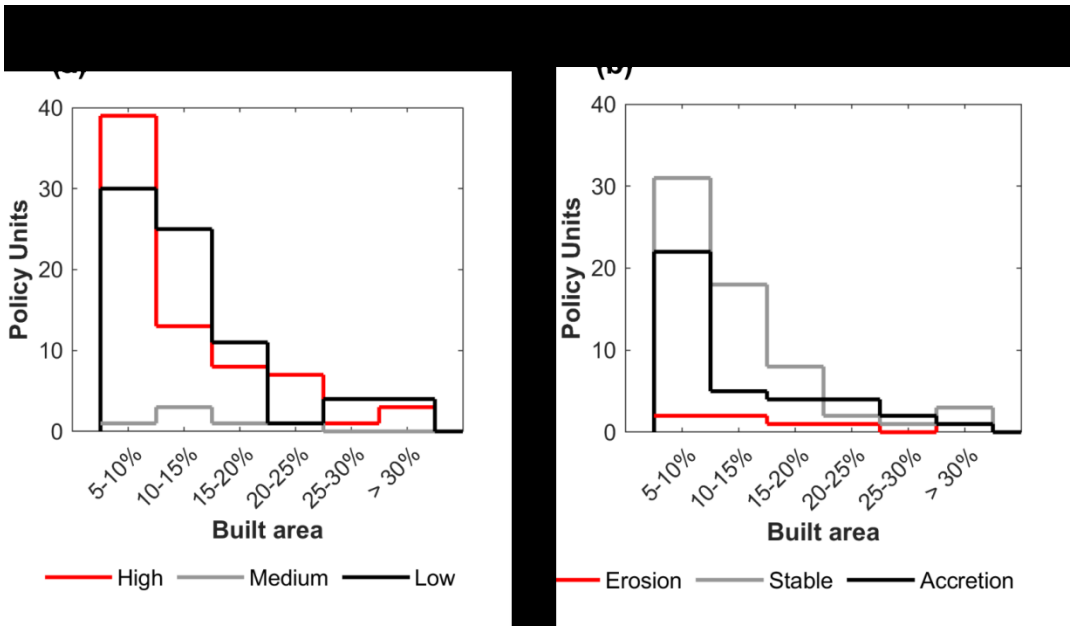

Figure 2.5 Proportion of developed area exposed to (a) coastal flooding and (b) modes of shoreline change.

Table 2.2 Defenses on the coastal floodplain.

	Policy Units	%	Length [km]	%	Population	%	Buildings	%
Natural	266	19.5	281.1	9.1	6,789	0.9	2,436	1.2
Engineered	71	5.2	83.1	2.7	8,227	1.1	2,125	1.1
Combined	843	61.8	2,212.1	71.8	682,002	92.7	191,016	92.4

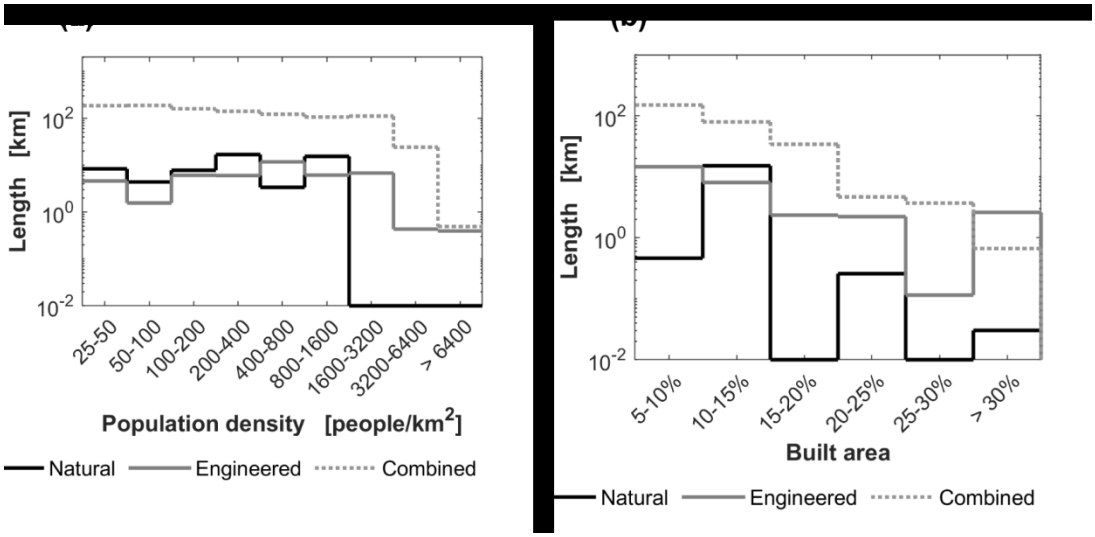

Figure 2.6 Plots of (a) population and (b) buildings protected by coastal defenses. *Natural* refers to Policy Units that rely on natural structures for their protection against floods or coastal erosion; *engineered* comprises areas exclusively protected with hard defenses; and *combined* includes both natural and engineered defenses.

Under the current Shoreline Management Plans, we find that 66% (over 2,000 km) of the coastal-floodplain coastline and 93% of the coastal-floodplain population (683,381 people) are associated with a *Hold-the-Line* (HTL) policy (**Fig. 2.7**), in which the existing defense line is maintained or upgraded. Policy alternatives of *No Active Intervention* (NAI) apply to 21% (less than 700 km) of the coastal-floodplain coastline, and *Managed Realignment* (MR) only 12% (381 km). Both policies tend to be more common in areas with lower population density (**Fig. 2.7**). An *Advance-the-Line* (ATL) policy for land reclamation is rarely invoked (**Table 2.3**).

Table 2.3 Shoreline Management Plans strategies in the Short-Term (2005-2025) and Long-Term (2056–2105).

	Strategy	Policy Units	%	Length [km]	%	Population	%	Buildings	%
Short-Term	ATL	2	0.2	9.8	0.3	2,519	0.3	489	0.2
	HTL	775	56.8	2,029.3	65.9	683,381	92.9	190,114	91.9
	MR	160	11.7	380.7	12.4	28,719	3.9	10,357	5
	NAI	427	31.3	659.0	21.4	21,011	2.9	5,826	2.8
Long-Term	HTL	662	48.5	1,713.7	55.7	652,090	88.6	178,212	86.2
	MR	232	17.0	659.6	21.4	63,388	8.6	23,188	11.2
	NAI	466	34.2	702.7	22.8	20,122	2.7	5,351	2.6

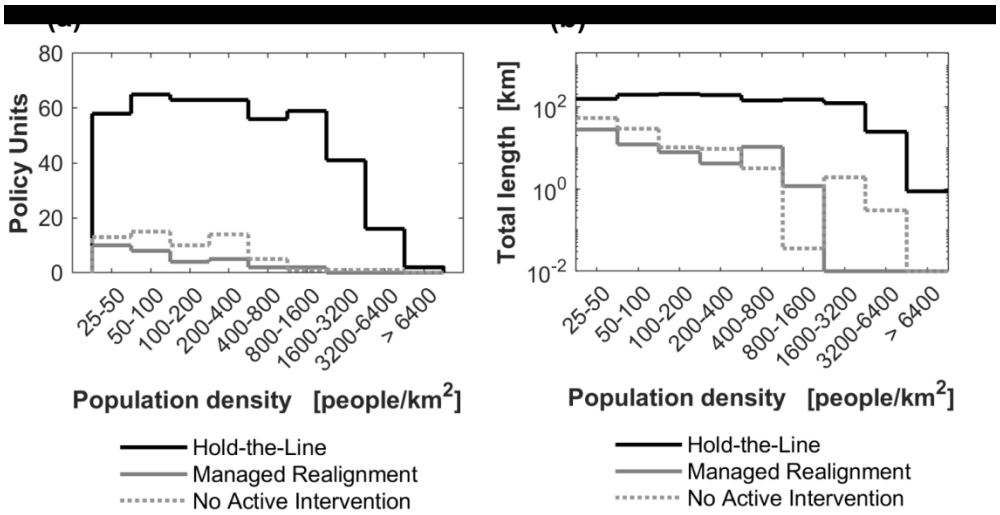

Figure 2.7 Strategic policies defined in the Shoreline Management Plans for the Short-Term horizon (2005–2025).

If recommendations for future epochs in the current Shoreline Management Plans are implemented, we estimate that the number of coastal floodplain Policy Units under *Hold-the-Line* (HTL) policies in the 2100s would reduce by 15% (spanning 1,714 km), affecting 4% of the present coastal-floodplain population (31,290 people) (**Fig. 2.8a**, **Table 2.3**). Meanwhile, the number of coastal-floodplain Policy Units under *Managed Realignment* (MR) would increase by more than 45% (to span 660 km) and approximately double the number of people living behind that designation (**Fig. 2.8b**). Although the application of *No Active Intervention* (NAI) policies is also expected to increase by 9% in the coming decades, the policy adjustments would affect 4% of the coastal-floodplain population (**Fig. 2.8c**). There are no *Advance-the-Line* (ATL) plans expected in the long term (**Table 2.3**).

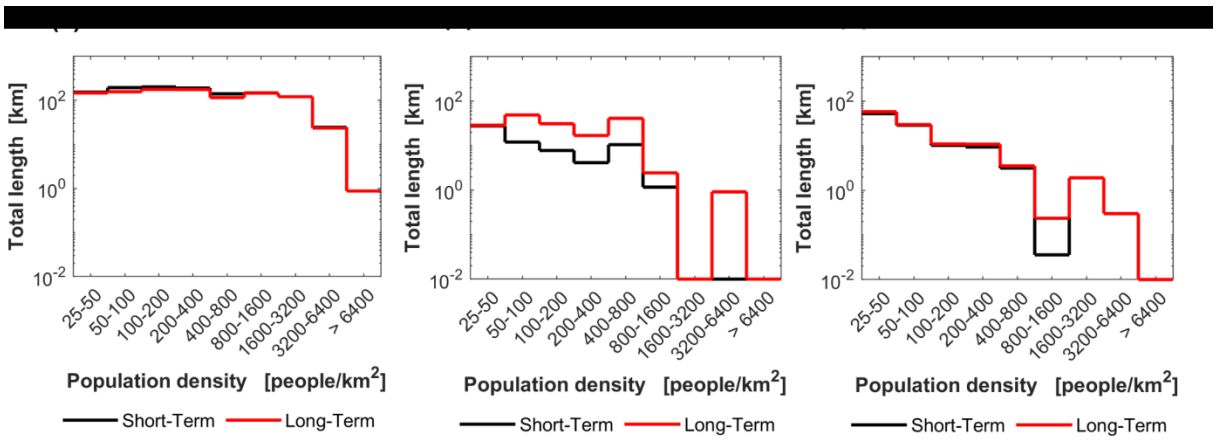

Figure 2.8 Differences in affected coastal-floodplain population under shifts in long-term (2056–2105) Shoreline Management Policies: (a) Hold-the-Line, (b) Managed Realignment and (c) No Active Intervention.

2.5.2 Patterns of social disadvantage

Potential social disparities in coastal risk are revealed when the coastal floodplains are parsed according to disadvantage scores in the national “River and Coastal Flood Disadvantage Index”. We find significant differences between low and high-disadvantage areas in terms of natural hazards, coastal defenses, and policy recommendations. Of the coastal-floodplain Policy Units, 32% reflect high and 25% low disadvantage scores, respectively. Nearly 44% (1,400 km) of the coastal-floodplain coastline and 70% (3,000 km^2) of the total coastal floodplain area are classified as highly disadvantaged. Policy Units with low disadvantage scores only represent 15% of the coastal-floodplain coastline (451 km) and 4% of the coastal floodplain (168 km^2). The marked difference in total coastal-floodplain area for high and low disadvantage is explained in part by the few large, rural coastal floodplains associated with high disadvantage that extend far inland (**Fig. 2.9a**). That said, the overwhelming majority of the population and buildings on the coastal floodplain are found in areas of high disadvantage; areas of low disadvantage account for barely 1% of the total population and buildings (**Table 2.4**).

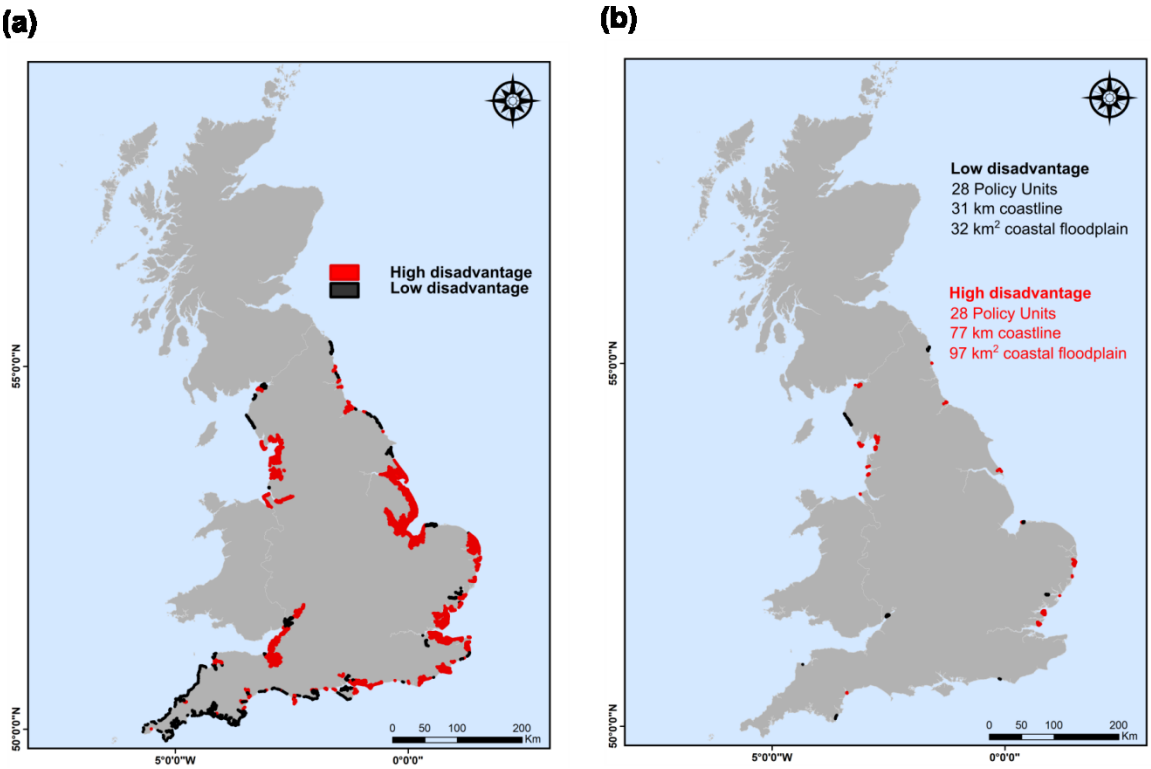

Figure 2.9 Social disadvantage reported in the national River and Coastal Flood Disadvantage Index, mapped to coastal floodplain extents. (a) Policy Units with low and high disadvantage scores; (b) Policy Units with high and low disadvantage scores and exposed to both a high likelihood of flooding and long-term shoreline erosion. Summary statistics are provided in Table 4.

Exposure to coastal flooding also differs by social disadvantage (**Figs. 2.10a-b**; **Table 2.4**). Where the likelihood of flooding is high, the total area of the coastal floodplain with high disadvantage scores (660 km^2) is nearly five times greater than the equivalent area with low disadvantage (139 km^2). In terms of relative proportion, however, these high-likelihood zones account for 83% and 22% of the total coastal-floodplain area associated with low and high disadvantage, respectively. These areas include approximately half the population and buildings associated with low disadvantage, and 12% of the population and buildings associated with high disadvantage. For exposure to shoreline-change hazard, a majority of coastal floodplain Policy Units are classified as stable or accreting (**Figs. 2.10c-d**; **Table 2.4**). Only 9% of Policy Units with low disadvantage and 11% with high disadvantage are in zones of long-term erosion, but the total length of coastal-floodplain coastline associated with high disadvantage (153 km) is nearly three times greater than the length associated with low disadvantage (54 km). There are 28 coastal floodplain Policy Units (2%) classified as highly disadvantaged and exposed to both coastal flooding and long-term coastal erosion (**Fig. 2.9b**), with approximately 3,000 people and 800 buildings located in these areas (<0.5% of the total population and buildings on the coastal floodplain).

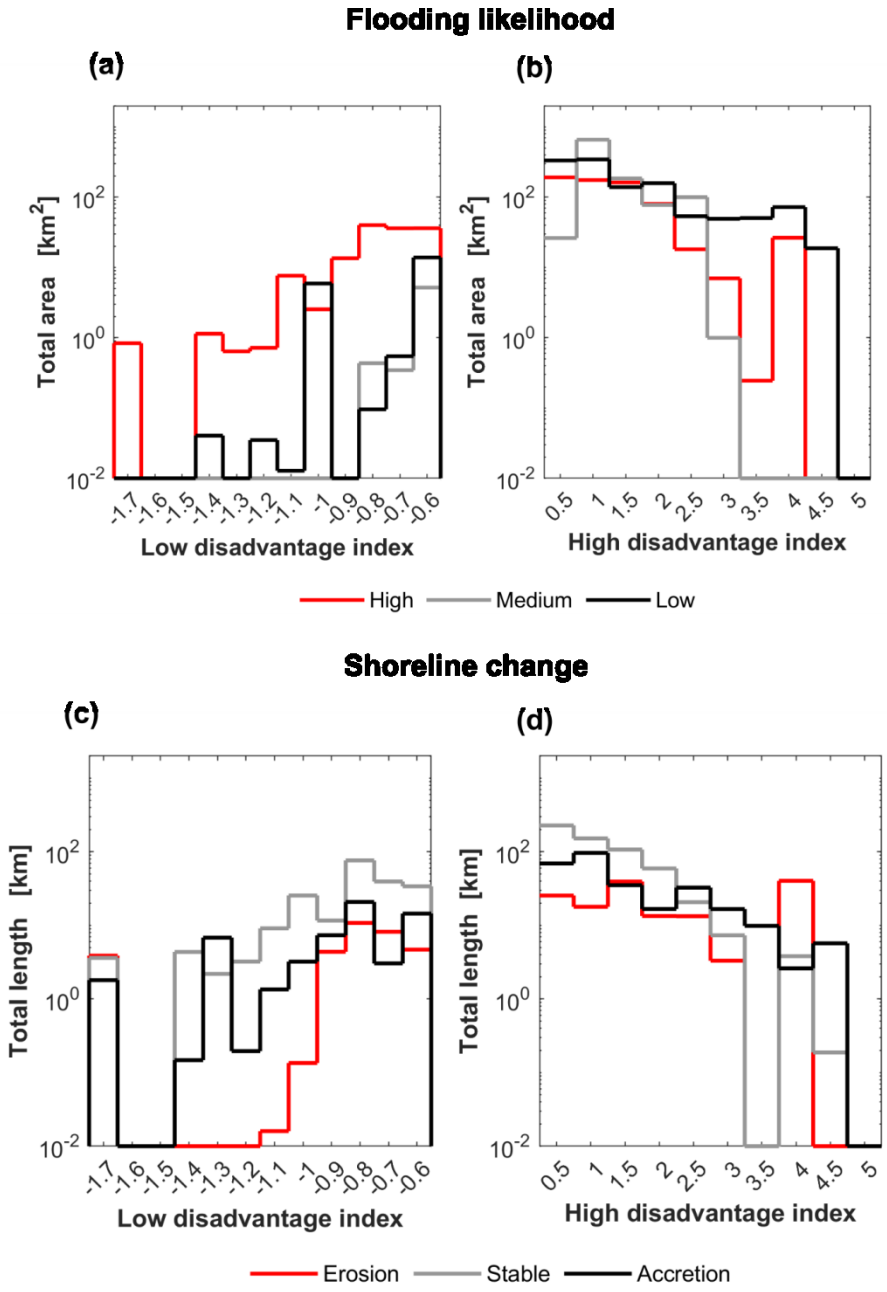

Figure 2.10 Social disparities in exposure to natural hazards: flood likelihood in areas of (a) low and (b) high disadvantage, and distribution of shoreline change in areas of (c) low and (d) high disadvantage.

Table 2.4 Summary statistics for high and low disadvantaged areas.

		Policy Units	%	Length [km]	%	Area [km2]	%	Pop.	%	Build.	%
HIGH DISADVANTAGE	**Total**	**442**	**31.5**	**1358.1**	**44.1**	**2,964.8**	**69.7**	**616,628**	**83.8**	**175,177**	**84.7**
SMP Short-Term	ATL	2	0.5	9.8	0.7	11.1	0.4	2,519	0.4	489	0.3
	HTL	318	73.9	1,057.5	77.9	2,497.1	84.2	569,417	92.3	161,401	92.1
	MR	42	9.8	145.4	10.7	269.1	9.1	27,108	4.4	9,119	5.2
	NAI	68	15.8	145.4	10.7	187.5	6.3	17,583	2.9	4,168	2.4
SMP Long-Term	HTL	277	64.4	901.4	66.4	2,285.4	77.1	543,822	88.2	151,818	86.7
	MR	84	19.5	306.9	22.6	510.4	17.2	55,966	9.1	19,705	11.2
	NAI	65	15.1	146.8	10.8	168.3	5.7	16,812	2.7	3,619	2.1
Coastal defenses	Natural	31	7.2	36.9	2.7	55.3	1.9	3,024	0.5	1,585	0.9
	Engineered	17	3.9	22.9	1.7	12.1	0.4	3,761	0.6	1,017	0.6
	Combined	328	76.3	1,126.2	82.9	2,655.9	89.6	587,266	95.2	165,437	94.4
Flood likelihood	High	245	56.9	630.9	46.5	660.3	22.3	78,709	12.8	20,075	11.5
	Medium	15	3.5	112.7	8.3	1,047.8	35.3	157,326	25.5	52,445	29.9
	Low	167	38.8	613.3	45.2	1,256.3	42.4	380,584	61.7	102,654	11.5
Shoreline change	Erosion	45	10.5	153.1	11.3	292.0	9.8	30,994	5.0	8,039	4.6
	Stable	204	47.4	578.5	42.6	805.7	27.2	128,789	20.9	37,013	21.1
	Accretion	85	19.8	302.4	22.3	1,554.2	52.4	405,796	65.8	116,929	66.7
LOW DISADVANTAGE	**Total**	**340**	**24.9**	**451.2**	**14.7**	**167.6**	**3.9**	**6,423**	**0.9**	**2,675**	**1.3**
SMP Short-Term	HTL	123	36.2	141.2	31.3	80.5	48.0	5,493	85.5	1961	73.3
	MR	35	10.3	51.1	11.3	21.7	12.9	318	5.0	252	9.4
	NAI	182	53.5	258.9	57.4	65.5	39.1	612	9.5	462	17.3
SMP Long-Term	HTL	96	28.3	114.4	25.4	63.9	38.1	4,810	74.9	1,714	64.1
	MR	47	13.8	80.1	17.7	37.8	22.6	1,018	15.8	472	17.6
	NAI	197	57.9	256.6	56.9	66.0	39.3	595	9.3	489	18.3
Coastal defenses	Natural	113	33.2	95.4	21.1	17.7	10.5	172	2.7	161	6.0
	Engineered	21	6.2	13.6	3.0	3.1	1.8	2,290	35.7	458	17.1
	Combined	148	43.5	230.1	51.0	126.7	75.6	2,971	46.3	1,592	59.5
Flood likelihood	High	305	89.7	407.8	90.4	139.3	83.1	2,911	45.3	1,504	56.2
	Medium	6	1.8	5.6	1.3	5.9	3.5	943	14.7	209	7.8

		Policy Units	%	Length [km]	%	Area [km2]	%	Pop.	%	Build.	%
	Low	28	8.2	31.9	7.1	20.5	12.2	2,567	40.0	954	35.7
Shoreline change	Erosion	30	8.8	53.9	3.6	32.4	19.3	832	13.0	367	13.7
	Stable	180	52.9	781.4	52.7	82.2	49.1	705	11.0	561	21.0
	Accretion	64	18.8	201.7	13.6	29.5	17.6	1,525	23.7	728	27.2

We also find that coastal floodplain Policy Units with low disadvantage rely more than their high-disadvantage counterparts on natural forms of coastal protection. Approximately 33% of low-disadvantage coastal floodplain Policy Units (95 km of coastline) have natural barriers as their only form of coastal protection (**Fig. 2.11a**), in contrast to only 7% (37 km) of high-disadvantage coastal floodplain Policy Units (**Fig. 2.11b**, **Table 2.4**). "Combined" defenses predominate in high-disadvantage areas (**Fig. 2.11b**), with nearly 1,200 km of coastline fronted by both natural and engineered protection. However, the proportion of engineered defenses in these "combined" reaches is greater where the disadvantage is high (**Fig. 2.12d**), such that, on average, more than half of the protections in place are engineered. Conversely, in low-disadvantage areas, almost 70% of the defenses in "combined" reaches are natural (**Table 2.4**). The proportion of hard engineering increases with population and building density across both categories of disadvantage (**Figs. 2.12b-c**).

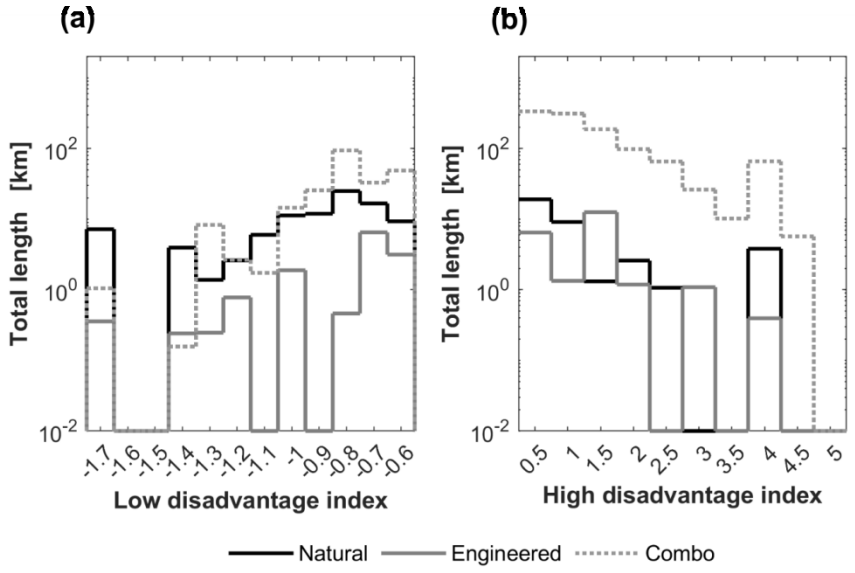

Figure 2.11 Distribution of coastal defenses in areas of (a) low and (b) high disadvantage.

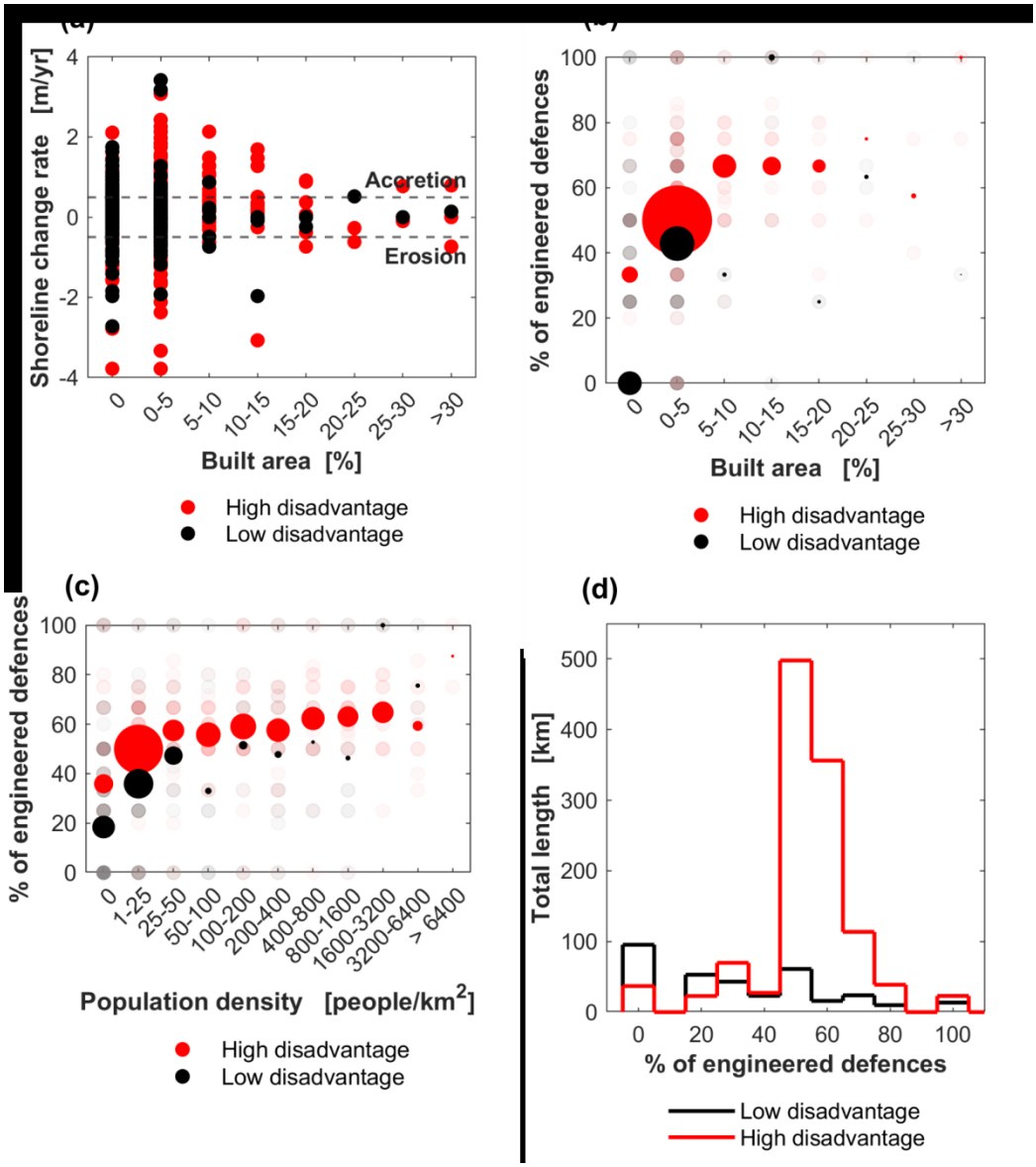

Figure 2.12 Relationships between the components of coastal risk in high and low disadvantage areas. (a) Relationship between rates of shoreline change (hazard) and coastal-floodplain development intensity (exposure). (b) Percentage of engineered defenses (vulnerability) relative to building density and (c) population density (exposure); symbols in (b) and (c) are scaled by total length, and medians (dark circles) are superimposed atop the full range of distributions (light circles). (d) Distribution of total shoreline length (exposure) in relation to the percentage of engineered defenses in high and low disadvantage areas (vulnerability).

Current strategic plans indicate more No Active Intervention in areas of low disadvantage (**Fig. 2.13a**): nearly 260 km (57%) of the coastal-floodplain coastline in low-disadvantage zones follow the “do nothing” strategy, compared to 145 km (11%) implementing this policy where disadvantage is high. *Hold-the-Line* policies, on the other hand, are applied in more than 1,000 km of coastal-floodplain coastline with high disadvantage (**Fig. 2.13b**); in low-disadvantage areas, the same strategy extends less than 150 km. Over the long term (2056–2105), areas of low (**Fig. 2.13c**) and high disadvantage (**Fig. 2.13d**) alike will follow the

national trend, with *Hold-the-Line* policies being replaced by *Managed Realignment*, but the number of Policy Units applying *No Active Intervention* strategies is expected to increase only in low disadvantaged areas (**Table 2.4**).

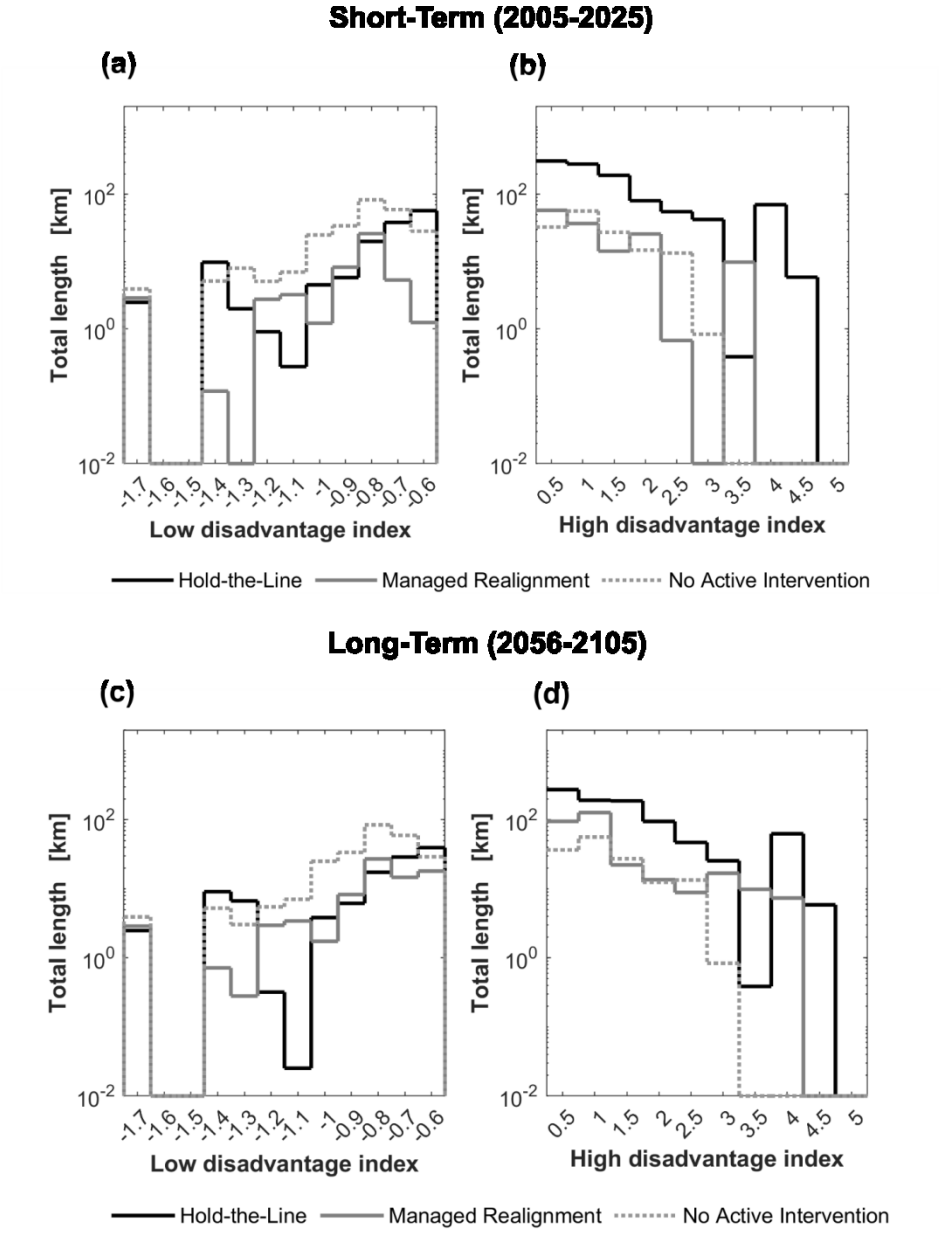

Figure 2.13 Distribution of strategic policies according to Shoreline Management Plans: (a) low and (b) high disadvantage areas for the Short-Term horizon (2005–2025) and (c) low and (d) high disadvantage areas for the Long-Term horizon (2056–2105).

2.6 Implications

2.6.1 Comparative patterns

Analyses of shoreline change along the Atlantic Coast of the USA have found a positive relationship between shoreline change rate and the intensity of coastal development, finding shoreline erosion more prevalent where the coast is unoccupied and accretion where the

coast is densely populated (Armstrong and Lazarus, 2019a; Hapke et al., 2013). One explanation for this positive relationship is that areas of intensive coastal development tend to aggressively counteract shoreline erosion with engineering interventions such as beach nourishment (Armstrong and Lazarus, 2019a), which involves widening an eroded beach with sand imported from outside the local littoral system. There is no UK-scale dataset for beach nourishment comparable to the one for the USA maintained by the Program for the Study of Developed Shorelines (PSDS, 2021), and beach nourishment is not included among the coastal defenses listed in the national dataset from the Channel Coast Observatory. However, for England, we find indications of a similar kind of relationship between rates of shoreline change and coastal-floodplain development intensity (**Fig. 2.12**). Our results show both negative and positive rates of shoreline change—zones of erosion and accretion—where development pressures from population and buildings are low, and an apparent convergence toward "shoreline stability" (little or negligible long-term change) where development is high (**Fig. 2.12a**). This convergence is consistent with the median percentage of engineered defenses tending to increase, and then saturate, with population and building density (**Figs. 2.12b-c**). We echo the conclusion offered by Hapke et al. (2013) for the US Mid-Atlantic, that "the influence of development…appears to override the geomorphological signal of shoreline behavior, an important consideration for interpretations of investigations of change along developed coasts. Only along sparsely developed coasts does the shoreline respond as expected with respect to the coastal geomorphology."

Beyond development, the disparities we explore between areas of low and high social disadvantage in England's coastal floodplains are another important consideration for investigations of coastal change, and signal a notable contrast with coastal demographic trends in the USA. While since the 1970s the coastal USA has experienced disproportionate population growth and a concentration of wealth in coastal real estate (Armstrong et al., 2016; Crossett et al., 2013; Lazarus et al., 2018), over the same timeframe English seaside towns and communities have been hollowing out (House of Lords, 2019; Walton and Browne, 2010; Zsamboky et al., 2011). The fact that coastal flood and erosion hazard is compounded to a greater extent in areas of high disadvantage (**Fig. 2.9b**; **Table 2.4**) raises complex political issues regarding how to navigate these places toward coastal futures that are both socially and environmentally sustainable (CCC, 2018; House of Lords, 2019).

2.6.2 Spatial relationships alongshore

Although we can superimpose data layers for components of coastal risk and examine their spatial relationships, our analysis does not include the kind of dynamics that real hazard events can impose upon a physical landscape. Without morphodynamic modeling we cannot otherwise determine, for example, whether a breach in coastal defenses associated with one Policy Unit will divert flood waters into another, thus revealing spatial connectivity between

floodplains. Morphodynamic modeling remains computationally expensive over such extended spatial scales, but represents a necessary step in a clearer understanding of compounded coastal hazard and connectivity-related exposure on defended coastal floodplains.

Nor are we able to account for ways in which Policy Units may be connected (or isolated) by littoral processes like wave-driven alongshore sediment transport. Detailed analysis of wave forcing, alongshore sediment flux, and shoreline change along the Anglian coast, in southeast England, shows that while there is a predominant wave climate that tends to drive sediment flux from north to south, there are local zones of reversal, and that emphasis on the prevailing pattern belies significant variability in conditions operating at smaller spatial and faster time scales (Burningham and French, 2017). The Policy Units underpinning the Shoreline Management Plans of the UK were intended, by original design, to reflect the boundaries of large-scale littoral cells (Nicholls et al., 2013), but if the reaches of those circulatory systems shift with climate-driven changes in wave climate, for example, then the edges of neighboring Shoreline Management Plans may begin to blur. Understanding and accounting for mobile boundaries between governance units remains a significant challenge in coastal management (Lazarus et al., 2016).

2.6.3 Data gaps and opportunities for insight

In undertaking this analysis, we found that the UK lacks the comprehensive datasets of coastal hazard, exposure, and defenses required to make informed, forward-looking decisions for sustainable management of coastal systems – now, and under future climate change (Lazarus et al., 2021). We used a Landsat-derived dataset of shoreline-change trends (Luijendijk et al., 2018) because it was the only dataset that offered national coverage. The UK Environment Agency's "National Coastal Erosion Risk Map" is useful (Environment Agency, 2019c), but comprises binned projections of future change based on past erosion rates and is thus a step removed from the data that underpins it. The Environment Agency also holds an inventory of flood defense assets in the "National Flood and Coastal Defence Database"—presently archived—that aimed to compile "consistent methods of asset condition target setting, asset inspection and reporting on fluvial and sea flood defense assets" and support "investment decisions and enables prioritisation of works around the country based on risk" (Environment Agency, 2010). However, the inventory "does not currently apply to coastal erosion assets" (Environment Agency, 2010) and only includes assets under the auspices of the Environment Agency, thus missing any defenses under the jurisdiction of local authorities. The UK also lacks any comprehensive record of beach nourishment projects, despite their widespread application—the often-cited review of European beach nourishment practices by Hanson et al. (2002) is nearly two decades old. Digital catalogs of building footprints and infrastructure networks—current, and rendered

from historical maps—should improve quantitative assessments of development patterns in space and time. But overall, the lack of integrated datasets from local to national scales around the UK—and the patchiness of public availability—presents a substantial hurdle to a detailed accounting of coastal risk, to evidence-based explanations for disparities in social disadvantage and their dynamics at the coast, and to data-driven policy planning for coastal sustainability.

2.7 Conclusions

Analyzing components of coastal risk (hazard, exposure, and vulnerability) at the national scale for England, we find that areas associated with high social disadvantage are disproportionately affected by coastal flooding and erosion hazard, relying on high proportions of engineered defenses and extensions of a *Hold-the-Line* shoreline-management policy, even as government investment in hard coastal defenses is expected to become economically unsustainable under future climate-driven forcing (CCC 2018). Our effort to synthesize a national-scale portrait of coastal risk highlighted substantive data gaps in present states and behaviors of coastal hazards, exposure, and defenses, and in the historical trajectories from which existing coastal risk has arisen. Morphodynamic modeling can surely improve assessments of coastal hazard impacts, especially in terms of spatial connectivity among coastal floodplains and in sediment-transport cells alongshore. But ahead of that, basic investment in collating, formalizing, managing, and enabling public access to national-scale geomatics, infrastructure, and demographics datasets will deliver an outsized advance in evidence-based insight into UK coastal risk.

2.8 Acknowledgments

This research has been supported by the Natural Environment Research Council (grant no. NE/S016651/1) and a Southampton Marine and Maritime Institute Doctoral Studentship to S.A. The authors thank the *NERC UK Climate Resilience CoastalRes* team and project stakeholders for helpful discussions.

Chapter 3 Paper 2: The revalorizing effect of beach nourishment

This manuscript is currently in progress and undergoing review with the respective coauthors. We anticipate making minor or moderate adjustments and revisions before its submission.

Initial authors: Aldabet S., Lazarus E.D., Armstrong S.B.

Aldabet S. contributed to the investigation, methodology, formal analysis, writing, data curation; Lazarus E.D. contributed to the conceptualization, investigation, methodology, formal analysis, writing, supervision, project administration, funding acquisition; Armstrong S.B. contributed to the conceptualization and methodology.

3.1 Abstract

Coastal zones in the United States are highly vulnerable to climate change hazards. Yet, they undergo sustained population growth and increased building density, leading to more densely developed environments. Here, we investigate spatial development patterns in New Jersey and Florida, two well-known hotspots of coastal risk, combining large-scale housing information containing extensive structural and economic data with locations of historical beach nourishment projects. Our results indicate that properties in nourishing areas tend to be larger, more expensive, and exhibit higher growth rates over time in both regions. The consistent findings across multiple datasets and locations suggest that the observed pattern of increased exposure to coastal risk is not limited to specific geographic areas, but rather represents a pervasive trend characterizing developed coastlines throughout the United States.

3.2 Introduction

Coastal zones are highly susceptible to climate change hazards (Nicholls and Cazenave, 2010; Seneviratne et al., 2021; Wong et al., 2014). Yet, they are the most densely populated and economically active regions on the planet, with growth rates often outpacing those of inland areas—a trend that is expected to continue in the future (McGranahan et al., 2007; Neumann et al., 2015; Wong et al., 2014). In the United States, coastal counties comprise only 17% of the land area but house over half of the country's population (Crossett et al., 2013; 2004). Despite decades of regulations aimed at mitigating their vulnerability, the US coastlines continue to undergo sustained population growth and increase in building density, leading to more densely developed environments. Even areas with a history of catastrophic

events have experienced rises in structure density over the last few decades, often exceeding average trends (Braswell et al., 2022; Iglesias et al., 2021; Lazarus et al., 2018).

Recognizing that increasing exposure in high-risk areas is a significant factor leading to higher losses from natural disasters (Cutter & Emrich, 2005; IPCC, 2012), there has been a growing interest in examining emerging patterns that might be contributing to the ongoing expansion of urban development in zones prone to hazards (Armstrong et al., 2016; Braswell et al., 2022; Iglesias et al., 2021; Lazarus et al., 2018). For instance, Armstrong et al. (2016) integrated a comprehensive property-level database, including structural characteristics like the year of construction and total living area, with the geographical locations of beach nourishment, a prevalent method of coastal protection. Their study, focused on understanding the factors influencing intensified coastal development along the Atlantic and Gulf Coasts of Florida, revealed a significant disparity in both the quantity and size of waterfront family homes between regions protected by beach nourishment and those lacking such protective measures. These empirical findings lend support to the notion of a potential positive feedback between hazard protection and urban development, a concept previously highlighted in existing literature (Burby, 2006; Burton and Cutter, 2008; Di Baldasarre et al., 2018; 2013; Kates et al., 2006; Montz and Tobin, 2008; Tobin, 1995; White, 1945; 1994). Furthermore, Armstrong et al.'s (2016) research unveiled an intriguing pattern: in nourished areas, the largest homes tend to be among the most recently built. This observation might suggest an enduring pattern among homeowners to take on increased risk by constructing larger residences in hazard-prone regions, a trend that has found support in other empirical investigations (Braswell et al., 2022; Lazarus et al., 2018).

Despite the unquestionable significance of this research, it is important to note that Armstrong et al.'s (2016) study encountered specific data limitations that constrained their findings. The property-level dataset used in their analysis lacked essential tax-related details, such as property values and sale dates. Consequently, the study's results were confined to a snapshot of the spatial characteristics of the built environment at the time of assessment. Additionally, the assessment of property values depended on indirect criteria, specifically property size. These limitations are common when investigating dynamics that require comprehensive housing data encompassing both physical and socio-economic attributes. Access to such data is often hindered by challenges like inconsistent availability, associated costs, privacy concerns, or infrequent updates of existing datasets (Lu et al., 2013). Nonetheless, emerging data sources, including remote sensing, industry-generated data (e.g., Google Maps, Microsoft Maps), volunteered geographic information (e.g., OpenStreetMaps), and cadastral and tax data, are increasingly providing easily accessible data on building stock and its attributes. These sources have the potential to become valuable assets in the context of coastal risk research.

In cases where structural variables, such as house type or total living area, are unavailable, alternative data sources, like building footprints derived from remote sensing, can serve as reasonable substitutes (Lu et al., 2013). While the plan-view area of a building may not provide a perfectly accurate measurement—as it could either underestimate the total living space of multi-story houses or overstate the area of single-story homes with extensive covered porches—it still offers a valuable estimate for assessing. For example, in the study conducted by Lazarus et al. (2018), residential building footprints were manually extracted from satellite imagery to examine long-term development trends in hurricane-prone regions over 5 to 14 years. Their findings revealed that reconstruction efforts often led to the creation of larger and more densely built environments, consequently increasing exposure to natural disasters. This counterintuitive trend, referred to as *building back bigger* (Lazarus et al., 2018), received further confirmation from Braswell et al. (2022), who used gridded historical settlement data layers from HISDAC-US, derived from Zillow's ZTRAX database, to analyze building patterns in areas at risk of sea-level rise. Their research concluded that high-risk coastal areas tend to exhibit denser and more intensively developed built environments compared to regions with lower risk levels.

Here, we leverage comprehensive housing datasets encompassing both structural and economic information, in conjunction with the locations of beach nourishment projects, to investigate spatial development patterns in two coastal regions that are widely recognized as hotspots for coastal risk: New Jersey and Florida. New Jersey, the most densely populated state in the US (Cooper et al., 2008), houses approximately 7.15 million people, constituting roughly 80% of its population, in coastal areas (NOAA, 2022). Its barrier islands, with a population density of 915 permanent residents per square kilometer, rank second only to those in New York (Zhang and Leatherman, 2011). Yet, New Jersey's coastlines are highly susceptible to Nor'easters, severe storms, and hurricanes, which have resulted in numerous billion-dollar disasters (NOAA, 2022). Since the 1990s, the state has faced the impact of 27 significant storms, including the devastating Hurricane Sandy in 2012 and the more recent Hurricane Ida in 2021. Similarly, Florida, which boasts the longest extent of barrier islands in the country (Zhang and Leatherman, 2011), has experienced the effects of 86 storms in recent decades, including eleven major hurricanes classified as Category 3 to 5. Consequently, both regions have a rich history of beach replenishment programs dating back to the 1930s-1940s, accounting for 13% and 20% of the total beach nourishment projects conducted in the United States during the 20th century, respectively (Campbell and Benedet, 2006; Elko et al., 2021).

This research primarily focuses on New Jersey's barrier islands due to the availability of an extensive tax record dataset spanning over two decades (1995-2016), which includes physical attributes like building location, property type, total living area, and other typically hard-to-obtain data, such as sale date and price. When classifying the barrier island

municipalities into nourishing and non-nourishing zones (**Fig. 3.1a**), we find that, even though some municipalities nourish more than others (**Fig. 3.1b**), the cumulative number of beaches using these practices has steadily increased since the 1930s, and most especially since the 1960s (**Fig. 3.1c**), when this practice gained popularity throughout the United States (Trembanis et al., 1999) and Europe (Hanson et al., 2002). While the number of non-nourishing municipalities is higher (**Fig. 3.1d**), the municipal sections of the barrier islands that had at least one beach nourishment event between 1995 and 2016 are larger (**Fig. 3.1e**) and have a longer Atlantic shoreline length (**Fig. 3.1f**). Consequently, there is a greater concentration of houses in nourishing zones compared to non-nourishing municipalities (20,647 and 12,903 properties, respectively). Additionally, we observe that houses located in areas with beach nourishment practices tend to have higher property values, commanding an average premium of 12% compared to residences in non-nourishing areas. Property prices also exhibit a positive correlation with proximity to the beach, meaning that houses closer to the beach tend to have higher prices. Houses in nourishing areas are also larger. Although there is a general trend of increasing property size over time, the proportion of houses undergoing expansion is notably higher in nourishing municipalities (30%) compared to non-nourishing zones (23%). The former also exhibit higher growth rates in terms of property size compared to their non-nourished counterparts.

We confirm the validity of the identified patterns in New Jersey using two distinct methodologies. Firstly, we use the HISDAC-US historical layers (Leyk and Uhl, 2018), derived from an independent housing database (ZTRAX), to assess changes in built-up intensity along New Jersey’s barrier islands from 1995 to 2015. Our analysis reveals a consistent upward trend, notably prominent in areas with beach nourishment projects. Secondly, we investigate whether this expansion of the built environment is similarly evident in other vulnerable regions, such as Florida. By examining data from the Florida Department of Revenue's tax database spanning the years 2012-2017, we show that shorefront family homes along Florida’s Atlantic and Gulf coasts, especially those in nourishing zones, not only exhibit larger sizes and higher values but also demonstrate notable growth rates over time. Remarkably, this trend persists even in towns like Naples or Palm Beach, which have endured recurrent damage from disruptive storms.

The consistency of our findings across diverse datasets and regions provides compelling evidence that increased exposure to coastal risk is a persistent pattern along developed coastlines in the United States. These observations emphasize the pressing need for comprehensive policy interventions aimed at mitigating the risks associated with ongoing coastal development and enhancing the resilience of coastal communities to natural hazards.

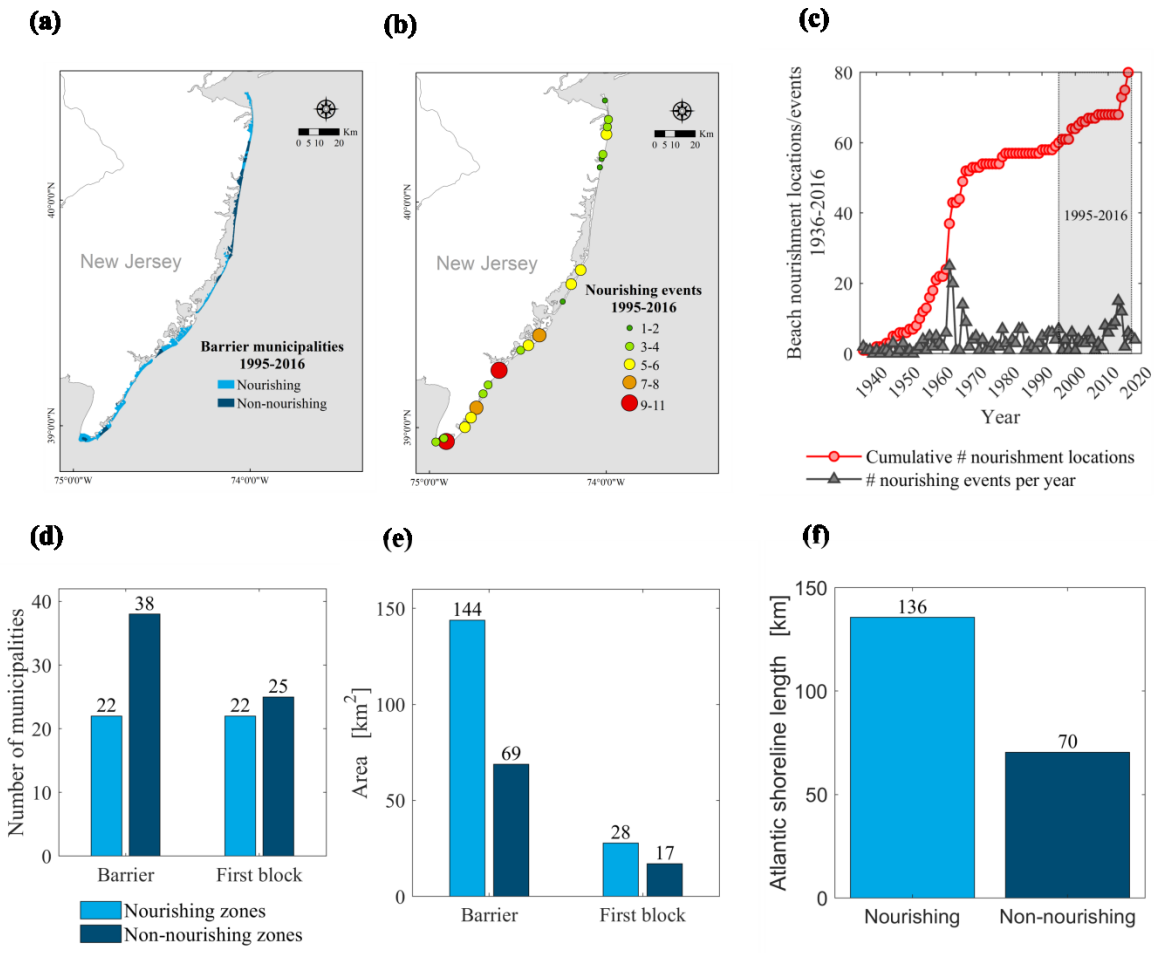

Figure 3.1 Beach nourishment in the barrier islands of New Jersey. (a) Barrier island outlines divided into nourishing (light blue) and non-nourishing (dark blue) municipalities. (b) Map of recorded beach nourishment projects carried out in the barrier islands of New Jersey between 1995 and 2016. (c) Cumulative number of beach nourishment locations between 1940 and 2020 on the barrier islands of New Jersey and number of nourishment events per year. The gray square highlights our period of study (1995-2016). (d) Number of nourishing and non-nourishing municipalities that have jurisdiction in the barrier islands of New Jersey and, most specifically, in the first block of properties from the Atlantic shoreline. (e) Total area (in km2) of the nourishing and non-nourishing barrier and first block municipal sections. (f) Total length (in km) of the Atlantic shoreline in nourishing and non-nourishing areas of the New Jersey barrier islands.

3.3 Data and methods

3.3.1 Study area

To be used as masks throughout the analysis, we generate two polygon layers defining the boundaries of our study areas: the New Jersey barrier islands and the first block of properties from the Atlantic shoreline.

In ArcMap 10.7, we convert a polyline dataset outlining New Jersey's coastline (NJDEP, 2015) into a polygon layer and select only those polygons that delineate the geographic contours of the barrier islands. With this layer, we proceed to create a second dataset focused solely on the first row of properties. To do this, we start with the outer boundaries of the barrier islands and digitize the inner limits by tracing the layout of the nearest major road to the ocean, using OpenStreetMap as reference basemap. The two resulting polygon layers are subdivided into municipal jurisdictions by intersecting them with a dataset describing New Jersey's administrative divisions (NJOGIS, 2020).

3.3.2 Tax records

We source data on real estate transactions from SR-1A forms for four coastal counties in New Jersey: Atlantic, Cape May, Monmouth, and Ocean (NJ Treasury, 2018). These databases contain details on property sales across New Jersey counties for defined timeframes, which in this case span from the earliest available year, 1988, up to 2016, which marks the year in which the data was collected. Each entry in the resulting datasets corresponds to a distinct transaction and encompasses details such as building location (defined by the address), property type, year of construction, total living area (measured in square feet), sale date, and sale price. Additionally, each property is assigned a unique identifier, referred to as PAMS_PIN, enabling the tracking of sales transactions for individual properties over the timeframe.

Using R, the SR1-A data retrieved is cleaned and processed to ensure its integrity. This involves filtering out records to retain only those pertaining to residential buildings, and excluding any that are incomplete, contain errors, or lack critical information. Specifically, we eliminate records of properties constructed or sold before 1900 or after 2016, transactions with sale prices below $1,000, and properties with a total area less than 270 square feet (approximately 25 square meters). This cleaning process yields a refined dataset consisting of almost 350,000 transactions (exactly 349,015) from an initial pool of 677,851, capturing the sales of 226,164 unique residential properties between the years 1995 and 2016. We convert property size measurements to square meters and account for economic changes over time by adjusting sale prices to 2016 dollars using the Consumer Price Index (CPI) inflation calculator (U.S. Bureau of Labor Statistics, 2021).

To georeference the SR1-A records, we connect our curated property database to an extensive, georeferenced parcel dataset for New Jersey (NJOGIS, 2018) using ArcMap 10.7. This connection is based on a join operation, with PAMS_PIN as the linking field. Leveraging the two polygon layers created previously as masks, we generate two specific subsets of the SR1-A data. The first subset encompasses all residential properties located within the boundaries of the New Jersey barrier islands, comprising 54,472 transactions over 33,550 distinct properties. The second subset focuses on properties situated within the first block, containing 8,748 transactions related to 4,624 unique properties.

While our primary research interest centers on the analysis of transaction data over time, in which properties may be listed repeatedly for different sales, certain parts of this study require focusing on individual properties instead of transactions. To address this, we compile two additional datasets that include only unique PAMS_PINs: one for the barrier islands and another for the first block of properties. In instances where a property has been sold multiple times, possibly reflecting changes in size and value, we incorporate only the data from the most recent sale, capturing the latest characteristics of each property.

3.3.3 Beach nourishment

Beach nourishment, a soft engineering method that involves importing sand to counteract coastal erosion and increase beach width, is examined in this study through the historical database of beach nourishment projects, maintained by the Program for the Study of Developed Shorelines at Western Carolina University (PSDS, 2021). Recognized as the most detailed resource of its kind, the database identifies nourishment activities by listing the beach's name alongside its approximate two-dimensional coordinates (latitude and longitude).

In ArcMap 10.7, we import the beach nourishment dataset as a point layer using projects' coordinates, and remove any records conducted outside our designated study period. We then overlay the two polygon masks on the point layer of beach nourishment projects, classifying municipalities as "nourishing" if they have undertaken one or more beach nourishment projects between 1995 and 2016, evidenced by the presence of corresponding points within their boundaries. Municipalities without any projects in this timeframe are categorized as "non-nourishing" areas.

3.3.4 Historical Settlement Data Compilation for the United States (HISDAC-US)

The Historical Settlement Data Compilation of the United States, or HISDAC-US (Leyk and Uhl in 2018; Leyk et al. in 2020), provides a comprehensive description of the built environment across most of the contiguous United States for the period 1810-2015. Derived from property records compiled from the Zillow Transaction and Assessment Dataset

(ZTRAX), the database comprises gridded settlement layers generated at a 5-year temporal resolution and 250-meter spatial resolution. HISDAC-US offers various measures of settlement characteristics, including the year of the earliest construction, the count of built-up property records, and the built-up intensity (BUI), which represents the total gross indoor area of all built-up properties within a grid cell for a specific year. Here, we leverage the BUI layers to examine the evolution of coastal development in New Jersey's barrier islands during our timeframe and explore potential disparities between nourishing and non-nourishing municipalities.

In ArcMap 10.7, we load datasets from 1995, 2000, 2005, 2010, and 2015 and then clip them to match the boundaries of our defined study areas using mask layers for the barrier islands and the first block of properties. To monitor the evolution of built-up areas, we convert the clipped rasters into point layers, where each point indicates a specific level of built-up intensity. Additionally, we introduce a new integer field to each point to assign it a unique identifier. Subsequently, we perform a spatial join between these point layers and the polygons delineating the barrier islands and the first block properties, which are categorized by municipalities and labeled according to their beach nourishment status. This step allows us to identify the HISDAC-US points located within either nourishing or non-nourishing zones across our study areas.

3.3.5 Building footprints

Property taxes, such as those found in the SR-1A records, typically provide information about the total living area of the property, which includes the size of all the floors that constitute a house. Yet, despite its high accuracy, this metric is often unavailable, especially for large-scale analyses. Consequently, prior research has turned to using building footprints as an alternative to investigate spatial and temporal differences in house size (Lazarus et al., 2018). Given our access to the total living area, we have the opportunity to compare this with plan-view areas, enabling us to evaluate the feasibility of using building footprints when detailed property size data is not readily available.

For this analysis, we extract building footprints for the barrier islands of New Jersey from the US Building Footprints database (Microsoft, 2021). Initially, we identify 118,999 features overlapping with the boundaries of our study area. Using ArcMap 10.7, we refine this selection to include only those features that entirely fall within our composite of residential parcels, previously connected to SR1-A data via the PAMS_PIN. To enhance the precision of the resulting dataset, we exclude any feature smaller than 25 square meters, aiming to eliminate potential inaccuracies caused by slivers, digitization errors, or dataset overlaps. Subsequently, we execute a join operation in R to match the refined building footprints with the property tax records, using the unique PAMS_PIN as the key field. This procedure allows

us to simultaneously monitor each property's maximum total living space (as reported in the SR1-A data) alongside its covered footprint area (given by the Microsoft data). From this process, we derive a dataset encompassing 15,414 unique properties on the barrier islands and 1,685 unique properties in the first block. Each property is additionally associated with its corresponding municipality and categorized into either nourishing or non-nourishing zones, determined by their engagement in beach nourishment initiatives.

3.3.6 Florida

To explore whether similar trends are observable in other regions of the United States, we build upon the research conducted by Armstrong et al. (2016) and investigate changes in the size and value of shorefront single-family homes sold on the Atlantic and Gulf coasts of Florida between 2012 and 2017. For that, we acquire tax data from the Florida Department of Revenue in the form of Florida Parcel Statewide datasets, which are readily accessible through the Florida Geographic Data Library. The datasets cover the years 2012, 2014, 2015, and 2017 (Florida Department of Revenue, 2012; 2014; 2015; 2017). These collections feature parcel polygons for all listed properties within those years, alongside detailed attributes such as construction year, total living space, total property assessment, and occasionally, information on sale dates and sale prices.

Due to the large volume of entries in the Florida Department of Revenue datasets, we use ArcMap 10.7 to isolate properties situated within the first 50 meters of the shoreline, and keep only those identified as "single-family" homes. Because of prevalent inaccuracies and omissions in the sales data, in this case we use the "total assessment" field to evaluate property value, and the years of the datasets themselves, rather than sale dates, to facilitate comparisons over time. We then concatenate the resulting layers in a dataset encompassing 327,351 transactions associated with 114,315 distinct properties. To ensure data accuracy and consistency, we undertake a data cleaning process in R that excludes properties with a total living area less than 25 square meters and a total assessment value lower than $10,000. This results in a refined dataset comprising 324,728 transactions, representing 113,438 unique properties.

Following the methodology outlined by Armstrong et al. (2016), we use ZIP codes rather than municipalities, as they offer a more comprehensive coverage. We keep only those polygons that intersect with oceanfront properties and classify them based on the presence or absence of beach nourishment projects within each ZIP code, labeling them as nourishing or non-nourishing zones. Considering the relatively short duration of our study period in this region (2012-2017), we align with the timeframe used in the New Jersey analysis for identifying nourishing zones, specifically defining them as areas that have undergone at least one

beach replenishment project between 1995 and 2016, according to the PSDS beach nourishment database.

3.3.7 United States

To establish a national framework for our regional analysis, we use housing metrics sourced from the U.S. Census Bureau, specifically within the category of “Single-family sold”, which roughly corresponds to the SR-1A “Residential” class. For our analysis, we extract the annual mean house size and sale price of all single-family properties sold in the United States. These metrics are obtained from the “Square Feet” and “Sale Price” items, respectively (U.S. Census Bureau, 2021a; 2021b). Property size is converted to square meters, and property sale prices are adjusted to reflect 2016 US dollars using the Consumer Price Index (CPI) inflation calculator (U.S. Bureau of Labor Statistics, 2021).

3.4 Results

3.4.1 Increased property price

Between 1995 and 2016, the average price of residential properties sold in New Jersey’s barrier islands significantly exceeds the national average, standing at over three times the national figure ($3,900/m^2 compared to $1,410/m^2; **Fig. 3.2a**). While national property prices remain relatively stable over this period, property values on the barrier islands exhibit an upward trend from 2005 to 2010, reaching a peak at $5,568/m^2, before experiencing a 36% decline to $4,104/m^2 between 2010 and 2016. When comparing nourishing and non-nourishing areas, we find that houses in municipalities engaged in nourishment practices are, on average, 12% more expensive ($4,059/m^2) than those in non-nourishing areas ($3,616/m^2). However, the general decrease in property prices between 2010 and 2016 narrows this difference, with houses in both areas selling at comparable prices in the later years of the period. Properties located on the first block follow a similar trend (**Fig. 3.2b**), with prices being 11% higher in nourishing areas ($5,801/m^2) compared to non-nourishing zones ($5,223/m^2). In general, the average price for properties sold on the first block ($5,584/m^2) is 43% higher than the average for the entire barrier-island area and nearly five times the national average. Note that these figures incorporate all transactions, which could entail multiple values for the same property if it was sold more than once during the study period.

Fig. 3.2c-d provides a more comprehensive perspective on the relationship between property prices and distance from the Atlantic coast. In this case, the data used pertains to individual properties, rather than transactions. For properties with multiple transactions, the analysis relies on the size and price recorded during the most recent sale. We find that nearly all residential properties on the barrier islands, amounting to 99.8% of all houses, are

situated within 2.5 kilometers of the coastline (**Fig. 3.2c**), illustrating the narrowness of these geomorphological units, with the only exceptions being in Lower Township, a nourishing municipality. Concerning property values, a clear correlation is evident, where houses located closer to the shoreline command higher prices, particularly in nourishing areas. The average price per square meter in the barrier islands stands at $4,064, rising to $6,116 for properties in the first block. Among the first-block properties, those built within 500 meters of the beach, constituting 97% of all first-block properties, have an average price of $6,222/m^2. This value further increases to $6,960/m^2 for properties within 100 meters of the beach (representing 37% of first-block properties) and reaches $8,082/m^2 for those within the first 50 meters of the beach (comprising 8% of homes in the first block). Moreover, the proportion of first-block houses located closer to the ocean is higher in nourishing areas (**Fig. 3.2d**), with 58%, 64%, and 80% of the properties built within 500 meters, 100 meters, and 50 meters of the shoreline, respectively, situated in municipalities that nourish.

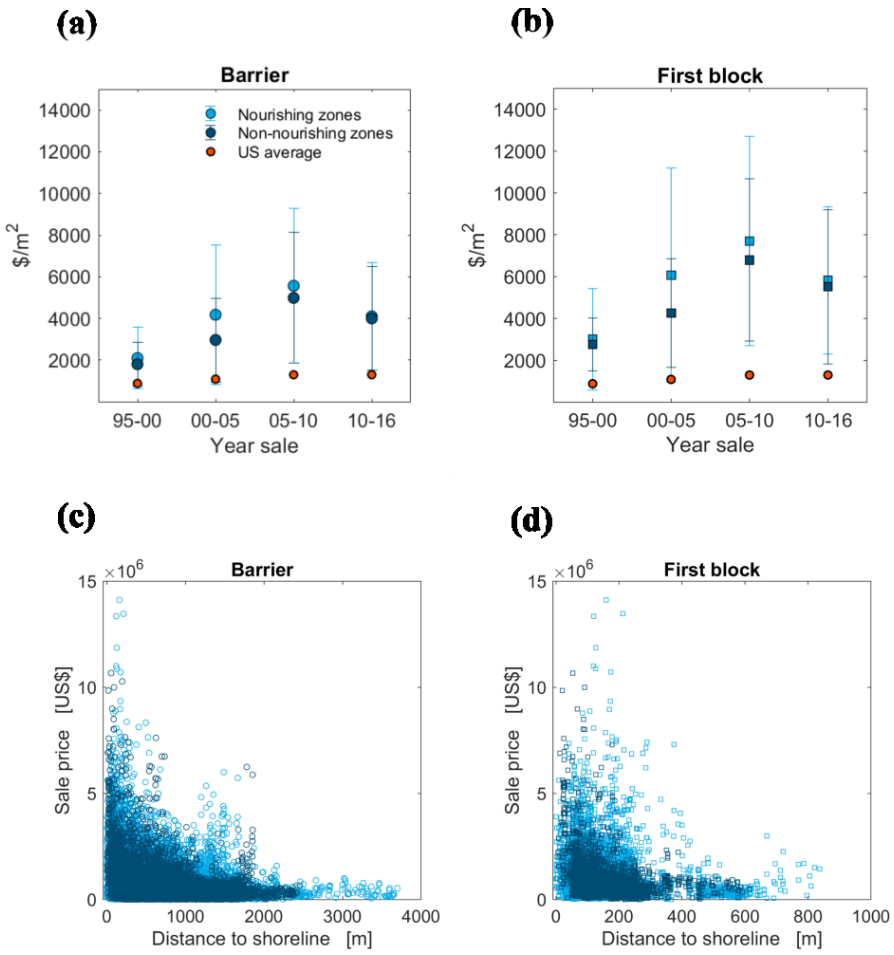

Figure 3.2 The revalorizing effect of beach nourishment. Evolution of mean house price (in $/m^2) for residential properties sold in the barrier islands of New Jersey (a) and the first block of properties from the Atlantic shoreline (b) between 1995 and 2016, compared to the national average. Relationship between sale prices (in $)

and distance to the shoreline (in meters) for barrier islands (c) and first-block residential properties (d).

3.4.2 Increased property size

Residential properties sold in New Jersey's barrier islands between 1995 and 2016 are, on average, 43% smaller than the national average for the same time period (157 m^2 compared to 223 m^2, respectively). Comparing property sizes in nourishing and non-nourishing zones, we find that houses on the barrier islands in nourishing areas are, on average, 4% larger than those built in non-nourishing towns (**Fig. 3.3a**). This difference becomes more pronounced for first-block houses, which are more influenced by the presence or absence of nourishing practices. As shown in **Fig. 3.3b**, first-block houses in nourishing municipalities are, on average, 13% larger (168 m^2) than those in non-nourishing areas (148 m^2), although these differences vary considerably over time. During the initial half of the study period (1995-2005), houses sold in areas with nourishing events are over 25% larger compared to those in non-nourishing zones, while in the latter half (2005-2015) the difference is less pronounced at 7%.

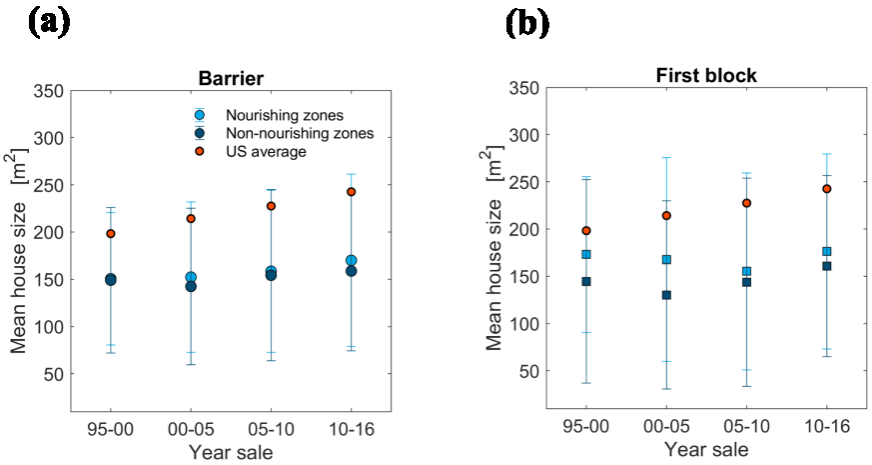

Figure 3.3 Changes in mean house size in the barrier islands of New Jersey (a) and the first block of properties from the Atlantic shoreline (b) between 1995 and 2016.

When examining changes in the total living area of residential properties that were sold more than once between 1995 and 2016, we find that a significant portion of homes experience an increase in size over time, particularly in nourishing municipalities. About 30% of barrier properties in nourishing areas grow in size over the study period, while 55% remain unchanged and only 15% experience a decrease (**Fig. 3.4a**). Similarly, in the first block of properties, 30% increase in total living area over time, and only 17% decrease it (**Fig. 3.4b**). Conversely, in non-nourishing areas, the proportion of houses growing in size over time is lower, both in the barrier islands and in the first block of properties. **Figs. 3.4c-d** indicate that

23% of the barrier-island houses and 22% of the first-block properties expand between 1995 and 2016, while the vast majority remain unchanged (66% and 71%, respectively).

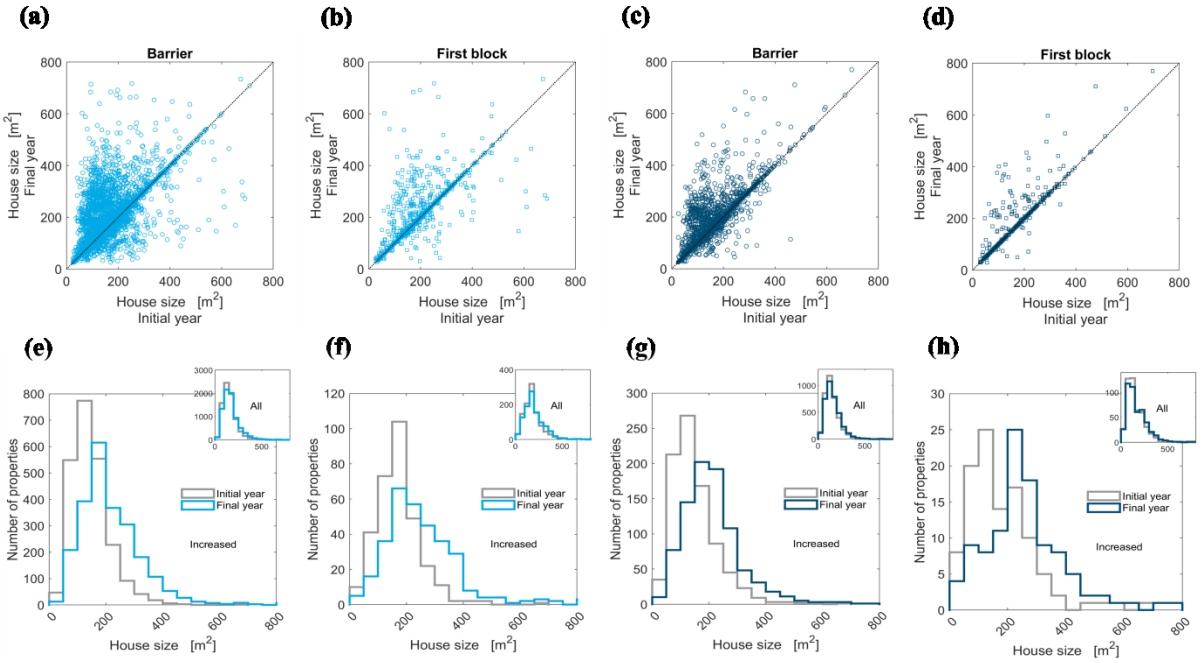

Figure 3.4 Changes in property size for houses sold more than once between 1995 and 2016 in the barrier islands of New Jersey and in the first block of properties. The scatterplots (a-d) compare the size of these properties the first and last time a sale was recorded in the tax database, both in nourishing (a-b) and non-nourishing municipalities (c-d). The histograms (e-h) represent the distributions of properties that increased their size over time according to their total living area the first time they were sold (in gray) and the last time their size was recorded in the database (in blue), both in nourishing (e-f) and non-nourishing areas (g-h). Insets in e-h show initial and final year distributions of all properties in a-d.

When considering only properties that increase in size over time, the statistical distributions reveal similar trends in both nourishing and non-nourishing areas. In the barrier islands, houses in nourishing municipalities increase by 50%, going from an average of 145 m^2 at their first recorded sale to 217 m^2 at their last recorded sale (**Fig. 3.4e**). Properties in non-nourishing zones experience slightly less growth (42%), increasing from an average size of 150 m^2 to 213 m^2 (**Fig. 3.4g**). In the first block, on the other hand, there are barely differences in size growth over time between nourishing and non-nourishing zones. On average, first-block houses in nourishing municipalities increase by 48%, growing from an average of 171 m^2 when first recorded to 253 m^2 when last appearing in the database (**Fig. 3.4f**). Similarly, in non-nourishing areas, their average size increases by 47%, from 175 m^2 to 256 m^2 (**Fig. 3.4h**).

3.4.3 Increased built-up intensity

We also examine changes in coastal development on New Jersey's barrier islands between 1995 and 2015 using gridded settlement layers from HISDAC-US (Leyk and Uhl, 2018), which are derived from property data compiled in the Zillow Transaction and Assessment Dataset (ZTRAX). Focusing on the built-up intensity (BUI), defined as the sum of the gross indoor area of all properties located in a grid cell in a given year, we find that both nourishing and non-nourishing municipalities experience similar growth patterns, although the increase is slightly higher in areas that nourish. Over the study period, total gross building area increases by 37% in nourishing municipalities (**Fig. 3.5a**) and by 36% in non-nourishing zones (**Fig. 3.5c**) for the barrier islands of New Jersey. As shown in **Figs. 3.5c-d**, the differences between nourishing and non-nourishing zones are also similar in the first block of properties (42% and 41%, respectively), although the growth rate in these areas is exceeds the barrier-island average.

When examining the evolution of the mean building intensity per cell between 1995 and 2015, we do observe that gross indoor area is consistently higher in municipalities that nourish, both in the barrier islands (**Fig. 3.5e**) and in the first block of properties (**Fig. 3.5f**). On average, nourishing zones are 5% more intensively developed than non-nourishing areas in the barrier islands, and 6% in the first block of properties. This difference is more pronounced in 2005 when the total built-up area is 7% higher in the barrier islands and almost 9% higher in the first block of properties.

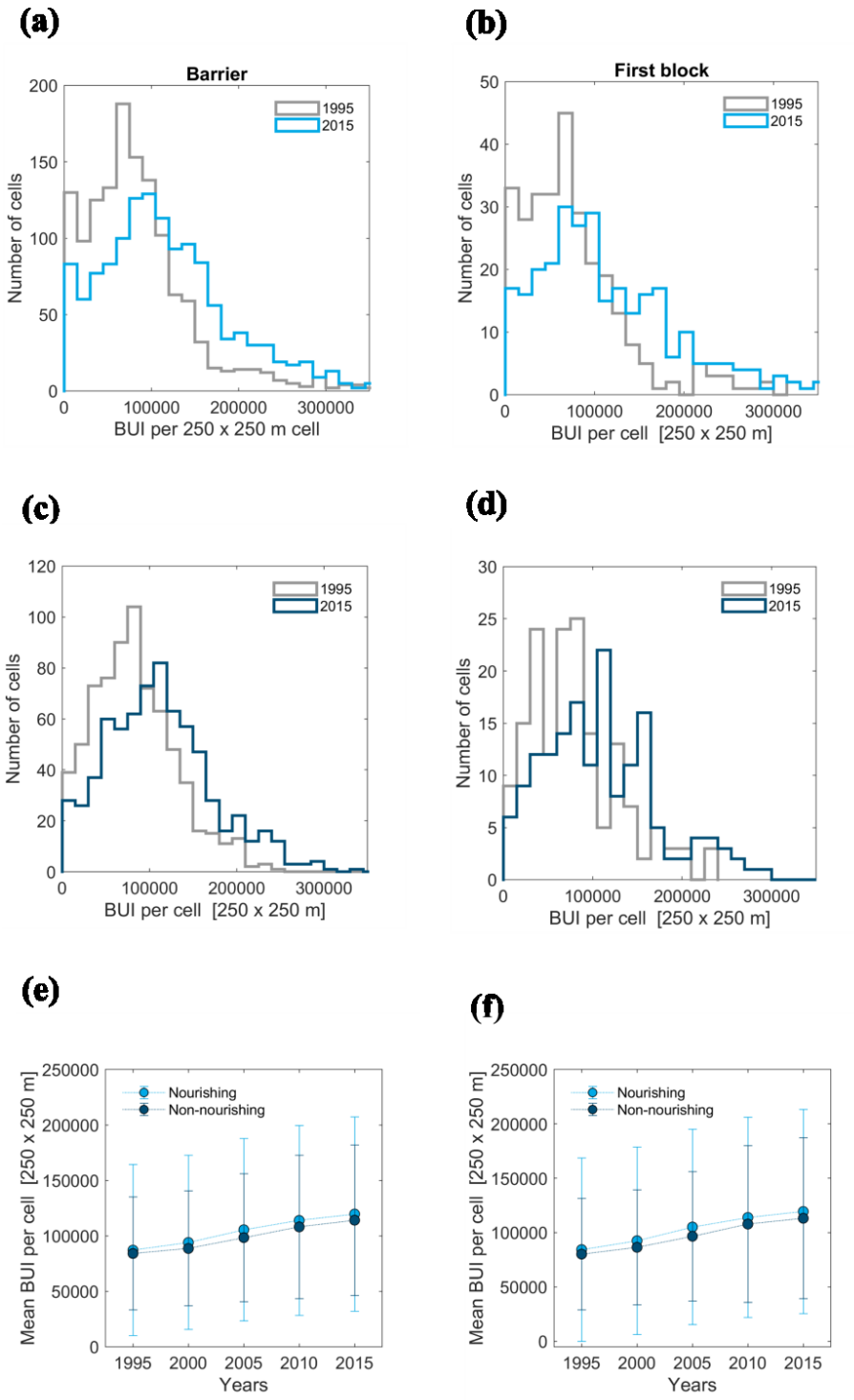

Figure 3.5 Changes in built-up intensity from 1995 to 2015 according to the HISDAC-US database. (a-b) Comparisons in built-up intensity for all raster cells located in nourishing areas of the barrier islands of New Jersey and the first block of properties. (c-d) Comparisons in built-up intensity for barrier and first-block cells located in non-nourishing municipalities. (e-f) Evolution of the mean built-up intensity during our period of study in nourishing and non-nourishing municipalities of the barrier islands and the first block of properties.

3.4.4 Scaling relationships

3.4.4.1 Sale price versus property size

We examine the correlation between house size and house wealth using samples of the tax database containing data for unique properties, rather than transaction records. Thus, for properties that are listed multiple times in the database, we specifically consider the sale price and total living area values recorded during their most reacent sale. Our findings reveal a positive linear relationship between property size and property price, indicating that larger homes typically command higher prices. This relationship holds true for both nourishing and non-nourishing municipalities in the barrier islands (**Fig. 3.6a**), with the most notable effect observed in the first block (**Fig. 3.6b**).

It is important to note that, even after our cleaning process, the tax databases still contain some records with questionable values, including very small areas or extremely low sale prices. Consequently, a larger sample size introduces greater variability among the analyzed variables. Therefore, the coefficient of determination (R^2) tends to be higher in non-nourishing areas, especially in the first block of properties, which has the smallest sample size.

3.4.4.2 Total living area versus plan-view area

We solely rely on the total living area reported in SR-1A forms, which includes the combined area of all floors of a property, for all calculations in our analysis. However, accessing this metric for large-scale analyses might pose challenges. In such situations, building footprints can serve as a viable alternative when other data is unavailable. Here, we explore how building footprints scale relative to total living area using footprint data from the Microsoft database. Our results show that, on average, the total living area is 11% larger than building footprints in the barrier islands (**Fig. 3.6c**), and 23% greater in the first block (**Fig. 3.6d**). Applying these scaling factors to mean footprint values would enable comparisons with statistics based on total living area.

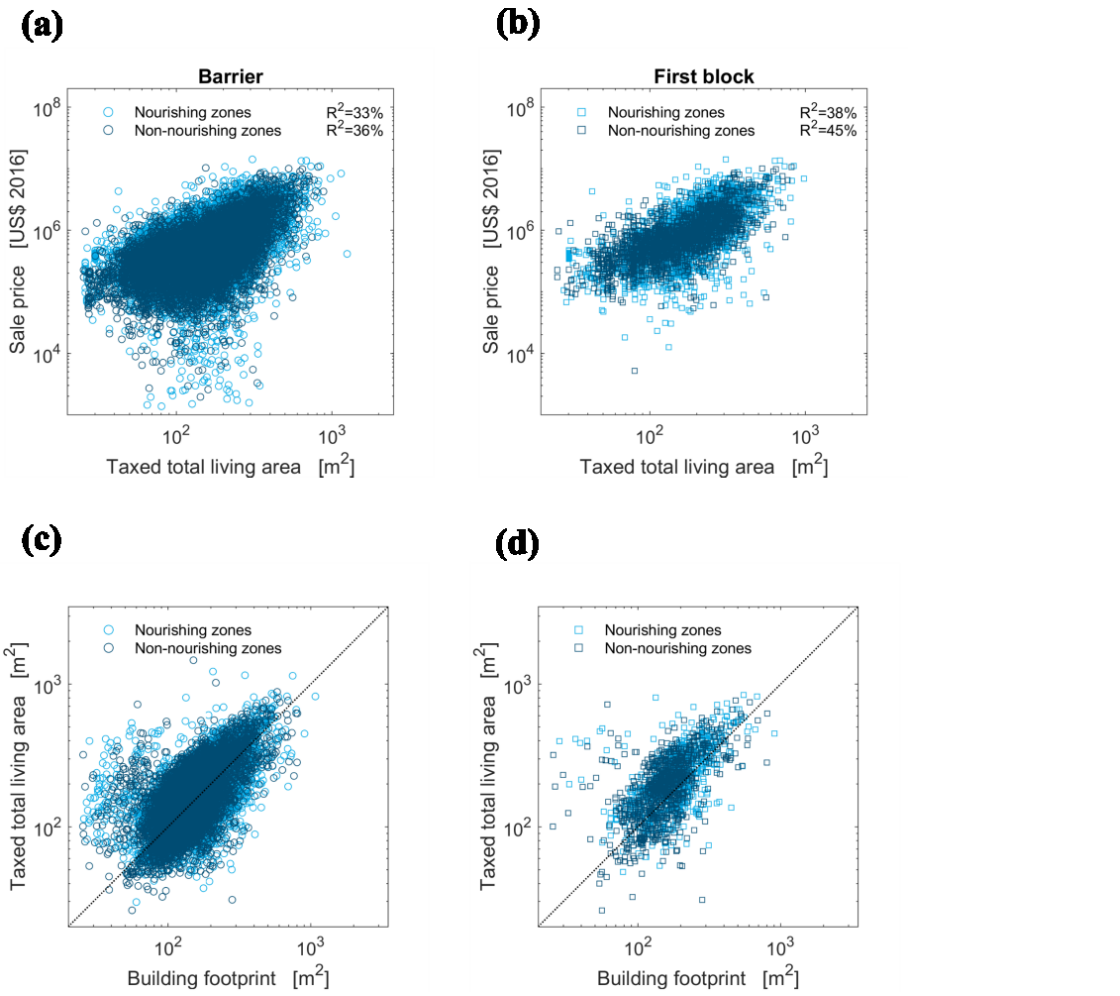

Figure 3.6 Scaling relationships between sale price and total living area (a-b) and total living area and building footprint (c-d) in the barrier islands of New Jersey and the first block of properties.

3.4.5 Florida

Analyzing changes in property prices along the Atlantic and Gulf Coasts of Florida from 2012 to 2017, we find that shorefront family houses in Florida are nearly twice the national average, with prices averaging $2,490/m² compared to the national average of $1,402/m². Nourishing zones generally exhibit 32% higher values than non-nourishing areas ($2,810/m² and $2,136/m², respectively), with a global increase of 21% in property value over the study period (**Fig. 3.7a**). Comparison between the Atlantic and Gulf coasts (**Figs. 3.7b-c**) reveals significant differences between the two regions. Houses on the Gulf Coast are, on average, 27% more affordable than those on the Atlantic Coast ($2,225/m² and $2,829/m², respectively), and show the greatest disparity between nourishing and non-nourishing areas. Houses on the Atlantic Coast are 9% more valuable in nourishing ($2,930/m²) than in non-nourishing zones ($2,697/m²), while on the Gulf Coast, properties in nourishing areas are 53% more expensive than those in non-nourishing areas, with average prices of 2,702 $/m² and 1,764 $/m², respectively.

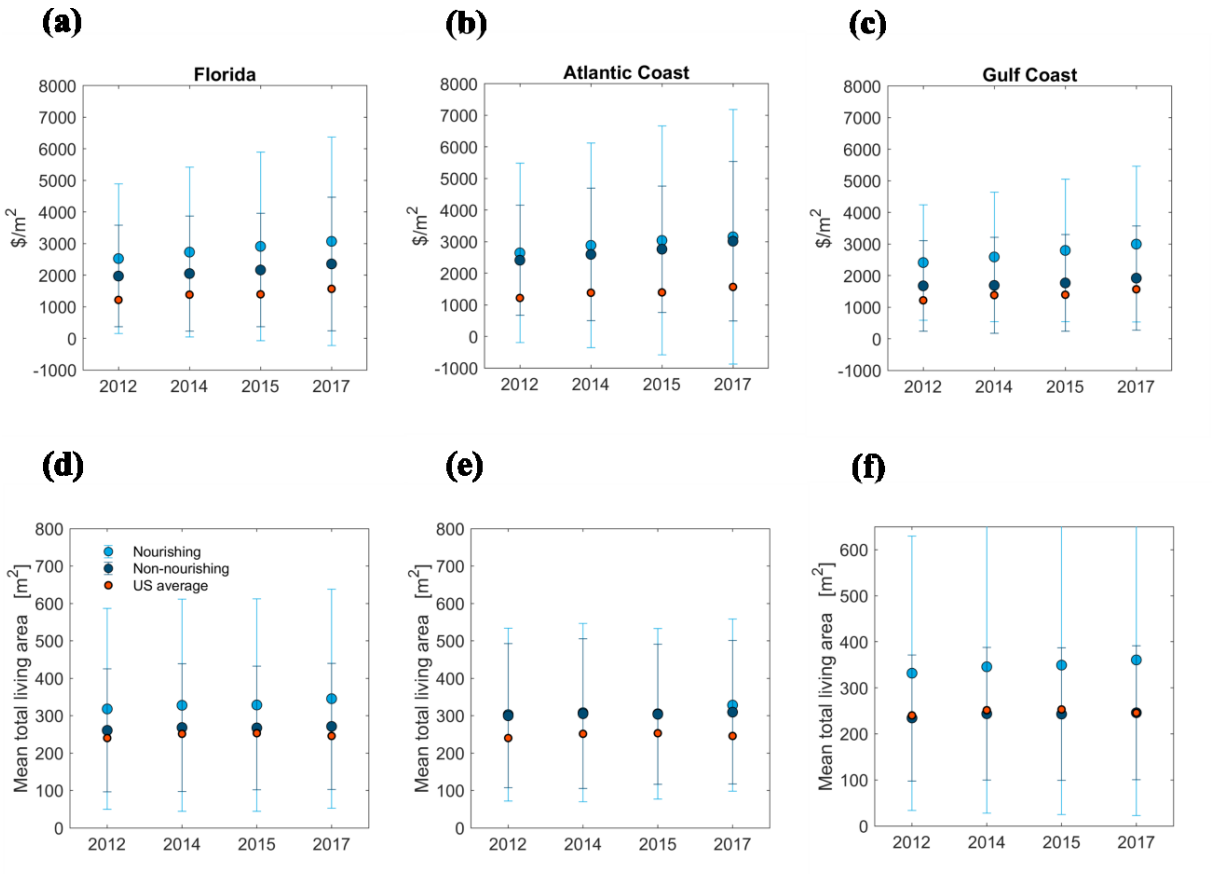

Figure 3.7 Changes in property price (a-c) and property size (d-f) of shorefront single-family houses in the Atlantic and Gulf Coasts of Florida.

Our study also indicates that properties located along the Atlantic and Gulf Coasts of Florida are, on average, 21% larger than the national average during the period of 2012-2017 (300 m^2 and 247 m^2, respectively). Additionally, shorefront family houses tend to be 24% larger in nourishing areas than in non-nourishing towns, with average sizes of 330 m^2 and 267 m^2, respectively (**Fig. 3.7d**). We also observe a more significant increase in property size over time in nourishing areas (9%) compared to non-nourishing zones (4%), with notable differences between the Atlantic and Gulf coasts. Overall, properties located on the Atlantic Coast are 5% larger than those on Florida's Gulf Coast, with similar average sizes observed in both nourishing and non-nourishing zones (311 m^2 and 305 m^2, respectively; **Fig. 3.7e**). Conversely, properties situated on the Gulf Coast exhibit greater variation, with houses in nourishing areas being 30% larger than those in non-nourishing zones (347 m^2 and 242 m^2, respectively; **Fig. 3.7f**). Notably, while the mean house size in non-nourishing zones along the Gulf Coast is comparable to the national average, properties situated in nourishing areas exceed the US average by 40%.

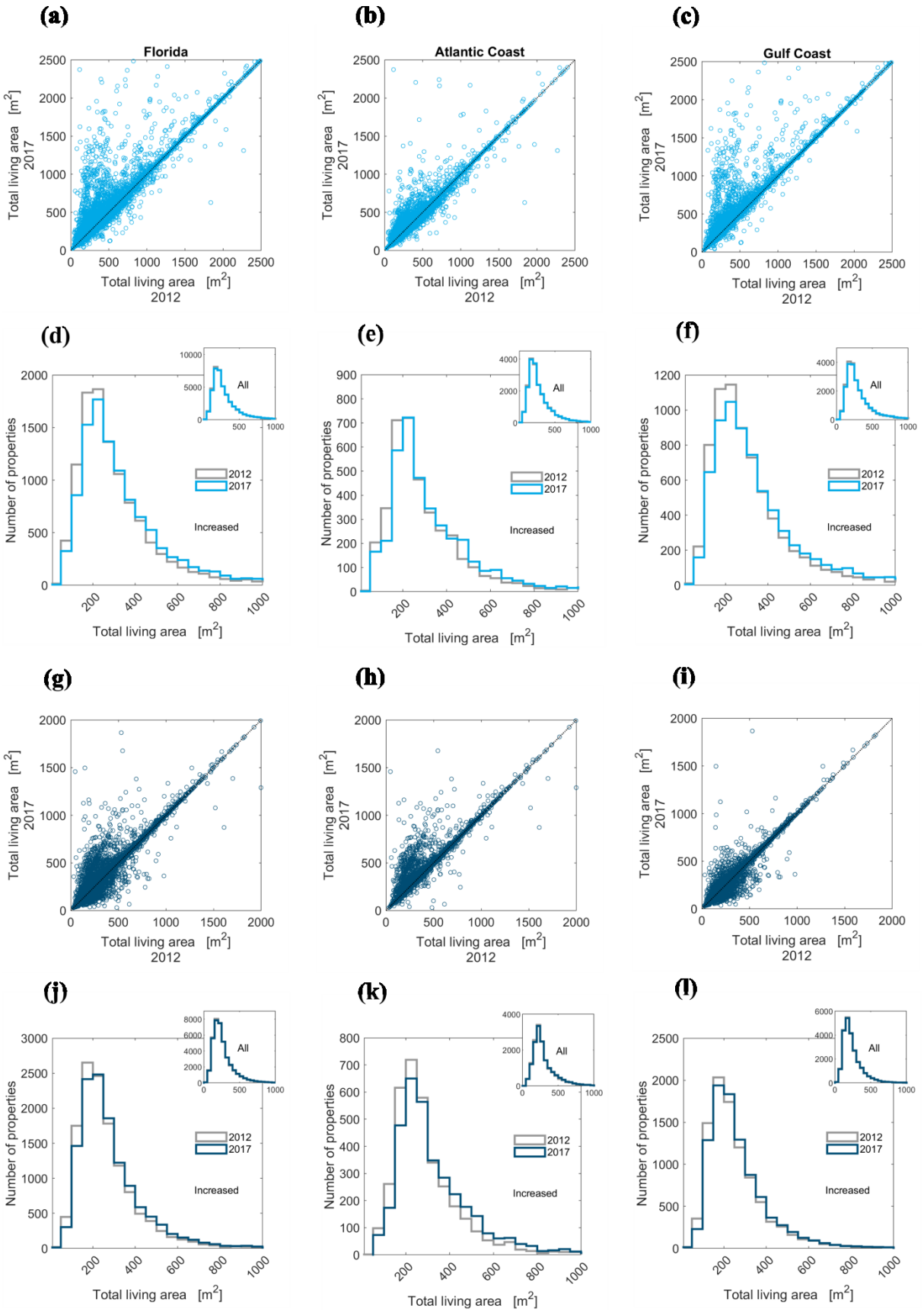

Figure 3.8 Changes in property size for houses sold more than once between 2012 and 2017 in the Atlantic and Gulf Coasts of Florida. The scatterplots compare the size of these properties the first and last time a sale was recorded in the tax database in nourishing (a-c) and non-nourishing municipalities (g-i). The histograms represent the distributions of properties that increased their size over time according to their

total living area the first time they were sold (in gray) and the last time their size was recorded in the database (in blue), both in nourishing (d-f) and non-nourishing areas (j-l). Insets in the histograms show initial and final year distributions of all properties in the database.

As in the analysis conducted in New Jersey, we examine changes in total living area over time in Florida by tracking properties that appear more than once in the database. We find a significant increase in the mean size of single-family homes, particularly in nourishing areas. Shorefront family homes situated in nourishing communities in Florida experience 26% increase in size between 2012 and 2017, with an average growth rate of 3% (from 322 m^2 to 332 m^2; **Fig. 3.8a**). This growth, however, is not evenly distributed across regions. Properties on the Atlantic Coast exhibit a modest 1.4% increase (from 301 m^2 to 305 m^2; **Fig. 3.8b**), while homes on the Gulf Coast see a more significant 5% increase (from 341 to 357 m^2; **Fig 3.8c**). Additionally, a higher percentage of properties on the Gulf Coast (31%) undergo size increases over time compared to their counterparts on the Atlantic Coast (19%).

Similarly, 33% of shorefront family homes in non-nourishing areas experience an increase in size between 2012 and 2017. However, the rate of growth is lower than that in nourishing areas, with only a 1.4% increase. Interestingly, on the Atlantic Coast, non-nourishing communities witness the most substantial increase in property size (2.7%), with average sizes growing from 300 m^2 to 308 m^2 (**Fig. 3.8h**). On the Gulf Coast, on the other hand, nearly 40% of properties located in non-nourishing areas register an increase in property size, but the average size sees minimal change between 2012 and 2017, going from 242 m^2 to 244 m^2 (**Fig. 3.8i**).

When considering only properties that experience an increase in size over time, the statistical distributions indicate a consistent growth in property size along the coasts of Florida. However, the growth rate is higher in nourishing areas (16%, from an average of 320 m^2 in 2012 to 370 m^2 in 2017; **Fig. 3.8d**) than in non-nourishing zones (8%, from 268 m^2 to 288 m^2; **Fig. 3.8j**). When conducting a coast-to-coast comparison, we see that the Atlantic Coast experiences a similar increase of 14% in both nourishing and non-nourishing areas, although houses in nourishing zones are slightly larger (304 m^2 in 2012 and 348 m^2 in 2017; **Fig. 3.8e**) than those in non-nourished towns (298 m^2 in 2012 and 341 m^2 in 2017; **Fig. 3.8k**). Conversely, the Gulf Coast shows a significant difference between nourishing and non-nourishing areas. Homes in nourishing zones not only exhibit significantly larger sizes compared to those in non-nourishing zones, but they also demonstrate a 16% increase in size over time, growing from 328 m^2 to 381 m^2 (**Fig. 3.8f**). Properties in non-nourishing areas, on the other hand, only show a 5% increase during the same period (from 256 m^2 to 268 m^2; **Fig. 3.8l**).

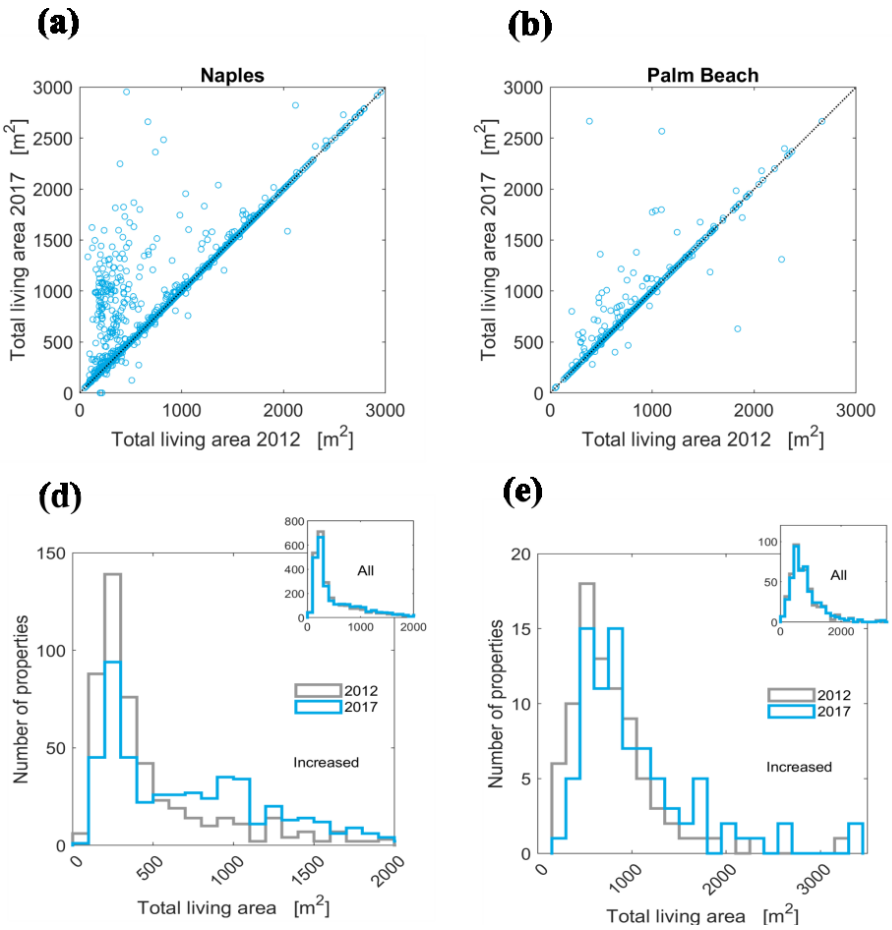

Figure 3.9 Changes in property size for houses sold more than once between 2012 and 2017 in two storm-prone locations: Naples and Palm Beach. The scatterplots (a-b) compare the size of these properties the first and last time a sale was recorded in the tax database, and the histograms (c-d) represent the distributions of properties that increased their size over time, according to their total living area the first time they were sold (in gray) and the last time their size was recorded in the database (in blue). Insets in the histograms show initial and final year distributions of all properties in the database.

The ongoing growth in property size along the Atlantic and Gulf coasts of Florida carries significant implications for storm-prone coastal towns like Naples on the Gulf Coast or Palm Beach on the Atlantic Coast. Despite facing recurrent property and infrastructure damage, a substantial percentage of shorefront single-family homes in these regions undergo expansion over the study period. In Naples, approximately 21% of homes located in ZIP codes with nourishing events experience an increase in size between 2012 and 2017 (**Fig. 3.9a**), showing an average growth rate of 59% (from 556 m^2 to 886 m^2; **Fig. 3.9c**). Similarly, in Palm Beach, 18% of properties increase their size between 2012 and 2017 (from 808 m^2 to 1,046 m^2), with a 30% growth rate (**Fig. 3.9b**).

3.5 Implications

3.5.1 The revalorizing effect of beach nourishment

Previous empirical research in specific coastal communities has shown that beach nourishment has a revalorizing effect on shorefront properties. Wide beaches and closer proximity to the shoreline increase property values (Landry et al., 2003; Pompe and Rinehart, 1995; Qiu and Gopalakrishnan, 2018) and help property owners maintain house prices stable (Blackwell et al., 2010). However, conclusions drawn from case studies are location-specific and may not necessarily extend to larger spatial scales (Di Baldasarre et al., 2018; Laundry et al., 2003). Hence, the present study seeks to investigate the impact of beach nourishment on property values at a more extensive geographical scope, encompassing two distinct geographical regions. The objective is to demonstrate that the proposed relationship remains consistent regardless of local management practices, policies, or regulations.

Our results are suggestive that beach replenishment has a large and positive effect on property values. Residential properties sold in New Jersey and Florida command a premium of 12% and 32%, respectively, compared to houses in non-nourishing zones. Furthermore, it is evident that properties situated closer to the beach tend to command higher prices than those located farther inland, particularly in municipalities that undergo nourishment efforts (**Figs. 3.4c-d**). Specifically, our research in New Jersey reveals that first-block houses are, on average, 50% more expensive than those on the barrier islands ($6,116/m^2 and $4,064/m^2, respectively), and approximately 10% more valuable in nourishing zones compared to non-nourishing areas ($6,359/m^2 and $5,770/m^2, respectively). These findings align with prior assertions that beach nourishment can elevate property prices, not only for oceanfront properties but also for non-waterfront houses located a few rows inland (Kriesel and Friedman, 2002).

The revalorizing effect of beach nourishment on property values can be assessed by examining not only its effect on sale prices but also its influence on property sizes. In fact, in instances where economic data is unavailable, the size of a house can serve as an indicator for assessing relative property wealth (Armstrong et al., 2016). In our analysis of the relationship between property size and price, we consistently observe that larger houses tend to command higher sale prices than smaller dwellings (**Fig. 3.6a-b**). Furthermore, properties sold in areas with beach nourishment tend to exhibit larger sizes compared to those in non-nourishing towns. For instance, in New Jersey, first-block properties sold in nourishing municipalities are 14% larger than those in non-nourishing municipalities. In Florida, shorefront houses in nourishing towns are 24% bigger, although there are noticeable variations between the East and Gulf Coasts: while on the Atlantic Coast the mean house size is similar in both areas (311 m^2 and 305 m^2, respectively), houses in nourishing areas of

the Gulf Coast are 30% bigger than those in non-nourishing towns (347 m^2 and 242 m^2, respectively).

Ultimately, our research suggests that nourishing areas tend to have a higher proportion of high-value properties, regardless of the region analyzed or the metric used to measure property wealth. This overarching trend could be indicative of the intertwined nature of property values and coastal protection. Wide and protected beaches may lead to high-value coastal development, which then requires further protection (Armstrong et al., 2016; McNamara et al., 2015; Mileti, 1999; Nordstrom, 2004). Without coastal protection, house values on vulnerable coastlines would likely experience vastly different outcomes (Lazarus, 2014; Mileti, 1999; Werner and McNamara, 2007).

3.5.2 Increased exposure in high-risk coastal development in nourishing areas

Increasing exposure has been identified as a key driver of worsening losses from natural events (Cutter & Emrich, 2005; Iglesias et al., 2021; IPCC, 2012; Lazarus et al., 2018). In the United States, a notable 57% of existing structures are situated in regions prone to natural hazards. Moreover, both population and urban development in these vulnerable areas are steadily increasing, particularly along hazardous coastlines (Braswell et al., 2022; Iglesias et al., 2021). Coastal communities in the US are characterized by denser and more intensely developed built environments compared to inland areas, even in regions with an elevated risk of catastrophic events (Braswell et al., 2022). Hurricane-prone zones, for example, are more developed than areas not at risk and have experienced more rapid increases in building density over time (Braswell et al., 2022; Iglesias et al., 2021). Our findings not only confirm the existence of this widespread pattern of increased exposure in high-risk coastal development but also provide evidence that beach nourishment may be a catalyst for these unintended dynamics.

This analysis, based on multiple appearances of properties in tax databases, provides evidence that houses are gradually increasing in size over time, thereby contributing to heightened exposure in coastal areas prone to hazards, such as the barrier islands of New Jersey and the Atlantic and Gulf coasts of Florida. Moreover, the expansion of coastal development varies significantly between nourishing and non-nourishing zones. A notably higher proportion of larger properties are located in nourishing areas, which also exhibit a faster growth rate in property size. In New Jersey, there is approximately a 30% increase in the size of residential properties sold in nourishing zones between their first and last recorded measurement in the database for the period 1995-2016. In contrast, non-nourishing areas, although they also exhibit a growing trend in housing size over time, have a lower proportion of properties (23%) with increased sizes compared to nourishing areas, and the rate of growth is also slower (42%). A comparable pattern is observed in Florida from 2012 to

2017, with nourishing zones experiencing higher growth rates (3%) than non-nourishing zones (1.4%), despite both having similar proportions of properties expanding in size over that period (26% and 33%, respectively).

Considering that the disparities between nourishing and non-nourishing regions are consistently observed across datasets originating from different sources and geographic regions, it is unlikely that these spatial correlations are mere coincidences. Nonetheless, we conduct another evaluation to determine if similar development patterns emerge from alternative data sources and metrics. For that, we use the HISDAC-US data layers, which are derived from a separate database (ZTRAX) containing unique housing transaction data. Specifically, we investigate changes in the built-up intensity (BUI) of New Jersey's barrier islands between 1995 and 2015. The results confirm that coastal development has been steadily on the rise since 1995, with slightly more pronounced growth rates in nourishing areas. Additionally, nourishing municipalities exhibit higher development density, particularly in proximity to the beach. Grid cells within the first block of properties display more elevated built-up intensity levels and growth rates in comparison to the barrier islands as a whole, suggesting that areas nearer to the beach are experiencing more rapid increases in building exposure over time.

3.5.3 Growth patterns in vulnerable zones

Considering that Florida, particularly its Gulf coast, is considered one of the most relevant hotspots for hurricane-induced coastal flooding worldwide (Sajjad et al., 2020), we also explore development patterns in two areas prone to recurrent hurricane and tropical storm impacts. Naples, situated on the Gulf Coast, has encountered 43 hurricanes and tropical storms since the 1950s. Notable recent events include Hurricane Wilma in 2005, a major tropical storm in 2008 (Fay), and Hurricane Irma in 2017, which made landfall a short distance south of Naples with sustained winds exceeding 100 mph (~180 km/h). Similarly, Palm Beach, located on the Atlantic Coast, has been affected by 73 hurricanes and tropical storms between 1950 and 2021. Among these, Hurricanes Frances and Jeanne in 2004 caused significant damage, including eight fatalities, considerable infrastructure destruction, and extended power outages. Additionally, Hurricane Wilma in 2005 resulted in moderate damage to numerous buildings, infrastructure, and trees.

Despite the well-acknowledged effects of coastal hazards and the recurring property and infrastructure damage experienced in these two regions, our findings reveal that approximately 20% of the shorefront single-family homes sold in Naples and Palm Beach increase in size from 2012 to 2017. Notably, properties that experience size growth show an average increase of 59% in Naples and 30% in Palm Beach, suggesting a potential "building back bigger" trend in these hurricane-prone areas. These results corroborate previous

assertions highlighting escalating exposure of residential assets in locations with a history of catastrophic events, despite decades of regulatory initiatives aimed at reducing vulnerability in developed coastal areas (Braswell et al., 2022; Lazarus et al., 2018). While this development patterns likely arise from a combination of multiple—and compounded—factors, the presence of hazard protection measures likely plays a significant role. Both Naples and Palm Beach have implemented numerous beach nourishment projects over the past decades, safeguarding their shorelines and valuable assets from recurrent flooding and severe beach erosion. Consequently, while the underlying natural processes driving these hazards remain unaltered, hazard defenses may mitigate or obscure the apparent impact of natural events, potentially fostering development in these high-risk areas (Armstrong et al., 2016; Burby, 2006; Di Baldassarre et al., 2018; 2013; Tobin, 1995; White, 1945).

3.5.4 Building footprints as a proxy for total living area

Empirically uncovering these emerging trends necessitates access to comprehensive housing data capturing the structural characteristics of the built environment. Variables such as the number of rooms, lot dimensions, or the total living area, which adds up the area of all floors comprising a property, not only provide insights into the physical attributes of the properties under study but also serve as widely accepted proxies for evaluating property values (Sirmans et al., 2005). Yet, obtaining accurate and up-to-date housing data can pose significant challenges, especially when conducting large-scale analyses. Some of these databases may lack consistent availability or regular updates, and issues related to privacy and associated costs can present barriers to accessibility (Lu et al., 2013). In such scenarios, remotely sensed data, which can be directly extracted from satellite imagery or obtained as Geographic Information System (GIS) data files from openly accessible datasets, may serve as acceptable surrogates for certain structural attributes.

Building footprints, for instance, approximately match the area of a single-story property. Consequently, they can serve as a viable substitute for total living area when evaluating exposure, making inferences about property values, or exploring changes in the built environment over time. With advancements in deep learning and the growing accessibility of highly detailed imagery, building footprints also emerge as invaluable tools for rapid post-disaster damage assessment of infrastructure, emergency management, and recovery efforts (Berezina and Liu, 2022; Calantropio et al., 2021; Liu et al., 2022). However, it is important to note that plan-view footprints may sometimes underestimate the total living area of multi-story properties or overestimate the area of single-story homes with extensive covered porches. Thus, to facilitate comparisons with national statistics derived from total living area, it becomes necessary to estimate the scaling relationship between the two metrics and subsequently apply the corresponding scaling factors to the mean footprints (Lazarus et al., 2018). For the barrier islands of New Jersey, we find that total living area is,

on average, ~11% bigger than the mean building footprint, and ~23% higher in the first block of properties (**Fig. 3.6c-d**). Thus, in the absence of more accurate data, the application of these scaling factors would have rendered building footprints a viable substitute for assessing property size and a reasonable proxy for property value, enabling comparisons with other datasets providing total living area.

3.6 Conclusions

Although increasing exposure has been acknowledged as a major factor in the exacerbation of losses from natural hazards, development in coastal areas continues to grow in both size and number of structures (Cutter & Emrich, 2005; IPCC, 2012; Lazarus et al., 2018; Iglesias et al., 2021). This pervasive trend highlights a paradoxical relationship between coastal development and natural hazards, where the implementation of protective measures, such as beach nourishment, may inadvertently encourage continued urban growth in high-risk coastal areas (Armstrong et al., 2016; Burby, 2006; Burton and Cutter, 2008; Di Baldasarre et al., 2018; Di Baldasarre et al., 2013; Kates et al., 2006; Montz and Tobin, 2008; Tobin, 1995; White, 1945). Our findings in New Jersey and Florida indicate that residential properties sold in areas undergoing beach nourishment tend to be larger, more expensive, and experience more rapid growth rates compared to those in non-nourishing zones. The trend of increased property size over time is also observed in storm-prone areas facing recurrent damage, such as Naples or Palm Beach. These findings underscore a prevalent trend of heightened exposure in high-risk coastal development and point to beach nourishment as a potential factor contributing to these unintended dynamics.

To comprehend the intricate relationship between coastal development and natural hazards, it is essential to gain access to comprehensive data encompassing the physical and socio-economic attributes of residential properties. While property tax records, as those used in our research, offer precise insights, their accessibility can be limited due to privacy concerns and financial constraints. Consequently, our study underscores the potential of satellite-derived data, particularly building footprints, as a reliable alternative for assessing property size and a reasonable proxy for property value when alternative data sources are unavailable. Furthermore, other openly accessible resources such as the historical data layers compiled on the HISDAC-US database, which derive from proprietary records, also represent valuable tools for assessing exposure and tracking the evolution of built environments over time.

The consistent findings obtained in this study, irrespective of the dataset source or the geographic region under investigation, offer robust evidence that the associations between protection measures and heightened coastal risk exposure are not confined to specific cases or locations. Instead, they reveal a pervasive pattern that typifies developed coastlines across the United States. These unforeseen dynamics highlight the pressing need for

comprehensive policy interventions aimed at mitigating the risks associated with ongoing coastal development and enhancing the resilience of coastal communities in the face of more frequent and severe natural hazards.

3.7 Acknowledgments

The authors gratefully acknowledge support from a Southampton Marine and Maritime Institute Doctoral Studentship (to SA), and Dan Ciarletta for help accessing New Jersey tax records.

Chapter 4 Paper 3: Thresholds in road network functioning on US Atlantic and Gulf barrier islands

Paper published as:

Aldabet, S., Goldstein, E. B., & Lazarus, E. D. (2022) “Thresholds in Road Network Functioning on US Atlantic and Gulf Barrier Islands”, *Earth’s Future*, 10(5), e2021EF002581. DOI: 10.1029/2021EF002581

Aldabet, S. contributed to the investigation, methodology, formal analysis, writing and data curation; Goldstein, E. B. contributed to the conceptualization, investigation, methodology, formal analysis, and writing; Lazarus, E. D. contributed to conceptualization, investigation, methodology, formal analysis, writing, supervision, funding acquisition.

4.1 Abstract

Barrier islands predominate the Atlantic and Gulf coastlines of the USA, where population and infrastructure growth exceed national trends. Forward-looking models of barrier island dynamics often include feedbacks with real estate markets and management practices aimed at mitigating damage to buildings from natural hazards. However, such models thus far do not account for networks of infrastructure, such as roads, and how the functioning of infrastructure networks might influence management strategies. Understanding infrastructure networks on barrier islands is an essential step toward improved insight into the future dynamics of human-altered barriers. Here, we examine thresholds in the functioning of 72 US Atlantic and Gulf Coast barrier islands. We use digital elevation models to assign an elevation to each intersection in each road network. From each road network we sequentially remove intersections, starting from the lowest elevation. We use the maxima of the second giant connected component to identify a specific intersection—and corresponding elevation—at which functioning of the network fails, and we match the elevation of each critical intersection to local annual exceedance probabilities for extreme high-water levels. We find a range of failure thresholds for barrier island road network functioning, and also find that no single metric—absolute elevation, annual exceedance probability, or a quantitative metric of robustness—sufficiently ranks the susceptibility of barrier road networks to failure. Future work can incorporate thresholds for road network into forward-looking models of barrier island dynamics that include hazard-mitigation practices for protecting infrastructure.

4.2 Introduction

Barrier islands predominate the Atlantic and Gulf coastlines of the USA (Mulhern et al., 2017; Stutz & Pilkey, 2011). An estimated 4,300–4,700 km of open coast is parceled into as many as 282 islands (Dolan et al., 1980; Mulhern et al., 2017, 2021; Stutz & Pilkey, 2011), of which approximately a quarter have been described as “urbanized” (Dolan et al., 1980; Dolan & Lins, 2000). These host more than 1.4 million permanent residents (Zhang & Leatherman, 2011) and a disproportionate number of high-value properties (Nordstrom, 2004). Over recent decades, population growth and expansion of the built environment on US barrier islands have continued at rates that exceed national trends (McNamara & Lazarus, 2018; NOAA, 2013; Stutz & Pilkey, 2011; Zhang & Leatherman, 2011), unchecked by damaging impacts of large storms (Godschalk et al., 1989; Lazarus et al., 2018).

The future dynamics of “urbanized” barrier islands will be determined by their built environments, and the persistence of localized hazard-mitigation practices (e.g., seawalls, breakwaters, groynes, beach nourishment, dune construction) to protect against storm impacts, chronic erosion, and sea-level rise (Armstrong & Lazarus, 2019; Lazarus et al., 2016; Lazarus & Goldstein, 2019; Lazarus et al., 2021; McNamara et al., 2015; McNamara & Keeler, 2013; McNamara & Lazarus, 2018; Miselis & Lorenzo-Trueba, 2017; McNamara & Werner, 2008a, 2008b; Nordstrom, 1994, 2004; Rogers et al., 2015). Construction and protection of the built environment in barrier settings alters natural pathways of sediment transport, which in turn redistributes and reapportions local sediment budgets (Nordstrom, 1994, 2004). Changes in the sediment budget in turn change spatial patterns of hazard exposure, to which coastal management and planning must respond. Research into this feedback, which has come to typify human-altered coastlines, has tended to emphasize the comparative morphological state of the barrier environment (McNamara & Werner, 2008a, 2008b) or to focus on the economic dynamics reflected in real-estate and property values (Armstrong & Lazarus, 2019; Armstrong et al., 2016; Gopalakrishnan et al., 2016, 2011; Lazarus et al., 2016; McNamara et al., 2015; McNamara & Keeler, 2013; McNamara & Lazarus, 2018; McNamara et al., 2011; Smith et al., 2009; Williams et al., 2013). Much of this work uses numerical modeling to explore and understand potential thresholds in the human–environmental system that might drive barriers toward different management regimes—or even abandonment. However, subsumed in the spatial domains of these modeling exercises, but not addressed directly, are the networks of critical infrastructure—roads and public utilities—that are fundamental to the fabric of built environments. These networks connect physical spaces, with their own thresholds in functioning where failure may be abrupt.

Investigating infrastructure networks on developed barrier islands for thresholds in functioning—which could necessitate changes in management and planning—is an essential step toward improved insight and foresight into how human-altered barriers may evolve in

the future. The analysis we present here examines potential thresholds in the functioning of US Atlantic and Gulf barrier island road networks. In the US, road networks tend to be the principal way in which people and goods reach and move within developed barrier islands, and are vital to hazard evacuation, emergency response, and recovery operations during and after catastrophic storms (Anarde et al., 2018; Darestani et al., 2021; Frazier et al., 2013; Godschalk et al., 1989; Velasquez-Montoya et al., 2021). Road network disruptions—mechanisms that cause reductions in mobility or increases in the costs necessary to maintain the desired levels of mobility (Markolf et al., 2019)—are common on barrier islands during hurricanes, tropical storms, and nor'easters (Dolan & Lins, 2000; Hardin et al., 2012; Krynock et al., 2005; Nordstrom, 2004; Nordstrom & Jackson, 1995; Spanger-Siegfried et al., 2014; Velasquez-Montoya et al., 2021), and also occur as a result of king tides, sea-level anomalies, groundwater flooding, or other factors that lead to nuisance or "sunny day" flooding (Fant et al., 2021; Hino et al., 2019; Housego et al., 2021; Jacobs et al., 2018; Moftakhari et al., 2018, 2015, 2017; Praharaj et al., 2021). Road disruptions can lead to major socio-economic impacts, isolating neighborhoods, compromising evacuation, and preventing people from accessing critical services (Balomenos et al., 2019; Dong, Esmalian, et al., 2020; Jenelius & Mattson, 2012; Spanger-Siegfried et al., 2014; Suarez et al., 2005). The maintenance and restoration of other critical systems—electricity, water supply, communications—often depends on a functioning road system (Chang, 2016; Johansen & Tien, 2018; Mattson & Jenelius, 2015; Nicholson & Du, 1997).

Because road systems are networks, they can be investigated with the quantitative tools of graph theory (Albert & Barabási, 2002; Boeing, 2017, 2019, 2020; Callaway et al., 2000; Holme et al., 2002; Iyer et al., 2013; Jamakovic & Uhlig, 2008; Kirkley et al., 2018; Moreira et al., 2009; Porta et al., 2006; Tian et al., 2019). Note that network analyses have also been variously applied to coastal morphology and dynamics in non-built environments (Hiatt et al., 2021; Passalacqua, 2017; Pearson et al., 2020; Tejedor et al., 2018). Within the large and rapidly expanding body of research into climate-driven disruptions to critical infrastructure (Faturechi & Miller-Hooks, 2015; Jaroszweski et al., 2014; Markolf et al., 2019; Neumann et al., 2021; Wang et al., 2020), a subset is exploring specifically the exposure and susceptibility of infrastructure to different drivers of flood disturbance. In addition to graph-based methods, recent work has focused on investigating disruption to road networks using techniques from agent-based traffic simulation paired with hydrodynamic models of flooding, specifically to look at travel time delays (e.g., Hummel et al., 2020; Papakonstantinou et al., 2019). Studies consider road and other transportation networks in urban coastal settings (de Bruijn et al., 2019; Kasmalkar et al., 2020, 2021; Kermanshah & Derrible, 2017; Pezza & White, 2021; Plane et al., 2019; Rotzoll & Fletcher, 2013; Sadler et al., 2017; Suarez et al., 2005; Sweet et al., 2014) and in fluvial floodplains and upland catchments (Abdulla & Birgisson, 2021; Arrighi et al., 2021; Dave et al., 2021; Dong, Esmalian, et al., 2020; Dong et al., 2022; Evans et al., 2020; Hummel et al., 2020; Kelleher & McPhillips, 2020;

Papakonstantinou et al., 2019; Pregnolato et al., 2017; Singh et al., 2018; Versini et al., 2010; Wang et al., 2019); others focus on water-treatment systems in low-lying coastal regions (Hummel et al., 2018) or multiple layers of infrastructure networks (Douglas et al., 2016; Habel et al., 2020, 2017; Koks et al., 2019; Neumann et al., 2021). To understand and forecast the future dynamics of developed barrier islands, more inquiry is needed to link thresholds in road network functioning to the physical forces that drive coastal change.

Here, we examine the drivable road networks of 72 barrier islands along the Atlantic and Gulf Coasts of the USA (Figure 1), selected because their networks contain >100 nodes. First, we cast the road network of each barrier island as a separate graph of nodes (intersections) connected by edges (road segments). We use spatially extensive digital elevation models to assign an elevation to each node (intersection) in each road network. For each barrier island, we sequentially remove nodes from the network, starting from the lowest elevation, and identify the critical node—with its corresponding elevation—at which each barrier island road network crosses a threshold of functioning. We then link the elevation of each critical node to the local annual exceedance probability curve for extreme high-water levels. Our analysis demonstrates a method to identify specific physical locations that, if disrupted by flooding or a flood-related hazard (e.g., road damage, debris/sediment accumulation), could trigger functional failure in an island road network. We organize the components of this threshold, which varies by barrier island, in terms of common metrics—elevation and annual exceedance probabilities—to facilitate their incorporation into forward-looking modeling of developed barrier island dynamics.

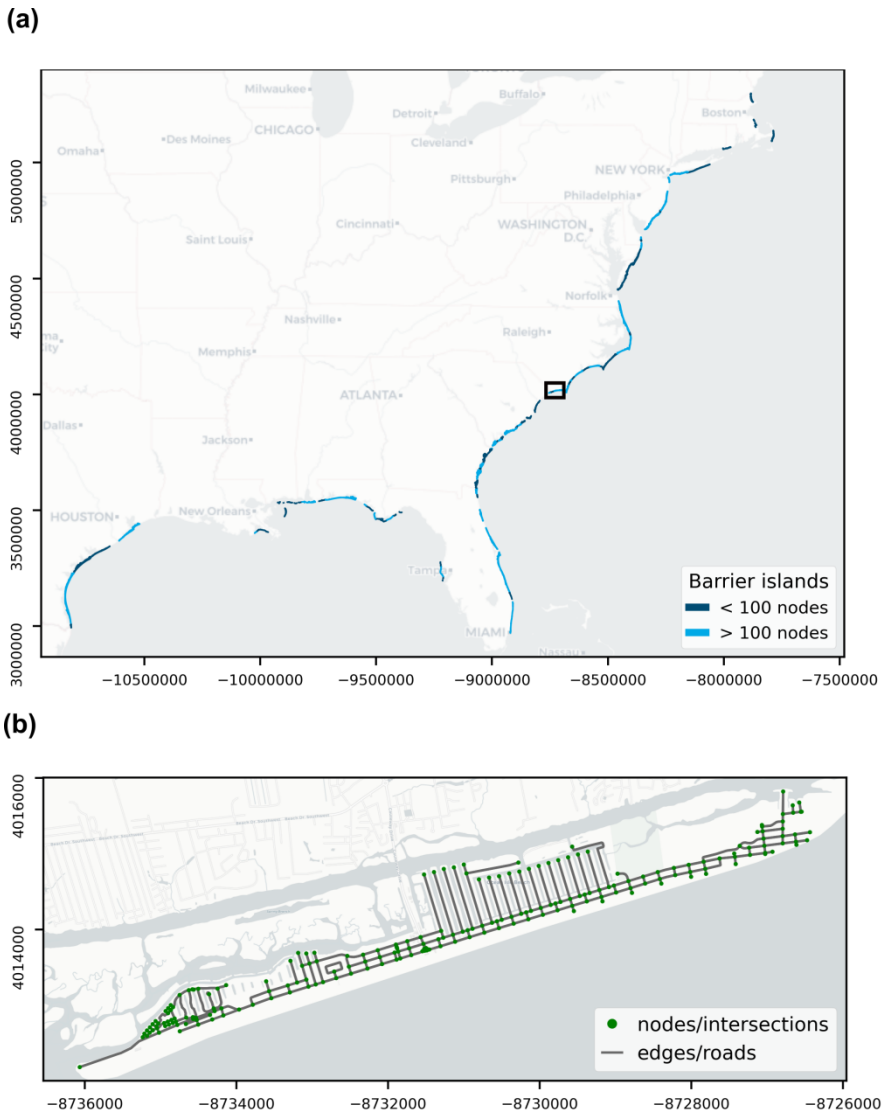

Figure 4.1 US Atlantic and Gulf Coast barrier islands considered in this study, and their road networks. (a) Map of 184 barrier islands (Mulhern et al., 2017, 2021), of which 74 have road networks with >100 nodes (intersections). Of those, 72 (light blue) overlap with tiles currently available in the Continuously Updated Digital Elevation Model data from NOAA (Amante et al., 2021; CIRES, 2014). Box shows location of example barrier in panel below. (b) Example of drivable road network at Ocean Isle, North Carolina, USA, in which intersections are represented as nodes and roads as edges. Maps shown in Web Mercator projection (EPSG:3857).

4.3 Methods

Our workflow for investigating US Atlantic and Gulf barrier island road networks is shown in Figure 4.2. We discuss each step in the sequence below.

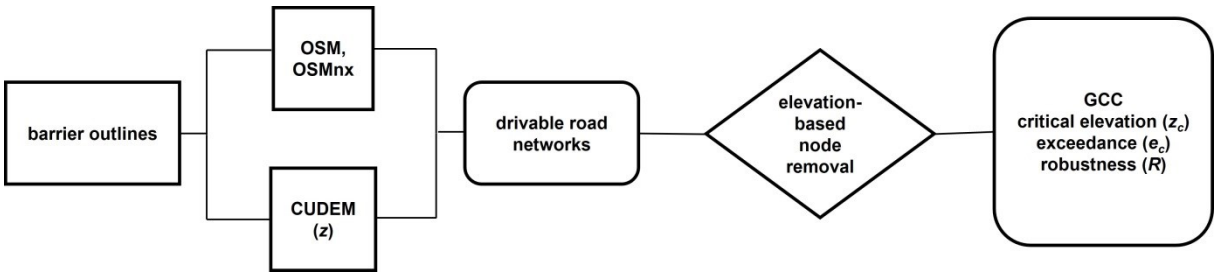

Figure 4.2 Methodological workflow for assessing robustness to flood-induced failures in road networks on US Atlantic and Gulf barrier islands. Abbreviations are as follows: OSM is Open Street Map; OSMnx is an analytical toolbox (Boeing, 2017). CUDEM is the NOAA Continuously Updated Digital Elevation Model (Amante et al., 2021; CIRES, 2014). GCC is the giant connected component of a network, or the large cluster of nodes connected in the original network.

4.3.1 Road networks and topography

To isolate barrier island road networks, we used digitized perimeters of 184 barrier islands along the Atlantic and Gulf Coasts of the USA as spatial boundaries (Mulhern et al., 2017, 2021) and extracted the drivable road networks from Open Street Map (OSM) with OSMnx (Boeing, 2017). Cast as networks, road intersections are encoded as nodes and road segments are edges. We excluded connections between an island and the mainland (i.e., bridges, causeways, etc.) as well as other possible transportation pathways on islands, such as bikeways and walkways.

Of the 184 barriers considered, 108 have drivable road networks, according to their classification within OSM. Of those, 103 overlapped with tiles currently available in the NOAA Continuously Updated Digital Elevation Model (CUDEM), a set of 1/9 Arc-Second resolution bathymetric and topographic tiles for the coastal USA (Amante et al., 2021; CIRES, 2014). Note that some of these 103 networks are sandy tracks or access roads, or networks with very few nodes. For statistically meaningful metrics of network structure, we restricted our analysis to barriers with drivable road networks of at least 100 nodes (Figure 4.1). This reduced our sample to 72 barriers. We determined the elevation of each node (road intersection) in each network by spatially querying the CUDEM dataset.

The size of this subset is broadly consistent—despite very different selection criteria—with the count by Dolan et al. (1980), who identified 70 barrier islands as “urbanized.” We did not attempt to reconcile differences in reported numbers of US Atlantic and Gulf barrier islands: Dolan et al. (1980) report 282 islands; Stutz and Pilkey (2011) report 277; Mulhern et al. (2017, 2021) digitized 184. Note that several developed barrier islands are missing from Mulhern et al. (2017), but we use this dataset from Mulhern et al. (2017, 2021) because it is the only barrier compilation that is openly accessible.

4.3.2 Network response to node removal

The susceptibility of a network to the failure of its components is typically explored by nullifying or removing nodes and calculating metrics that reflect network functioning (Abdulla & Birgisson, 2021; Iyer et al., 2013; Li et al., 2015; Newman, 2010; Schneider et al., 2011; Wang et al., 2019). For example, when enough of the network is removed, travel between any two nodes (intersections) becomes impossible or requires long travel distances (and time) on the network. We removed nodes from a network based on a ranked list by elevation—from lowest to highest—in contrast to removing nodes randomly (a common approach, e.g., Albert & Barabási, 2002). Node removal in this way mimics a simplified "bathtub" flooding scenario (e.g., Abdulla & Birgisson, 2021; Wang et al., 2019), which assumes that nodes become nullified because they are actively flooded, damaged by flooding, and/or unusable because of debris and/or sand deposited on the road. We assumed that the removal of a node causes the immediate disconnection of all its connected edges. This work thus considered node removal exclusively. Because road intersections can be abstracted as points, they can be linked to specific elevations in a straightforward way. Since edges encode segments of roadway, an alternate strategy could preferentially remove network edges, or both edges and nodes. Edge removal would require dense sampling of elevation data along each edge of a road network to accurately locate lowest road elevation and calculate other summary metrics (e.g., mean road elevation). Future work should address whether the inclusion of edges significantly improves (or otherwise substantively changes) the results of this kind of analysis. Network metrics were calculated using NetworkX (Hagberg et al., 2008).

For road networks, the original network is connected in a single large cluster—the giant connected component (or giant component). As nodes in the original network are serially removed, the network breaks into smaller networks. Here, we tracked the size of these subnetworks relative to the size of the giant component. Specifically, as the fraction of nodes removed (q) increases and the first giant component degrades, we tracked the size of the second-largest cluster—the second giant connected component (Figure 4.3a). The network crosses a critical threshold at q_c, when the first giant component fragments and the size of the second giant component becomes maximal (Li et al., 2015; Wang et al., 2019). Generally, the higher q_c—that is, the more nodes that can be removed before the giant component fragments—the less prone the network is to failure (Newman, 2010). The critical threshold (q_c) can be linked to a specific node that causes the failure of the network (Figure 4.3b) and to the elevation of that node, which we refer to as the critical elevation (z_c).

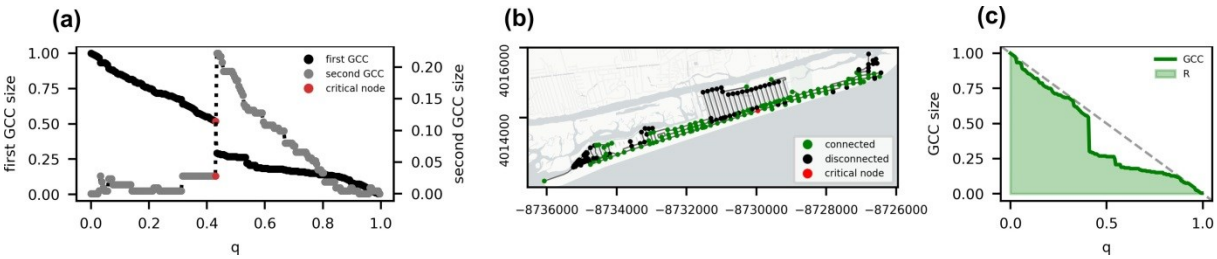

Figure 4.3 Examples illustrating the methodology used to (a) explore the size decay of the first and second GCCs, (b) identify the critical node that leads to the fragmentation of the network, and (c) quantify overall network robustness to elevation-based node removal. Barrier example shown here is the drivable network at Ocean Isle, North Carolina, USA. In (a), the vertical axes show the first (left) and second (right) GCC size as a fraction of nodes in the original network, as a function of the fraction of nodes removed (q). Red dot in panels (a) and (b) marks the critical node in the GCC and in real physical space, respectively. In panel (c), robustness R is taken as the area (light green) under the decay curve for the first GCC (bold green). Dashed gray line shows the inverse 1:1 reference line, indicating the theoretical maximum for R = 0.5. Maps like the example shown in (b) for all 72 barrier road networks with >100 nodes can be found in the data repository.

The relative importance of a node to the connectivity of a network is often measured in terms of centrality (e.g., Newman, 2010). Our focus here is specifically on quantifying network failure—which is related to but distinct from calculating node centrality and network connectivity. Determining the relative importance of a node to the potential failure (or robustness) of a network is typically treated as a percolation-type problem (Abdulla & Birgisson, 2021; Callaway et al., 2000; Dong, Mostafizi, et al., 2020; Li et al., 2015; Wang et al., 2019), and assessed in terms of threshold behavior in the giant connected component (Newman, 2010; Schneider et al., 2011). Relationships between metrics for network connectivity and percolation are not necessarily straightforward (Newman, 2010), in part because many metrics of network topology are autocorrelated, making them poorly suited tools for distinguishing among networks with different structures (Bounova & de Weck, 2012; Jamakovic & Uhlig, 2008).

4.3.3 Extreme water levels

Comparison of coastal barrier islands solely on the basis of topographic elevation (i.e., one barrier is higher or lower than another) is not meaningful unto itself because of local differences in tidal forcing and extreme water level statistics. For example, road networks on higher-standing barriers subject to frequent extreme storms might be more prone to flooding than road networks on lower-lying barriers subject to fewer storms. To provide meaningful

comparisons among the broad geospatial distribution of barriers in our sample, we recast all node (intersection) elevations to local annual exceedance probabilities of extreme water events.

Extreme water levels have been used to examine the direct and indirect impacts of coastal floods on transportation systems and assess the susceptibility of the network to flood-induced failure (Fant et al., 2021; Habel et al., 2020; Jacobs et al., 2018; Pezza & White, 2021). Annual exceedance probabilities and average recurrence intervals are commonly applied for infrastructure design and assessment of flood risk (Apel et al., 2004, 2006; Hackl et al., 2018; Haigh et al., 2014; Sweet & Park, 2014; Vitousek et al., 2017; Wahl et al., 2017). Average recurrence intervals, also known as return periods, provide an estimation of the time elapsed between events of the same magnitude; annual exceedance probability refers to the likelihood that high-water levels exceed a certain elevation in any given year (Haigh et al., 2014). For example, a flood with an annual exceedance probability of 0.01 corresponds to an event that has a 1% chance of annual occurrence, or an average recurrence interval of 100 years. (Return period can be understood as the inverse of exceedance probability.)

Extreme value analysis (EVA)—the branch of statistics that deals with the estimation and prediction of rare values within a series (Coles, 2001)—has been applied broadly to analyses of observed and simulated extreme high-water levels to quantify the probability of occurrence (and/or return period) of extreme events (Vitousek et al., 2017; Wahl et al., 2017; Zervas, 2013). One of the most common EVA methods is block maxima, which considers the maximum of all recorded values within a block of time (i.e., days, months, or years) and approximates extreme values using a Generalized Extreme Value (GEV; Coles, 2001; Zervas, 2013) distribution. The GEV distribution is described by three parameters—location (μ), scale (σ), and shape (ξ)—that refer, respectively, to the center of the distribution, the deviation around the mean, and the tail behavior of the distribution. The shape parameter determines the extreme distribution used: Gumbel ($\xi = 0$), Frèchet ($\xi > 0$), or Weilbull ($\xi < 0$). Using long-term monthly tide gauge records from the 112 US stations operated by the Center for Operational Oceanographic Products and Services, Zervas (2013) followed a GEV approach to characterize the distributions of extreme high and low-water levels and produce exceedance probability curves for each station. For each barrier island in this analysis, we generated extreme high-water level annual exceedance probability curves by sampling the Gumbel distribution described by the three reported GEV parameters (Zervas, 2013) for the tidal station closest to that barrier by straight-line distance. Note that this use of straight-line distance is an assumption, as extremes may differ based on factors such as bathymetry, geometry of adjacent coastal landforms, and dynamics of the forcing event (e.g., direction of storm propagation). We then estimated annual exceedance probabilities for the critical node of each barrier network, which we refer to as the critical exceedance, e_c. We thus linked each critical node to a specific annual exceedance probability. All calculation was done using the

Python ecosystem, for example, Scipy (Virtanen et al., 2020) and Numpy (Harris et al., 2020). Note that the choice of extreme value analysis applied to a data set has the greatest effect on events with the lowest likelihood of occurrence (Wahl et al., 2017). Because high-likelihood events are of particular interest to us in this analysis, the Gumbel distributions that we use to reproduce the estimates reported by Zervas (2013) are sufficient: a different method of extreme value analysis would result in different probabilities for the low-likelihood events from these tide gauges, but estimates for high-likelihood events will be effectively the same.

4.3.4 Network robustness

Having focused on identifying a single critical node for each island and defining a critical threshold for each barrier road network in terms of elevation (and exceedance probability), we next examined the overall network robustness of each barrier. The purpose of this step is to provide a summary metric for network functioning that includes but is not limited to the occurrence of the critical threshold: for example, determining how much of the original road network is still connected when any given percentage of the nodes is removed. Calculating whole-network robustness permitted us to compare barrier road networks in terms of their entire architecture, rather than solely by comparing aspects of a single critical node (e.g., its elevation and the related exceedance value).

We used the robustness metric *R* proposed by Schneider et al. (2011), which measures the summed size of the giant connected component as nodes are removed (Figure 4.3c):

$$R = \frac{1}{N}\sum_{Q=1}^{N} s\,(Q)$$

where *N* refers to the total number of nodes in the network, *Q* to the number of nodes removed, and *s(Q)* is the fraction of nodes in the giant component after removing *Q* nodes. The normalization factor 1/N allows comparison between networks of different sizes. The resulting *R* values range between 1/*N* (for a star graph) to 0.5 (a fully connected network; Schneider et al., 2011). Note that we evaluated network robustness in two ways: by removing nodes in rank order of elevation (lowest to highest) and by random node removal (e.g., Wang et al., 2019). Other studies have investigated how *R* changes with non-random but abstracted network disruptions (Iyer et al., 2013), and how *R* varies in transportation networks, specifically, with different types of disruptions (Dong, Mostafizi, et al., 2020; Wang et al., 2019).

4.4 Results

4.4.1 Barrier island road networks

Of the 184 barrier islands considered in this analysis (Mulhern et al., 2017, 2021), 74 have drivable road networks with more than 100 nodes, and only 72 overlap with CUDEM tiles. These 72 islands account for 65% of the total US Atlantic and Gulf barrier island area (3,082 km^2 out of 4,716 km^2) and 60% of the US Atlantic and Gulf barrier island shoreline length (4,282 km out of 7,150 km) delineated in the dataset by Mulhern et al. (2017, 2021). On average, the 72 islands with networks of >100 nodes are typically three times larger (43 km^2) than barrier islands with small or no drivable road networks (15 km^2). Almost 90% of the 72 islands (63 barriers) are smaller than 100 km^2, and ~60% (42 barriers) are smaller than 25 km^2 (Figure 4.4a). Road network size is variable, ranging between 19 and 678 km of total road length (143 km on average; Figure 4.4b) and between 111 and 3,486 intersections (739 nodes on average; Figure 4.4c). Approximately 20% of these drivable networks (16 networks) have more than 200 km of total street length, and more than 25% (19 networks) have more than 1,000 nodes. The average node elevation for the 72 road networks with >100 nodes is 2.5 m (Figure 4.4d). Of all nodes in the dataset, ~65% sit between 1 and 3 m elevation (34,438 nodes out of 53,214), and ~8% (4,516 nodes) are below 1 m elevation. Conversely, barely 7% of all road intersections (3,695 nodes) are located above 5 m elevation, and only 0.5% (265 nodes) are above 10 m elevation.

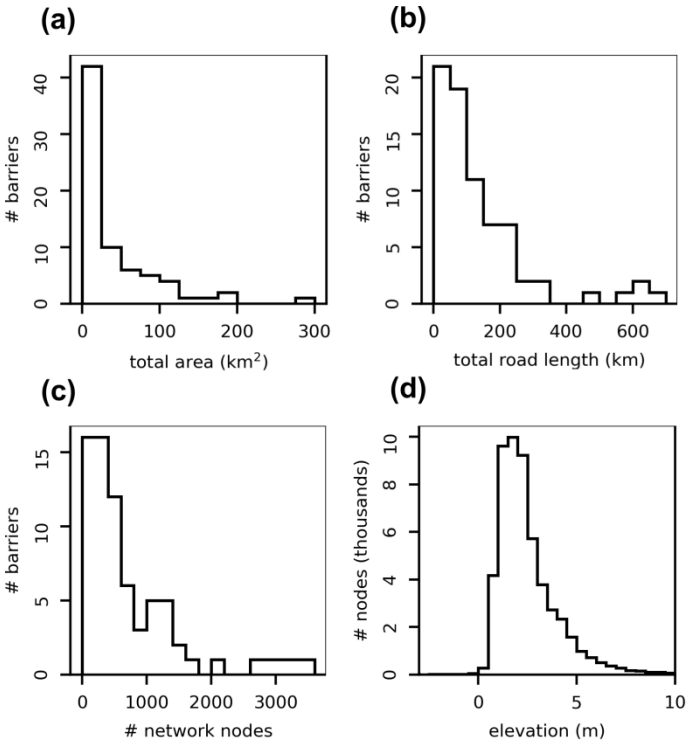

Figure 4.4 Summary statistics for 72 US Atlantic and Gulf barrier-island road networks with >100 nodes. Panels show distributions of (a) total area, (b) total road length, and

(c) the number of networked nodes for all 72 barriers. Panel (d) shows the distribution of elevation for all networked nodes in all 72 barriers.

4.4.2 Elevation-based node removal

Elevation plays a primary role in determining the sequence of road closures, where intersections at the lowest elevations are expected to be among the first disrupted during floods (e.g., Abdulla & Birgisson, 2021): disruption might include being submerged by the flood, being physically damaged by flood water, and being buried under debris and/or sediment deposited by flooding. The aggregate compilation of all networked node elevations shows that most nodes sit below 5 m (Figure 4.4d). We also plot each node in a given network in ranked order of elevation, from lowest to highest, for all 72 barriers with networks >100 nodes—a representation akin to a hypsometric curve (Figure 4.5a)—which demonstrates the topographic similarity of these road networks despite the geographic distribution of the barriers on which they are situated. For each road network, we used the ranked order of node elevation to sequentially remove nodes, from lowest to highest, and plot the corresponding size of the first giant connected component (Figure 4.5b). We find that two general modes of behavior emerge. In one mode, the giant component decreases linearly with each node removed: as one node is removed from network, one node is removed from the giant component. This occurs as the removed nodes come from areas at the extremities of the network, or where the network is highly connected and nodes are linked by multiple edges (i.e., removal of a single intersection from a gridded network). In the other mode, the removal of a single node results in a sharp drop in giant component size. An example of this is the loss of a single node that links two parts of an island, each with its own cluster of nodes. Large, abrupt changes in the size of the giant component indicate the presence of nodes whose removal results in the fragmentation of the network. Thus, although these 72 barrier networks appear similar topographically, node removal on the basis of elevation does not yield identical curves because of differences in local network architecture (Figure 4.5b).

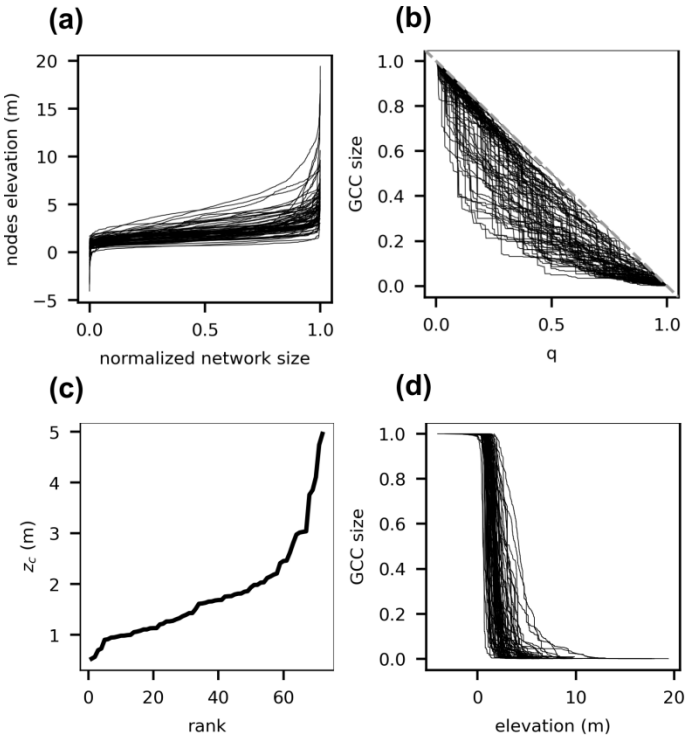

Figure 4.5 Network effects of node removal based on ranked list of elevation (from low to high). (a) Elevation of each networked node, sorted into a ranked list from lowest to highest, for 72 barriers with networks with >100 nodes. Network size is normalized to 1. (b) Size decay of each giant connected component under sequential node removal by elevation, from lowest to highest. Gray dashes are the inverse 1:1 reference line. (c) Elevation of the critical node (zc) for each of the 72 road networks with >100 nodes, ranked from lowest to highest. (d) Size decay of each giant connected component as a function of node elevation.

We find that for all 72 road networks with >100 nodes, the elevation of the critical node (z_c)—the node whose removal from the network simultaneously reduces the size of the first giant component and maximizes the size of the second giant component—lies below 5 m (Figure 4.5c). Moreover, 85% (61 networks) have critical nodes below 2.5 m; 44% (32 networks) have critical nodes below 1.5 m; and 18% (13 networks) have a critical node below 1 m. Unlike the more varied curves apparent when the size of the giant component is plotted as a function of the fraction of nodes removed (Figure 4.5b), plotting the size of the giant component as a function of the elevation of each node removed emphasizes the precarity implied by such low elevations for critical nodes (Figure 4.5d): the size of the giant component decays all but instantaneously as node elevation increases. However, similarly low-lying topography does not equate to similar likelihoods of flooding. For that, we needed to consider geographic differences in extreme water level.

4.4.3 Extreme water levels

Inferring road network susceptibility to failure purely in terms of node elevation is not meaningful. Tidal range varies along the US Atlantic and Gulf coastline, as does exposure to extreme high-water levels (i.e., hurricanes, nor'easters, and sea-level anomalies). We therefore connected each barrier road network node elevation to estimated local exceedance probabilities of extreme high-water levels. As a result, nodes at the same elevation but on different barrier islands can be associated with markedly different annual exceedance probabilities (Figure 4.6a). We find that 44 of the 72 barrier networks (61%) have critical nodes at elevations associated with annual exceedance probabilities >0.01 (greater than 1% per year, or an average recurrence time of once every 100 years; Figure 4.6b). Of those, 25 networks—over a third of the barriers sampled—yield critical thresholds in annual exceedance probability at or above 0.1 (10% chance per year, or an average recurrence time of once every 10 years). The critical elevation for those nodes is, on average, just above 1 m elevation (Figure 4.6c). Generally, we find that local critical exceedance (e_c) is associated with the elevation of the critical node (z_c; Figure 4.6c).

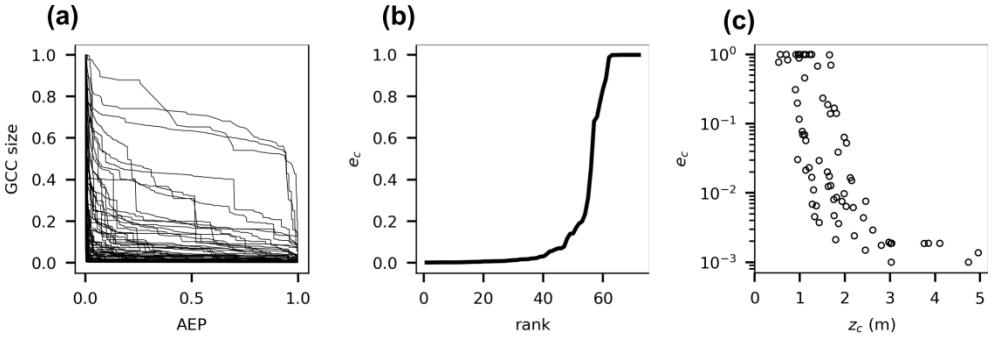

Figure 4.6 Relationships between road networks and extreme water levels. (a) Size decay of the giant connected component versus annual exceedance probability (AEP) of extreme high-water events, based on the elevation of each node removed. (b) Barrier islands ranked according to exceedance probability of the critical node (e_c). (c) Relationship between the exceedance probability of the critical node for each barrier (e_c) as a function of the critical-node elevation (z_c).

4.4.4 Road network robustness

We calculated road network robustness to measure the ability of the road network architecture to withstand node removal. Recall that robustness (R) is the normalized, summed size of the giant connected component as nodes are removed (Equation 4.1, after Schneider et al., 2011). We first focus on robustness by removing nodes in order of elevation (low to high). For the 72 barriers with networks >100 nodes, we show the giant component as a function of the fraction of nodes removed (as in Figure 4.5b), now colored by the corresponding R value (Figure 4.7a). When the size of the giant component decreases

linearly with each successive node removed—as shown by the inverse 1:1 reference line (gray dashes)—the area under the curve is maximized, and so is the associated *R* value (*R* = 0.5). Color makes the gradient in *R* visually apparent: low values (purples) are associated with the farthest excursions from the 1:1 reference line, and high values (yellows) are concentrated closest to the reference line.

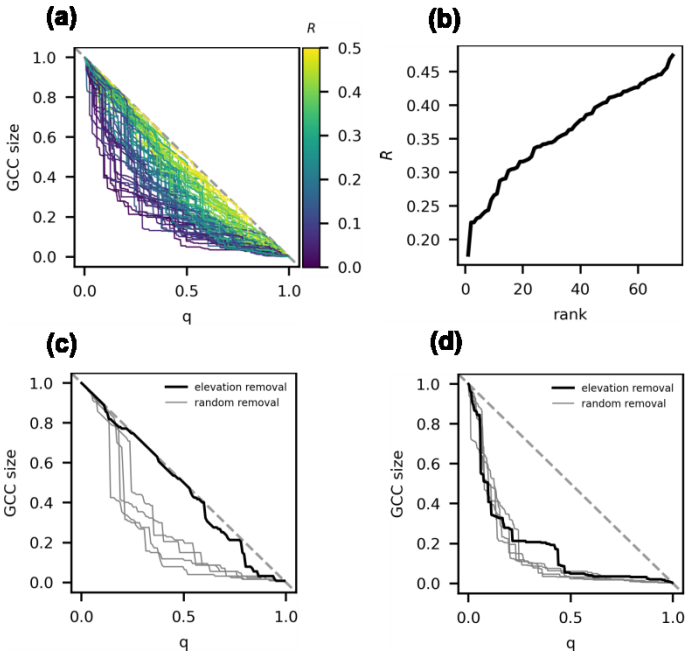

Figure 4.7 Road network robustness. (a) Normalized giant connected component size as a function of fraction of network nodes removed (as in Figure 4.5b), where color represents values of robustness (purple ~ low; yellow ~ high). Dashed gray inverse 1:1 reference line denotes the curve for perfectly linear GCC decay with a theoretical maximum robustness of R = 0.5. (b) Rank-order plot of robustness values for the 72 barriers with >100 nodes. (c) Decay of giant component as a function of fraction of nodes removed for a network with high robustness to flooding disturbance (black line; R = 0.47; island FL28 in Mulhern et al. (2021)). Solid gray lines show comparatively distinct decay curves for the same network under random node removal. (d) Decay of giant component as a function of fraction of nodes removed for a network with low robustness to flooding disturbance (black line; R = 0.17; island SC1 in Mulhern et al. (2021)). Solid gray lines show similar decay curves for the same network under random node removal.

Approximately 35% of the networks (26 islands) have $R > 0.4$, with four networks above 0.45. Nearly half of the barriers analyzed (32 islands) fall within the range $0.3 < R < 0.4$, and the remaining 20% of the networks (14 islands) have $R < 0.3$, with one network below 0.2 (Figure 4.7b). The highest R values in our sample illustrate behavior close to an end-member situation, where the giant component decreases almost linearly until nearly two-thirds of the nodes in the network are removed ($q_c \sim 0.6$)—at which point, the network begins to

disintegrate (Figure 4.7c). By contrast, networks with low *R* values are characterized by abrupt reductions in the size of the giant component with the removal of a small fraction of nodes (Figure 4.7d).

Related work on flood-driven disruptions to road networks has demonstrated quantitative differences between the behavior of the giant component with preferential removal of nodes by elevation versus random node removal (Abdulla & Birgisson, 2021; Wang et al., 2019). We likewise show that a given network can have high robustness to elevation-based node removal, yet low robustness to random node removal (Figure 4.7c). Barriers with higher mean elevation tend to have critical nodes at higher elevations, and therefore be more tolerant of elevation-based node removal—but are no less prone to failure under random removal. Note that networks with low robustness values for elevation-based removal tend to show little difference between elevation-based removal versus random removal (Figure 4.7d), suggesting an intrinsic low robustness in their network architecture that is independent of removal order type.

4.5 Implications

4.5.1 No single metric can be used to rank barrier susceptibility to disruption

Taken together, the key variables explored in this work—critical node elevation (z_c), critical exceedance (e_c), and robustness (R)—provide a window into the complexity of elevation-based disturbance to road networks on seemingly similar barrier environments. Collating these three variables in a parallel-coordinates plot shows that the ranking of barriers changes depending on the metric (Figure 8). Here, the barriers are first ranked by critical elevation (z_c) in ascending order (left column), then by critical annual exceedance probability (e_c) in descending order (middle column), and then by robustness (R) in ascending order (right column). The top of the plot thus uniformly corresponds to barrier networks that are less susceptible to disturbance based on each metric. Barrier islands are colored according to their elevation rank (sequence in first column), and each color tracks across the other two columns for e_c and R. Connecting lines cross as individual barriers change places in the respective rankings. This result illustrates a key insight: a barrier network might appear worryingly susceptible to disturbance on a ranked list according to one variable but reassuringly strong according to another. That is, a network might have a notably low critical node elevation, but be situated in a place unlikely to be affected by extreme high-water levels, and/or be characterized by an architecture with high robustness to elevation-controlled (i.e., flooding) disturbance. Cognate studies of hazard-driven disturbance to road networks have reached similar conclusions regarding the elusiveness of a single, definitive, ranking metric that captures network susceptibility to failure (Kermanshah & Derrible, 2017).

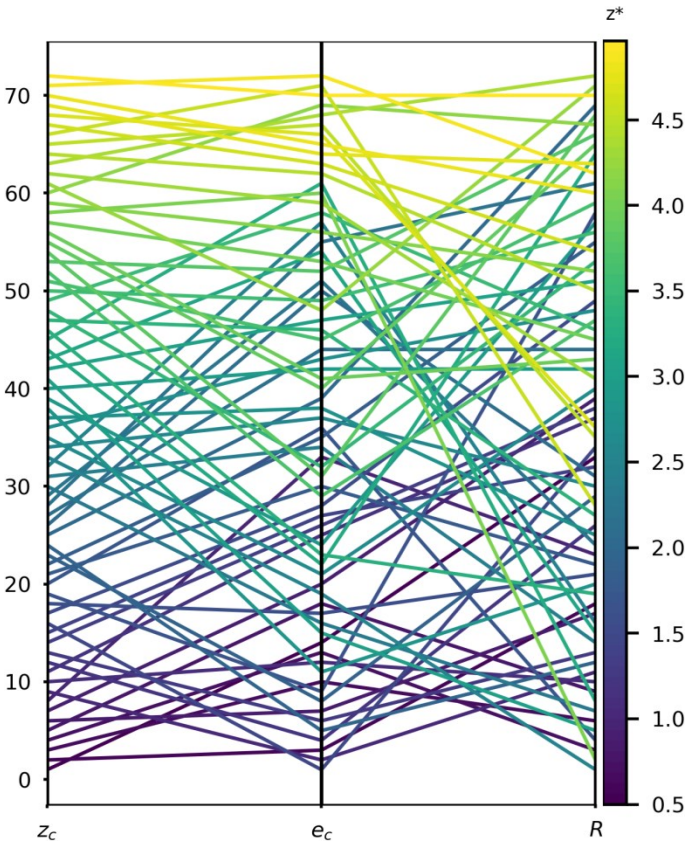

Figure 4.8 Parallel-coordinates plot of critical node elevation (z_c), exceedance probability (e_c), and robustness (R) for barriers with road networks of >100 nodes. In each column, respectively, barriers (labeled at far left) are ranked by z_c in ascending order, by e_c in descending order, and by R in ascending order. Each barrier is colored by z_c, and that color follows each barrier across the plot as its relative rank changes for e_c and R.

4.5.2 Caveats: non-stationarity and interdependencies in hazard forcing

Our analysis does not account for non-stationarity in environmental forcing, which is needed for work like this to be incorporated in future-looking modeling of barrier island dynamics. Our results are therefore indicative of road network robustness to disturbance on US Atlantic and Gulf barriers based on past conditions, but likely underestimate annual exceedance probabilities for critical nodes (e_c) in the future, as even high-likelihood events become more frequent. Future work should incorporate and explore the effects of forcing non-stationarity (e.g., Buchanan et al., 2017; Cheng & AghaKouchak, 2014; Ezer & Atkinson, 2014; Kirezci et al., 2020; Moftakhari et al., 2015; Sweet & Park, 2014; Taherkhani et al., 2020; Tebaldi et al., 2012; Vitousek et al., 2017; Wahl et al., 2017). We anticipate that the primary effect of non-stationarity would be to raise critical exceedance over time across the dataset, driving more barriers—some more rapidly than others—toward high if not guaranteed annual exceedance probabilities.

We also do not explicitly consider flood drivers or specific impacts of flooding (e.g., standing water, road damage, traffic flow, debris and sediment deposition), and instead focus on network disruption based purely on elevation. Future work can incorporate observations on how road networks are impacted by relative contributions of specific drivers from marine sources (Serafin et al., 2017) and others, such as pluvial (Dave et al., 2021; Evans et al., 2020; Kelleher & McPhillips, 2020; Neumann et al., 2021; Pregnolato et al., 2017) or groundwater flooding (Habel et al., 2020, 2017; Plane et al., 2019; Rotzoll & Fletcher, 2013), or the potential importance of variability in flood duration (Arrighi et al., 2021; Darestani et al., 2021; de Bruijn et al., 2019; Najibi & Devineni, 2018; Pezza & White, 2021; Sweet et al., 2014). Adding traffic dynamics either through graph-based approaches (e.g., Dong et al., 2022), or agent-based traffic simulations (e.g., Hummel et al., 2020; Papakonstantinou et al., 2019) would also enrich future work, as would further investigation of material and mechanical properties of roadways to understand the event conditions likely to cause permanent damage (e.g., Khan et al., 2014, 2017; Mallick et al., 2017).

As empirical and modeled data for constructing annual exceedance probabilities for extreme high-water levels continue to improve (Muis et al., 2020; Tadesse & Wahl, 2021; Woodworth et al., 2016), so too will analyses of infrastructural robustness to flooding at specific localities—which might involve recalculating probabilities of infrastructural failure under non-stationary forcing (Cheng & AghaKouchak, 2014) and/or including the mitigating or exacerbating effects of coastal landscape morphodynamics (Anarde et al., 2018; Darestani et al., 2021; Velasquez-Montoya et al., 2021). Nevertheless, gaining insight into the probability distribution—and non-stationarity—of multi-source flood magnitude and frequency will also require a proliferation of accessible, comprehensive, multi-layer datasets (Habel et al., 2020). For example, our annual exceedance probabilities do not explicitly account for changes in each component of the total water level, and accounting for changing wave climates can significantly increase predictions of future total water levels (e.g., Vitousek et al., 2017). Emerging multi-layer datasets will not only include environmental forcings, but also different types of susceptible infrastructure (Emanuelsson et al., 2014; Neumann et al., 2021), of which road networks are only one: recent works in this expanding research space consider wastewater treatment facilities (Hummel et al., 2018), storm-water conduits (Habel et al., 2020), rail and tunnel systems (Douglas et al., 2016; Koks et al., 2019), and interdependencies across multiple infrastructure systems (Najafi et al., 2021).

4.5.3 Identifying hotspots of concern

Our analysis offers a computationally efficient way of exploring (with open-access data sets) barrier island road network robustness to disturbance from extreme high-water events. The resulting isolation of a critical node associated with large-scale network failure is essentially a first-order diagnostic, derived from the assumption, a priori, that topography is a key control

on flood susceptibility. To test if flood-driven failure of coastal (and other floodplain) road networks is fundamentally a function of topography at critical nodes will require sustained observation of real settings (e.g., Plane et al., 2019). But if borne out, then this work demonstrates how specific nodes, or sets of nodes, in a road network might be targeted in planning strategies for climate adaptation at local scales—especially where resources for adaptation are limited, and specific actions (e.g., raising a road surface over a given distance) may have noticeable effect on the impact of increasingly frequent disturbances.

Local actions at critical nodes in road networks—and other networked infrastructure—are important because, as our results illustrate, the local failure of a critical node triggers a nonlocal failure of the larger network in which it sits. Climate-driven, local disruptions with nonlocal consequences represent a vital concern not only for physical networks of critical infrastructure (Arrighi et al., 2021; Hummel et al., 2018; Li et al., 2015), but also for the emplacement of hazard defenses, which can displace or amplify hazard impacts alongshore (Ells & Murray, 2012; Lazarus et al., 2016; Wang et al., 2018) or downstream (Tobin, 1995). Our analysis suggests that if the critical node of a road network is elevated, for example, by a local intervention that rearranges the three-dimensional network topology, then a different node elsewhere in the network will become the new critical junction. However, if the new critical node corresponds to a significantly lower annual exceedance probability, then the functional susceptibility of the network will have improved in kind—as long as other interventions, such as hazard defenses, do not likewise displace flooding impacts in unintentionally confounding ways.

Broadly, our findings contribute to a diverse and rapidly expanding body of work concerning climate-driven impacts to infrastructure (Faturechi and Miller-Hooks, 2015; Jaroszweski et al., 2014; Markolf et al., 2019; Neumann et al., 2021; Wang et al., 2020), and pertain to forward-looking discourse on sustainable urban systems, including calls for “developing new data and methods to understand current drivers and interactions among natural, human-built, and social systems in urban areas as they impact multiple sustainability outcomes across scales” (ACERE, 2018). Our work here is focused on barrier islands along the US Atlantic and Gulf Coasts, but a similar effort could be applied to other low-lying coastal systems vulnerable to flooding, such as coral atolls (e.g., Storlazzi et al., 2018). Development of simple diagnostics for infrastructure susceptibility in built environments with high exposure to natural hazard should only become more promising with improved accessibility to high-resolution geospatial data for natural and human systems. Specifically, our results can contribute to forward-looking predictions of barrier island dynamics. Future work can incorporate thresholds for road network functioning into barrier island models. Numerical models could include human actions and management strategies that acknowledge thresholds in infrastructure functioning and incorporate hazard-mitigation practices that aim

to protect infrastructure. We anticipate that feedbacks between sediment dynamics and infrastructure will also contribute to future barrier island dynamics.

4.6 Acknowledgments

EBG and EDL thank Katherine Anarde, Beth Sciaudone, Kenny Ells, and Dylan McNamara for fruitful discussions. We thank Julia Mulhern and Cari Johnson for sharing data and making it openly accessible; we also thank the Editor, an anonymous reviewer, and Stuart Pearson for helpful comments. The authors gratefully acknowledge support from a Southampton Marine and Maritime Institute Doctoral Studentship (to SA), The Leverhulme Trust (RPG-2018-282, to EDL and EBG), and an Early-Career Research Fellowship from the Gulf Research Program of the National Academies of Sciences, Engineering, and Medicine (to EBG). The content is solely the responsibility of the authors and does not necessarily represent the official views of the Gulf Research Program of the National Academies of Sciences, Engineering, and Medicine.

Chapter 5 Synthesis and conclusions

5.1 Key insights

5.1.1 Built environments as human-landscape systems

Despite widespread awareness of coastal hazards, built environments, which include human-made structures and complex infrastructure networks, continue to expand, increasing the potential for disaster. Rapid population growth and expansion of human settlements in low-lying coastal areas are causing unexpected variations in hazard exposure that amplify the risk confronted by coastal regions and impose greater financial strain on already vulnerable societies. Even areas previously unfamiliar with natural hazards are increasingly prone to damage due to the combination of more frequent and severe natural events (Seneviratne et al., 2021) and the expansion and densification of human settlements (Ashley et al., 2014; Ashley and Strader, 2016; Iglesias et al., 2021). By adopting a conceptual framework that recognizes built environments as interconnected human-natural systems and incorporates them into risk assessments, we can thoroughly examine the essential components of risk—hazards, exposure, and vulnerability—as interdependent variables rather than isolated elements. This broader perspective not only acknowledges the significant role of built environments in shaping and impacting risk but also has the potential to reveal valuable insights into self-reinforcing feedbacks and unforeseen dynamics that narrower perspectives tend to overlook (Haff, 2003; Lazarus et al., 2016; Nordstrom, 1994; Werner & McNamara, 2007).

The connections between built environments, a primary indicator of exposure, and the other risk components can be investigated through various approaches and methodologies. For instance, we could examine the entire built-up footprint area and get an overview of the overall extent of human-altered landscapes (Braswell et al., 2022; Iglesias et al., 2021). Alternatively, we could focus on specific elements of the built environment, such as residential properties (Armstrong et al., 2016; Lazarus et al., 2018) or road networks (Aldabet et al., 2022), to understand their interactions with risk dynamics. Through a non-diachronic approach, we could assess the present physical and socio-economic characteristics of the system and its contribution to risk (Armstrong et al., 2016), while incorporating a temporal dimension would allow us to explore the historical evolution of the built environment and reveal the underlying processes and dynamics that have shaped its current state (Lazarus et al., 2018).

In this thesis, coastal built environments are conceptualized as coupled human-landscape systems, allowing for a thorough analysis of the empirical connections between their physical and socio-economic aspects that potentially amplify coastal risk. Across its chapters, the research employs varied methodologies, spans different time frames, and examines multiple structural elements, consistently focusing on extensive spatial scales and relying solely publicly accessible data. This systematic approach adheres to the three main objectives outlined in Chapter 1:

- To examine coastal built environments as interconnected human-natural systems, identifying empirical relationships between their natural and socio-economic components.
- To conduct analyses over extensive spatial extents, moving beyond the limitations of traditional, localized case studies.
- To rely exclusively on publicly available data.

Building on this framework, Chapter 2 presented a comprehensive evaluation of coastal risk across the open coast of England, exploring the complex interplay between its three fundamental components: exposure, hazard, and vulnerability (blue triangle in **Fig. 5.1**). Here, exposure encompassed population and building footprints, while coastal flooding and shoreline erosion represented the hazard component. Vulnerability, meanwhile, was assessed using a social disadvantage index and the presence of engineered hazard protection. The scarcity of historical data necessitated a non-diachronic approach, providing a snapshot of the built environment and coastal communities at the time of the assessment. Despite these data constraints, detailed further in section 5.1.2, the research preserved its wide geographical coverage and commitment to using only publicly available data sources.

Moving to the United States, where the abundance of publicly available, large-scale data broadened the scope of analysis, Chapter 3 delved into the comparison of the exposure and vulnerability components (green oval in **Fig. 5.1**), while subtly integrating the hazard element, given the study's focus on storm-prone coastal regions. In this case, residential properties were used to represent the exposure component, and vulnerability was based on property wealth and reliance on beach nourishment practices. Importantly, the inclusion of historical data in this chapter proved essential in enabling a more complete exploration of evolving development patterns and improving the comprehension of potential dynamics that contribute to increased risk.

Finally, Chapter 4 explored interactions between the hazard and exposure components along the developed barrier islands of the US (pink oval in **Fig. 5.1**), seeking to comprehend the susceptibility of vulnerable built environments to significant failures. In this study, the exposure element was represented by road networks, which are critical for societal functioning, while a bathtub coastal flooding scenario was used to model the hazard

component. This assessment primarily aimed at evaluating the capacity of the analyzed road networks to withstand extreme high-water events and identifying critical physical locations that, if disrupted, could lead to a complete functional failure of the entire system.

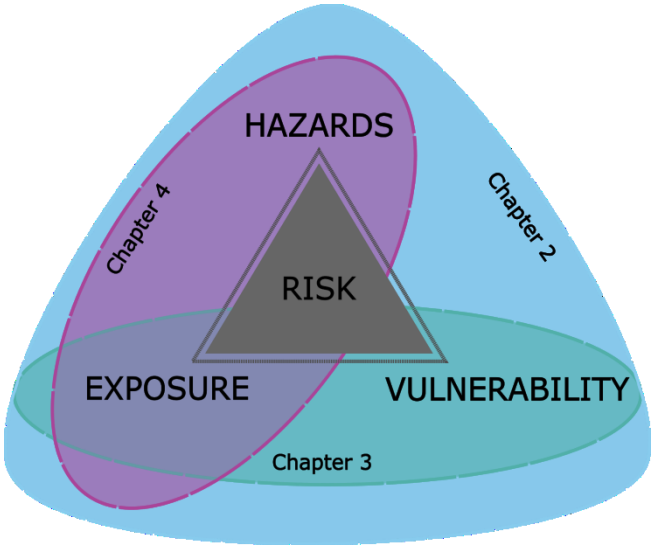

Figure 5.1 Interrelations between the components of risk explored in this thesis: hazard, exposure and vulnerability in Chapter 2, exposure and vulnerability in Chapter 3 and hazard and exposure in Chapter 4.

5.1.2 Advantages and drawbacks of large-scale analysis

Regardless of the approach taken to investigate the relationship between coastal development and coastal risk, it is crucial to consider the significance of scale and the limitations associated with localized case studies. While conventional case studies can offer valuable insights into specific risk dynamics such as the *levee effect*, their findings might not be easily extrapolated to larger scales due to their unique characteristics and processes (Di Baldasarre et al., 2018; Landry et al., 2003). To address this limitation, it becomes necessary to either compare multiple case studies to identify common patterns or conduct large-scale analyses that unveil widespread relationships (Collenteur et al., 2015; Di Baldasarre et al., 2018; Schultz and Elliott, 2013). Consequently, as stated in Chapter 1, a primary objective of this thesis was to examine the role of the built environment on coastal risk on a scale that allowed for more generalized conclusions than conventional case studies.

Conducting research at such scales, however, presents significant challenges, particularly regarding data availability and consistency. Data for large-scale analyses are often fragmented, scattered across different organizations, proprietary, or even nonexistent. The analysis conducted in Chapter 2, for instance, faced significant limitations due to the absence of comprehensive, standardized, and easily accessible datasets for evaluating coastal risk at a national level in the UK. These data constraints hindered our ability to thoroughly examine

spatiotemporal risk patterns resulting from the interactions among coastal hazards, exposure, vulnerability, and management interventions on a large scale, thus restricting our initial scope of work. While narrowing the analysis to a specific location in England might have mitigated some of these limitations and provided more detailed insights, it did not align with the broader dynamics that this thesis aimed to explore. Therefore, the next two chapters shifted the geographical focus to the United States, where comprehensive large-scale data was more readily available. Nonetheless, the challenges encountered during this research underscored the importance of relevant open-access data and prompted us to advocate for a dedicated open data portal in the UK, specifically addressing coastal erosion, flood risk, and resilience (Lazarus et al., 2021). The following points highlight the most significant data constraints experienced during this investigation:

Lack of temporal data

Despite our efforts, we encountered significant challenges in acquiring temporal data related to coastal defenses and building footprints. This limitation severely hindered our ability to explore spatial dynamics such as the *levee effect* on a large scale, thereby restricting our understanding of their broader implications. Throughout the assessment, attempts to access comprehensive publicly available datasets encompassing building footprints spanning multiple years across the entire study area, the coastal floodplains of England, were unsuccessful. The temporal data the Ordnance Survey Service provided, obtained upon request, was limited to a specific area within 100 meters of the shoreline, regrettably misaligned with the intended spatial scope. Additionally, the dataset on coastal defenses lacked temporal information regarding the implementation, maintenance, functionality, or repairs of the defenses, further restricting the analysis.

Incomplete coastal defenses

The Environment Agency's (EA) "National Flood and Coastal Defence Database" (presently archived) or the currently available "Spatial Flood Defences" dataset both aimed to compile a collection of data on flood and coastal defenses owned or managed by the EA. However, its coverage, restricted to assets within the Agency's jurisdiction and excluding coastal erosion defenses managed by other authorities, limited our comprehensive understanding of the broader coastal defense landscape. To address this gap, we used a coastal defenses dataset provided by the Channel Coastal Observatory (CCO, 2020), which encompasses both engineered and natural structures and offers a more extensive coverage along the English coastline. However, this dataset presents its own limitations as it does not extend to estuarine shorelines, where defenses are also present, and does not include information on beach nourishment projects, which is a significant gap considering their relevance to coastal risk management. In fact, there is a lack of comprehensive information on the application, cost, volume, and spatial extent of beach nourishment projects across the country. The

review conducted by Hanson et al. (2002) on European beach nourishment practices is outdated and, unlike the publicly available dataset maintained by the Program for the Study of Developed Shorelines (PSDS) in the US, which was used in Chapter 3, the underlying dataset of the review is not publicly accessible.

Disparities in the geographical range of coastal flooding

We defined the coastal floodplain using the "Flood Map for Planning (Rivers and Sea)" datasets (EA 2019a; 2019b), which provide information on the source of flooding (e.g., coastal or fluvial). However, these datasets did not consider the likelihood of flooding so, to determine the probability of these events, we relied on the Environment Agency's "Risk of Flooding by Rivers and Sea" dataset (EA 2019d). Yet, it is important to note that there are spatial discrepancies between the polygons representing the two data sources. These differences primarily arise because the first dataset does not account for the presence of coastal defenses in determining flooding extent, while the second dataset incorporates existing coastal defenses to assess flood probabilities.

Limited English-wide coastal erosion data

To represent the coastal erosion hazard on a spatial scale matching the coastal defenses dataset, we ultimately relied on a global dataset derived from Landsat data (Luijendijk et al., 2018). This dataset provides estimated rates of shoreline change in meters per year at transects spaced 500 meters apart along the coast. Although only validated for sandy beaches, the selection of this dataset was based on its extensive and standardized coverage of shoreline change, surpassing the boundaries of sub-national regions. England-wide coastal erosion data from the "futurecoast" project (DEFRA, 2002) theoretically exists, but is not readily accessible and has remained inactive for two decades. Likewise, the publicly available Environment Agency "National Coastal Erosion Risk Map" (EA, 2019c) is a derivative product consisting of binned projections of future change based on historical erosion rates, which made it inappropriate for our analytical purposes.

5.1.3 Comparative patterns in coastal risk

Despite the aforementioned limitations, Chapter 2 reflects the maximum level of understanding of spatial relationships among risk components achievable with the available open-access data, yielding results that closely align with earlier studies relying on proprietary data or modeling outcomes from contracted consultancies (CCC, 2018; Rözer and Surminski, 2020; Sayers, 2018; Zsamboky et al., 2011). Consistently, this previous research demonstrated a steady upward trend in residential development within floodplains over the past few decades, highlighting the increased exposure to natural hazards experienced by socially disadvantaged communities. Chapter 2 of this thesis further emphasizes the

disproportionate vulnerability of regions with significant social disadvantages to coastal flooding and shoreline erosion.

Specifically, the analysis reveals that approximately 16% of the population in England's coastal floodplain areas, around 113,880 individuals, resides in high-risk flood zones with an annual probability of flooding greater than 1 in 30 years. Among them, about 6,200 people and over 2,200 buildings are also challenged by chronic shoreline erosion. Consequently, the majority of coastal floodplain communities heavily rely on engineered defenses and the *Hold-the-Line* coastal management policy, which aims to maintain or enhance existing protection. These structures cover roughly 75% of the coastal floodplain shoreline and are often supplemented by natural features such as beaches and marshes, which provide additional protection against wave energy and flood damage. This setup effectively protects a significant portion of the coastal floodplain population and buildings against high-frequency, low-intensity natural hazards. However, future climate-driven forces are anticipated to challenge the effectiveness of these defenses, and continued government investment in hard coastal infrastructure is economically unviable (CCC, 2018). Future coastal management approaches may therefore lead to an approximately 15% reduction in the protected coastline area under the *Hold-the-Line* policy by 2100, doubling the number of people residing in *Managed Realignment* areas, and increasing the implementation of the *No Active Intervention* policy.

Our findings also show that most of the population and buildings on the coastal floodplain are found in areas of high social disadvantage. The convergence of coastal hazards in areas with high levels of disadvantage presents complex political challenges in steering these vulnerable regions towards socially and environmentally sustainable coastal futures (CCC, 2018; House of Lords, 2019). Residents with low incomes are particularly at risk, as their circumstances often lead them to reside in hazard-prone areas that are more affordable (McGranahan et al., 2007), and are less likely to have insurance coverage or resources for adequate disaster preparedness and recovery (England and Knox, 2014).

In the UK, coastal communities have unique characteristics that make them especially vulnerable to climate hazards, including aging populations, geographic and social isolation, inadequate housing conditions, higher unemployment rates, and lower wages (Zsamboky et al., 2011). The seasonal nature of their trade has contributed to a continuous decline in business activity and job opportunities, particularly impacting the younger generation (Centre for Social Justice, 2013). Recent reports show that around 71% of coastal towns in England and Wales have slower population and employment growth rates compared to national averages, whereas only 47% of non-coastal towns exhibit the same trend (Office for National Statistics, 2020). Coastal regions also experience higher levels of deprivation when compared to their non-coastal counterparts. The economic stagnation and lack of skilled

workforce experienced in these towns have caused property prices to decline significantly due to decreased demand (Centre for Social Justice, 2013). Consequently, former tourist accommodations and small businesses have been repurposed as affordable housing options, attracting especially vulnerable groups such as care leavers, individuals with substance abuse or mental health issues, and ex-offenders. This concentration of vulnerable individuals in certain coastal towns not only strains public services but also intensifies their vulnerability, to such an extent that:

> "...the British seaside has been perceived as a sort of national embarrassment.… [T]here are many smaller towns on the coast that have seen their unique selling point diminish.… Their sense of isolation and 'end of the line' feel has left small town, seaside communities overlooked and feeling unloved by the Government, local councils, service providers and businesses alike."
>
> **House of Lords (2019), pg. 6**

Interestingly, coastal demographic trends in the US present a stark contrast to those observed in English seaside towns. While the latter have experienced a decline in population over the past few decades (House of Lords, 2019; Zsamboky et al., 2011), most coastal areas of the US have seen a disproportionate growth in population and a concentration of wealth in coastal real estate since the 1970s (Armstrong et al., 2016; Crossett et al., 2013; Lazarus et al., 2018). Coastal communities in the US exhibit denser and more intensely developed built environments compared to inland areas, and even regions with a history of devastating events have witnessed an increase in the number of structures in recent decades, often exceeding average trends (Braswell et al., 2022; Lazarus et al., 2018). In barely 17% of the total land area, US coastal counties accommodate more than half of the country's population (Crossett et al., 2004; Crossett et al., 2013) and a significant number of high-value properties (Nordstrom, 2004). The continuous expansion of the built environment in these areas has increased the number of vulnerable "targets", raising the probability of hazards impacting developed land and triggering disasters that affect a larger population and more valuable assets (Ashley & Stradler, 2016). If current development patterns persist, approximately 2.5 million coastal properties in the US, worth about $1.07 trillion, will be at risk of chronic flooding by the end of the century (Union of Concerned Scientists, 2018). Therefore, despite their inherent differences, coastal communities in the UK and the US are escalating their susceptibility to coastal hazards and will encounter considerable challenges associated with coastal risk in the coming decades.

5.1.4 Unintended consequences of hazard protection

Although it is widely recognized that increasing exposure plays a pivotal role in the long-term amplification of economic losses from natural disasters (Cutter & Emrich, 2005; Iglesias et

al., 2021; Lazarus et al., 2018), evidence suggests that populations and their built environments continue to expand within physically vulnerable regions, including most coastal regions worldwide (Ashley & Strader, 2016; Braswell et al., 2022; Chen et al., 2019; Iglesias et al., 2021; McGranahan et al., 2007; Neumann et al., 2015; Nicholls & Small 2002). This paradoxical trend has sparked increasing interest in studying underlying dynamics that may be contributing to these emerging development patterns (Armstrong et al., 2016; Braswell et al., 2022; Iglesias et al., 2021; Lazarus et al., 2018). Notably, a growing body of research points to the unintended effects of hazard protection, which may inadvertently encourage development in areas prone to disasters (Burby, 2006; Burton and Cutter, 2008; Di Baldassarre et al., 2018; 2013; Kates et al., 2006; Montz and Tobin, 2008; Tobin, 1995; White, 1945), creating a false sense of safety among the protected communities, who often underestimate, minimize or even deny risk (De Marchi and Scolobig, 2012). This belief reduces risk awareness and preparedness—potentially increasing the vulnerability of the exposed communities—and sustains continuous urban development in disaster-prone areas. Thus, the presence of defenses drives development and, in turn, increased exposure demands more protection (McNamara & Werner, 2008a; 2008b; Werner & McNamara, 2007), locking the system into self-reinforcing feedbacks that can eventually lead to disaster traps (Lazarus, 2022b).

In this thesis, the absence of temporal data in Chapter 2 posed a limitation in assessing the influence of hazard defense implementation on coastal development in England and, consequently, obtaining a more comprehensive understanding of their contribution to the exacerbation of coastal risk at larger scales. However, by shifting the analysis to the United States, where publicly available data is more readily accessible, it was possible to explore how certain management practices may inadvertently contribute to the escalation of coastal risk. Specifically, the beach nourishment database maintained by the Program for the Study of Developed Shorelines (PSDS) at Western Carolina University (PSDS, 2021) served as a valuable resource in Chapter 3 to study the impact of this particular form of protection on the evolution of the coastal built environment.

Beach nourishment, the practice of importing sand to replenish and widen eroding beaches, has been the primary strategy in the US since the 1970s for protecting coastal development from the adverse effects of coastal hazards and the potential loss of properties (NRC, 2014). Yet, beyond its protective role, beach nourishment also generates economic benefits. Wide beaches, often achieved through nourishment practices, can be seen as a form of natural capital, contributing to the economic growth of tourism-related businesses, enhancing the value of oceanfront properties facing coastal hazards, and benefiting coastal communities as a whole through factors such as real estate values, hotel occupancy rates, and sales taxes (Lazarus et al., 2011). Previous research has consistently emphasized the positive influence of beach nourishment on property values, leading to stability or even an increase in

oceanfront house prices in areas prone to coastal hazards (Blackwell et al., 2010; Landry et al., 2003; Pompe and Rinehart, 1995; Qiu and Gopalakrishnan, 2018). For instance, the study conducted by Qiu and Gopalakrishnan (2018) in Nags Head, North Carolina, revealed that investments in beach nourishment resulted in a significant increase of 11.7% to 16.5% in house prices for shorefront properties located on nourished beaches. Yet, conclusions drawn from case studies tend to be location-specific and may not be applicable at larger scales (Laundry et al., 2003; Di Baldasarre et al., 2018). For this reason, Chapter 3 of this thesis aimed to investigate the wider implications of beach nourishment on property values in two prominent geographical regions of the US: the barrier islands of New Jersey and the Atlantic and Gulf Coasts of Florida.

Our findings demonstrate that beach nourishment has a significant and positive impact on property values at a large scale, suggesting that local management practices, policies, or regulations do not influence observed patterns. During the analyzed periods, residential houses in municipalities benefiting from nourishment in New Jersey and Florida were sold at premiums of 12% and 32%, respectively, compared to houses located in non-nourished areas. Proximity to the beach also played a role, as homes closer to the beach commanded higher prices, particularly in towns that underwent nourishment projects. Additionally, beach nourishment correlated with larger residential properties. In New Jersey, homes located on the first block from the beach were on average 14% larger in nourished municipalities than in non-nourished ones, while in Florida, shorefront houses in nourished towns were 24% larger.

Incorporating a temporal dimension on the analysis, our study also reveals a consistent trend of increasing house sizes over time, resulting in a higher level of exposure in coastal areas vulnerable to hazards. Notably, this expansion of coastal development is more pronounced and rapid in nourished zones compared to non-nourished areas. Even areas frequently affected by natural hazards experienced a noticeable pattern of properties becoming larger. For example, storm-prone municipalities such as Naples and Palm Beach witnessed substantial growth in house size between 2012 and 2017, with growth rates of 59% and 30% respectively, underscoring a clear trend of *building back bigger* (Lazarus et al., 2018). These findings support previous claims that residential assets in areas with a history of catastrophic events are increasingly exposed to risks, despite efforts to reduce vulnerability in developed coastal areas (Braswell et al., 2022; Lazarus et al., 2018).

Overall, the consistent disparities observed between nourishing and non-nourishing regions imply that areas under protective measures tend to show more pronounced trends of development. Furthermore, the presence of this connection between protection and development across different datasets and within two distinct large-scale geographical regions strongly indicates that these spatial associations are not random or limited to local

influences. Instead, they potentially unveil a prevalent pattern that characterizes well-developed coastlines across the United States.

5.1.5 Networks of critical infrastructure in evolving human-landscape systems

Developed coastal environments undergo continuous transformations as a result of management decisions, interventions for hazard mitigation, and intentional manipulation of natural landforms (McNamara & Lazarus, 2018). The construction and protection of coastal built environments, for example, have a profound impact on the natural pathways of sediment transport, leading to the redistribution and reassignment of local sediment budgets (Nordstrom, 1994, 2004). Modifications in sediment dynamics, in turn, have significant implications for the spatial patterns of hazard exposure, demanding adaptive measures from coastal management and planning.

Dynamic coastal environments such as barrier islands, which are in constant change due to the action of waves, tides, currents, and winds (Mulhern et al., 2017), are particularly susceptible to human interventions that modify their natural settings and destabilize their spatiotemporal processes (McNamara and Lazarus, 2018). Yet, most barrier islands in the world are under huge development pressure (Stutz and Pilkey, 2011), resulting in intricate interactions between human activities and coastal changes that elevate the potential for environmental disasters (Dolan and Lins, 2000; Mcnamara and Lazarus, 2018; Zhang and Leatherman, 2011). Consequently, the future trajectory of these islands relies heavily on the resilience of their built environments and the effectiveness of localized hazard-mitigation measures (e.g., seawalls, beach nourishment, dune construction) implemented to protect them against storm impacts, chronic erosion, and rising sea levels (Armstrong and Lazarus, 2019a; Lazarus et al., 2016; Lazarus and Goldstein, 2019; McNamara and Keeler, 2013; McNamara and Lazarus, 2018; McNamara and Werner, 2008a, 2008b; McNamara et al., 2015; Miselis and Lorenzo-Trueba, 2017; Nordstrom, 1994, 2004; Rogers et al., 2015).

Integral to the fabric of these built environments are networks of critical infrastructure, such as roads and public utilities, which connect physical spaces and support the well-being and quality of life of individuals (Jennelius and Mattson, 2012). In the United States, road networks serve as the primary means of transportation for people and goods on barrier islands and are vital to hazard evacuation, emergency response, and post-disaster recovery operations (Anarde et al., 2018; Darestani et al., 2021; Frazier et al., 2013; Godschalk et al., 1989; Velasquez-Montoya et al., 2021). Yet, these roads face recurrent disruptions—mechanisms that cause reductions in mobility or increases in the costs necessary to maintain the desired levels of mobility (Markolf et al., 2019)—during hurricanes, tropical storms, and nor’easters (Dolan & Lins, 2000; Hardin et al., 2012; Krynock et al., 2005; Nordstrom, 2004; Nordstrom and Jackson, 1995; Spanger-Siegfried et al., 2014; Velasquez-Montoya et al.,

2021), as well as a result of king tides, sea-level anomalies, groundwater flooding, or other factors that lead to nuisance or “sunny day” flooding (Fant et al., 2021; Hino et al., 2019; Housego et al., 2021; Jacobs et al., 2018; Moftakhari et al., 2018; 2015; 2017; Praharaj et al., 2021). These road network disruptions can have significant socio-economic impacts, isolating neighborhoods, compromising evacuation efforts, and impeding access to critical services (Balomenos et al., 2019; Dong et al., 2020; Jenelius and Mattson, 2012; Spanger-Siegfried et al., 2014; Suarez et al., 2005). Even the maintenance and restoration of other critical systems (e.g. electricity, water supply, and communications) often rely on a functioning road network (Chang, 2016; Johansen and Tien, 2018; Mattson and Jenelius, 2015; Nicholson and Du, 1997).

Examining infrastructure networks on developed barrier islands is therefore crucial for identifying thresholds in their functioning that could lead to large-scale breakdowns and compromise the functionality of the entire built environment. Such analyses or modeling exercises may also inform necessary changes in management and planning and provide valuable insights into the future of these delicate human-landscape systems. The analysis conducted in Chapter 4 of this thesis explores a method for identifying key physical locations that, if disrupted by flooding, could trigger functional failure in barrier-island road networks. The components of this threshold, which differ across barrier islands, are organized using three metrics: the elevation of the critical node responsible for network collapse, the annual exceedance probability associated with that elevation, and the overall robustness of the network to flood-induced failures.

Elevation plays a primary role in determining the sequence of road closures, as intersections at the lowest elevations are expected to be among the first disrupted during floods (Abdulla and Birgisson, 2021). Given the low topography of the analyzed islands, our findings indicate that a significant portion of their road networks are at risk of flood-induced failure. Most road intersections are situated below 5 meters elevation, with nearly half (44%) of the critical nodes—intersections whose disruption leads to the collapse of the network—located below 1.5 meters and the majority (85%) below 2.5 meters. But inferring road network susceptibility to failure purely in terms of node elevation is not meaningful, due to local and regional variations in tidal range and exposure to extreme high-water levels. Thus, connecting the elevation of each barrier road network node to the estimated local exceedance probabilities of extreme high-water levels, we find that nodes at the same elevation but on different barrier islands could be associated with markedly different flood probabilities. Similarly, when examining the overall robustness of these networks, which provides an assessment of the entire network’s architecture and its ability to withstand the successive disturbance of nodes, we observe that some networks that were initially considered highly susceptible to flood-induced failures, due to the elevation and/or exceedance probability of their critical node, exhibit notable resistance to elevation-controlled disturbances like flooding.

The results of this study suggest that no single metric can be used to determine the barrier susceptibility to disruption, as:

> "...different metrics can capture different properties of robustness of a system, which can be contrasted with results captured from the other metrics."
>
> **Kermanshah and Derrible (2017), p. 162**

A barrier network that may initially exhibit a high susceptibility to disturbance based on one metric could demonstrate considerable resilience based on another. For instance, a network with a critical node at a very low elevation could be positioned in a place unlikely to be impacted by extreme high-water levels, and/or possess an architectural design with inherent strength against elevation-controlled disturbances like flooding. Yet, the analysis offers a simple method to explore road network robustness against extreme high-water events, using open-access data.

The identification of a critical node leading to network failure is a valuable initial diagnostic based on the assumption that topography influences flood susceptibility. Further observation of natural settings will be required to verify whether flood-driven failures of coastal and other floodplain road networks are fundamentally linked to topography at critical nodes. But, if supported, this approach would highlight specific nodes or groups of nodes in a road network, which, if targeted in climate adaptation planning at local scales—especially in resource-constrained situations—could significantly enhance the overall functionality of the network. If the critical node of a road network were elevated by a local intervention that rearranged the three-dimensional network topology, a different node elsewhere in the network would become the new critical junction. But if that new critical node had a significantly lower annual exceedance probability, then the functional susceptibility of the network to failure would have improved, as long as other human interventions, such as hazard defenses, do not likewise displace flooding impacts in unintentionally confounding ways.

Nevertheless, it is important to acknowledge that our analysis did not account for changing environmental conditions, which play a vital role in predicting future barrier island dynamics. Consequently, while our results provide valuable insights into road network robustness based on historical conditions, they may underestimate the susceptibility to failure under future scenarios. Similarly, the study presented in Chapter 4 focused solely on network disruption based on elevation, without considering other flood drivers (e.g., marine, pluvial, groundwater…) or flooding consequences such as standing water, road damage, traffic flow, or sediment deposition.

5.1.6 Impact of coastal engineering on the risk triangle

This dissertation examines the dynamic interactions among the elements of risk—hazard, exposure, and vulnerability— and their combined effects on coastal risk, as illustrated by the Risk Triangle in **Fig. 5.1**. Within this framework, coastal engineering interventions, which fall here under the vulnerability component, are of particular importance, as they have the dual potential to either mitigate or exacerbate coastal risk. This dichotomy challenges the traditional belief that engineering always reduces vulnerability, suggesting instead that it can also enhance it, as argued in this thesis.

Beach nourishment, for example, stands out as an effective method against coastal erosion. It provides cost benefits in both construction and maintenance compared to traditional structural methods, and helps prevent economic declines (Alexandrakis et al., 2015). Widely recognized as a cost-efficient solution, beach nourishment is frequently recommended to protect vulnerable coastal communities and their economies (e.g., Spencer et al., 2022). Beyond preserving revenues from beach tourism, nourishment plays a crucial role in mitigating storm-induced damage to coastal properties and infrastructure, thereby stabilizing or even enhancing their market values (Blackwell et al., 2010; Landry et al., 2003; Pompe and Rinehart, 1995; Qiu & Gopalakrishnan, 2018). Empirical evidence presented in Chapter 3 underscores this revalorizing effect of beach nourishment, demonstrating that areas benefitting from such interventions feature a higher number of residences, which are also larger and command higher market values compared to regions without nourishment efforts.

Thus, at first glance, engineered coastal defenses seem to reshape the risk triangle by ostensibly diminishing exposure to coastal threats. However, this perceived reduction can lead to an ironic outcome: while the immediate perception of risk may be lowered through these defensive actions, the resulting increase in development—driven by an enhanced sense of security—unintentionally raises the potential for damage by concentrating more assets and population in areas inherently susceptible to coastal hazards (Burby, 2006; Burton and Cutter, 2008; Di Baldassarre et al., 2018; 2013; Kates et al., 2006; Montz and Tobin, 2008; Tobin, 1995; White, 1945). This paradox highlights the complex impact of engineering interventions on coastal risk, supporting the thesis's claim that coastal defenses, rather than mitigating risk, may inadvertently amplify it.

Maintaining the effectiveness of coastal defenses crucially hinges on proper management, consistent upkeep, and timely upgrades. These requirements grow more and more pressing as climate change and sea-level rise pose increasing challenges. The dilemma emerges when the sustainability of these defenses is questioned, potentially leading to their neglect or abandonment. This scenario is not hypothetical; as outlined in Chapter 2, despite calls for greater maintenance funding for the UK's flood defense systems to maintain their operational efficiency and cost-effectiveness, the coming decades may see a heightened risk of their

failure or neglect, thereby intensifying the vulnerability to coastal flooding and erosion (Committee on Climate Change, 2018; Priestley and Allen, 2017). In light of these growing threats, it is likely that continuous investment will be necessary not only to keep existing defenses operational but also to enhance and expand them to cope with more severe impacts. Failing to implement these critical updates could severely compromise existing safety measures and significantly escalate risks, turning areas that were once considered safe into potential disaster hotspots.

Yet, in spite of the uncertainties of climate change and the substantial financial demands of coastal management, the persistent and widespread coastal engineering efforts that support human development along the global coastlines continue to drive urbanization trends in regions that will inevitably require sustained investment to ensure their safety. Recent decades have witnessed the rise of coastal mega-projects designed to attract luxury real estate investments, with prominent examples in Gulf nations such as the Palm Islands in Dubai, The Pearl in Doha, and Durrat Al Bahrain on Bahrain Island. Aggressive urban developments have dramatically transformed coastlines around the world, replacing natural landscapes with artificial structures to accommodate growing populations. The world's longest man-made dike, the 33-kilometer Saemangeum Seawall in South Korea, illustrates how extensive engineering efforts can profoundly alter landscapes and ecosystems (Baek et al., 2024; Lee et al., 2018). Consequently, although these developments and technological advancements have driven economic growth and human expansion, they also stress fragile coastal ecosystems (Williams et al., 2022) and modify ecological and physical dynamics in ways that could heighten coastal risk and its related expenses (Lazarus, 2022b).

As the detrimental impacts of extensive coastal urbanization become increasingly apparent, there has been a significant rise in environmental management research, prompting demands for stricter environmental regulations and enhanced management practices in vulnerable regions (Burt and Bartholomew, 2019). Despite these concerns, the continuing necessity for coastal engineering to protect communities and promote development remains. This has led to the adoption of innovative strategies like the Netherlands' "Sand Engine" initiative ("ZandMotor" in Dutch). This pioneering mega-nourishment project leverages natural processes to distribute 21 million cubic meters of sand along the coastline, offering a more sustainable method to strengthening coastal defenses (Luijendijk et al., 2017). However, the long-term effectiveness and ecological impacts of such nature-based solutions still demand persistent monitoring and in-depth research to be fully understood (Huisman et al., 2021).

5.2 Future work

This thesis underlines the importance of studying coastal built environments as interconnected human-landscape systems to gain valuable insights into their current state and future development. However, throughout this investigation, it became evident that exploring the dynamics of developed coastlines on a large scale presents significant challenges. Detailed housing data offers valuable insights into the physical attributes of the built environment (as outlined in Chapter 3) and can even serve as a proxy to assess property values (Armstrong et al., 2016; Lu et al., 2013; Sirmans et al., 2005). Yet, Chapter 2 demonstrated that acquiring comprehensive and up-to-date building data at large scales might be difficult due to inconsistent availability, further compounded by privacy and cost issues (Lu et al., 2013). Collections of geocoded housing and property-level data, such as the Zillow Transaction and Assessment Dataset (ZTRAX) used to create the Historical Settlement Data Compilation for the US (HISDAC-US; Leyk & Uhl, 2018), remain predominantly proprietary and not universally available for all countries. Similarly, national censuses may provide essential information about population density, distribution, and the characteristics of the built environment, but their resource-intensive, costly, and time-consuming nature results in infrequent implementation, particularly within developing countries. Hence, future research success in this field will hinge upon the availability of high-quality, comprehensive data accurately representing the physical, socioeconomic, and operational aspects of the built environment and its infrastructure networks. Promisingly, the forward-looking discourse on sustainable urban systems includes calls for “developing new data and methods to understand current drivers and interactions among natural, human-built, and social systems in urban areas as they impact multiple sustainability outcomes across scales” (ACERE, 2018).

Increasing accessibility to high-resolution geospatial data for both natural and human systems also offers an encouraging prospect for gaining deeper insights into the interconnections between risk components in built environments exposed to natural hazards. Over the last decades, Earth observations (EO), particularly satellite remote sensing, have become a valuable resource for assessing exposure and vulnerability factors, including urbanization and land management practices (Le Cozannet et al., 2020), as well as for monitoring coastal hazards and their drivers (Melet et al., 2020). Remote sensing technology enables the rapid acquisition of urban attributes, such as buildings or roads, and serves as a valuable tool for quantifying the built environment and assessing the spatiotemporal dimensions of physical exposure in disaster risk assessments (Ehrlich and Tenerelli, 2013). The geometric characteristics of building footprints, for example, can be used as proxy variables for investigating development trends in areas prone to hazards (Lazarus et al., 2018), or for assessing building resistance to flood impacts and estimating flood-related losses (Cerri et al., 2021). Thus, the growing availability of building-level data through

industry sources like Google (Sirko et al., 2021) and Microsoft, along with volunteered geographic information platforms such as OpenStreetMap (Atwal et al., 2022), or OpenCityModel, expands the potential for future research on built environments in other extensive geographical regions, including those with limited resources and potential data scarcity.

Other satellite-derived outputs can also be leveraged to surmount data limitations, particularly when assessing socioeconomic indicators that may prove difficult to obtain through conventional methods. For instance, researchers have used satellite-derived nightlight intensity as a surrogate for income and economic growth (Henderson et al., 2012), to delineate developed urban regions (Shi et al., 2012), predict high-resolution spatial employment density (Barzin et al., 2021), or to examine long-term relationships between human proximity to rivers, floods, and flood protection levels (Mård et al., 2018). In this context, cloud-based platforms like Google Earth Engine and Microsoft's Planetary Computer emerge as potent tools that significantly enhance the available resources, providing robust and efficient channels for both accessing and conducting advanced analysis of pre-processed satellite imagery. Moreover, they grant access to a comprehensive array of geospatial information, including aspects such as land cover, elevation, temperature, and vegetation.

In the European setting, where, as evidenced in Chapter 2, acquiring large-scale datasets has proven challenging, upcoming investigations exploring the influence of built environments on coastal risk could greatly benefit from the use of data originating from recent EU-funded initiatives such as CoCliCo (Coastal Climate Core Service; grant agreement No. 101003598). This project brings together European institutions and scholars with well-established expertise in broad-scale coastal risk assessment, research, and geospatial data management. The primary goal is to establish an open-source web platform that offers relevant and high-quality geospatial information layers on dominant risk drivers, thereby facilitating decision-making processes related to coastal risk management and strategies for adapting to rising sea levels. As a team member at Vizzuality, one of the consortium partners, I am currently engaged in this project, providing scientific support to the design and communication team.

Future work could also harness emerging data products like the Historical Settlement Data Compilation for Spain (HISDAC-ES; Uhl et al., 2023). This database integrates cadastral and building data to furnish a comprehensive collection of finely detailed gridded surfaces describing the physical, functional, and temporal facets of the built environment in Spain. Its public accessibility allows for conducting long-term, multi-dimensional analyses of the built environment in other large-scale coastal regions that have experienced substantial urban

land growth and increased exposure to flooding and shoreline erosion in recent decades, such as the Mediterranean coastline of Spain (Olcina et al., 2010, 2016).

5.3 Reflections

It is indeed puzzling that, despite the prevailing awareness of natural hazards and their capacity to inflict severe impacts on built environments, urban and population expansion continues unabated in regions susceptible to catastrophic events. This situation prompts critical questions about the underlying forces and dynamics that shape the decision-making processes in land development, particularly considering the increased risks posed by climate change in the coming decades. Even well-intentioned initiatives aimed at mitigating these impacts often result in unintended consequences that worsen already precarious situations. Historical reviews of early 20th-century levee constructions (Segoe, 1937; White, 1945), or the catastrophic failures during Hurricane Katrina (Burby, 2006), reveal a consistent theme: safety measures paradoxically increase risk. This observation prompts a vital question: Why does this cycle of hazardous development and repeated disasters continue? Do we need more research, or are there other impediments preventing the effective use of our knowledge?

The persistent reliance on progressively sophisticated engineering solutions to support development may reflect a deep-rooted conviction in our capacity to master and reshape nature. This mindset could stem from a lack of awareness of the consequences—as evidenced by De Marchi and Scolobig (2012)—or it could even represent a kind of hubris that drives us to overlook historical lessons in our quest for expansion, frequently under an illusory sense of safety that could result in catastrophic consequences. To truly comprehend the situation and potentially identify a more sustainable approach to coexist with nature, a thorough reassessment of our urban planning and disaster risk management strategies is required. This reevaluation should encourage the adoption of more sustainable and prudent strategies that recognize the limits of our control over nature and take into account the interconnected nature of our human-altered landscapes. Therefore, effective disaster risk reduction and adaptation strategies necessitate a comprehensive examination of the socio-economic, environmental, and policy factors that fuel the expansion of built environments in hazard-prone zones.

Expanding on these discussions, this thesis conceives coastal built environments as complex human-landscape systems that operate over vast spatial scales and extended timeframes. Earlier research was mostly theoretical (Mileti, 1999; Smith et al., 2009; Werner and McNamara, 2007) or focused on specific locations and events (e.g., Burby, 2006). However, a significant advancement is evident in Armstrong's (2019) pioneering work, which leveraged *big data* from diverse sources to establish a comprehensive framework for understanding

coastal risk, enabling the visualization of dynamic interactions involving hazards, exposure, and vulnerability over extended periods. Building upon this foundational work, the present thesis delves deeper into the dynamics of developed coastlines, placing special emphasis on the potential role of built environments in amplifying risks within coastal areas, ultimately intensifying the financial and social burdens faced by vulnerable communities.

Understanding the complex interplay between our actions and the consequences of natural hazards is essential for driving positive change. Although disaster research is well-established, its insights need to move beyond academic circles and reach a broader audience. By incorporating this knowledge into policy-making and increasing awareness among residents of these areas, we can foster more sustainable living practices and strengthen community resilience.

List of References

Abdulla, B., and Birgisson, B. (2021) 'Characterization of vulnerability of road networks to random and nonrandom disruptions using network percolation approach', *Journal of Computing in Civil Engineering*, 35(1), 04020054. DOI: 10.1061/(asce)cp.1943-5487.0000938

ACERE - Advisory Committee for Environmental Research and Education (2018) *Sustainable Urban Systems: Articulating a Long-Term Convergence Research Agenda. A Report from the NSF Advisory Committee for Environmental Research and Education.* Prepared by the Sustainable Urban Systems Subcommittee. DOI: 10.13140/RG.2.2.31234.94406

Aldabet, S., Goldstein, E. B., and Lazarus, E. D. (2022) 'Thresholds in road network functioning on US Atlantic and Gulf barrier islands', *Earth's Future*, 10(5), e2021EF002581. DOI: 10.1029/2021EF002581

Alexandrakis, G., Manasakis, C., & Kampanis, N. A. (2015) 'Valuating the effects of beach erosion to tourism revenue. A management perspective', *Ocean & Coastal Management*, 111, pp. 1-11. DOI: 10.1016/j.ocecoaman.2015.04.001

Aerts, J. C., Botzen, W. W., Emanuel, K., Lin, N., De Moel, H., and Michel-Kerjan, E. O. (2014) 'Evaluating flood resilience strategies for coastal megacities', *Science*, 344(6183), pp. 473-475. DOI: 10.1126/science.1248222

Albert, R., and Barabási, A. L. (2002) 'Statistical mechanics of complex networks', *Reviews of Modern Physics*, 74(1), pp. 47–97. DOI: 10.1103/revmodphys.74.47

Amante, C., Stroker, K., Love, M., Stiller, M., Carignan, K., and Arcos, N. (2021) 'Coastal Digital Elevation Models (DEMs) to Support Storm Surge Inundation Modeling'. Presented at 101st American Meterological Society Annual Meeting (virtual). Link to reference.

Anarde, K. A., Kameshwar, S., Irza, J. N., Nittrouer, J. A., Lorenzo-Trueba, J., Padgett, J. E., et al. (2018) 'Impacts of hurricane storm surge on infrastructure vulnerability for an evolving coastal landscape', *Natural Hazards Review*, 19(1), 04017020. DOI: 10.1061/(asce)nh.1527-6996.0000265

Apel, H., Thieken, A. H., Merz, B., and Blöschl, G. (2004) 'Flood risk assessment and associated uncertainty', *Natural Hazards and Earth System Sciences*, 4(2), pp. 295–308. DOI: 10.5194/nhess-4-295-2004

Apel, H., Thieken, A. H., Merz, B., and Blöschl, G. (2006) 'A probabilistic modelling system for assessing flood risks', *Natural Hazards*, 38(1), pp. 79–100. DOI: 10.1007/s11069-005-8603-7

Armstrong, S. B. (2019) *Exploring unintended feedbacks between coastal hazard, exposure, and vulnerability*. Doctoral dissertation, University of Southampton.

Armstrong, S. B., and Lazarus, E. D. (2019a) 'Masked shoreline erosion at large spatial scales as a collective effect of beach nourishment', *Earth's Future*, 7(2), pp. 74-84. DOI: 10.1029/2018ef001070

Armstrong, S. B., and Lazarus, E. D. (2019b) 'Reconstructing patterns of coastal risk in space and time along the US Atlantic coast, 1970–2016', *Natural Hazards and Earth System Sciences*, 19(11), pp. 2497-2511. DOI: 10.5194/nhess-2019-159-rc1

Armstrong, S. B., Lazarus, E. D., Limber, P. W., Goldstein, E. B., Thorpe, C., and Ballinger, R. C. (2016) 'Indications of a positive feedback between coastal development and beach nourishment', *Earth's Future*, 4(12), pp. 626-635. DOI: 10.1002/2016EF000425

Arrighi, C., Pregnolato, M., and Castelli, F. (2021) 'Indirect flood impacts and cascade risk across interdependent linear infrastructures', *Natural Hazards and Earth System Sciences*, 21(6), pp. 1955–1969. DOI: 10.5194/nhess-21-1955-2021

Ashley, W. S., and Strader, S. M. (2016) 'Recipe for disaster: How the dynamic ingredients of risk and exposure are changing the tornado disaster landscape', *Bulletin of the American Meteorological Society*, 97(5), pp. 767-786. DOI: 10.1175/bams-d-15-00150.1

Ashley, W. S., Strader, S., Rosencrants, T., and Krmenec, A. J. (2014) 'Spatiotemporal changes in tornado hazard exposure: The case of the expanding bull's-eye effect in Chicago, Illinois', *Weather, Climate, and Society*, 6(2), pp. 175-193. DOI: 10.1175/WCAS-D-13-00047.1

Atwal, K. S., Anderson, T., Pfoser, D., and Züfle, A. (2022) 'Predicting building types using OpenStreetMap', *Scientific Reports*, 12(1), article number 19976. DOI: 10.1038/s41598-022-24263-w

Baek, J. Y., Guerreiro, C. V., Kim, J., Nam, J., & Jo, Y. H. (2024) 'Coastal environmental changes after the Saemangeum seawall construction', *Frontiers in Marine Science*, 10, 1307218.

Balaguer, P., Sarda, R., Ruiz, M., Diedrich, A., Vizoso, G., and Tintore, J. (2008) 'A proposal for boundary delimitation for integrated coastal zone management initiatives', *Ocean & Coastal Management*, 51(12), pp. 806-814. DOI: 10.1016/j.ocecoaman.2008.08.003

Balomenos, G. P., Hu, Y., Padgett, J. E., and Shelton, K. (2019) 'Impact of coastal hazards on residents' spatial accessibility to health services', *Journal of Infrastructure Systems*, 25(4), article number 04019028. DOI: 10.1061/(asce)is.1943-555x.0000509

Barzin, S., Avner, P., Rentschler, J., and O'Clery, N. (2022) *Where are All the Jobs? A Machine Learning Approach for High Resolution Urban Employment Prediction in Developing Countries*. The World Bank. DOI: 10.1596/1813-9450-9979

Batibeniz, F., Ashfaq, M., Diffenbaugh, N. S., Key, K., Evans, K. J., Turuncoglu, U. U., and Önol, B. (2020) 'Doubling of U.S. Population exposure to climate extremes by 2050', *Earth's Future*, 8(4), article number e2019EF001421. DOI: 10.1029/2019EF001421

Berezina, P., and Liu, D. (2022) 'Hurricane damage assessment using coupled convolutional neural networks: a case study of hurricane Michael', *Geomatics, Natural Hazards and Risk*, 13(1), pp. 414-431. DOI: 10.1080/19475705.2022.2030414

Blackwell, C., Sheldon, S., and Lansbury, D. (2011) 'Beach Re-Nourishment and Property Value Growth: The Case of Folly Beach, South Carolina', *South Carolina* (February 11, 2011). DOI: 10.2139/ssrn.1760018

Boeing, G. (2017) 'OSMnx: New methods for acquiring, constructing, analyzing, and visualizing complex street networks', *Computers, Environment and Urban Systems*, 65, pp. 126–139. DOI: 10.1016/j.compenvurbsys.2017.05.004

Boeing, G. (2019) 'Urban spatial order: Street network orientation, configuration, and entropy', *Applied Network Science*, 4(1), pp. 1–19. DOI: 10.1007/s41109-019-0189-1#Abs1

Boeing, G. (2020) 'A multi-scale analysis of 27,000 urban street networks: Every US city, town, urbanized area, and Zillow neighborhood', *Environment and Planning B: Urban Analytics and City Science*, 47(4), pp. 590–608. DOI: 10.1177/2399808318784595

Bounova, G., and de Weck, O. (2012) 'Overview of metrics and their correlation patterns for multiple-metric topology analysis on heterogeneous graph ensembles', *Physical Review E*, 85(1), article number 016117. DOI: 10.1103/physreve.85.016117

Braswell, A. E., Leyk, S., Connor, D. S., and Uhl, J. H. (2022) 'Creeping disaster along the US coastline: Understanding exposure to sea level rise and hurricanes through historical development', *PLoS one*, 17(8), article number e0269741. DOI: 10.1371/journal.pone.0269741

Brody, S. D., Zahran, S., Highfield, W. E., Grover, H., and Vedlitz, A. (2008) 'Identifying the impact of the built environment on flood damage in Texas', *Disasters*, 32(1), pp. 1-18. DOI: 10.1111/j.1467-7717.2007.01024.x

Brody, S. D., Zahran, S., Maghelal, P., Grover, H., and Highfield, W. E. (2007) 'The rising costs of floods: Examining the impact of planning and development decisions on property damage in Florida', *Journal of the American Planning Association*, 73(3), pp. 330-345. DOI: 10.1080/01944360708977981

Buchanan, M. K., Oppenheimer, M., and Kopp, R. E. (2017) 'Amplification of flood frequencies with local sea level rise and emerging flood regimes', *Environmental Research Letters*, 12(6), article number 064009. DOI: 10.1088/1748-9326/aa6cb3

Burby, R. J. (2006) 'Hurricane Katrina and the paradoxes of government disaster policy: Bringing about wise governmental decisions for hazardous areas', *The annals of the American Academy of Political and Social Science*, 604(1), pp. 171-191. DOI: 10.1177/0002716205284676

Burningham, H., and French, J. (2017) 'Understanding coastal change using shoreline trend analysis supported by cluster-based segmentation', *Geomorphology*, 282, pp. 131-149. DOI: 10.1016/j.geomorph.2016.12.029

Burt, J. A., and Bartholomew, A. (2019) 'Towards more sustainable coastal development in the Arabian Gulf: Opportunities for ecological engineering in an urbanized seascape', *Marine pollution bulletin*, 142, pp. 93-102. DOI: 10.1016/j.marpolbul.2019.03.024

Burton, C., and Cutter, S. L. (2008) 'Levee failures and social vulnerability in the Sacramento-San Joaquin Delta area, California', *Natural hazards review*, 9(3), pp. 136-149. DOI: 10.1061/(ASCE)1527-6988(2008)9:3(136)

Calantropio, A., Chiabrando, F., Codastefano, M., and Bourke, E. (2021) 'Deep learning for automatic building damage assessment: application in post-disaster scenarios using UAV data', *ISPRS Annals of the Photogrammetry, Remote Sensing and Spatial Information Sciences*, 1, pp. 113-120. DOI: 10.5194/isprs-annals-V-1-2021-113-2021

Callaway, D. S., Newman, M. E., Strogatz, S. H., and Watts, D. J. (2000) 'Network robustness and fragility: Percolation on random graphs', *Physical Review Letters*, 85(25), article number 5468. DOI: 10.1103/physrevlett.85.5468

Campbell, T. J., and Benedet, L. (2006) 'Beach nourishment magnitudes and trends in the US', *Journal of Coastal Research*, 39, pp. 57-64. Link to reference.

CCC - Committee on Climate Change (2018) Managing the coast in a changing climate. Link to reference.

CCC - Committee on Climate Change (2016) UK Climate Change Risk Assessment 2017 Evidence Report. Link to reference.

CCO - Channel Coastal Observatory (2014) *National defences 2014 (dataset)*. Link to reference.

CEMHS - Center for Emergency Management and Homeland Security (2022) *The State of Disaster. Summary of losses, 1960-2020 (SHELDUS v20)*. Arizona State University. Link to reference.

Centre for Social Justice (2013) *Turning the Tide, Social justice in five seaside towns.* Link to reference.

Cerri, M., Steinhausen, M., Kreibich, H., and Schröter, K. (2021) 'Are OpenStreetMap building data useful for flood vulnerability modelling?', *Natural Hazards and Earth System Sciences*, 21(2), pp. 643-662. DOI: 10.5194/nhess-21-643-2021

Chang, S. E. (2016) 'Socioeconomic impacts of infrastructure disruptions', *Oxford research encyclopedias: Natural hazard science*. Oxford University Press. DOI: 10.1093/acrefore/9780199389407.013.66

Chen, Y., Xie, W., and Xu, X. (2019) 'Changes of population, built-up land, and cropland exposure to natural hazards in China from 1995 to 2015', *International Journal of Disaster Risk Science*, 10, pp. 557-572. DOI: 10.1007/s13753-019-00242-0

Cheng, L., and AghaKouchak, A. (2014) 'Nonstationary precipitation intensity-duration-frequency curves for infrastructure design in a changing climate', *Scientific Reports*, 4(1), pp. 1–6. DOI: 10.1038/srep07093

Church, M. (2010) 'The trajectory of geomorphology', *Progress in Physical Geography*, 34(3), pp. 265–286. DOI: 10.1177/0309133310363992

CIRES - Cooperative Institute for Research in Environmental Sciences (2014) *Continuously Updated Digital Elevation Model (CUDEM) – 1/9 Arc-Second Resolution Bathymetric-Topographic Tiles.* NOAA National Centers for Environmental Information. DOI: 10.25921/ds9v-ky35

Coles, S. (2001) *An introduction to statistical modeling of extreme values*. Springer-Verlag.

Collenteur, R. A., De Moel, H., Jongman, B., and Di Baldassarre, G. (2015) 'The failed-levee effect: Do societies learn from flood disasters?', *Natural Hazards*, 76, pp. 373-388. DOI: 10.1007/s11069-014-1496-6

Cooper, J. A. G., and McKenna, J. (2009) 'Boom and bust: the influence of macroscale economics on the world's coasts', *Journal of Coastal Research*, 25(3), pp. 533-538. DOI: 10.2112/09A-0001.1

Cooper, M. J., Beevers, M. D., and Oppenheimer, M. (2008) 'The potential impacts of sea level rise on the coastal region of New Jersey, USA', *Climatic Change*, 90(4), pp. 475-492. DOI: 10.1007/s10584-008-9422-0

Cooper, N. J., Barber, P. C., Bray, M. J., and Carter, D. J. (2002) 'Shoreline management plans: a national review and engineering perspective', *Proceedings of the Institution of Civil Engineers-Water and Maritime Engineering*, 154(3), pp. 221-228. Thomas Telford Ltd. DOI: 10.1680/wame.2002.154.3.221

CRED and UNDRR (2020) *Human cost of disasters: an overview of the last 20 years, 2000–2019*. DOI: 10.18356/79b92774-en

Crichton, D. (1999). 'The risk triangle', *Natural disaster management*, 102(3), pp. 102-103.

Crichton, D. (2008) 'Role of insurance in reducing flood risk', *The Geneva Papers on Risk and Insurance-Issues and Practice*, 33, pp. 117-132. DOI: 10.1057/palgrave.gpp.2510151

Crossett, K., Ache, B., Pacheco, P. and Haber, K. (2013) *National Coastal Population Report, Population Trends from 1970 to 2020*. NOAA State of the Coast Report Series, US Department of Commerce, Washington.

Crossett, K. M., Culliton, T. J., Wiley, P. C., & Goodspeed, T. R. (2004) *Population trends along the coastal United States: 1980–2008*. Coastal trends report series. National Oceanic and Atmospheric Administration, National Ocean Service, Management and Budget Office, Special Projects, 86.

Crutzen, P. J. (2002) 'The 'anthropocene'', *Journal de Physique IV (Proceedings)* 12(10), pp. 1-5. EDP sciences. DOI: 10.1051/jp4:20020447

Cutter, S. L., Boruff, B. J., & Shirley, W. L. (2003) 'Social vulnerability to environmental hazards', *Social Science Quarterly*, 84(2), pp. 242-261. DOI: 10.1111/1540-6237.8402002

Cutter, S. L., and Emrich, C. (2005) 'Are natural hazards and disaster losses in the US increasing?', *EOS, Transactions American Geophysical Union*, 86(41), pp. 381-389. DOI: 10.1029/2005eo410001

Cutter, S. L., and Finch, C. (2008) 'Temporal and spatial changes in social vulnerability to natural hazards', *Proceedings of the national academy of sciences*, 105(7), pp. 2301-2306. DOI: 10.1073/pnas.0710375105

Darestani, Y. M., Webb, B., Padgett, J. E., Pennison, G., and Fereshtehnejad, E. (2021) 'Fragility analysis of coastal roadways and performance assessment of coastal transportation systems subjected to storm hazards', *Journal of Performance of Constructed Facilities*, 35(6), article number 04021088. DOI: 10.1061/(asce)cf.1943-5509.0001650

Dave, R., Subramanian, S. S., and Bhatia, U. (2021) 'Extreme precipitation induced concurrent events trigger prolonged disruptions in regional road networks', *Environmental Research Letters*, 16(10), article number 104050. DOI: 10.1088/1748-9326/ac2d67

Davidson-Arnott, R., Bauer, B., and Houser, C. (2019) 'Introduction to coastal processes and geomorphology'. Cambridge university press.

de Bruijn, K. M., Maran, C., Zygnerski, M., Jurado, J., Burzel, A., Jeuken, C., and Obeysekera, J. (2019) 'Flood resilience of critical infrastructure: Approach and method applied to Fort Lauderdale, Florida', *Water*, 11(3), article number 517. DOI: 10.3390/w11030517

De Marchi, B., and Scolobig, A. (2012) 'The views of experts and residents on social vulnerability to flash floods in an Alpine region of Italy', *Disasters*, 36(2), pp. 316-337. DOI: 10.1111/j.1467-7717.2011.01252.x

DEFRA (2002) *FutureCoast*. Link to reference.

DEFRA (2006) *Shoreline Management Plan Guidance Volume 1: Aims and Requirements.* Department for Environment, Food and Rural Affairs, London. Link to reference.

Department for Levelling Up, Housing & Communities (2019). *English Indices of Deprivation 2019.* Link to reference.

Di Baldassarre, G., Kreibich, H., Vorogushyn, S., Aerts, J., Arnbjerg-Nielsen, K., Barendrecht, M., ... and Ward, P. J. (2018) 'Hess Opinions: An interdisciplinary research agenda to explore the unintended consequences of structural flood protection', *Hydrology and Earth System Sciences*, 22(11), pp. 5629-5637. DOI: 10.5194/hess-22-5629-2018

Di Baldassarre, G., Viglione, A., Carr, G., Kuil, L., Salinas, J. L., and Blöschl, G. (2013) 'Socio-hydrology: conceptualising human-flood interactions', *Hydrology and Earth System Sciences*, 17(8), pp. 3295-3303. DOI: 10.5194/hess-17-3295-2013

Di Baldassarre, G., Viglione, A., Carr, G., Kuil, L., Yan, K., Brandimarte, L., and Blöschl, G. (2015) 'Debates—Perspectives on socio-hydrology: Capturing feedbacks between physical and social processes', *Water Resources Research*, 51(6), pp. 4770-4781. DOI: 10.1002/2014wr016416

Dolan, R., and Lins, H. F. (2000) *The outer banks of North Carolina.* US Geological Survey Professional Paper 1177–B, US Government Printing Office.

Dolan, R., Hayden, B., andLins, H. (1980) 'Barrier Islands: The natural processes responsible for the evolution of barrier islands and for much of their recreational and

aesthetic appeal also make them hazardous places for humans to live', *American Scientist*, 68(1), pp. 16–25. Link to reference.

Dong, S., Esmalian, A., Farahmand, H., and Mostafavi, A. (2020) 'An integrated physical-social analysis of disrupted access to critical facilities and community service-loss tolerance in urban flooding', *Computers, Environment and Urban Systems*, 80, article number 101443. DOI: 10.1016/j.compenvurbsys.2019.101443

Dong, S., Gao, X., Mostafavi, A, and Gao, J. (2022) 'Modest flooding can trigger catastrophic road network collapse due to compound failure', *Communications Earth & Environment*, 3, article number 38. DOI: 10.1038/s43247-022-00366-0

Dong, S., Mostafizi, A., Wang, H., Gao, J., and Li, X. (2020) 'Measuring the topological robustness of transportation networks to disaster-induced failures: A percolation approach', *Journal of Infrastructure Systems*, 26(2), article number 04020009. DOI: 10.1061/(asce)is.1943-555x.0000533

Douglas, E. M., Kirshen, P. H., Bosma, K., Watson, C., Miller, S., and McArthur, K. (2016) 'Simulating the impacts and assessing the vulnerability of the central artery/tunnel system to sea level rise and increased coastal flooding', *Journal of Extreme Events*, 3(04), article number 1650013. DOI: 10.1142/s2345737616500135

Ehrlich, D., Melchiorri, M., Florczyk, A. J., Pesaresi, M., Kemper, T., Corbane, C., ... and Siragusa, A. (2018). 'Remote sensing derived built-up area and population density to quantify global exposure to five natural hazards over time.' *Remote Sensing*, 10(9), article number 1378. DOI: 10.3390/rs10091378

Ehrlich, D., and Tenerelli, P. (2013) 'Optical satellite imagery for quantifying spatio-temporal dimension of physical exposure in disaster risk assessments', *Natural Hazards*, 68, pp. 1271-1289. DOI: 10.1007/s11069-012-0372-5

Elko, N., Briggs, T. R., Benedet, L., Robertson, Q., Thomson, G., Webb, B. M., and Garvey, K. (2021) 'A century of US beach nourishment', *Ocean & Coastal Management*, 199, article number 105406. DOI: 10.1016/j.ocecoaman.2020.105406

Ells, K., and Murray, A. B. (2012) 'Long-term, non-local coastline responses to local shoreline stabilization', *Geophysical Research Letters*, 39(19). DOI: 10.1029/2012gl052627

Emanuelsson, M. A. E., McIntyre, N., Hunt, C. F., Mawle, R., Kitson, J., and Voulvoulis, N. (2014) 'Flood risk assessment for infrastructure networks', *Journal of Flood Risk Management*, 7(1), pp. 31–41. DOI: 10.1111/jfr3.12028

England, K., and Knox, K. (2015) *Targeting flood investment and policy to minimise flood disadvantage*. York: Joseph Rowntree Foundation. Link to reference.

Environment Agency (2018). *Estimating the economic costs of the 2015 to 2016 winter floods*. Bristol: Environment Agency. Link to reference.

Environment Agency (2019a) *Flood Map for Planning (Rivers and Sea) - Flood Zone 2*. Link to reference.

Environment Agency (2019b) *Flood Map for Planning (Rivers and Sea) - Flood Zone 3*. Link to reference.

Environment Agency (2019c) *National Coastal Erosion Risk Mapping (NCERM) - National (2018 - 2021)*. Link to reference.

Environment Agency (2010) *The Coastal Handbook*. Link to reference.

Environment Agency (2019d) *Risk of Flooding from Rivers and Sea*. Link to reference.

Environment Agency (2019e) *Shoreline Management Plan Mapping*. Link to reference.

Evans, B., Chen, A. S., Djordjević, S., Webber, J., Gómez, A. G., and Stevens, J. (2020) 'Investigating the effects of pluvial flooding and climate change on traffic flows in Barcelona and Bristol', *Sustainability*, 12(6), article number 2330. DOI: 10.3390/su12062330

Ezer, T., and Atkinson, L. P. (2014) 'Accelerated flooding along the US East Coast: On the impact of sea-level rise, tides, storms, the Gulf Stream, and the North Atlantic Oscillations', *Earth's Future*, 2(8), pp. 362–382. DOI: 10.1002/2014ef000252

Fant, C., Jacobs, J. M., Chinowsky, P., Sweet, W., Weiss, N., Sias, J. E., et al. (2021) 'Mere nuisance or growing threat? The physical and economic impact of high tide flooding on US road networks', *Journal of Infrastructure Systems*, 27(4), article number 04021044. DOI: 10.1061/(asce)is.1943-555x.0000652

Faturechi, R., and Miller-Hooks, E. (2015) 'Measuring the performance of transportation infrastructure systems in disasters: A comprehensive review', *Journal of Infrastructure Systems*, 21(1), article number 04014025. DOI: 10.1061/(asce)is.1943-555x.0000212

Fleming, C. A. (1992) 'The development of coastal engineering', *Coastal zone planning and management*, pp. 5-20. Thomas Telford Publishing. DOI: 10.1680/czpam.19041.0002

Florida Department of Revenue (2012) *Florida Parcel Data Statewide-2012.* Florida Geographic Data Library. Link to reference.

Florida Department of Revenue (2014) Florida Parcel Data Statewide-2014. Florida Geographic Data Library. Link to reference.

Florida Department of Revenue (2015) Florida Parcel Data Statewide-2015. Florida Geographic Data Library. Link to reference.

Florida Department of Revenue (2017) *Florida Parcel Data Statewide-2017.* Florida Geographic Data Library. Link to reference.

Frazier, T. G., Thompson, C. M., Dezzani, R. J., and Butsick, D. (2013) 'Spatial and temporal quantification of resilience at the community scale', *Applied Geography*, 42, pp. 95–107. DOI: 10.1016/j.apgeog.2013.05.004

Godschalk, D. R., Brower, D. J., and Beatley, T. (1989) *Catastrophic coastal storms: Hazard mitigation and development management.* Duke University Press

Gopalakrishnan, S., Landry, C. E., Smith, M. D., and Whitehead, J. C. (2016) 'Economics of coastal erosion and adaptation to sea level rise' *Annual Review of Resource Economics*, 8, pp. 119–139. DOI: 10.1146/annurev-resource-100815-095416

Gopalakrishnan, S., Smith, M. D., Slott, J. M., and Murray, A. B. (2011) 'The value of disappearing beaches: A hedonic pricing model with endogenous beach width', *Journal of Environmental Economics and Management*, 61(3), pp. 297–310. DOI: 10.1016/j.jeem.2010.09.003

Habel, S., Fletcher, C. H., Anderson, T. R., and Thompson, P. R. (2020) 'Sea-level rise induced multi-mechanism flooding and contribution to urban infrastructure failure', *Scientific Reports*, 10(1), pp. 1–12. DOI: 10.1038/s41598-020-60762-4

Habel, S., Fletcher, C. H., Rotzoll, K., and El-Kadi, A. I. (2017) 'Development of a model to simulate groundwater inundation induced by sea-level rise and high tides in Honolulu, Hawaii', *Water Research*, 114, pp. 122–134. DOI: 10.1016/j.watres.2017.02.035

Hackl, J., Lam, J. C., Heitzler, M., Adey, B. T., and Hurni, L. (2018) 'Estimating network related risks: A methodology and an application in the transport sector', *Natural Hazards and Earth System Sciences,* 18(8), pp. 2273–2293. DOI: 10.5194/nhess-18-2273-2018

Haff, P., (2003) 'Neogeomorphology, prediction, and the anthropic landscape', *Geophysical Monograph-American Geophysical Union*, 135, pp. 15–26. DOI: 10.1029/135GM02

Hagberg, A., Swart, P., and S Chult, D. (2008) *Exploring network structure, dynamics, and function using NetworkX (No. LA-UR-08-05495; LA-UR-08-5495).* Los Alamos, NM, USA: Los Alamos National Lab (LANL).

Haigh, I. D., MacPherson, L. R., Mason, M. S., Wijeratne, E. M. S., Pattiaratchi, C. B., Crompton, R. P., and George, S. (2014) 'Estimating present day extreme water level exceedance probabilities around the coastline of Australia: Tropical cyclone-induced storm surges', *Climate Dynamics*, 42(1–2), pp. 139–157. DOI: 10.1007/s00382-012-1653-0

Hallegatte, S., Rentschler, J., and Rozenberg, J. (2019) *Lifelines: The resilient infrastructure opportunity.* World Bank Publications. DOI: 10.1596/978-1-4648-1430-3

Hanson, H., Brampton, A., Capobianco, M., Dette, H. H., Hamm, L., Laustrup, C., ... and Spanhoff, R. (2002) 'Beach nourishment projects, practices, and objectives—a European overview', *Coastal Engineering*, 47(2), pp. 81-111. DOI: 10.1016/S0378-3839(02)00122-9

Hapke, C. J., Kratzmann, M. G., and Himmelstoss, E. A. (2013) 'Geomorphic and human influence on large-scale coastal change', *Geomorphology*, 199, pp. 160-170. DOI: 10.1016/j.geomorph.2012.11.025

Hardin, E., Mitasova, H., and Overton, M. (2012) 'GIS-based analysis of storm vulnerability change at Pea Island, NC', *Coastal Engineering Proceedings*, 1(33). DOI: 10.9753/icce.v33.management.75

Harris, C. R., Millman, K. J., van der Walt, S. J., Gommers, R., Virtanen, P., Cournapeau, D., et al. (2020) 'Array programming with NumPy', *Nature*, 585(7825), pp. 357–362. DOI: 10.1038/s41586-020-2649-2

He, Y., Thies, S., Avner, P., and Rentschler, J. (2021) 'Flood impacts on urban transit and accessibility—A case study of Kinshasa', *Transportation research part D: transport and environment*, 96, article number 102889. DOI: 10.1016/j.trd.2021.102889

Henderson, J. V., Storeygard, A., and Weil, D. N. (2012) 'Measuring economic growth from outer space', *American Economic Review*, 102(2), pp. 994-1028. DOI: 10.1257/aer.102.2.994

Herring, S. C., Christidis, N., Hoell, A., Hoerling, M. P., and Stott, P. A. (2020) 'Explaining extreme events of 2018 from a climate perspective', *Bulletin of the American Meteorological Society*, 101(1), pp. S1–S134. DOI: 10.1175/BAMS-ExplainingExtremeEvents2018.1

Hiatt, M., Addink, E. A., and Kleinhans, M. G. (2021) 'Connectivity and directionality in estuarine channel networks', *Earth Surface Processes and Landforms*, 47(3), pp. 807–824. DOI: 10.1002/esp.5286

Hinkel, J., Lincke, D., Vafeidis, A. T., Perrette, M., Nicholls, R. J., Tol, R. S., ... and Levermann, A. (2014) 'Coastal flood damage and adaptation costs under 21st century sea-level rise', *Proceedings of the National Academy of Sciences*, 111(9), pp. 3292-3297.

Hino, M., Belanger, S. T., Field, C. B., Davies, A. R., and Mach, K. J. (2019) 'High-tide flooding disrupts local economic activity', *Science Advances*, 5(2), article number eaau2736. DOI: 10.1126/sciadv.aau2736

Holme, P., Kim, B. J., Yoon, C. N., and Han, S. K. (2002) 'Attack vulnerability of complex networks', *Physical Review E*, 65(5), article number056109. DOI: 10.1103/physreve.65.056109

Hooke, R. L., (1994) 'On the Efficacy of Humans as Geomorphic Agents', *GSA Today*, 4(9), pp. 223–225.

Hooke, R. L., (2000) 'On the history of humans as geomorphic agents', *Geology,* 28(9), pp. 843–846. DOI: 10.1130/0091-7613(2000)28

House of Lords (2019). *The future of seaside towns.* House of Lords Select Committee on Regenerating Seaside Towns and Communities. London: The Stationery Office. Link to reference.

Housego, R., Raubenheimer, B., Elgar, S., Cross, S., Legner, C., and Ryan, D. (2021) 'Coastal flooding generated by ocean wave-and surge-driven groundwater fluctuations on a sandy barrier island', *Journal of Hydrology*, 603, article number 126920. DOI: 10.1016/j.jhydrol.2021.126920

Hummel, M. A., Berry, M. S., and Stacey, M. T. (2018) 'Sea level rise impacts on wastewater treatment systems along the US coasts', *Earth's Future*, 6(4), pp. 622–633. DOI: 10.1002/2017ef000805

Hummel, M. A., Tcheukam Siwe, A., Chow, A., Stacey, M. T., and Madanat, S. M. (2020) 'Interacting infrastructure disruptions due to environmental events and long-term climate change', *Earth's Future*, 8(10), article number e2020EF001652. DOI: 10.1029/2020ef001652

Huisman, B.J.A., Wijsman, J.W.M., Arens, S.M., Vertegaal, C.T.M., van der Valk, L., Donk, S.C., Vreugdenhil, H.S.I., Taal, M.D. (2021) *10-years evaluation of the Sand Motor : results of the Monitoring- and Evaluation Program (MEP) for the period 2011 to 2021.* Link to reference.

Hutton, N. S., Tobin, G. A., and Montz, B. E. (2019) 'The levee effect revisited: Processes and policies enabling development in Yuba County, California', *Journal of Flood Risk Management*, 12(3), article number e12469. DOI: 10.1111/jfr3.12469

Iglesias, V., Braswell, A. E., Rossi, M. W., Joseph, M. B., McShane, C., Cattau, M., ... and Travis, W. R. (2021) 'Risky development: Increasing exposure to natural hazards in the United States', *Earth's future*, 9(7), article number e2020EF001795. DOI: 10.1029/2020EF001795

IPCC (2012) *Summary for Policymakers*. In: Managing the Risks of Extreme Events and Disasters to Advance Climate Change Adaptation [Field, C.B., V. Barros, T.F. Stocker, D. Qin, D.J. Dokken, K.L. Ebi, M.D. Mastrandrea, K.J. Mach, G.-K. Plattner, S.K. Allen, M.

Tignor, and P.M. Midgley (eds.)]. A Special Report of Working Groups I and II of the Intergovernmental Panel on Climate Change. Cambridge University Press, Cambridge, UK, and New York, NY, USA, pp. 1-19. Link to reference.

IPCC (2022) *Annex II: Glossary* [Möller, V., R. van Diemen, J.B.R. Matthews, C. Méndez, S. Semenov, J.S. Fuglestvedt, A. Reisinger (eds.)]. In: Climate Change 2022: Impacts, Adaptation and Vulnerability. Contribution of Working Group II to the Sixth Assessment Report of the Intergovernmental Panel on Climate Change [H.-O. Pörtner, D.C. Roberts, M. Tignor, E.S. Poloczanska, K. Mintenbeck, A. Alegría, M. Craig, S. Langsdorf, S. Löschke, V. Möller, A. Okem, B. Rama (eds.)]. Cambridge University Press, Cambridge, UK and New York, NY, USA, pp. 2897–2930, DOI: 10.1017/9781009325844.029

Ishtiaque, A., Estoque, R. C., Eakin, H., Parajuli, J., and Rabby, Y. W. (2022) 'IPCC's current conceptualization of 'vulnerability' needs more clarification for climate change vulnerability assessments', *Journal of Environmental Management*, 303, article number 114246. DOI: 10.1016/j.jenvman.2021.114246

Iyer, S., Killingback, T., Sundaram, B., and Wang, Z. (2013) 'Attack robustness and centrality of complex networks', *PLoS One*, 8(4), article number e59613. DOI: 10.1371/journal.pone.0059613

Jacobs (2018) *Research to assess the economics of coastal change management in England and to determine potential pathways for a sample of exposed communities*. Report commissioned by the Committee on Climate Change.

Jacobs, J. M., Cattaneo, L. R., Sweet, W., and Mansfield, T. (2018) 'Recent and future outlooks for nuisance flooding impacts on roadways on the US East Coast', *Transportation Research Record*, 2672(2), pp. 1–10. DOI: 10.1177/0361198118756366

Jamakovic, A., and Uhlig, S. (2008) 'On the relationships between topological measures in real-world networks', *Networks and Heterogeneous Media*, 3(2), pp. 345–359. DOI: 10.3934/nhm.2008.3.345

Janković, V., and Schultz, D. M. (2017) 'Atmosfear: Communicating the effects of climate change on extreme weather', *Weather, Climate, and Society*, 9(1), pp. 27-37. DOI: 10.1175/wcas-d-16-0030.1

Jaroszweski, D., Hooper, E., and Chapman, L. (2014) 'The impact of climate change on urban transport resilience in a changing world', *Progress in Physical Geography*, 38(4), pp. 448–463. DOI: 10.1177/0309133314538741

Jenelius, E., and Mattsson, L. G. (2012) 'Road network vulnerability analysis of area-covering disruptions: A grid-based approach with case study', *Transportation Research Part A: Policy and Practice*, 46(5), pp. 746–760. DOI: 10.1016/j.tra.2012.02.003

Johansen, C., and Tien, I. (2018) 'Probabilistic multi-scale modeling of interdependencies between critical infrastructure systems for resilience', *Sustainable and Resilient Infrastructure*, 3(1), pp. 1–15. DOI: 10.1080/23789689.2017.1345253

Kasmalkar, I. G., Serafin, K. A., Miao, Y., Bick, I. A., Ortolano, L., Ouyang, D., and Suckale, J. (2020) 'When floods hit the road: Resilience to flood-related traffic disruption in the San Francisco Bay Area and beyond', *Science Advances*, 6(32), article number eaba2423. DOI: 10.1126/sciadv.aba2423

Kasmalkar, I. G., Serafin, K. A., and Suckale, J. (2021) 'Integrating urban traffic models with coastal flood maps to quantify the resilience of traffic systems to episodic coastal flooding', *MethodsX*, 8, article number 101483. DOI: 10.1016/j.mex.2021.101483

Kates, R. W., Colten, C. E., Laska, S., and Leatherman, S. P. (2006) 'Reconstruction of New Orleans after Hurricane Katrina: a research perspective', *Proceedings of the National Academy of Sciences*, 103(40), pp. 14653-14660. DOI: 10.1073/pnas.0605726103

Kelleher, C., and McPhillips, L. (2020) 'Exploring the application of topographic indices in urban areas as indicators of pluvial flooding locations', *Hydrological Processes*, 34(3), pp. 780–794. DOI: 10.1002/hyp.13628

Kermanshah, A., and Derrible, S. (2017) 'Robustness of road systems to extreme flooding: Using elements of GIS, travel demand, and network science', *Natural Hazards*, 86(1), pp. 151–164. DOI: 10.1007/s11069-016-2678-1

Khan, M. U., Mesbah, M., Ferreira, L., and Williams, D. J. (2014) 'Development of road deterioration models incorporating flooding for optimum maintenance and rehabilitation strategies', *Road and Transport Research*, 23(1), pp. 3–24. DOI: 10.3316/informit.323776325188349

Khan, M. U., Mesbah, M., Ferreira, L., and Williams, D. J. (2017) 'Estimating pavement's flood resilience', *Journal of Transportation Engineering, Part B: Pavements*, 143(3), article number 04017009. DOI: 10.1061/jpeodx.0000007

Kirezci, E., Young, I. R., Ranasinghe, R., Muis, S., Nicholls, R. J., Lincke, D., and Hinkel, J. (2020) 'Projections of global-scale extreme sea levels and resulting episodic coastal flooding over the 21st Century', *Scientific Reports*, 10(1), pp. 1–12. DOI: 10.1038/s41598-020-67736-6

Kirkley, A., Barbosa, H., Barthelemy, M., and Ghoshal, G. (2018) 'From the betweenness centrality in street networks to structural invariants in random planar graphs', *Nature Communications*, 9(1), pp. 1–12. DOI: 10.1038/s41467-018-04978-z

Koks, E. E., Rozenberg, J., Zorn, C., Tariverdi, M., Vousdoukas, M., Fraser, S. A., et al. (2019) 'A global multi-hazard risk analysis of road and railway infrastructure assets', *Nature Communications*, 10(1), pp. 1–11. DOI: 10.1038/s41467-019-10442-3

Kriesel, W., and Friedman, R. (2002) *Coastal hazards and economic externality: implications for beach management policies in the American South East*. Heinz Center Discussion Paper. Link to reference.

Krynock, L. W., Shelden, J. G., and Martin, J. D. (2005) 'Highway vulnerability along NC 12 – Ocracoke Island, North Carolina.' *Presented at Solutions to Coastal Disasters Conference 2005*, pp. 423–432. DOI: 10.1061/40774(176)43

Landry, C. E., Keeler, A. G., and Kriesel, W. (2003) 'An economic evaluation of beach erosion management alternatives', *Marine Resource Economics*, 18(2), pp. 105-127. DOI: 10.1086/mre.18.2.42629388

Lavalle, C., Gomes, C. R., Baranzelli, C., and Batista e Silva, F. (2000) *Coastal zones, Policy alternatives impacts on European Coastal Zones, 2000-2050*. Joint Research Centre, European Commission. Link to reference.

Lavell, A., Oppenheimer, M., Diop, C., Hess, J., Lempert, R., Li, J., and Myeong, S. (2012) *Managing the risks of extreme events and disasters to advance climate change adaptation. A special report of working groups I and II of the intergovernmental panel on climate change (IPCC)*, pp. 25-64. DOI: 10.1017/cbo9781139177245.004

Lazarus, E. D. (2014) 'Threshold effects of hazard mitigation in coastal human–environmental systems', *Earth Surface Dynamics*, 2(1), pp. 35-45. DOI: 10.5194/esurf-2-35-2014

Lazarus, E. D. (2017) 'Toward a global classification of coastal anthromes', *Land*, 6(1), 13. DOI: 10.3390/LAND6010013

Lazarus, E. D. (2022a) 'A conceptual beachhead: 'Beaches and dunes of human-altered coasts' by Karl F. Nordstrom (1994)', *Progress in Physical Geography: Earth and Environment*, 46(3), pp. 481-490. DOI: 10.1177/03091333211054679

Lazarus, E. D. (2022b) 'The disaster trap: Cyclones, tourism, colonial legacies, and the systemic feedbacks exacerbating disaster risk', *Transactions of the Institute of British Geographers*, 47(2), pp. 577-588. DOI: 10.1111/tran.12516

Lazarus, E. D., Aldabet, S., Thompson, C. E., Hill, C. T., Nicholls, R. J., French, J. R., ... and Penning-Rowsell, E. C. (2021) 'The UK needs an open data portal dedicated to coastal flood and erosion hazard risk and resilience', *Anthropocene Coasts*, 4(1), pp. 137-146. DOI: 10.1139/anc-2020-0023

Lazarus, E. D., Ellis, M. A., Brad Murray, A., and Hall, D. M. (2016) 'An evolving research agenda for human-coastal systems', *Geomorphology*, 256, pp. 81–90. DOI: 10.1016/j.geomorph.2015.07.043

Lazarus, E. D., and Goldstein, E. B. (2019) 'Is there a bulldozer in your model?', *Journal of Geophysical Research: Earth Surface*, 124(3), pp. 696–699. DOI: 10.1029/2018jf004957

Lazarus, E. D., Goldstein, E. B., Taylor, L. A., and Williams, H. E. (2021) 'Comparing patterns of hurricane washover into built and unbuilt environments', *Earth's Future*, 9(3), article number e2020EF001818. DOI: 10.1029/2020ef001818

Lazarus, E. D., Limber, P. W., Goldstein, E. B., Dodd, R., and Armstrong, S. B. (2018) 'Building back bigger in hurricane strike zones', *Nature Sustainability*, 1(12), pp. 759-762. DOI: 10.1038/s41893-018-0185-y

Lazarus, E. D., McNamara, D. E., Smith, M. D., Gopalakrishnan, S., and Murray, A. B. (2011) 'Emergent behavior in a coupled economic and coastline model for beach nourishment', *Nonlinear Processes in Geophysics*, 18(6), pp. 989–999. DOI: 10.5194/npg-18-989-2011

Le Cozannet, G., Kervyn, M., Russo, S., Ifejika Speranza, C., Ferrier, P., Foumelis, M., ... and Modaressi, H. (2020) 'Space-based earth observations for disaster risk management', *Surveys in geophysics*, 41, pp. 1209-1235. DOI: 10.1007/s10712-020-09586-5

Leafe, R., Pethick, J., and Townend, I. (1998) 'Realizing the benefits of shoreline management', *Geographical Journal*, pp. 282-290. DOI: 10.2307/3060617

Lee, J. K., Chung, O. S., Park, J. Y., Kim, H. J., Hur, W. H., Kim, S. H., & Kim, J. H. (2018) 'Effects of the Saemangeum Reclamation Project on migratory shorebird staging in the Saemangeum and Geum Estuaries, South Korea', *Bird Conservation International*, 28(2), pp. 238-250.

Leuttich, R. A., Baecher, G. B., Bell, S. B., Berke, P. R., Corotis, R. B., Cox, D. T., ... and van Dongeren, A. (2014) *Reducing coastal risk on the east and gulf coasts.* The National Academies Press, Washington.

Leyk, S., and Uhl, J. H. (2018) 'HISDAC-US, historical settlement data compilation for the conterminous United States over 200 years', *Scientific data*, 5(1), pp. 1-14. DOI: 10.1038/sdata.2018.175

Leyk, S., Uhl, J. H., Connor, D. S., Braswell, A. E., Mietkiewicz, N., Balch, J. K., and Gutmann, M. (2020) 'Two centuries of settlement and urban development in the United States', *Science Advances*, 6(23), article number eaba2937. DOI: 10.1126/sciadv.aba2937

Li, D., Fu, B., Wang, Y., Lu, G., Berezin, Y., Stanley, H. E., and Havlin, S. (2015) 'Percolation transition in dynamical traffic network with evolving critical bottlenecks', *Proceedings of the National Academy of Sciences USA*, 112(3), pp. 669–672. DOI: 10.1073/pnas.1419185112

Lichter, M., Vafeidis, A. T., Nicholls, R. J., and Kaiser, G. (2011) 'Exploring data-related uncertainties in analyses of land area and population in the 'Low-Elevation Coastal Zone' (LECZ)'. *Journal of Coastal Research*, 27(4), pp. 757-768. DOI: 10.2112/JCOASTRES-D-10-00072.1

Lindley, S., O'Neill, J., Kandeh, J., Lawson, N., Christian, R., and O'Neill, M. (2011) *Climate change, justice and vulnerability*. Joseph Rowntree Foundation, York.

Liu, C., Sepasgozar, S. M., Zhang, Q., and Ge, L. (2022) 'A novel attention-based deep learning method for post-disaster building damage classification', *Expert Systems with Applications*, 202, article number 117268. DOI: 10.1016/j.eswa.2022.117268

Lu, Z., Im, J., Quackenbush, L. J., and Yoo, S. (2013) 'Remote sensing-based house value estimation using an optimized regional regression model', *Photogrammetric Engineering & Remote Sensing*, 79(9), pp. 809-820. DOI: 10.14358/PERS.79.9.809

Luijendijk, A., Hagenaars, G., Ranasinghe, R., Baart, F., Donchyts, G., and Aarninkhof, S. (2018) 'The state of the world's beaches', *Scientific Reports*, 8(1), article number 6641. DOI: 10.1038/s41598-018-24630-6

Luijendijk, A. P., Ranasinghe, R., de Schipper, M. A., Huisman, B. A., Swinkels, C. M., Walstra, D. J., & Stive, M. J. (2017) 'The initial morphological response of the Sand Engine: A process-based modelling study', *Coastal engineering*, 119, pp. 1-14. DOI: 10.1016/j.coastaleng.2016.09.005

Mallick, R., Tao, M., Daniel, J., Jacobs, J., and Veeraragavan, A. (2017) 'Vulnerability of roadways to flood-induced damage', *Journal of Flood Risk Management*, 10, pp. 301–313. DOI: 10.1111/jfr3.12135

Mård, J., Di Baldassarre, G., & Mazzoleni, M. (2018) 'Nighttime light data reveal how flood protection shapes human proximity to rivers', *Science Advances*, 4(8), article number eaar5779. DOI: 10.1126/sciadv.aar5779

Markolf, S. A., Hoehne, C., Fraser, A., Chester, M. V., and Underwood, B. S. (2019) 'Transportation resilience to climate change and extreme weather events—Beyond risk and robustness', *Transport Policy*, 74, pp. 174–186. DOI: 10.1016/j.tranpol.2018.11.003

Mattsson, L. G., and Jenelius, E. (2015) 'Vulnerability and resilience of transport systems—A discussion of recent research', Transportation Research Part A: Policy and Practice, 81, pp. 16–34. DOI: 10.1016/j.tra.2015.06.002

McGranahan, G., Balk, D., and Anderson, B. (2007) 'The rising tide: Assessing the risks of climate change and human settlements in low elevation coastal zones', *Environment and Urbanization,* 19(1), pp. 17–37. DOI: 10.1177/0956247807076960

McNamara, D. E., Gopalakrishnan, S., Smith, M. D., and Murray, A. B. (2015) 'Climate adaptation and policy-induced inflation of coastal property value', *PloS one*, 10(3), article number e0121278. DOI: 10.1371/journal.pone.0121278

McNamara, D. E., and Keeler, A. (2013) 'A coupled physical and economic model of the response of coastal real estate to climate risk', *Nature Climate Change*, 3(6), pp. 559–562. DOI: 10.1038/nclimate1826

McNamara, D. E., and Lazarus, E. D. (2018) 'Barrier islands as coupled human–landscape systems', *Barrier dynamics and response to changing climate*, pp. 363-383. DOI: 10.1007/978-3-319-68086-6_12

McNamara, D. E., Lazarus, E. D., and Goldstein, E. B. (2023) 'Human–coastal coupled systems: Ten questions', *Cambridge Prisms: Coastal Futures*, 1, article number e20. DOI: 10.1017/cft.2023.8

McNamara, D. E., Murray, A. B., and Smith, M. D. (2011) 'Coastal sustainability depends on how economic and coastline responses to climate change affect each other', *Geophysical Research Letters*, 38, article number L07401. DOI: 10.1029/2011GL047207

McNamara, D. E., and Werner, B. T. (2008a) 'Coupled barrier island–resort model: 1. Emergent instabilities induced by strong human-landscape interactions', *Journal of Geophysical Research: Earth Surface*, 113(F1). DOI: 10.1029/2007jf000840

McNamara, D. E., and Werner, B. T. (2008b) 'Coupled barrier island–resort model: 2. Tests and predictions along Ocean City and Assateague Island National Seashore, Maryland', *Journal of Geophysical Research: Earth Surface*, 113(F1). DOI: 10.1029/2007jf000841

Melet, A., Teatini, P., Le Cozannet, G., Jamet, C., Conversi, A., Benveniste, J., and Almar, R. (2020) 'Earth observations for monitoring marine coastal hazards and their drivers', *Surveys in Geophysics*, 41, pp. 1489-1534. DOI: 10.1007/s10712-020-09594-5

Microsoft (2021) *US Building Footprints*. GitHub Repository. Link to reference.

Millennium Ecosystem Assessment (2005), 'Ecosystems and Human Well-Being: Current State and Trends', Washington, DC: Island Press, p. 516. Link to reference.

Mileti, D. (1999) 'Disasters by Design: A Reassessment of Natural Hazards in the United States', Washington, DC: Joseph Henry Press. DOI: 10.17226/5782

Miselis, J. L., and Lorenzo-Trueba, J. (2017) 'Natural and human-induced variability in barrier-island response to sea level rise', *Geophysical Research Letters*, 44(23), pp. 11–922. DOI: 10.1002/2017gl074811

Moftakhari, H. R., AghaKouchak, A., Sanders, B. F., Allaire, M., and Matthew, R. A. (2018) 'What is nuisance flooding? Defining and monitoring an emerging challenge', *Water Resources Research*, 54, pp. 4218–4227. DOI: 10.1029/2018wr022828

Moftakhari, H. R., AghaKouchak, A., Sanders, B. F., Feldman, D. L., Sweet, W., Matthew, R. A., and Luke, A. (2015) 'Increased nuisance flooding along the coasts of the United States due to sea level rise: Past and future', *Geophysical Research Letters*, 42(22), pp. 9846–9852. DOI: 10.1002/2015gl066072

Moftakhari, H. R., AghaKouchak, A., Sanders, B. F., and Matthew, R. A. (2017) 'Cumulative hazard: The case of nuisance flooding', *Earth's Future*, 5(2), pp. 214–223. DOI: 10.1002/2016ef000494

Montz, B. E., and Tobin, G. A. (2008) 'Livin'large with levees: Lessons learned and lost', *Natural Hazards Review*, 9(3), pp. 150-157. DOI: 10.1061/(ASCE)1527-6988(2008)9:3(150)

Moreira, A. A., Andrade, J. S., Jr., Herrmann, H. J., and Indekeu, J. O. (2009) 'How to make a fragile network robust and vice versa', *Physical Review Letters*, 102(1), article number 018701. DOI: 10.1103/physrevlett.102.018701

Muis, S., Apecechea, M. I., Dullaart, J., de Lima Rego, J., Madsen, K. S., Su, J., et al. (2020) 'A high-resolution global dataset of extreme sea levels, tides, and storm surges, including future projections', *Frontiers in Marine Science*, 7, article number 263. DOI: 10.3389/fmars.2020.00263

Mulhern, J. S., Johnson, C. L., and Martin, J. M. (2017) 'Is barrier island morphology a function of tidal and wave regime?' *Marine Geology*, 387, pp. 74–84. DOI: 10.1016/j.margeo.2017.02.016

Mulhern, J. S., Johnson, C. L., and Martin, J. M. (2021) 'Data for: Is barrier island morphology a function of tidal and wave regime?', *Hive*. DOI: 10.7278/S50d-5pzj-r9vr

Murdock, A. P., Harfoot, A. J. P., Martin, D., Cockings, S., and Hill, C. (2015) *OpenPopGrid: an open gridded population dataset for England and Wales*. GeoData, University of Southampton.

Murray, A. B., Gopalakrishnan, S., McNamara, D. E., and Smith, M. D. (2013) 'Progress in coupling models of human and coastal landscape change', *Computers and geosciences*, 53, pp. 30-38. DOI: 10.1016/j.cageo.2011.10.010

Najafi, M. R., Zhang, Y., and Martyn, N. (2021) 'A flood risk assessment framework for interdependent infrastructure systems in coastal environments', *Sustainable Cities and Society*, 64, article number 102516. DOI: 10.1016/j.scs.2020.102516

Najibi, N., and Devineni, N. (2018) 'Recent trends in the frequency and duration of global floods', *Earth System Dynamics*, 9(2), pp. 757–783. DOI: 10.5194/esd-9-757-2018

Neumann, B., Vafeidis, A. T., Zimmermann, J., and Nicholls, R. J. (2015) 'Future coastal population growth and exposure to sea-level rise and coastal flooding - A global assessment', *PLoS ONE*, 10(3). DOI: 10.1371/journal.pone.0118571

Newman, M. (2010) *Networks: An introduction*. Oxford University Press.

Nicholls, R. J., and Cazenave, A. (2010) 'Sea-level rise and its impact on coastal zones', *Science*, 328(5985), pp. 1517-1520. DOI: 10.1126/science.1185782

Nicholls, R. J., and Small, C. (2002) 'Improved estimates of coastal population and exposure to hazards released', *Eos, Transactions American Geophysical Union*, 83(28), pp. 301-305. DOI: 10.1029/2002EO000216

Nicholls, R. J., Townend, I. H., Bradbury, A. P., Ramsbottom, D., and Day, S. A. (2013) 'Planning for long-term coastal change: experiences from England and Wales', *Ocean Engineering*, 71, pp. 3-16. DOI: 10.1016/j.oceaneng.2013.01.025

Nicholls, R., Zanuttigh, B., Vanderlinden, J. P., Weisse, R., Silva, R., Hanson, S., ... and Koundouri, P. (2015) 'Developing a holistic approach to assessing and managing coastal flood risk', *Coastal risk management in a changing climate*, pp. 9-53. Butterworth-Heinemann. DOI: 10.1016/b978-0-12-397310-8.00002-6

Nicholson, A., and Du, Z. P. (1997) 'Degradable transportation systems: An integrated equilibrium model', *Transportation Research Part B: Methodological*, 31(3), pp. 209–223. DOI: 10.1016/s0191-2615(96)00022-7

NJDEP (2015) *Coastline of New Jersey, Edition 20150501 (Land_coastline_2007)*. New Jersey Department of Environmental Protection. Bureau of Geographic Information System (BGIS). Link to reference.

NJOGIS (2020) *Municipal boundaries of New Jersey*. New Jersey Office of Information Technology, Office of GIS. Link to reference.

NJOGIS (2018) *Parcels and MOD-IV Composite of New Jersey*. New Jersey Office of Information Technology, Office of GIS. Link to reference.

NJ Treasury (2018) *Division of Taxation – Statistical Information.* Link to reference.

NOAA (2022) *New Jersey*. Available at Link to reference.

Nordstrom, K. F. (1994) 'Beaches and dunes of human-altered coasts', *Progress in Physical Geography*, 18(4), pp. 497–516. DOI: 10.1177/030913339401800402

Nordstrom, K. F. (2004) *Beaches and Dunes of Developed Coasts*. Cambridge, UK: Cambridge University Press.

Nordstrom, K. (2005) 'Beach nourishment and coastal habitats: research needs to improve compatibility', *Restoration Ecology*, 13(1), pp. 215-222. DOI: 10.1111/j.1526-100x.2005.00026.x

Nordstrom, K. F. (2014) 'Living with shore protection structures: a review', *Estuarine, coastal and shelf science*, 150, pp. 11-23. DOI: 10.1016/j.ecss.2013.11.003

Nordstrom, K. F., and Jackson, N. L. (1995) 'Temporal scales of landscape change following storms on a human-altered coast, New Jersey, USA', *Journal of Coastal Conservation*, 1(1), pp. 51–62. DOI: 10.1007/BF02835562

NRC - National Research Council (2014) Reducing coastal risk on the East and Gulf coasts. DOI: 10.17226/18811

Office for National Statistics (2020) *Coastal Towns in England and Wales: October 2020*. Available at Link to reference.

Olcina, J., Hernández, M., Rico, A. M., and Martínez, E. (2010) 'Increased risk of flooding on the coast of Alicante (Region of Valencia, Spain)', *Natural Hazards and Earth System Sciences*, 10(11), pp. 2229-2234. DOI: 10.5194/nhess-10-2229-2010

Olcina, J., Sauri, D., Hernández, M., & Ribas, A. (2016) 'Flood policy in Spain: a review for the period 1983-2013', *Disaster Prevention and Management*, 25(1), pp. 41-58. DOI: 10.1108/DPM-05-2015-0108

Ordnance Survey Service (2019) *Edina Digimap: OS Open Map - Local* [SHAPE geospatial Data], Scale 1:10000, Tiles: nt,nu,nx,ny,nz,ov,sd,se,sh,sj,sk,so,sp,sr,ss,st,su,sw,sx,sy,sz,ta,tf,tg,tl,tm,tq,tr,tv.

Papakonstantinou, I., Lee, J., and Madanat, S. M. (2019) 'Optimal levee installation planning for highway infrastructure protection against sea level rise', *Transportation Research Part D: Transport and Environment*, 77, pp. 378–389. DOI: 10.1016/j.trd.2019.02.002

Passalacqua, P. (2017) 'The Delta Connectome: A network-based framework for studying connectivity in river deltas', *Geomorphology*, 277, pp. 50–62. DOI: 10.1016/j.geomorph.2016.04.001

Pearson, S. G., van Prooijen, B. C., Elias, E. P., Vitousek, S., and Wang, Z. B. (2020) 'Sediment connectivity: A framework for analyzing coastal sediment transport pathways', *Journal of Geophysical Research: Earth Surface*, 125(10), article number e2020JF005595. DOI: 10.1029/2020jf005595

Penning-Rowsell, E. C. (2015) 'A realistic assessment of fluvial and coastal flood risk in England and Wales', *Transactions of the Institute of British Geographers*, 40(1), pp. 44-61. DOI: 10.1111/tran.12053

Pérez, J. M. G. (2010). 'The real estate and economic crisis: An opportunity for urban return and rehabilitation policies in Spain', *Sustainability*, 2(6), pp. 1571-1601. DOI: 10.3390/su2061571

Pezza, D. A., and White, J. M. (2021) 'Impact of the duration of coastal flooding on infrastructure', *Public Works Management & Policy*, 26(2), pp. 144–163. DOI: 10.1177/1087724x20915918

Plane, E., Hill, K., and May, C. (2019) 'A rapid assessment method to identify potential groundwater flooding hotspots as sea levels rise in coastal cities', *Water*, 11(11), article number 2228. DOI: 10.3390/w11112228

Pompe, J. J., and Rinehart, J. R. (1995) 'The value of beach nourishment to property owners: storm damage reduction benefits', *Review of Regional Studies*, 25(3), pp. 271-286. DOI: 10.52324/001c.9010

Porta, S., Crucitti, P., and Latora, V. (2006) 'The network analysis of urban streets: A dual approach', *Physica A: Statistical Mechanics and its Applications*, 369(2), pp. 853–866. DOI: 10.1016/j.physa.2005.12.063

Praharaj, S., Chen, T. D., Zahura, F. T., Behl, M., and Goodall, J. L. (2021) 'Estimating impacts of recurring flooding on roadway networks: A Norfolk, Virginia case study', *Natural Hazards*, 107, pp. 2363–2387. DOI: 10.1007/s11069-020-04427-5

Pregnolato, M., Ford, A., Glenis, V., Wilkinson, S., and Dawson, R. (2017) 'Impact of climate change on disruption to urban transport networks from pluvial flooding', *Journal of Infrastructure Systems*, 23(4), article number 04017015. DOI: 10.1061/(asce)is.1943-555x.0000372

Priestley, S., and Allen, G. (2017) *Flood risk management and funding*. Briefing Paper CBP07514. House of Commons Library, 47.

PSDS (2021). *Beach nourishment database*. Program for the Study of Developed Shorelines. Western Carolina University. Link to reference.

Qiu, Y., and Gopalakrishnan, S. (2018) 'Shoreline defense against climate change and capitalized impact of beach nourishment', *Journal of Environmental Economics and Management*, 92, pp. 134-147. DOI: 10.1016/j.jeem.2018.08.013

Ramsbottom, D., Sayers, P., and Panzeri, M. (2012) *Climate change risk assessment for the floods and coastal erosion sector. Defra Project Code GA0204*. Report to Defra, London, UK. Link to reference.

Rentschler, J., Avner, P., Marconcini, M., Su, R., Strano, E., and Hallegatte, S. (2022) 'Global evidence of rapid urban growth in flood zones since 1985', *Nature*, 622, pp. 87–92. DOI: 10.1038/s41586-023-06468-9

Rogers, L. J., Moore, L. J., Goldstein, E. B., Hein, C. J., Lorenzo-Trueba, J., and Ashton, A. D. (2015) 'Anthropogenic controls on overwash deposition: Evidence and consequences', *Journal of Geophysical Research: Earth Surface*, 120(12), pp. 2609–2624. DOI: 10.1002/2015JF003634

Rotzoll, K., and Fletcher, C. H. (2013) 'Assessment of groundwater inundation as a consequence of sea-level rise', *Nature Climate Change*, 3(5), pp. 477–481. DOI: 10.1038/nclimate1725

Rözer, V., and Surminski, S. (2020) *New Build Homes, Flood Resilience and Environmental Justice-Current and Future Trends Under Climate Change Across England and Wales*. Grantham Research Institute on Climate Change and the Environment. Link to reference.

Sadler, J. M., Haselden, N., Mellon, K., Hackel, A., Son, V., Mayfield, J., et al. (2017) 'Impact of sea-level rise on roadway flooding in the Hampton Roads region, Virginia', *Journal of Infrastructure Systems*, 23(4), article number 05017006. DOI: 10.1061/(asce)is.1943-555x.0000397

Sajjad, M., Lin, N., and Chan, J. C. (2020) 'Spatial heterogeneities of current and future hurricane flood risk along the US Atlantic and Gulf coasts', *Science of the total environment*, 713, article number 136704. DOI: 10.1016/j.scitotenv.2020.136704

Salgado, K., and Martinez, M. L. (2017) 'Is ecosystem-based coastal defense a realistic alternative? Exploring the evidence'. *Journal of Coastal Conservation*, 21, pp. 837-848. DOI: 10.1007/s11852-017-0545-1

Samuels, P., and Gouldby, B., (2009) *Language of Risk: Project Definitions (Second Edition)*. Link to reference.

Sayers, P. (2018) *GIS-based assessment of coastal flood and erosion risk in England*. Link to reference.

Sayers, P., Horritt, M., Penning Rowsell, E., & Fieth, J. (2017) *Present and future flood vulnerability, risk and disadvantage: A UK scale assessment*. Link to reference.

Schneider, C. M., Moreira, A. A., Andrade, J. S., Havlin, S., and Herrmann, H. J. (2011) 'Mitigation of malicious attacks on networks', *Proceedings of the National Academy of Sciences USA*, 108(10), pp. 3838–3841. DOI: 10.1073/pnas.1009440108

Schultz, J., and Elliott, J. R. (2013) 'Natural disasters and local demographic change in the United States', Population and Environment, 34, pp. 293-312. DOI: 10.1007/s11111-012-0171-7

Segoe, L. (1937) *Flood control and the cities*.

Seneviratne, S. I., Zhang, X., Adnan, M., Badi, W., Dereczynski, C., Di Luca, A., ... and Zhou, B. (2021). *11 Chapter 11: weather and climate extreme events in a changing climate*. Link to reference.

Serafin, K. A., Ruggiero, P., and Stockdon, H. F. (2017) 'The relative contribution of waves, tides, and nontidal residuals to extreme total water levels on US West Coast sandy beaches', *Geophysical Research Letters*, 44(4), pp. 1839–1847. DOI: 10.1002/2016gl071020

Shi, K., Huang, C., Yu, B., Yin, B., Huang, Y., and Wu, J. (2014) 'Evaluation of NPP-VIIRS night-time light composite data for extracting built-up urban areas', *Remote Sensing Letters*, 5(4), pp. 358-366. DOI: 10.1080/2150704X.2014.905728

Singh, P., Sinha, V. S. P., Vijhani, A., and Pahuja, N. (2018) 'Vulnerability assessment of urban road network from urban flood', *International Journal of Disaster Risk Reduction*, 28, pp. 237–250. DOI: 10.1016/j.ijdrr.2018.03.017

Sirko, W., Kashubin, S., Ritter, M., Annkah, A., Bouchareb, Y. S. E., Dauphin, Y., ... and Quinn, J. (2021) 'Continental-scale building detection from high resolution satellite imagery', *arXiv preprint arXiv:2107.12283*. DOI: 10.48550/arXiv.2107.12283

Sirmans, S., Macpherson, D., and Zietz, E. (2005) 'The composition of hedonic pricing models', *Journal of Real Estate Literature*, 13(1), pp. 3-43. Lin to reference.

Small, C., and Nicholls, R. J. (2003) 'A global analysis of human settlement in coastal zones', *Journal of Coastal Research*, pp. 584-599.

Smith, B. D., and Zeder, M. A. (2013) 'The onset of the Anthropocene', *Anthropocene*, 4, pp. 8-13. DOI: 10.1016/j.ancene.2013.05.001

Smith, M. D., Slott, J. M., McNamara, D., and Murray, A. B. (2009) 'Beach nourishment as a dynamic capital accumulation problem', *Journal of Environmental Economics and Management*, 58(1), pp. 58-71. DOI: 10.1016/j.jeem.2008.07.011

Spanger-Siegfried, E., Fitzpatrick, M., and Dahl, K. (2014) *Encroaching tides: How sea level rise and tidal flooding threaten US East and Gulf Coast communities over the next 30 years*. Union of Concerned Scientists. Link to reference.

Spielman, S. E., Tuccillo, J., Folch, D. C., Schweikert, A., Davies, R., Wood, N., & Tate, E. (2020) 'Evaluating social vulnerability indicators: criteria and their application to the Social Vulnerability Index', *Natural hazards*, 100, pp. 417-436. DOI: 10.1007/s11069-019-03820-z

Storlazzi, C. D., Gingerich, S. B., Van Dongeren, A. P., Cheriton, O. M., Swarzenski, P. W., Quataert, E., et al. (2018) 'Most atolls will be uninhabitable by the mid-21st century because of sea-level rise exacerbating wave-driven flooding', *Science Advances*, 4(4), article number eaap9741. DOI: 10.1126/sciadv.aap9741

Strader, S. M., and Ashley, W. S. (2015) 'The expanding bull's-eye effect', *Weatherwise*, 68(5), pp. 23-29. DOI: 10.1080/00431672.2015.1067108

Stutz, M. L., and Pilkey, O. H. (2011) 'Open-ocean barrier islands: Global influence of climatic, oceanographic, and depositional settings', *Journal of Coastal Research*, 27(2), pp. 207–222. DOI: 10.2112/09-1190.1

Suarez, P., Anderson, W., Mahal, V., and Lakshmanan, T. R. (2005) 'Impacts of flooding and climate change on urban transportation: A systemwide performance assessment of the Boston Metro Area', *Transportation Research Part D: Transport and Environment*, 10(3), pp. 231–244. DOI: 10.1016/j.trd.2005.04.007

Sweet, W. V., and Park, J. (2014) 'From the extreme to the mean: Acceleration and tipping points of coastal inundation from sea level rise', *Earth's Future*, 2(12), pp. 579–600. DOI: 10.1002/2014ef000272

Sweet, W., Park, J., Marra, J., Zervas, C., and Gill, S. (2014) *Sea level rise and nuisance flood frequency changes around the United States.* NOAA Technical Report NOS CO-OPS 073. Link to reference.

Tadesse, M. G., and Wahl, T. (2021) 'A database of global storm surge reconstructions', *Scientific Data*, 8(1), pp. 1–10. DOI: 10.1038/s41597-021-00906-x

Taherkhani, M., Vitousek, S., Barnard, P. L., Frazer, N., Anderson, T. R., and Fletcher, C. H. (2020) 'Sea-level rise exponentially increases coastal flood frequency', *Scientific Reports*, 10(1), pp. 1–17. DOI: 10.1038/s41598-020-62188-4

Tebaldi, C., Strauss, B. H., and Zervas, C. E. (2012) 'Modelling sea level rise impacts on storm surges along US coasts', *Environmental Research Letters*, 7(1), article number 014032. DOI: 10.1088/1748-9326/7/1/014032

Tejedor, A., Longjas, A., Passalacqua, P., Moreno, Y., and Foufoula-Georgiou, E. (2018) 'Multiplex networks: A framework for studying multiprocess multiscale connectivity via coupled-network theory with an application to river deltas', *Geophysical Research Letters*, 45(18), pp. 9681–9689. DOI: 10.1029/2018gl078355

Theobald, D. M., Kennedy, C., Chen, B., Oakleaf, J., Baruch-Mordo, S., and Kiesecker, J. (2020) 'Earth transformed: detailed mapping of global human modification from 1990 to 2017', *Earth System Science Data*, 12(3), pp. 1953-1972. DOI: 10.5194/essd-12-1953-2020

Theobald, D. M., Kennedy, C., Chen, B., Oakleaf, J., Baruch-Mordo, S., and Kiesecker, J. (2021) *Data for detailed temporal mapping of global human modification from 1990 to 2017 (v1.4) [Data set]*. Zenodo. DOI: 10.5281/zenodo.5338803

Thumerer, T., Jones, A. P., and Brown, D. (2000) 'A GIS based coastal management system for climate change associated flood risk assessment on the east coast of England', *International Journal of Geographical Information Science*, 14(3), pp. 265-281. DOI: 10.1080/136588100240840

Tian, J., Yu, M., Ren, C., and Lei, Y. (2019) 'Network-scape metric analysis: A new approach for the pattern analysis of urban road networks', *International Journal of Geographical Information Science*, 33(3), pp. 537–566. DOI: 10.1080/13658816.2018.1545234

Tobin, G. A. (1995) 'The levee love affair: a stormy relationship?', *JAWRA Journal of the American Water Resources Association*, 31(3), pp. 359-367. DOI: 10.1111/j.1752-1688.1995.tb04025.x

Townend, I. H., Fleming, C. A., McLaren, P., and Hunter-Blair, A. (1990) 'A regional study of coastal morphology', *Coastal Engineering*, pp. 2589-2602. DOI: 10.1061/9780872627765.199

Trembanis, A. C., Pilkey, O. H., and Valverde, H. R. (1999) 'Comparison of beach nourishment along the US Atlantic, Great Lakes, Gulf of Mexico, and New England shorelines', *Coastal Management*, 27(4), pp. 329-340. DOI: 10.1080/089207599263730

Uhl, J. H., Royé, D., Burghardt, K., Aldrey Vázquez, J. A., Borobio Sanchiz, M., and Leyk, S. (2023) 'HISDAC-ES: Historical Settlement Data Compilation for Spain (1900–2020)', *Earth System Science Data Discussions*, 1-51. Preprint. DOI: 10.5194/essd-2023-53

Union of Concerned Scientists (2018) *Underwater: Rising Seas, Chronic Floods, and the Implications for US Coastal Real Estate*. Link to reference.

UNISDR (2015) *Sendai framework for disaster risk reduction 2015–2030*. Proceedings of the Third United Nations World Conference on DRR, Sendai, Japan. Link to reference.

U.S. Bureau of Labor Statistics (2021) *CPI Inflation Calculator*. Link to reference.

U.S. Census Bureau (2021a) *Square Feet*. Link to reference.

U.S. Census Bureau (2021b) *Sale Price*. Link to reference.

Van Aalst, M. K. (2006) 'The impacts of climate change on the risk of natural disasters', *Disasters*, 30(1), pp. 5-18. DOI: 10.1111/j.1467-9523.2006.00303.x

Velasquez-Montoya, L., Sciaudone, E. J., Smyre, E., and Overton, M. F. (2021) 'Vulnerability indicators for coastal roadways based on barrier island morphology and shoreline change predictions', *Natural Hazards Review*, 22(2), article number 04021003. DOI: 10.1061/(asce)nh.1527-6996.0000441

Versini, P. A., Gaume, E., and Andrieu, H. (2010) 'Assessment of the susceptibility of roads to flooding based on geographical information–test in a flash flood prone area (the Gard region, France)', *Natural Hazards and Earth System Sciences*, 10(4), pp. 793–803. DOI: 10.5194/nhess-10-793-2010

Virtanen, P., Gommers, R., Oliphant, T. E., Haberland, M., Reddy, T., Cournapeau, D., et al. (2020) 'SciPy 1.0: Fundamental algorithms for scientific computing in Python', *Nature Methods*, 17, pp. 261–272. DOI: 10.1038/s41592-019-0686-2

Vitousek, S., Barnard, P. L., Fletcher, C. H., Frazer, N., Erikson, L., and Storlazzi, C. D. (2017) 'Doubling of coastal flooding frequency within decades due to sea-level rise', *Scientific reports*, 7(1), pp. 1-9. DOI: 10.1038/s41598-017-01362-7

Vitousek, P. M., Mooney, H. A., Lubchenco, J., and Melillo, J. M. (1997) 'Human domination of Earth's ecosystems', *Science*, 277(5325), pp. 494-499. DOI: 10.1126/science.277.5325.494

Vousdoukas, M. I., Mentaschi, L., Voukouvalas, E., Verlaan, M., and Feyen, L. (2017) 'Extreme sea levels on the rise along Europe's coasts', *Earth's Future*, 5(3), pp. 304-323. DOI: 10.1002/2016EF000505

Wahl, T., Haigh, I. D., Nicholls, R. J., Arns, A., Dangendorf, S., Hinkel, J., and Slangen, A. B. (2017) 'Understanding extreme sea levels for broad-scale coastal impact and adaptation analysis', *Nature Communications*, 8(1), pp. 1–12. DOI: 10.1038/ncomms16075

Walton, J. K., and Browne, P. (2010) *Coastal Regeneration in English Resorts-2010*. Coastal Communities Alliance. Link to reference.

Walker, I. J., Davidson-Arnott, R. G., Bauer, B. O., Hesp, P. A., Delgado-Fernandez, I., Ollerhead, J., & Smyth, T. A. (2017) 'Scale-dependent perspectives on the geomorphology and evolution of beach-dune systems', *Earth-Science Reviews*, 171, pp. 220-253. DOI: 10.1016/j.earscirev.2017.04.011

Wang, R. Q., Stacey, M. T., Herdman, L. M. M., Barnard, P. L., and Erikson, L. (2018) 'The influence of sea level rise on the regional interdependence of coastal infrastructure', *Earth's Future*, 6(5), pp. 677–688. DOI: 10.1002/2017ef000742

Wang, T., Qu, Z., Yang, Z., Nichol, T., Clarke, G., and Ge, Y. E. (2020) 'Climate change research on transportation systems: Climate risks, adaptation and planning', *Transportation Research Part D: Transport and Environment*, 88, article number 102553. DOI: 10.1016/j.trd.2020.102553

Wang, W., Yang, S., Stanley, H. E., and Gao, J. (2019) 'Local floods induce large-scale abrupt failures of road networks', *Nature Communications*, 10(1), pp. 1–11. DOI: 10.1038/s41467-019-10063-w

Werner, B. T., and McNamara, D. E. (2007) 'Dynamics of coupled human-landscape systems', *Geomorphology*, 91(3–4), pp. 393–407. DOI: 10.1016/j.geomorph.2007.04.020

White, G. F. (1945) *Human adjustment to floods*. *Research Paper*, 29, article number 225. Department of Geography, University of Chicago.

White, G. F. (1994) 'A perspective on reducing losses from natural hazards', *Bulletin of the American Meteorological Society*, 75(7), pp. 1237-1240. DOI: 10.1175/1520-0477(1994)075<1237:aporlf>2.0.co;2

White, G. F. (1975) *Flood hazard in the United States: A research assessment*. Institute of Behavioral Science, University of Colorado

Williams, Z. C., McNamara, D. E., Smith, M. D., Murray, A. B., and Gopalakrishnan, S. (2013) 'Coupled economic-coastline modeling with suckers and free riders', *Journal of Geophysical Research: Earth Surface*, 118(2), pp. 887–899. DOI: 10.1002/jgrf.20066

Williams, B. A., Watson, J. E., Beyer, H. L., Klein, C. J., Montgomery, J., Runting, R. K., ... and Wenger, A. (2022) 'Global rarity of intact coastal regions' *Conservation Biology*, 36(4), article number e13874. DOI: 10.1111/cobi.13874

Wisner, B., Blaikie, P., Cannon, T., and Davis, I. (2004). *At Risk: Natural Hazards, People's Vulnerability, and Disasters (2nd ed.)*. London; New York: Routledge. DOI: 10.1007/s11069-006-9000-6

Wong, P. P., Losada, I. J., Gattuso, J.-P., Hinkel, J., Khattabi, A., McInnes, K. L., Saito, Y., et al. (2014). Coastal systems and low-lying areas. In C. B. Field, V. R. Barros, D. J. Dokken, K. J. Mach, M. D. Mastrandrea, T. E. Bilir, M. Chatterjee, et al. (Eds.), Climate Change 2014: *Impacts, Adaption, and Vulnerability. Part a: Global and Sectoral Aspects. Contribution of Working Group II to the Fifth Assessment Report of the Intergovernmental Panel on Climate Change*, pp. 361–409. Cambridge, UK and New York, NY, USA: Cambridge University Press.

Woodworth, P. L., Hunter, J. R., Marcos, M., Caldwell, P., Menéndez, M., and Haigh, I. (2016) 'Towards a global higher-frequency sea level dataset', *Geoscience Data Journal*, 3(2), pp. 50–59. DOI: 10.1002/gdj3.42

Zervas, C. (2013) *Extreme water levels of the United States 1893–2010*. NOAA Technical Report NOS CO-OPS 067, Silver Spring, Maryland. Link to reference.

Zhang, K., and Leatherman, S. (2011) 'Barrier island population along the US Atlantic and Gulf coasts', *Journal of Coastal Research*, 27(2), pp. 356–363. DOI: 10.2112/JCOASTRES-D-10-00126.1

Zsamboky, M., Fernández-Bilbao, A., Smith, D., Knight, J., and Allan, J. (2011). *Impacts of climate change on disadvantaged UK coastal communities.* Joseph Rowntree Foundation, pp. 1-63. Link to reference.